

**Deanship of Graduate Studies  
Al-Quds University**



**Synthesis and Study of Structure of Mixed-Ligand  
Mononuclear Coordination Compound of Copper,  
Nickel with 2,2'-Bipyrazine Ligand and Bidentate  
Nitrogenous Bases.**

**Afnan Ribhee Abdallah Mansour**

**M.Sc. Thesis**

**Jerusalem –Palestine**

**1444 / 2023**

**Synthesis and Study of Structure of Mixed-Ligand Mononuclear Coordination Compound of Copper, Nickel with 2,2'-Bipyrazine Ligand and Bidentate Nitrogenous Bases.**

Prepared by

**Afnan Ribhee Abdallah Mansour**

B.Sc. Chemistry. Al-Quds University/ Palestine

Supervisor: Dr. Hussein Alkam

A thesis submitted in partial fulfillment of requirement for the degree of the Master of Applied and Industrial Technology, Al-Quds University.

**1444 / 2023**

**Al-Quds University**  
**Deanship of Graduate Studies**  
**Applied and Industrial Technology Program**



## **Thesis Approval**

**Synthesis and Study of Structure of Mixed-Ligand Mononuclear Coordination Compound of Copper, Nickel with 2,2'-Bipyrazine Ligand and Bidentate Nitrogenous Bases.**

Prepared by: Afnan Ribhee Abdallah Mansour  
Registration No: 21512730

Supervisor: Dr. Hussein Alkam

Master thesis submitted and accepted, Date: 20/ 5 /2023.

The names and signatures of the examining committee members are as follows:

1- Head of Committee/ Dr. Hussein Alkam

Signature.....

2- Internal Examiner/ Dr. Wadie Sultan

Signature .....

3- External Examiner/ Dr. Sami Makharza

Signature.....

**Jerusalem-Palestine**

**1444 / 2023**


## **Dedication**

This thesis is dedicated to the sake of Allah, my Creator and my Master. A special feeling of gratitude to my loving parents, Ribhee and Fatima whose words of encouragement. To all of those who encouraged me and helped me; my son Fadi, my brothers obaida and Mohammad, my sweet sister Jannat, my aunt Anaam and any my honey friends, my Dr. Hatem Abu Hilal, my Dr. Abd Al-Halim Ayad, my supervisor Dr. Hussein Alkam, my teachers and work colleagues in college of Science & Technology, to my beloved University; Al-Quds University.

Afnan R. Mansour

## **Declaration**

I certify that this thesis submitted for the degree of master is the result of my own research, except where otherwise acknowledged, and this thesis (or any part of the same) has not been submitted for a higher degree to any other university or institute.

Signed..........

Afnan Ribhee Abdallah Mansour

Date: 20 / 5 / 2023

## **Acknowledgements**

My offer gratitude and thanks to Allah, for giving me a huge perseverance and persistence in completing my thesis. I am very happy to express thankfulness to all who helped and encouraged me to keep going in my educations. Special thanks to my advisor my bachelor's to my master's degrees Dr. Hussein Alkam, for his assistance and recommendations on my experiments and analysis. Special thanks are given to Professor Dr. Antonios Hatzidimitriou from Aristotle University of Thessaloniki, and to Prof. Dr. Matthias Wagner and Dr. Michael Bolte from J.-W.-Goethe-University for their efforts in solving the X-ray structures. Special thanks and appreciation to my colleagues in the chemistry department at Al Quds University for their helping. I would like also to give my thanks to Mrs. Maryam Faroun in the Nanotechnology center at Al-Quds University, and to Dr. Mahmoud Khatib for helping. At least, a great thankful is given to my sweet family and friends for supporting, helping and motivating me during this period.

## Abstract:

The construction of varied networks architectures has been accomplished by incorporating a variety of transition metal coordination geometries in ligand design. Nitrogen-based heterocycles represent a worthy example of ligands that react with metal ions, providing a significant role in the improvement of inorganic complexes and future synthetic works.

There are series of new synthesized complexes that contain either copper(II) or nickel(II) metal atom with homoleptic and/or mixed-ligand as 2,2'-bipyrazine, 2,2'-dipyridylamine, 2-(aminomethyl)pyridine. The structures of the coordination compounds which are  $[\text{Cu}(\text{amp})_2(\text{NO}_3)_2]$  where amp: 2-(aminomethyl)pyridine,  $[(\text{bpz})\text{Cu}(\text{OH})(\text{ClO}_4)(\text{H}_2\text{O})]_2 \cdot \text{H}_2\text{O}$ ,  $[\text{Cu}(\text{bpz})_3](\text{ClO}_4)_2 \cdot 2\text{CH}_3\text{CN}$  where bpz: 2,2'-bipyrazine,  $[\text{Cu}(\text{dipyam})(\text{H}_2\text{O})(\text{pca})]\text{ClO}_4$  where dipyam: 2,2'-dipyridylamine, pca: 2-pyrazinecarboxylate,  $[\text{Ni}(\text{dipyam})_2(\text{bpz})](\text{ClO}_4)_2$  and  $[\text{Cu}(\text{bpz})_2(\text{H}_2\text{O})](\text{NO}_3)_2$  have been characterized based on several techniques as single crystal X-ray diffraction, FTIR spectroscopy and thermal analysis (DSC), and characterized in detail of ligands by FTIR spectroscopy.

The Cu(II) atom in a new  $[\text{Cu}(\text{amp})_2(\text{NO}_3)_2]$  compound has six coordinated with four nitrogen atoms of 2-(aminomethyl)pyridine (amp) ligands, and with two oxygen atoms of the coordinated nitrate molecule. A distorted octahedral coordination geometry around copper Cu(II) atom. The crystal is monoclinic, with space group  $P2_1/c$  and the unit cell dimensions  $a = 8.6377$  (7),  $b = 8.9833$  (6),  $c = 9.9958$  (8) Å,  $\beta = 99.430^\circ$ ,  $Z = 2$  and  $V = 765.14$  (10) Å<sup>3</sup>. The crystal packing is stabilized by C-H...O and N-H...O hydrogen bonds between the pyridine and amino groups of amp ligand with the oxygen atoms of coordinated nitrate molecule. The chains also are reinforced by C-H...O interactions between the CH group of the amp ligand and oxygen atom of nitrate ligand of neighboring chain. Adjacent Cu chains overlapping with others by  $\pi$ - $\pi$  stacking interactions connecting by two 2-(aminomethyl)pyridine ligand.

The structure of the dimer  $[(\text{bpz})\text{Cu}(\text{OH})(\text{ClO}_4)(\text{H}_2\text{O})]_2 \cdot \text{H}_2\text{O}$  contains two separate centrosymmetric  $\mu$ -hydroxy copper(II) dimers, with two terminal 2,2'-bipyrazine ligands, two molecules of water and two perchlorate groups and one water molecule as solvent

molecule. The crystal are triclinic, with space group P-1 and the unit cell dimensions are  $a = 8.0391 (10)$ ,  $b = 8.1718 (9)$ ,  $c = 10.5662 (14) \text{Å}$ ,  $\alpha = 77.973 (5)$ ,  $\beta = 80.465 (6)$ ,  $\gamma = 84.271 (5)^\circ$ ,  $Z = 1$  and  $V = 667.98 (14) \text{Å}^3$ . The X-ray study shows that a distorted elongated tetragonal octahedral geometry around each copper(II) atom, where oxygen atoms of water and perchlorate particles located in the axial positions, while the two nitrogen atoms of 2,2'-bipyrazine ligand and two oxygen of the bridging hydroxo groups located in equatorial sites. The hydrogen bond are formed according to the nitrogens of pyrazine ligands, oxygen of perchlorate groups, hydroxide groups of coordinated water and crystallization water molecules.

The X-ray study of the new compound  $[\text{Cu}(\text{bpz})_3](\text{ClO}_4)_2 \cdot 2\text{CH}_3\text{CN}$  conclude to that Cu(II) center has distorted octahedral geometry and the crystal is monoclinic, with space group  $P2_1/c$  and the unit cell dimensions  $a = 11.2508(6)$ ,  $b = 22.1602(12)$ ,  $c = 13.6980(8) \text{Å}$ ,  $A = 90^\circ$ ,  $b = 90.302(5)^\circ$ ,  $g = 90^\circ$ ,  $Z = 4$  and  $V = 3415.1(3) \text{Å}^3$ . The crystal packing reveals different kinds of hydrogen bonds including, between acetonitrile and nitrogen atom of bpz ligands, oxygen atoms of perchlorate molecules, and hydrogen atom of bpz ligands and between hydrogen atom of acetonitrile and oxygen atom of perchlorate. Also, a Van Deer Waal interaction formed between the C-H of bpz with oxygen atom of  $\text{ClO}_4$ . The adjacent sheets are interact through the  $\pi$ -- $\pi$  interaction.

The in situ formed a new chelate  $[\text{Cu}(\text{dipyam})(\text{H}_2\text{O})(\text{pca})]\text{ClO}_4$  studied by X-ray and showed that Cu(II) atom has five coordinated by two nitrogen atoms of 2,2'-dipyridylamine, one nitrogen and one oxygen of 2-pyrazinecarboxylate (pca) ligand, one oxygen atom of coordinated water. The perchlorate molecule is a counter ion, A distorted square pyramid geometry around Cu(II) ion. The crystal is triclinic, with space group P-1 and the unit cell dimensions are  $a = 7.8943 (10)$ ,  $b = 9.9511 (14)$ ,  $c = 13.412 (2) \text{Å}$ ,  $\alpha = 98.908 (9)$ ,  $\beta = 106.079(8)^\circ$ ,  $\gamma = 112.715 (7)^\circ$ ,  $Z = 2$  and  $V = 892.2 (2) \text{Å}^3$ . The perchlorate anions bind the complex cations to produce a chain structure through  $\text{O}—\text{H}\cdots\text{O}$  close contacts and  $\text{C}—\text{H}\cdots\text{O}$  hydrogen bonds. The in situ forming of new ligand (pca) will encourage scientists to hypothesize a new methodology for C-C / C-N bond cleavage.

The new divalent nickel chelate  $[\text{Ni}(\text{dipyam})_2(\text{bpz})](\text{ClO}_4)_2$ , the X-ray structural analysis show that the Ni(II) atom is a hexacoordinated by two nitrogen atoms of 2,2'-bipyrazine ligand, and four nitrogen atoms of two 2,2'-dipyridylamine ligands. The two

perchlorate ion is a counter ion. The geometry of the compound is a distorted octahedral because of existing the three chelate rings binds with Ni(II) metal, including two (dipyam), one 2,2'-bipyrazine ligands, each 2,2'-dipyridylamine located at equatorial plane and at axial position, and 2,2'-bipyrazine ligands located at equatorial positions. The crystal structure is monoclinic, with space group C2/c the unit cell dimensions are  $a = 16.919 (3)$ ,  $b = 11.2635 (18)$ ,  $c = 17.588 (4) \text{ \AA}$ ,  $\beta = 113.037 (4)^\circ$ ,  $Z = 4$  and  $V = 3084.4 (10) \text{ \AA}^3$ . The perchlorate anions link the complex cations to form a chain structure through N—H $\cdots$ O close contacts and C—H $\cdots$ O hydrogen bonds, beside to 2,2'-bipyrazine ligand binds through C—H $\cdots$ N. The  $\pi\cdots\pi$  and/or C-H $\cdots\pi$  interactions that established by aromatic rings of pyridyl and pyrazinyl groups from adjacent sheet.

The new  $[\text{Cu}(\text{bpz})_2(\text{H}_2\text{O})](\text{NO}_3)_2$  complex investigated by X-ray analysis to find that Cu(II) atom is five coordinated with four nitrogen atoms of 2,2'-bipyrazine ligands, and with one oxygen atom of the water molecule. The two nitrate molecules as counter ion. A distorted trigonal bipyramidal geometry around copper Cu(II) atom. The crystal is Monoclinic, with space group C2/c and the unit cell dimensions  $a = 15.886 (6)$ ,  $b = 7.208 (4)$ ,  $c = 18.016 (7) \text{ \AA}$ ,  $\beta = 107.07 (4)$ ,  $Z = 4$  and  $V = 1972.2 (17) \text{ \AA}^3$ . The crystal packing is stabilized by hydrogen bond that formed according to nitrate anions which is acting as bridges to bond with the cations of the complex via O—H $\cdots$ N and O—H $\cdots$ O hydrogen bonds and C—H $\cdots$ O closed contacts.

These complexes may be able to play role in different fields either chemical, biological or electrical studies due to their ligands have expanded using in multi applications, for example, using in development of selective catalysis, preparation of supramolecular compounds, designing of pharmaceutical molecules that used in drug discovery studies, beside to their utilizing in electro-optic materials, semiconductor materials and magnetic materials.

# Contents

<b>List of Schemes.....</b>	<b>ix-x</b>
<b>List of Figures.....</b>	<b>xi-xvii</b>
<b>List of Tables.....</b>	<b>xviii-xix</b>
<b>List of Abbreviations.....</b>	<b>xx</b>
<b>Chapter One</b>	
<b>1.1 Introduction.....</b>	<b>1</b>
1.2 The importance of copper and nickel metals in coordination complexes.....	1-5
1.3 The importance of nitrogen heterocyclic compounds in forming complexes.....	6-9
1.4 2,2'-bipyrazine ligand.....	9-15
1.5 2,2'-dipyridylamine ligand.....	15-17
1.6 2-(Aminomethyl)pyridine ligand.....	17-19
1.7 pyrazine-2-carboxylate ligand.....	19-22
1.8 The role of mixed ligands in producing of new complexes.....	23-25
<b>1.9 Literature review.....</b>	<b>25</b>
1.9.1 Synthesis of 2,2'-bipyrazine ligand.....	25-28
1.9.2 Copper complexes.....	29-42
1.9.3 Nickel complexes.....	43-51
1.9.4 Other metals complexes.....	51-61
<b>1.10 Research Objectives.....</b>	<b>62</b>
<b>Chapter Two</b>	
<b>2.1 Materials.....</b>	<b>63</b>
<b>2.2 Methods.....</b>	<b>63-64</b>
2.2.1 Synthesis of 2,2'-bipyrazine (bpz)(C <sub>8</sub> H <sub>6</sub> N <sub>4</sub> ).....	63-64

2.2.2 Synthesis of coordination complexes.....	64
2.2.2.1 Synthesis of [Cu(amp) <sub>2</sub> (NO <sub>3</sub> ) <sub>2</sub> ] complex.....	64
2.2.2.1.1 Preparations.....	64
2.2.2.1.2 Crystal Data.....	65
2.2.2.2 Synthesis of [Cu(dipyam)(H <sub>2</sub> O)(pca)]ClO <sub>4</sub> complex .....	66
2.2.2.2.1 Preparations.....	66
2.2.2.2.2 Crystal Data.....	66-67
2.2.2.3 Synthesis of [Cu(bpz) <sub>2</sub> (H <sub>2</sub> O)](NO <sub>3</sub> ) <sub>2</sub> complex.....	67-68
2.2.2.3.1 Preparations.....	68
2.2.2.3.2 Crystal Data.....	68
2.2.2.4 Synthesis of [(bpz)Cu(OH)(ClO <sub>4</sub> )(H <sub>2</sub> O)] <sub>2</sub> .2H <sub>2</sub> O complex.....	68
2.2.2.4.1 Preparations.....	68
2.2.2.4.2 Crystal Data.....	69
2.2.2.5 Synthesis of [Ni(dipyam) <sub>2</sub> (bpz)](ClO <sub>4</sub> ) <sub>2</sub> complex.....	69
2.2.2.5.1 Preparations.....	69-70
2.2.2.5.2 Crystal Data.....	70
2.2.2.6 Synthesis of [Cu(bpz) <sub>3</sub> ](ClO <sub>4</sub> ) <sub>2</sub> .2CH <sub>3</sub> CN complex.....	71
2.2.2.6.1 Preparations.....	71
2.2.2.6.2 Crystal Data.....	71-72

## Chapter Three

<b>Results and Discussion.....</b>	<b>73</b>
3.1 [(bpz)Cu(OH)(ClO <sub>4</sub> )(H <sub>2</sub> O)] <sub>2</sub> .H <sub>2</sub> O complex.....	73-74
3.1.1 Crystal structure for [(bpz)Cu(OH)(ClO <sub>4</sub> )(H <sub>2</sub> O)] <sub>2</sub> .H <sub>2</sub> O.....	75-81
3.2 [Cu(bpz) <sub>2</sub> (H <sub>2</sub> O)](NO <sub>3</sub> ) <sub>2</sub> complex.....	82
3.2.1 Infrared spectroscopy.....	83
3.2.1.1 2,2'-bipyrazine (bpz) ligand.....	83-85
3.2.1.2 Infrared spectroscopy for [Cu(bpz) <sub>2</sub> (H <sub>2</sub> O)](NO <sub>3</sub> ) <sub>2</sub> .....	86-87
3.2.2 Thermal analysis.....	88
3.2.3 Crystal structure for [Cu(bpz) <sub>2</sub> (H <sub>2</sub> O)](NO <sub>3</sub> ) <sub>2</sub> .....	88-97
3.3 [Cu(dipyam)(H <sub>2</sub> O)(pca)]ClO <sub>4</sub> complex.....	97-98

3.3.1 Infrared spectroscopy.....	98-102
3.3.1.1 2,2'-dipyridylamine (dipyam) ligand.....	98-99
3.3.1.2 Infrared spectroscopy for [Cu(dipyam)(H <sub>2</sub> O)(pca)]ClO <sub>4</sub> ...	101-102
3.3.2 Thermal analysis.....	103
3.3.3 Crystal structure for [Cu(dipyam)(H <sub>2</sub> O)(pca)]ClO <sub>4</sub> .....	103-113
3.3.4 Breaking of 2,2'-bipyrazine Ring.....	114-116
3.4 [Cu(bpz) <sub>3</sub> ](ClO <sub>4</sub> ) <sub>2</sub> .2CH <sub>3</sub> CN complex.....	116
3.4.1 Infrared spectroscopy.....	116-119
3.4.2 Thermal analysis.....	119-120
3.4.3 Crystal structure for [Cu(bpz) <sub>3</sub> ](ClO <sub>4</sub> ) <sub>2</sub> .2CH <sub>3</sub> CN.....	120-130
3.4.4 Synthesis for [Cu(bpz) <sub>3</sub> ](ClO <sub>4</sub> ) <sub>2</sub> .2CH <sub>3</sub> CN complex.....	131
3.5 [Ni(dipyam) <sub>2</sub> (bpz)](ClO <sub>4</sub> ) <sub>2</sub> complex.....	131-132
3.5.1 Infrared spectroscopy.....	132-134
3.5.2 Crystal structure for [Ni(dipyam) <sub>2</sub> (bpz)](ClO <sub>4</sub> ) <sub>2</sub> .....	134-144
3.6 [Cu(amp) <sub>2</sub> (NO <sub>3</sub> ) <sub>2</sub> ] complex.....	145-146
3.6.1 Infrared spectroscopy.....	146
3.6.1.1 2-(aminomethyl)pyridine ligand.....	146-147
3.6.1.2 Infrared spectroscopy for [Cu(amp) <sub>2</sub> (NO <sub>3</sub> ) <sub>2</sub> ].....	148-150
3.6.2 Thermal analysis.....	151
3.6.3 Crystal structure for [Cu(amp) <sub>2</sub> (NO <sub>3</sub> ) <sub>2</sub> ] complex.....	151-161

## Chapter Four

4.1 Conclusion.....	162-164
4.2 Future work.....	165

## Chapter Five

References.....	166-199
-----------------	---------

## List of Schemes

<b>Scheme Number</b>	<b>Scheme Name</b>	<b>Page No.</b>
<b>Scheme 1.1</b>	2,2'-bipyrazine ligand provided various metal-binding patterns.	9
<b>Scheme 1.2</b>	2,2'-bipyrazine ligand provided four potential N binding sites and the flexibility of its structure around C-C bond center.	10
<b>Scheme 1.3</b>	Conformations of 2,2'-bipyrazine ligand (above) and its metal binding patterns (below).	11
<b>Scheme 1.4</b>	2,2'-bipyrimidine ligand (a) and 2,2'-bipyrazine ligand (b)	13
<b>Scheme 1.5</b>	View the structure of 2-(aminomethyl)pyridine or 2-picolyamine (ampy) ligand.	18
<b>Scheme 1.6</b>	View the structure of pyrazine-2-carboxylic acid (pcaH).	20
<b>Scheme 1.7</b>	View the synthesis of 2,2'-bipyrazine ligand, using 2-chloropyrazine as starting material.	26
<b>Scheme 1.8</b>	View of that Pd-catalyzed reductive of 2-chloropyrazine to produce 40% of bpz.	26
<b>Scheme 1.9</b>	View of that exposing of 2-iodopyrazine to optimized conditions to form 81% of bpz.	26
<b>Scheme 1.10</b>	View of synthesis of 2,2'-bipyrazine ligand by starting with pyrazine carboxylic acid.	28
<b>Scheme 1.11</b>	View of conditions that used to raise the yield % of 2,2'-bipyrazine ligand.	28
<b>Scheme 1.12</b>	View of conditions that used to get 42% yield of 2,2'-bipyrazine ligand.	28
<b>Scheme 1.13</b>	View the structure of cationic $[\text{Ni}(\text{dpamH})_2(\text{X-salo})]\text{Cl}$ complexes (X= 5-Cl, 5-Br, 5-CH <sub>3</sub> or 3-OCH <sub>3</sub> ).	49
<b>Scheme 1.14</b>	View the structure of cationic $[\text{Fe}(\text{bpy})_3]^{2+}$ complex.	60
<b>Scheme 2.1</b>	View the synthesis of 2,2'-bipyrazine ligand.	63

<b>Scheme 3.1</b>	View the proposed mechanism for the reaction of [Cu(dipyam)(H <sub>2</sub> O)(pca)]ClO <sub>4</sub>	116
<b>Scheme 3.2</b>	View the personal suggestion for the mechanism of breaking bond of 2,2'-bipyrazine ligand during the forming of [Cu(dipyam)(H <sub>2</sub> O)(pca)]ClO <sub>4</sub> complex.	116

## List of Figures

Figures Number	Figures Name	Page No.
<b>Figure 1.1</b>	(a) View of diverse configurations of 2,2'-dipyridylamine ligand and (b) view of three conformational arrangements of deprotonated from 2,2'-dipyridylamine ligand.	16
<b>Figure 1.2</b>	pca ligand has different coordination modes. (I) bidentate terminal (II) bidentate/N-monodentate bridge (III) bidentate/O-monodentate bridge (IV) bidentate/O,N-monodentate bridge (V) N-monodentate terminal pcaH ligand.	21
<b>Figure 1.3</b>	View different coordination modes of pca–metal complexes and polymers.	22
<b>Figure 1.4</b>	View of the complex unit $[\text{Cu}_2(\text{dpp})_2(\text{H}_2\text{O})_2(\text{NO}_3)_2(\text{ox})] \cdot 4\text{H}_2\text{O}$ with the atomic numbering.	29
<b>Figure 1.5</b>	View the section of the chain in $[\text{Cu}(\text{bpz})(\text{ox})]_n$ with the atomic numbering.	30
<b>Figure 1.6</b>	View of X-ray crystal structure for $[\text{Cu}(\text{dpa})_2(\text{dca})_2]$ showing the structure unit (pyridine rings of hydration not shown).	31
<b>Figure 1.7</b>	View of X-ray crystal structure for $[\text{Cu}(\text{D,L-phe})(\text{bpy})] \cdot (\text{ClO}_4)$ showing the structure unit (pyridine rings of hydration not shown).	32
<b>Figure 1.8</b>	View the structures of the compounds.	33
<b>Figure 1.9</b>	View a section of neutral $[\text{Cu}(\text{bpy})(\text{tcm})_2]_n$ chain with displaying the atomic numbering.	33
<b>Figure 1.10</b>	View the Tetranuclear $[\text{Cu}(\text{bpz})_4(\text{tcm})_8]$ complex with showing the atom numbering.	34
<b>Figure 1.11</b>	View the structure of $[\text{Cu}_2(\text{HL})_2(\text{bpy})_2(\text{H}_2\text{O})_2](\text{ClO}_4)_2 \cdot 2\text{H}_2\text{O}$ compound.	35
<b>Figure 1.12</b>	View of $[\text{Cu}(\text{bpy})(\text{NO}_3)_2]$ complex that used as a hybrid catalyst by placing it in proximity to DNA via non covalent interactions.	36
<b>Figure 1.13</b>	View the structure of $[\text{Cu}_2(\text{L4})(\text{ClO}_4)(\text{OH})(\text{CH}_3\text{OH})](\text{ClO}_4)$ complex.	37

<b>Figure 1.14</b>	View the structure of [Cu(L2)NO <sub>3</sub> ] complex, showing the partial atom numbering.	38
<b>Figure 1.15</b>	View of X-ray structure for [Cu(Bpy)(Gly)]ClO <sub>4</sub> complex, with showing the atomic numbering.	39
<b>Figure 1.16 a</b>	View of the structure for [Cu(NH <sub>2</sub> CH <sub>2</sub> CH <sub>2</sub> OH) <sub>2</sub> (NO <sub>3</sub> ) <sub>2</sub> ] complex.	40
<b>Figure 1.16 b</b>	View of the structure for [Cu(NH <sub>2</sub> CH <sub>2</sub> CH(CH <sub>3</sub> )OH) <sub>2</sub> (NO <sub>3</sub> ) <sub>2</sub> ] complex.	40
<b>Figure 1.17</b>	View the structure of [Cu(bpy) <sub>2</sub> (TaF <sub>6</sub> ) <sub>2</sub> ] complex.	41
<b>Figure 1.18</b>	View the structure of [Cu(bpy) <sub>3</sub> ][TaF <sub>6</sub> ] <sub>2</sub> complex.	42
<b>Figure 1.19</b>	View the structure of [Ni(ampy) <sub>2</sub> (NO <sub>3</sub> ) <sub>2</sub> ] complex.	43
<b>Figure 1.20</b>	View the structure of Ni(II) complex.	44
<b>Figure 1.21</b>	View the structure of [Ni(C <sub>10</sub> H <sub>8</sub> N <sub>2</sub> ) <sub>3</sub> ](ClO <sub>4</sub> ) complex, showing the atomic labeling.	45
<b>Figure 1.22</b>	View the structure of [Ni(dpa) <sub>2</sub> (N <sub>3</sub> ) <sub>2</sub> ].H <sub>2</sub> O complex, showing the atomic labelling.	46
<b>Figure 1.23</b>	View the structure of [Ni(bpy) <sub>2</sub> (NO <sub>3</sub> )](NO <sub>3</sub> ) complex.	46
<b>Figure 1.24</b>	View the structure of [Ni(ampy) <sub>2</sub> (tcm) <sub>2</sub> ] complex.	47
<b>Figure 1.25</b>	View the structure of [Ni(dpa) <sub>2</sub> (dca) <sub>2</sub> ] complex.	48
<b>Figure 1.26</b>	View the structure of [Ni(C <sub>8</sub> H <sub>7</sub> O <sub>3</sub> )(C <sub>10</sub> H <sub>8</sub> N <sub>2</sub> )]ClO <sub>4</sub> complex, with showing the atomic labelling.	48
<b>Figure 1.27</b>	View the structure of cationic [Ni(bz)(dipyam) <sub>2</sub> ] <sup>+</sup> complex.	50
<b>Figure 1.28</b>	View the structure of (a) [Ni(bpy) <sub>2</sub> (Bz)]NO <sub>3</sub> ·1.25H <sub>2</sub> O complex and (b) [Ni(Bz) <sub>2</sub> (bpy)] complex.	51
<b>Figure 1.29</b>	View the structure of [Zn(AMP) <sub>2</sub> (NO <sub>3</sub> ) <sub>2</sub> ] complex.	52
<b>Figure 1.30</b>	View the structure of [Zn(bpp)(pca)(MeOH)]ClO <sub>4</sub> complex.	53
<b>Figure 1.31</b>	View the structure of [Fe(bpy) <sub>3</sub> ](ttcH).2bpy.7H <sub>2</sub> O complex. The water molecules and hydrogen atoms of coordinated bpy are deleted for clarity.	53
<b>Figure 1.32</b>	View the structure of [Ag(sac)(ampy)] complex.	54
<b>Figure 1.33</b>	View the structure of [Co(bipy) <sub>3</sub> ](ClO <sub>4</sub> ) <sub>2</sub> complex.	55
<b>Figure 1.34</b>	View the structure of (a) [(amp) <sub>2</sub> FeCl <sub>2</sub> ] complex and (b) [(amp) <sub>2</sub> FeBr <sub>2</sub> ] complex.	56

<b>Figure 1.35</b>	View the structure of $[\text{Zn}(\text{bpy})_2(\text{CH}_3\text{COO})](\text{ClO}_4)\cdot\text{H}_2\text{O}$ complex.	56
<b>Figure 1.36</b>	View the structure of tetranuclear cation $[\{\text{cis-Pt}(\text{NH}_3)_2(2,2'\text{-bpz-N}4,\text{N}4')\}_4]^{8+}$ complex.	57
<b>Figure 1.37</b>	View the structure of $[\{\text{cis-Pt}(\text{NH}_3)_2(2,2'\text{-bpz-N}4,\text{N}4')\}_4](\text{NO}_3)_8\cdot 4\text{H}_2\text{O}$ complex with two nitrate anions and four water molecules cluster encapsulated.	58
<b>Figure 1.38</b>	View the structure of cation $[\text{Ru}(2,2'\text{-bipyridine})_2(\text{Hdpa})]^{2+}$ complex.	59
<b>Figure 1.39</b>	View the structure of cation $[\text{Co}^{\text{II}}_2(\text{L}^1)(\text{bpy})_2]^+$ complex.	60
<b>Figure 1.40</b>	View the structure of $[\text{Zn}(\text{bpy})_3]\text{Cl}_2$ complex.	61
<b>Figure 3.1</b>	View the structure of $[(\text{bpz})\text{Cu}(\text{OH})(\text{ClO}_4)(\text{H}_2\text{O})]_2\cdot\text{H}_2\text{O}$ complex with showing the atom numbering.	75
<b>Figure 3.2</b>	View the distance between Cu-ligand and the angle between Cu1-O-Cu1 of the $[(\text{bpz})\text{Cu}(\text{OH})(\text{ClO}_4)(\text{H}_2\text{O})]_2\cdot\text{H}_2\text{O}$ complex according to the X-ray analysis.	76
<b>Figure 3.3a</b>	View the crystal packing of $[(\text{bpz})\text{Cu}(\text{OH})(\text{ClO}_4)(\text{H}_2\text{O})]_2\cdot\text{H}_2\text{O}$ complex with showing the inter-intrachain H-bonds.	79
<b>Figure 3.3b</b>	View the crystal packing of the complex with showing inter-intrachain H-bonds within the unit cell.	80
<b>Figure 3.3c</b>	View the inter-intrachain H-bonds within unit cell.	80
<b>Figure 3.4</b>	View the distance of $\pi$ - $\pi$ stacking interaction between the 2,2'-bipyrazine ligand in the $[(\text{bpz})\text{Cu}(\text{OH})(\text{ClO}_4)(\text{H}_2\text{O})]_2\cdot\text{H}_2\text{O}$ complex.	81
<b>Figure 3.5</b>	FTIR for 2,2'-bipyrazine ligand.	85
<b>Figure 3.6</b>	The infrared spectra of the $[\text{Cu}(\text{bpz})_2(\text{H}_2\text{O})](\text{NO}_3)_2$ complex.	88
<b>Figure 3.7</b>	Differential Scanning Calorimetry (DSC) of $[\text{Cu}(\text{bpz})_2(\text{H}_2\text{O})](\text{NO}_3)_2$ complex.	89
<b>Figure 3.8</b>	View the structure of $[\text{Cu}(\text{bpz})(\text{H}_2\text{O})](\text{NO}_3)_2$ complex, with showing the atomic numbering.	90
<b>Figure 3.9</b>	View the structure packing of $[\text{Cu}(\text{bpz})_2(\text{H}_2\text{O})](\text{NO}_3)_2$ complex within the unit cell.	91

<b>Figure 3.10</b>	View the inter-intrachain H-bonds of the of [Cu(bpz) <sub>2</sub> (H <sub>2</sub> O)](NO <sub>3</sub> ) <sub>2</sub> complex.	92
<b>Figure 3.11 a</b>	View the distance between the Cu-ligand and the angle between N3 <sup>i</sup> -Cu1-N1 <sup>i</sup> of the [Cu(bpz) <sub>2</sub> (H <sub>2</sub> O)](NO <sub>3</sub> ) <sub>2</sub> according to the X-ray complex.	93
<b>Figure 3.11 b</b>	View the angles between the Cu-ligand of the [Cu(bpz) <sub>2</sub> (H <sub>2</sub> O)](NO <sub>3</sub> ) <sub>2</sub> complex according to the X-ray analysis.	95
<b>Figure 3.12</b>	View the crystal packing of [Cu(bpz) <sub>2</sub> (H <sub>2</sub> O)](NO <sub>3</sub> ) <sub>2</sub> complex with showing the inter-intrachain H-bonds.	96
<b>Figure 3.13</b>	View of the network around coordination water of the [Cu(bpz) <sub>2</sub> (H <sub>2</sub> O)](NO <sub>3</sub> ) <sub>2</sub> complex and nitrate anion.	97
<b>Figure 3.14</b>	View the π- π stacking interactions distance between the 2,2'-bipyrazine ligand in [Cu(bpz) <sub>2</sub> (H <sub>2</sub> O)](NO <sub>3</sub> ) <sub>2</sub> complex.	97
<b>Figure 3.15</b>	FTIR for 2,2'-dipyridylamine ligand.	100
<b>Figure 3.16</b>	The infrared spectra of the [Cu(dipyam)(H <sub>2</sub> O)(pca)]ClO <sub>4</sub> complex.	103
<b>Figure 3.17</b>	Differential Scanning Calorimetry (DSC) of [Cu(dipyam)(H <sub>2</sub> O)(pca)]ClO <sub>4</sub> complex.	104
<b>Figure 3.18</b>	View the structure of [Cu(dipyam)(H <sub>2</sub> O)(pca)]ClO <sub>4</sub> complex, with showing the atomic numbering.	105
<b>Figure 3.19</b>	View the structure packing of [Cu(dipyam)((H <sub>2</sub> O)(pca)]ClO <sub>4</sub> complex within unit cell.	106
<b>Figure 3.20 a</b>	View the distance between the Cu-ligand of the [Cu(dipyam)(H <sub>2</sub> O)(pca)]ClO <sub>4</sub> complex according to the X-ray complex.	107
<b>Figure 3.20 b</b>	View the angles between the Cu-ligand of the [Cu(dipyam)(pca)(H <sub>2</sub> O)]ClO <sub>4</sub> complex, (a) the angle between N4-Cu1-O1 (b) the angle between the N-Cu1-O3 (c) the angle between N4-Cu1-O3 (d) the angle between N3-Cu1-O3 (e) the angle between N1-Cu1-O1	109
<b>Figure 3.21</b>	View the inter-intrachain H-bonds of the [Cu(dipyam)(H <sub>2</sub> O)(pca)]ClO <sub>4</sub> complex.	110
<b>Figure 3.22</b>	View the network structure of [Cu(dipyam)(H <sub>2</sub> O)(pca)]ClO <sub>4</sub> complex with showing the inter intrachain H-bonds.	112

<b>Figure 3.23</b>	View the distance of $\pi$ - $\pi$ interaction 2-pyrazincarboxylate ligand at 3.635-3.812 Å° and between the 2,2'-dipyridylamine ligand at 4.002 Å° in the [Cu(dipyam)(H <sub>2</sub> O)(pca)]ClO <sub>4</sub> complex	113
<b>Figure 3.24</b>	View the weak interaction between N atom and C-H group of pca ligand of other sheet with distance value 2.540 Å° in the [Cu(dipyam)(H <sub>2</sub> O)(pca)]ClO <sub>4</sub> complex.	114
<b>Figure 3.25</b>	View the weak interaction between the NH group of 2,2'-dipyridylamine ligand and OH group of 2-pyrazine carboxylate ring in adjacent structure unit is 2.585 Å° and between the NH group of 2,2'-dipyridylamine ligand and oxygen (O3) of coordinated water is 2.618 Å° in the [Cu(dipyam)(H <sub>2</sub> O)(pca)]ClO <sub>4</sub> complex.	115
<b>Figure 3.26</b>	The infrared spectra of the [Cu(bpz) <sub>3</sub> ](ClO <sub>4</sub> ) <sub>2</sub> .2CH <sub>3</sub> CN.	114
<b>Figure 3.27</b>	Differential Scanning Calorimetry (DSC) of [Cu(bpz) <sub>3</sub> ](ClO <sub>4</sub> ) <sub>2</sub> .2CH <sub>3</sub> CN complex.	119
<b>Figure 3.28</b>	View the structure of [Cu(bpz) <sub>3</sub> ](ClO <sub>4</sub> ) <sub>2</sub> .2CH <sub>3</sub> CN complex, with showing the atomic numbering.	121
<b>Figure 3.29a</b>	View the structure packing of [Cu(bpz) <sub>3</sub> ](ClO <sub>4</sub> ) <sub>2</sub> .2CH <sub>3</sub> CN complex within the unit cell.	123
<b>Figure 3.29b</b>	View a part of unit cell for the [Cu(bpz) <sub>3</sub> ](ClO <sub>4</sub> ) <sub>2</sub> .2CH <sub>3</sub> CN complex.	123
<b>Figure 3.30</b>	View the bite distance and the distance between the Cu-ligand of the [Cu(bpz) <sub>3</sub> ](ClO <sub>4</sub> ) <sub>2</sub> .2CH <sub>3</sub> CN complex according to the X-ray complex.	124
<b>Figure 3.31</b>	View the bite angles between N atom of bpz ligands and Cu metal of [Cu(bpz) <sub>3</sub> ](ClO <sub>4</sub> ) <sub>2</sub> .2CH <sub>3</sub> CN complex.	126
<b>Figure 3.32</b>	View the inter-interaction H-bonds of the [Cu(bpz) <sub>3</sub> ](ClO <sub>4</sub> ) <sub>2</sub> .2CH <sub>3</sub> CN.	129
<b>Figure 3.33</b>	View the crystal packing of [Cu(bpz) <sub>3</sub> ](ClO <sub>4</sub> ) <sub>2</sub> .2CH <sub>3</sub> CN complex with showing the inter-interaction H-bonds.	130
<b>Figure 3.34</b>	View the $\pi$ - $\pi$ interaction distance between the atomic rings of the [Cu(bpz) <sub>3</sub> ](ClO <sub>4</sub> ) <sub>2</sub> .2CH <sub>3</sub> CN complex.	130

<b>Figure 3.35</b>	View the space-filling packing diagram of [Cu(bpz) <sub>3</sub> ](ClO <sub>4</sub> ) <sub>2</sub> ·2CH <sub>3</sub> CN complex, showing the interactions of adjacent chains.	131
<b>Figure 3.36</b>	The infrared spectra of the [Ni(dipyam) <sub>2</sub> (bpz)](ClO <sub>4</sub> ) <sub>2</sub> complex.	134
<b>Figure 3.37</b>	The ball and stick model represents the structure of the [Ni(dipyam) <sub>2</sub> (bpz)](ClO <sub>4</sub> ) <sub>2</sub> complex with the atom numbering.	136
<b>Figure 3.38</b>	View the structure packing of [Ni(dipyam) <sub>2</sub> (bpz)](ClO <sub>4</sub> ) <sub>2</sub> complex within unit cell.	137
<b>Figure 3.39 a</b>	The angles between N atoms of ligands & Ni metal of [Ni(dipyam) <sub>2</sub> (bpz)](ClO <sub>4</sub> ) <sub>2</sub> complex according to the X-ray complex.	138
<b>Figure 3.39 b</b>	View the value of angles between nitrogen that bonded with Ni(II) metal of [Ni(dipyam) <sub>2</sub> (bpz)](ClO <sub>4</sub> ) <sub>2</sub> complex, the color used to distinguish between them.	139
<b>Figure 3.40 a</b>	View the bite distance and the bite angles between N atoms of ligands and Ni metal of [Ni(dipyam) <sub>2</sub> (bpz)](ClO <sub>4</sub> ) <sub>2</sub> complex according to the X-ray.	140
<b>Figure 3.40 b</b>	View the value of bite angle between N <sup>3i</sup> —Ni1—N <sup>5i</sup> and bite distance between N(3 <sup>i</sup> )...N(5 <sup>i</sup> ) of [Ni(dipyam) <sub>2</sub> (bpz)](ClO <sub>4</sub> ) <sub>2</sub> complex.	141
<b>Figure 3.41</b>	View the distance between Ni metal and nitrogen ligands of [Ni(dipyam) <sub>2</sub> (bpz)](ClO <sub>4</sub> ) <sub>2</sub> complex.	142
<b>Figure 3.42</b>	View the inter-interaction H-bonds of the [Ni(dipyam) <sub>2</sub> (bpz)](ClO <sub>4</sub> ) <sub>2</sub> complex.	143
<b>Figure 3.43</b>	View the crystal packing of [Ni(dipyam) <sub>2</sub> (bpz)](ClO <sub>4</sub> ) <sub>2</sub> complex with showing the inter-interaction H-bonds.	144
<b>Figure 3.44</b>	View that perchlorate anion links with the cations of the [Ni(dipyam) <sub>2</sub> (bpz)](ClO <sub>4</sub> ) <sub>2</sub> complex; forming two-dimensional sheet.	145
<b>Figure 3.45</b>	View the distance of π–π stacking interactions connecting each 2,2'- bipyrazine and 2,2'-dipyridylamine ligands at 3.722 - 3.839 Å°	146
<b>Figure 3.46</b>	FTIR for 2-(aminomethyl)pyridine ligand.	148
<b>Figure 3.47</b>	The infrared spectra of [Cu(amp) <sub>2</sub> (NO <sub>3</sub> ) <sub>2</sub> ] complex.	151

<b>Figure 3.48</b>	Differential Scanning Calorimetry (DSC) of [Cu(amp) <sub>2</sub> (NO <sub>3</sub> ) <sub>2</sub> ] complex.	152
<b>Figure 3.49</b>	View the structure of [Cu(amp) <sub>2</sub> (NO <sub>3</sub> ) <sub>2</sub> ] complex, with showing the atomic numbering.	153
<b>Figure 3.50</b>	View the structure packing of [Cu(amp) <sub>2</sub> (NO <sub>3</sub> ) <sub>2</sub> ] complex within unit cell.	153
<b>Figure 3.51</b>	View the angles between N1-Cu-N2 & N1-Cu- N2' of the [Cu(amp) <sub>2</sub> (NO <sub>3</sub> ) <sub>2</sub> ] complex according to the X-ray complex.	154
<b>Figure 3.52</b>	View the distance between the Cu-amp ligand of the [Cu(amp) <sub>2</sub> (NO <sub>3</sub> ) <sub>2</sub> ] complex according to the X-ray.	155
<b>Figure 3.53a</b>	The angles between N and O atoms of the ligands and Cu metal of [Cu(amp) <sub>2</sub> (NO <sub>3</sub> ) <sub>2</sub> ] complex according to the X-ray complex.	157
<b>Figure 3.53b</b>	View the values of angles between nitrogen that bonded with Cu(II) metal of [Cu(amp) <sub>2</sub> (NO <sub>3</sub> ) <sub>2</sub> ] complex, the color used to distinguish between them.	158
<b>Figure 3.54</b>	View the bite distance and the bite angles between N atoms of ligands and Cu metal of [Cu(amp) <sub>2</sub> (NO <sub>3</sub> ) <sub>2</sub> ] complex according to the X-ray complex.	158
<b>Figure 3.55</b>	View the inter-interaction H-bonds of the [Cu(amp) <sub>2</sub> (NO <sub>3</sub> ) <sub>2</sub> ] complex.	159
<b>Figure 3.56</b>	View the crystal packing of [Cu(amp) <sub>2</sub> (NO <sub>3</sub> ) <sub>2</sub> ] complex with showing the inter-interaction H-bonds.	160
<b>Figure 3.57</b>	View the distance value of intermolecular hydrogen bonding between NH <sub>2</sub> group of the amp ligand with the oxygen atom of nitrate ligand of adjacent chain of [Cu(amp) <sub>2</sub> (NO <sub>3</sub> ) <sub>2</sub> ] complex; forming two-dimensional sheet.	161
<b>Figure 3.58</b>	View the distance value of C-H...O interactions by the CH group of the amp ligand with oxygen atom of nitrate ligand of adjacent chain [Cu(amp) <sub>2</sub> (NO <sub>3</sub> ) <sub>2</sub> ] complex.	162
<b>Figure 3.59</b>	View the distance of π-π stacking interactions connecting two (amp) ligand at 3.375 Å in the [Cu(amp) <sub>2</sub> (NO <sub>3</sub> ) <sub>2</sub> ] complex	162

## List of Tables

Table Number	Table Name	Page No.
<b>Table 1.1</b>	View of optimization of Pd-catalyzed reductive homocoupling of 2-halopyrazines.	27
<b>Table 2.1</b>	Crystal Data and Structure Refinement Parameters for [Cu(amp) <sub>2</sub> (NO <sub>3</sub> ) <sub>2</sub> ] complex.	65
<b>Table 2.2</b>	Crystal Data and Structure Refinement Parameters for [Cu(dipyam)(H <sub>2</sub> O)(pca)ClO <sub>4</sub> ] complex.	66-67
<b>Table 2.3</b>	Crystal Data and Structure Refinement Parameters for [Cu(bpz) <sub>2</sub> (H <sub>2</sub> O)](NO <sub>3</sub> ) <sub>2</sub> complex.	67-68
<b>Table 2.4</b>	Crystal Data and Structure Refinement Parameters for [(bpz)Cu(OH)(ClO <sub>4</sub> )(H <sub>2</sub> O)] <sub>2</sub> .2H <sub>2</sub> O complex.	68-69
<b>Table 2.5</b>	Crystal Data and Structure Refinement Parameters for [Ni(dipyam) <sub>2</sub> (bpz)](ClO <sub>4</sub> ) <sub>2</sub> complex.	70
<b>Table 2.6</b>	Crystal Data and Structure Refinement Parameters for [Cu(bpz) <sub>3</sub> ](ClO <sub>4</sub> ) <sub>2</sub> .2CH <sub>3</sub> CN complex.	71-72
<b>Table 3.1</b>	Bond length [Å] of [(bpz)Cu(OH)(ClO <sub>4</sub> )(H <sub>2</sub> O)] <sub>2</sub> .H <sub>2</sub> O complex.	77
<b>Table 3.2</b>	Bond angle [deg.] of [(bpz)Cu(OH)(ClO <sub>4</sub> )(H <sub>2</sub> O)] <sub>2</sub> .H <sub>2</sub> O complex.	78
<b>Table 3.3</b>	Hydrogen geometry (Å, °) of [(bpz)Cu(OH)(ClO <sub>4</sub> )(H <sub>2</sub> O)] <sub>2</sub> .H <sub>2</sub> O complex.	79
<b>Table 3.4</b>	Infrared frequencies (cm <sup>-1</sup> ) for the free 2,2'-bipyrazine and assignments.	83
<b>Table 3.5</b>	Comparison Infrared frequencies (cm <sup>-1</sup> ) of 2,2'-bipyrazine ligand of [Cu(bpz) <sub>2</sub> (H <sub>2</sub> O)](NO <sub>3</sub> ) <sub>2</sub> complex with the free 2,2'-bipyrazine ligand.	86
<b>Table 3.6</b>	Bond length [Å] of [Cu(bpz) <sub>2</sub> (H <sub>2</sub> O)](NO <sub>3</sub> ) <sub>2</sub> complex.	92- 93
<b>Table 3.7</b>	Bond angle [deg.] of [Cu(bpz) <sub>2</sub> (H <sub>2</sub> O)](NO <sub>3</sub> ) <sub>2</sub> complex.	93-94
<b>Table 3.8</b>	Hydrogen geometry (Å, °) of [Cu(bpz) <sub>2</sub> (H <sub>2</sub> O)](NO <sub>3</sub> ) <sub>2</sub> complex.	95
<b>Table 3.9</b>	Infrared frequencies (cm <sup>-1</sup> ) data for the 2,2'-dipyridylamine ligand and assignments.	99

<b>Table 3.10</b>	Infrared frequencies ( $\text{cm}^{-1}$ ) data for the 2-pyrazinecarboxylate ligand and assignments.	101
<b>Table 3.11</b>	Bond angle [deg.] of $[\text{Cu}(\text{dipyam})(\text{H}_2\text{O})(\text{pca})]\text{ClO}_4$ complex.	107-108
<b>Table 3.12</b>	Bond length [ $\text{Å}$ ] of $[\text{Cu}(\text{dipyam})(\text{H}_2\text{O})(\text{pca})]\text{ClO}_4$ complex.	108
<b>Table 3.13</b>	Hydrogen geometry ( $\text{Å}$ , $^\circ$ ) of $[\text{Cu}(\text{dipyam})(\text{H}_2\text{O})(\text{pca})]\text{ClO}_4$ complex.	111
<b>Table 3.14</b>	Comparison Infrared frequencies ( $\text{cm}^{-1}$ ) of 2,2'-bipyrazine ligand of $[\text{Cu}(\text{bpz})_3](\text{ClO}_4)_2 \cdot 2\text{CH}_3\text{CN}$ complex with the free 2,2'-bipyrazine ligand.	117
<b>Table 3.15</b>	Bond length [ $\text{Å}$ ] of $[\text{Cu}(\text{bpz})_3](\text{ClO}_4)_2 \cdot 2\text{CH}_3\text{CN}$ complex.	125
<b>Table 3.16</b>	Bond angle [deg.] of $[\text{Cu}(\text{bpz})_3](\text{ClO}_4)_2 \cdot 2\text{CH}_3\text{CN}$ complex.	126-127
<b>Table 3.17</b>	Hydrogen geometry ( $\text{Å}$ , $^\circ$ ) of $[\text{Cu}(\text{bpz})_3](\text{ClO}_4)_2 \cdot 2\text{CH}_3\text{CN}$ complex	128
<b>Table 3.18</b>	Infrared frequencies ( $\text{cm}^{-1}$ ) for $[\text{Ni}(\text{dipyam})_2(\text{bpz})](\text{ClO}_4)_2$ complex and assignments.	133
<b>Table 3.19</b>	Bond angle [deg.] of $[\text{Ni}(\text{dipyam})_2(\text{bpz})](\text{ClO}_4)_2$ complex.	137-138
<b>Table 3.20</b>	Bond length [ $\text{Å}$ ] of $[\text{Ni}(\text{dipyam})_2(\text{bpz})](\text{ClO}_4)_2$ complex.	141-142
<b>Table 3.21</b>	Hydrogen geometry ( $\text{Å}$ , $^\circ$ ) of $[\text{Ni}(\text{dipyam})_2(\text{bpz})](\text{ClO}_4)_2$ complex.	144
<b>Table 3.22</b>	Infrared frequencies ( $\text{cm}^{-1}$ ) for the 2-(aminomethyl)pyridine and assignments.	147
<b>Table 3.23</b>	Comparison Infrared frequencies ( $\text{cm}^{-1}$ ) of 2-(aminomethyl)pyridine ligand of $[\text{Cu}(\text{amp})_2(\text{NO}_3)_2]$ complex with the 2-(aminomethyl)pyridine ligand.	149
<b>Table 3.24</b>	Bond angle [deg.] of $[\text{Cu}(\text{amp})_2(\text{NO}_3)_2]$ complex.	156
<b>Table 3.25</b>	Bond length [ $\text{Å}$ ] of $[\text{Cu}(\text{amp})_2(\text{NO}_3)_2]$ complex.	159
<b>Table 3.26</b>	Hydrogen geometry ( $\text{Å}$ , $^\circ$ ) of $[\text{Cu}(\text{amp})_2(\text{NO}_3)_2]$ complex.	160

## Abbreviations

2,2'-bipyrazine	bpz
2,2'-bipyridine	bpy
Metal-2,2'-bipyrazine	M-bpz
Metal-2,2'-bipyridine	M-bpy
Hydrogen bonding	H-bonding
2,2'-bipyrimidine	bpym
2,2'-dipyridylamine	dipyam
Pyridyl groups	py
2-(aminomethyl)pyridine or 2-picolyamine	ampy
Pyrazine-2-carboxylic acid	pcaH
Pyrazine-2-carboxylate	pca
FTIR	Fourier transforms infrared spectroscopy
DSC	Differential Scanning Calorimetry
$\nu$	stretching
$\beta$	bending
$\gamma$	twisting
w	wagging
r	rocking
$\delta$	deformation
$\tau$	torsion
$\Phi$	ring breathing

# Chapter One

---

## **1.1 Introduction:**

The construction of a wide variety of network topologies has been achieved through ligand design with using of different transition metal coordination geometries.[1] Nitrogen-containing heterocycles is one of examples for ligands that interact with metal ions, in which it played a major role in the development of the inorganic complexes, and future synthetic work. [2]

## **1.2 The importance of copper and nickel metals in coordination complexes**

Copper is one of widely used metals, where it is one of the 25 most wealth elements in the earth. [3, 4] Its complexes are distinct in coordination chemistry and extensive redox chemistry. The coordination and geometry of them related and affected by the oxidation state of copper, where its oxidation states vary from 0 to +3. But +2 (cupric) and +1 (cuprous) are the most common. [3, 5]

For Cu(I) ion, in which its closed shell  $d^{10}$ , has the main coordination of four with tetrahedral geometry, however, the most commons are coordination of two with linear geometry and coordination of three with trigonal geometry. Their usually properties are diamagnetic and colorless, except if color emits from charge transfer by chelating ligands or affecting by the counter ion. On the other side, the coordination Cu(II) ion, in which its closed shell  $d^9$ , is usually in tetragonal coordination, with four short equatorial bonds and one or two longer axial bonds. Its complexes show rich physicochemical properties as copper(II) ion is paramagnetic. At least, the polynuclear copper clusters with diverse structural blocks generally could be reachable with appropriate bridged linkers. [3, 4, 6, 7]

In more details, the numerous of coordination structures that utilized by copper (I)/(II), lead to provide different coordinating ligands, which range from monodentate to hexadentate. [8] The coordination structure of copper(II) complexes variety from four to eight. The four-coordinate square planar environments is more common, then five-coordinate trigonal bipyramidal and square pyramidal arrangements, six-coordinate octahedral geometries, mostly showing tetragonal distortions. [8, 9, 10] While the usually structure of Cu(I) complexes is linear, in which its coordination number is 2, trigonal (CN

=3), or tetrahedral structure (CN=4). [8, 11] Each of coordination structures of copper(I) complexes has different characteristics. For example, the linear Cu(I) complexes are formed with a strong basic highly polarized ligands, however, they are insufficiently soluble. Another example is that stability of complexes Cu(I)/(II) ions essentially affected by various factors as geometry of the copper environment, number and nature of ligand [8]

Cu(II) ( $d^9$ ) complexes are being the most interest area studies; since Cu(II) metal had a single unpaired which could use for investigating of the nature of magnetic exchange interactions between the single unpaired electrons on two or more metal centers, and in which way this type of interaction is intermediated by the ligands that bridge the metal centers. [6, 12, 13]

Copper is one of essential micronutrients for all organisms that living in oxygen-rich environments. [14] Its uses expand in different fields and settings, including chemical reactions and physiological conditions because of its redox-active metal merit. [5] The easily changing in redox state enables the copper to coordinate a variety of ligands as carboxylate oxygen, imidazole nitrogen, etc. Also, redox property enables copper compounds to be used in medicine and clinical parts, due to its providing abundant pathways of biological activity. Whereas copper has a significant role in the function of many biological processes such as energy metabolism, mitochondrial respiration, antioxidation, collagen cross-linking. [5, 15, 16]

Nowadays, scientists turned to focus in copper complexes as were found to be the promising antitumor therapeutic agents, according to their acting by different biological mechanisms. [15] To be more accurate, Cu(II) sites show and play a significantly central role in biological metalloproteinase. [17] Likewise, copper is an essential fundamental in the development and functioning of multiple enzymes and proteins like cytochrome C oxidase and Cu/Zn superoxide dismutase, in which are participated in the processes of respiration, energy metabolism, and DNA synthesis. [3, 18, 19] Therapeutic efficacy of copper coordination complexes are not only efficient, but also they are less cost and safer alternative to classical platinum-containing chemotherapy. [3, 20] Beside to that, they show effective treatments as antimicrobial, antituberculosis, antimalarial, antifungal, and anti-inflammatory drugs. [21]

Furthermore, copper is not only considered as essential nutrient for living organism as animals, humans, and plant. But also, it is a vital component in regulating of the plant growth, including the chlorophyll formation and seed production. [22] As it involves in different enzyme systems that are responsible for the controlling the biochemical reactions in plant. Photosynthesis process is an instance that required copper to regulate the respiration of plant, with help the metabolism of carbohydrates and proteins. [22, 23] Additionally, it used to promote the plant disease. For example, Bordeaux mixture (copper sulfate) is commonly utilized in organic agriculture because of its low toxicity for human and environment. [24, 25]

Recent advancements in copper coordination complexes have appeared that they play critical roles in the photophysical and photo electrochemical applications. As catalysts, dye-sensitized, solar energy conversion, utilization and storage, light sensitizers, redox mediators, electron donors and catalytic centers. The results show that copper complexes are feasible to apply, better performing and better alternatives to use instead of other commonly used transition metals such as Co, Pt, Ir and Ru. [26]

In summary, the reasons for the copper metal and its complexes, and being special option to improve and synthesize process could not be counted, but there are several main points are mentioned. First, it is low-cost (much cheaper) than noble-metals, low toxicity, sustainable, more available (abundant) elements on earth. Second, copper has wide-ranging redox properties, with a variability of valence states ( $\text{Cu}^+$ ,  $\text{Cu}^{2+}$ , and  $\text{Cu}^{3+}$ ), and so applied in the expansion of electrocatalysts progress as lithium-ion battery anode materials and photocatalysts, and redox mediators in dye-sensitized solar cell. Third, copper could be a central metal in the enzyme as hemocyanin. Forth, its complexes are easy to form, with variety of coordination structures, this merit could be useful in designing of rod-like molecular arrays. Beside to that, it is an effective for all energy-related applications and rising of their performance. [3, 11, 27, 28]

In other perspective, researches attracted and attended to nickel complexes as they have appeared an important functions in different fields, such as bioinorganic and coordination chemistry. [29] Nickel is a crucial metal took part in multiple biological process. Therefore, its complexes have been interested for researchers according to their biological applicability, such as antiepileptic, anticonvulsant, antibacterial, antifungal,

antioxidant, antiaging agents, antimicrobial and anticancer/ antiproliferative activities. For example, nickel complexes have ability to inhibit the DNA repair process as they affect and interfere with the enzymes and proteins, which have critical function in mechanisms of DNA process as replication or repair. [29- 34] As a result, nickel has been identified as a component in many enzymes, and so it plays an important role in the metabolic reactions and becoming the key physiological functions in the organisms. [35]

Thus, it is an essential trace element for human beings, animals, microorganisms, and plants. This merit prompt researchers to pay more and more attention to this class of complexes for improving and synthesizing metal-based drugs, which targets many bioactivities. [29, 30, 33] Production of chiral amino acids via nickel(II) compounds is one of examples that present different features as high selectivity, high yield, low price, simple process and facile recovery of chiral ligand. [36] Beside to that, nickel complexes have an important role in biosynthesis reaction. Nickel, as example, shows a huge effect in the biosynthesis of the hydrogenase, carbon monoxide dehydrogenase. Also, it is found in bacteria as nickel-tetrapyrrole coenzyme, Cofactor F430 [37]

Furthermore, nickel heterocyclic carbene complexes are preferred category of precatalysts, which used in the organic transformations. They are favored to be an efficient for potential industrialization of these processes. That's because nickel has different properties such as low cost, easy to obtain, and spread frequently in the earth, where nickel is one of the most abundant metallic elements. [38] For instance, nickel complexes work as homogeneous catalysis reduction of ketones. [39] Also, organonickel(II) complexes are widely used in organometallic catalysis. Beside to that, several reports display that different transition metals as nickel used as efficient water-oxidizing catalysts under different conditions. [40, 41]

Moreover, efforts turned to choose nickel for developing efficient transition metal catalysts. That is because: first, its center is able to form various coordination environments as octahedral, square-planar and tetrahedral, which assist different steps of catalytic cycle. Second, Ni-complexes show an ability to catalyze C–C cross-coupling reactions. [42] The proceeding of catalytic cycle is going by using nickel- catalyzed reactions via its numerous oxidation states, which surrounds from -1 to +4. But divalent nickel (+2) is the most

common, and the central general analogue of nickel in biological systems. [43, 44] Therefore, that lead to be a valued precursors for assisting and supporting bimetallic catalysts. Because of combinations intimately associated with metals components, their stoichiometries can be accurately controlled and may also provide better control of the size. [45]

Generally, researches are going to design a new sustainable and potential catalytic system using unexpensive and available metals. Many studies are focus in the improving of 3d-transition metal based catalytic transformations as nickel because of cost effectiveness, variable oxidation states, facile oxidative addition of organic substrates on the nickel center, and low Ni-C bond strength. [41]

In addition to that, nickel is also considered as one of the most mainly used as raw material in manufacturing field as stainless steel and battery industry. [46] Also, it has a good resistance toward corrosive atmospheres, meaning that, it oxidized slowly by air at room temperature and so it is a corrosion-resistant. For that reason, historically, it used for coating chemistry equipment, painting iron and brass and industrialization certain kinds of alloys. Therefore, it is largely used in the electrical contact industry either as a barrier or as a final coating. [47, 48] At least, nickel diimine complexes have gained a large interest in electrocatalytic applications. [40]

All of applications and interest caring for nickel metal is because of its multiple chemical characteristics. One of them is nickel belongs to 3d group transition metals. Second, it is one of four elements that has ferromagnetic at approximately room temperature. Third, it is a naturally magnetostrictive material, meaning that if nickel metal exposed to magnetic field, a small changing might be happened in length. [37, 48] The magnetic property for nickel heterocyclic complexes because of that tetrahedral complexes are paramagnetic, whereas the square planar complexes are diamagnetic. However, octahedral complexes are formed when the having properties of magnetic at equilibrium state. These properties is occurring attributable to metallic bonding by delocalized d electrons and so creating a unity in which it increases by the number of shared electrons. [48]

### **1.3 The importance of nitrogen heterocyclic compounds in forming complexes**

Nitrogen heterocyclic (N- heterocyclic) compounds are one kind of aromatic carbon cycles organic compounds, in which it composed at least one nitrogen atom (heteroatom) that taking the place of a ring carbon atom or a complete CH=CH group. They are a fundamental for recognizing of life processes and to get a better quality for humanity. [49-53]

Their chemical structure is the key for the understanding of different properties such as physical, chemical, biological, or even technical. Besides to that, the aromaticity concept is the basis for justifying and realized of the structure, thus, the performance of heterocyclic compounds could be understood. As a result, their distinct structures are caused to have multi-using and so expand their significance in different fields. Adding to that, N- heterocyclic are the most discovered compounds due to their common spreading in nature; where more than 20 million chemical compounds currently registered, about one half contain heterocyclic systems. They are occurred naturally worth products for human and animal health as antibiotics, alkaloids, and cardiac glycosides. [52, 54-84]

Otherwise, their interest does not only measured by their abundance but also they are highlighted because of different reasons cantered in biological, chemical and technical applications. [52, 73, 74, 85] First, nitrogen heterocycles have a critical role in biochemistry and life process due to they participated in the chemical reactions of the creations body. In other words, they have been essential manifestations of life, for instance, providing of energy, transmission of nerve impulses, metabolism, and genetic information transfer. They also are main components of living cells as DNA, RNA, vitamins, enzymes and coenzymes, ATP and serotonin. At least, aromatic N- heterocyclic are the major constituents for abundant plant and animal hormones. [50, 78, 81, 84, 86-91] Secondly, the monitoring and remarkables of primitive life in nature contribute to reveal different healing ingredients. [52] Meaning that, the existing heterocycles in various natural products led to produce economical, efficient and active compounds that containing N-heterocyclic. [82, 92 – 98]

The applications of N- heterocyclic are countless including chemical, biological, pharmacy, medicine, herbicides, optics, electronics, agriculture, plastics, polymers, life

sciences and chemical genetics. Moreover, they are employed as additives and modifiers in a wide range of industries including cosmetics, reprography, information storage, solvents and vulcanization accelerators. [49, 50, 72, 75, 81 – 86, 99-106]

The continuous development life leads to take new applications of heterocycles, for example dyes, copolymers, photo-graphic fluorescent sensor, bleaching agents, and analytical reagents, and in the rubber industry antioxidants. Other products of technical importance as corrosion inhibitors, sensitizers, stabilizers include heterocycles in their structure. Furthermore, they performance as organic conductors, semiconductors, molecular wires, photo-voltaic cells, organic light-emitting diodes (OLEDs), light harvesting systems, optical data carriers, chemically controllable switches, and liquid crystalline compounds. In brief, N- heterocyclic is functionalized in any developed human society. In short, heterocycles offer a core source of novel aromatic compounds. Therefore, natural models are followed to invent and synthesize better developers like insecticides, pesticides, weed killers, rodenticides, and pharmaceuticals. [52, 73-75, 77, 79, 80, 82-84, 89, 91, 93-96, 98-101, 106, 107]

N-heterocyclic does not only display uses in agrochemicals, pharmaceutical applications and biological properties but also they have been on the forefront of attention in modern drug discovery and in the search of therapeutic agents, including synthesis, design, discovery and manufacturing of new drugs, in which heterocycles comprising around 60% are covered as a drug substances. Whereas their structure is a part of the pharmacophore itself and/or scaffolds for the correct spatial positioning of pharmacophore moieties. [50, 54 – 71, 75, 80-82, 84, 85, 87, 89, 105, 107, 123- 127]

Also, small heterocyclic molecules are considered “privileged” structures for the development of novel drugs. Meaning that, many pharmacological manufactures mimic the biological activity of natural products, in which it contains numerous heterocycles. The most advances views in fighting diseases, many chemically diverse heterocycles were synthesized, which afforded structural members with more desirable biological and physical properties, where nitrogen heterocyclic act as intermediate during synthesis of many biologically important compounds. [75, 83, 84, 100, 101, 116, 118, 119, 121, 128]

N- heterocyclic compounds represent the essential core of many biologically active natural products agents such as antifungal, anti-viral, anti-inflammatory, anti-bacterial, anti-tumoral, antimalarial activity and anti-oxidant activities agents, anti-asthmatic, antihypertensive, bronchodilatory, CCK antagonist, and lipoxygenase inhibition and in the treatment of infectious diseases. That diverse activities can be referred to the stability and operational efficiency of N- heterocyclic in human body, and to their ability to interact with DNA through hydrogen bonding. At the consequence, the enormous potential of heterocycles in the synthesis and design of new drugs. That continue to hold a central position in organic chemistry or becoming a biggest of the classical branches of organic chemistry. Especially, in the research areas of synthetic field because of their useful properties. The reason for that is the incorporation of a hetero atom in to a cyclic compound imparts new properties. Heterocycles are chemically more flexible and better able to cater the needs of biochemical systems. [49, 54-78, 81-85, 87, 89, 91, 93-96, 99-101, 103, 105-116, 127-131]

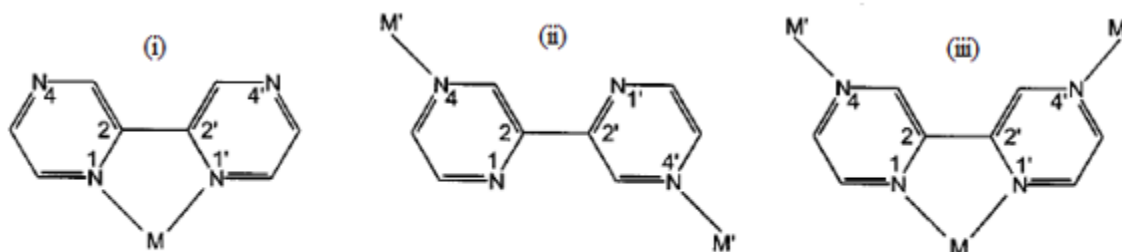
On one hand, their encountered structures and their biological and pharmaceutical relevance are led to develop new economical, efficient, selective synthetic strategies and synthetic transformations to access and testing new structures. A lot of them which are often heteroaromatic derivatives. Over and above that, nitrogen heterocyclic are ongoing to invent new uses across the chemical sciences used as an excellent role in metal-based catalytic reactions, organo catalytic carbene catalysis, where their strong binding with metal allow to enhance the stabilization of metallic colloids or surfaces. At least, they used as protecting groups, chiral auxiliaries, and they have been a worthy attention in improving of effective new methods to synthesise heterocycles. [51, 54, 62, 63, 75, 77, 102, 117, 123, 133-136]

The spreading applying of N- heterocyclic in different areas return to their unique interesting steric and electronic properties. N- heterocyclic as electron rich nitrogen heterocycles- is not only able to accept or donate a proton, but also they can simply make diverse weak interactions. They have different interactions that enhanced their role in vast fields as hydrogen bonding formation, dipole-dipole interactions, hydrophobic effects, van der Waals forces and  $\pi$ -stacking interactions. [89, 135]

In recent years, studied metal complex formation of 2,2'-bipyrazine as well as of selected other heterocyclic ligands such as 2-(aminomethyl)pyridine, 2,2'-dipyridylamine, with particular caring to synthesize unique metal-ligand compounds. [2, 137] Among nitrogen heterocycles, bipyrazine have been attracted special attention not because its importance as ligand in coordination chemistry but also as its existent in different applications as many bacterial studies, food, agriculture and medicine. [138]

#### **1.4 2,2'-bipyrazine ligand**

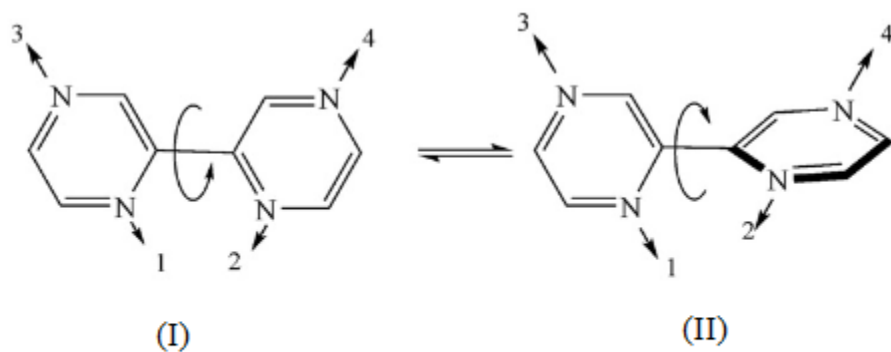
2,2'-bipyrazine (bpz) is one of most important multimodal N-heterocyclic ligand, as a resulting of forming discrete and polymeric metal complexes [137]. It has a typical property, in which it provided a large number of different metal-binding patterns. That is because of the availability of four ring N donor atoms and so it undergoes to the chelation mode. [139] N atoms (1,1'and/or 4,4') are involved in the coordination, and so different combinations of coordinate vectors are possible. According to scheme1.1 the mode (i) via N1 and N1' established a chelation mode, while mode (ii) or (iii) leads to create a molecular triangle based on geometry of M', either a hexanuclear, cup-shaped species forms (M' having a cis geometry), or a flat triangle (M' having a trans geometry). [140]



**Scheme 1.1** 2,2'-bipyrazine ligand provided various metal-binding patterns.<sup>[140]</sup>

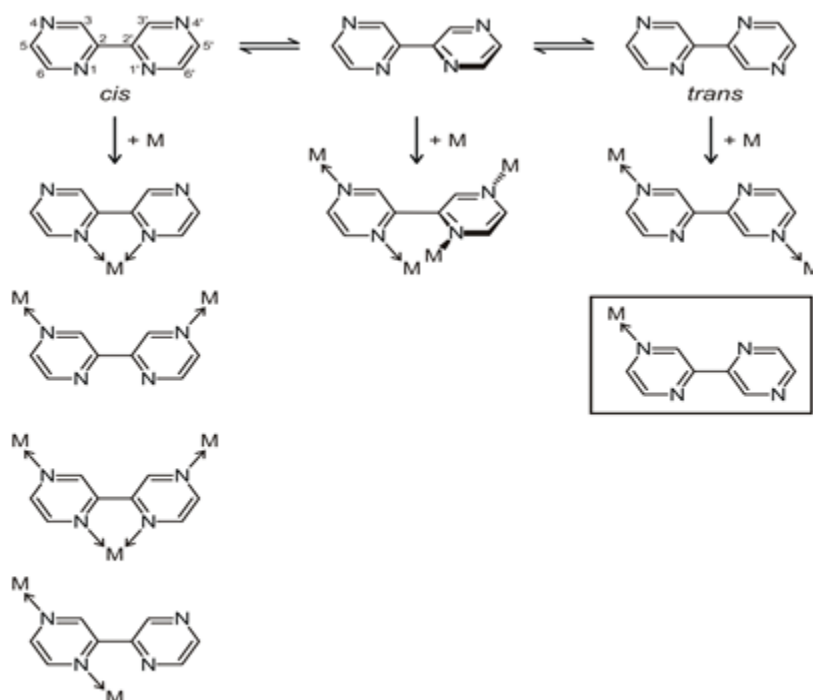
Adapting multi-modal bridging ligands as building units has gained attention in crystal engineering since they are capable of binding several metal centers in expected way to compose “preprogrammed” structural information and functionality. 2,2'-bipyrazine (bpz) is of specific attention among the adapting multi-modal bridging ligands not only due to its diversified binding capabilities but also to its structural flexibility about the central

C2–C2' bond (scheme 1.2), and so that facilitate the rotation around the C2–C2' bond to control network formation, and to give cis or trans isomers. [139, 141 – 144]



**Scheme 1.2** 2,2'-bipyrazine ligand provided four potential N binding sites and the flexibility of its structure around C-C bond center. [144]

According to that, various of molecular architectures are generated as a result of two different conformations of 2,2'-bipyrazine, which the two pyrazine halves oriented *cisoid* ( $C_{2v}$  symmetry) or *transoid* ( $C_{2h}$  symmetry), and the variable use of its four N-donor atoms (scheme 1.3). [137]



**Scheme 1.3** Conformations of 2,2'-bipyrazine ligand (above) and its metal binding patterns (below).<sup>[137]</sup>

At least, 2,2'-bipyrazine not just only provide two independent types of binding sites as the chelating bidentate site, and the two monodentate N-donor sites, but also two possible modes for bridging metal centers. These two bridging modes provide possible mechanism for generating two independent helices when reacted with a suitable metal center and thus, potentially, an asymmetric network. [1]

The 2,2'-bipyrazine (bpz) in comparison with 2,2'-bipyridine (bpy), has lower lying  $\pi^*$ -acceptor orbitals and higher orbital coefficients at the coordinating nitrogen centers. These properties lead to form the MLCT (metal-to-ligand charge transfer transition) and so guaranteed of strong metal/ligand interaction. [145 -147] The bipyrazine category is more powerful oxidizing agent in the excited state than the bipyridine category [148]. In comparison, the MLCT band of M-bpz (metal-2,2'-bipyrazine) complex is slightly higher in energy, and the lifetime of the emissive state is slightly longer than that of M-bpy (metal-2,2'-bipyridine) complex. [138(i)] Another difference, the M-bpz potentials are shifted more positive relative to that of M-bpy. [138(j)]

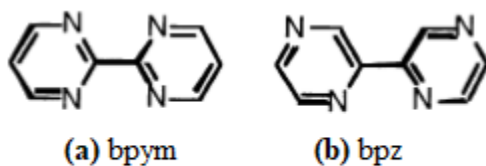
2,2'-bipyrazine considered as higher  $\pi$ -electron acceptor compared with other polypyridyl ligands. This merit could be benefit in different uses, where polypyridyl ligands with high  $\pi$ -electron acceptor properties employed in the synthesis of complexes as photosensitizers. [149] Much attention has been put to examination of polypyridyl complexes with respect to their characteristics, including photophysical, photochemical and redox properties [150(a-b)], with potential caring for many implementations such as energy conversion, [150(c-f)] water splitting, [150(g-h)] molecular machines [150(i-j)] or for biomedical applications. [150(k-m)]

2,2'-bipyrazine ligands possess non-chelating nitrogen atoms in their structure; the presence of these additional nitrogens enhancement of the  $\pi$ -deficiency of the ligand, has a great impact on the photophysics and photochemistry of the associated complexes. These additional nitrogen atoms can also be involved in H-bonding (hydrogen bonding) interactions, increasing the sensitivity of the complex to solvents. [150(a, n- o)]

Regarding to that, 2,2'-bipyrazine is not only reactive towards nucleophiles, but also has greater non-aromatic character comparing with other heterocycles as pyrimidines, bipyridine and phenanthroline based on chemical and experimental electron density analysis.[151] However, there are reports resulted in that there are factors lead to make the properties of 2,2'-bipyrazine (bpz) are similar to 2,2'-bipyrimidine (bpym) (scheme 1.4) such as their aromatic character, electroneutrality, planarity and presence of four nitrogen donors. On other hand, the relative arrangement of their nitrogens support creating of varied coordination modes. [24]

Also, the binding of bpz with different metals as Ag(I), Co(II), Ru(II), Pt(II), Pd(II) and Cu(II) show different coordination modes in comparing with bpym. For example, iron(II) compound,  $[\text{Fe}(\text{bpz})_3](\text{ClO}_4)_2 \cdot \text{H}_2\text{O}$ , was synthesized based on the studying and simulation the bpym complexes. The structural and magnetic characterization of  $[\text{Fe}(\text{bpz})_3](\text{ClO}_4)_2 \cdot \text{H}_2\text{O}$  compound displays the strong ligand field character of the bpz ligand toward iron(II) in line with what it was known for the related bpym ligand. In a near future, further efforts will be put to produce different homo and hetero-metallic bpz-containing metal compounds according to work that associated to bpym ligand. Ruthenium(II) complex  $[\text{RuII}(\text{bpz})_3]^{2+}$  was first reported in 1980 [24], its apparently favorable photoredox properties when compared with  $[\text{RuII}(\text{bpy})_3]^{2+}$  indicating substantial

promise. The scheme 1.4 below clarified the structure of 2,2'-bipyrimidine ligand (a) and 2,2'-bipyrazine ligand (b). [138(h), 152]



**Scheme 1.4** 2,2'-bipyrimidine ligand (a) and 2,2'-bipyrazine ligand (b). [138(h)]

The choosing of 2,2'-bipyrazine (bpz) ligand with metal complexes to utilize in different systems returns to its appropriate photophysical properties as long excited-state lifetimes and high luminescent efficiencies. In comparison between Ru-bpz complex with other Ru complexes as Ru-bpy complex is slightly higher in energy and the lifetime of the emissive state is slightly longer in water. [138(a), 153]

In addition, bpz could bind ruthenium to form complexes in which that contribute to improve or modify their properties. For instance, studies proved that Ru(bpz)<sub>3</sub>PF<sub>6</sub> complex is considered as a powerful photooxidant in which used for photo-redox transformations that produced because of oxidation process. [154(a-b), 155(a)]

Also, Ru complexes that has at least two  $\pi$ -deficient ligands as 2,2'-bipyrazine has oxidized or triggered with DNA through irradiation. [156, 157] In more details, the existing of 2,2'-bipyrazine, which is considered as an electron-deficient ligand, enables Ru complexes to photodamage DNA via direct electron abstraction [158] The result of study [Ru(bpz)<sub>3</sub>]<sup>2+</sup> complex, which Ru metal binds with tris 2,2'-bipyrazine ligand, showed that it is the most effective photo-oxidant.[159] The using of Cu/Zn SOD improved the photoreactivity of Ru(bpz)<sub>3</sub> toward DNA and that contributes to increase the DNA damage. The development of photo adduct formation probably returns to electron transfer from the enzyme to the excited Ru(bpz)<sub>3</sub>, referring to that an original electron removes from a metallo-protein to a poly-azaaromatic ruthenium complex. [160]

Likewise, 2,2'-bipyrazine's behavior in reactions is explained in terms allylic substitution and rearrangement mechanisms, and so varies of derivatives of bpz substituents are formed. That permitted to expand the description and a comparison of the

coordination power of the inner and outer nitrogen atoms of the bipyrazine with other ligands. These future details help in studying and predicting the metal complexation capacity of a given nitrogen atom. [151]

Although different studies took up searching for heterocycles units to building metal coordination complexes. Nevertheless 2,2'-bipyrazine subunit firstly has ability to bind different metal ions, secondly, its physical properties (i.e.  $\lambda_{\text{max}}$ : 296 nm and a molar absorbance up to  $14000 \text{ M}^{-1} \cdot \text{cm}^{-1}$ ) indicated to many possibilities to design new ligands for strongly luminescent lanthanides complexes. As well as to that, bipyrazine (bpz) contains both inner nitrogen coordination centers and external pH dependent electroactive centers that will be of interest for the development of both photoactive and electroactive assemblies. [151]

2,2'-bipyrazine could improve the properties of its derivatives. For example, the light emitting properties of the 6,6'-dichloro-2,2'-bipyraizne compound is obtained and studied in terms of absorption and emission spectra. Scientists found that bipyrazine functionalize on increasing the spectroscopic data as it is an electron-with-drawing central core. [161] On one hand, researches lead to that formation of double-stranded or more complex organometallic helical complexes depends on the nature of the metal and ligands.  $\text{Cu}^{\text{I}}$  complexing is one of concerns that scientists focused on to understand the mysterious traits with respect saturated heterotopic ligands, in which it can separate into one didentate "bipyridine" segment and one didentate "bi-pyrazine" segment upon complexation to metal ions. This means that only the same number of four inner nitrogen atoms could be engaged in the coordination with  $\text{Cu}^{\text{I}}$  to form a helicate, which is a coordination complex and not a chelate. [162]

Pyrazine derivatives used in collector–generator (C–G) technique that used to offer a basis in order to classify restrictions in homogeneous water oxidation catalysis, arising from coordinative deactivation with adding organic buffer bases plus competitive oxidation of the added base. [163]

There are some reports showed a new way to synthesize the coordination compounds with oligomeric or infinite metal chains by using aromatic ligands as bpz. The result of synthesis of  $[\text{HgX}_2(\text{bpyz})]_n(3\text{-Cl,X)Cl;3\text{-Br,X)Br}$ ; (bpyz) 2,2'-bipyrazine),

clarified that  $\text{Hg}_2\text{X}_2$  bridges is ubiquitous in the structural chemistry of mercury halides, the halide alone is not sufficient to induce linearity. However, the formation of linear Hg chains are influenced by assistance of  $\pi$ - $\pi$  interactions between coordinated ligands and halide bridges. [164]

The divalent metal complexes with aromatic ligands such as 2,2'-bipyrazine are likely to be incorporated into the 2D cavities of host molecule for the balance of the charge and interactions with aromatic rings, the unusual incorporation of the metal-2,2'-bpz complexes into the cavities of the host construct coordination polymers. [165]

### **1.5 2,2'-dipyridylamine ligand**

2,2'-dipyridylamine (dpa)  $[(\text{C}_5\text{H}_4\text{N})_2\text{-NH}]$  is one of the most interesting ligand that have two heteroaromatic pyridine donors [166 -168] because of its behave as a versatile ligand ranging from monodentate, chelating bi-dentate to bridging tri-dentate. [167, 169] Where, the two ring-nitrogen atoms act as electron-pair donors in most complexes, and in other complexes bridging amino nitrogen has donor properties. Dpa and its anion has different configurations in its coordination; anti-anti (where anti refers to the relation of the pyridyl nitrogens to the amine hydrogen), syn-syn, the free dpa ligand has a dimeric structure in which two dpa molecules are linked by  $\text{N-H}\cdots\text{N}$  hydrogen bonds, each dpa group exhibiting the various configuration in which that clarified in figure 1.1 (a) and (b) [169 – 172]

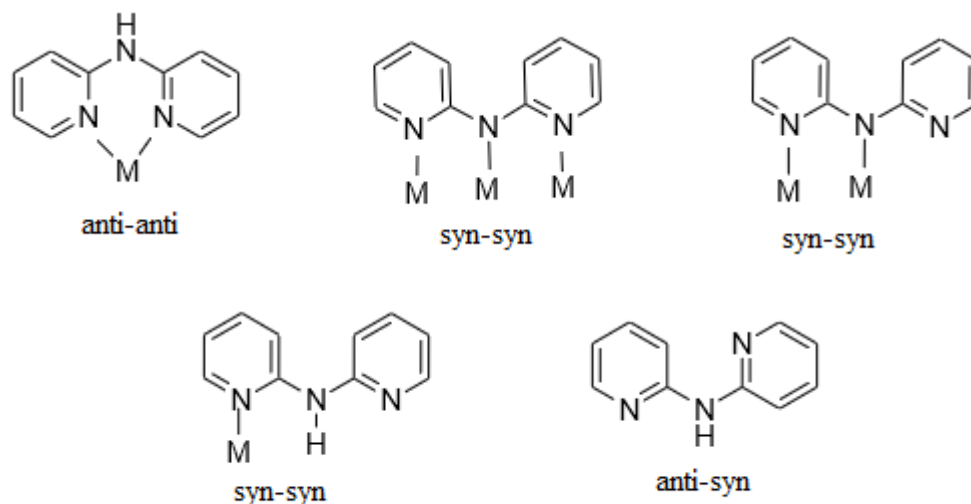


**Figure 1.1(a)** View of diverse configurations of 2,2'-dipyridylamine ligand (dpa).<sup>[171]</sup>

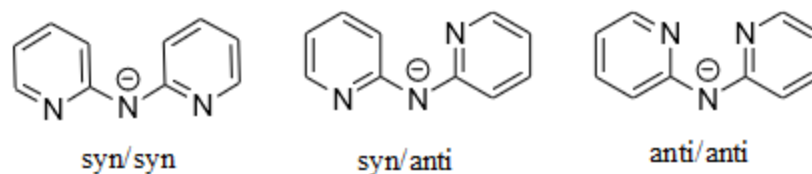


**Figure 1.1(b)** View the three conformational arrangement of deprotonated from 2,2'-dipyridylamine ligand.<sup>[171]</sup>

On one hand, dpa ligand has distinct merits. For example, hydrophobic interaction, or the aromatic ring stacking between the hetero atomic rings of dpa and the substituent group, as the amino acids, peptides and the DNA units. [166] Also, the pyridyl groups can rotate about the C(py)-N(amine) bond, which builds a certain degree of flexibility into the ligand system. That make it less rigid bidentate in terms of optical magnetic memory [173(a-b)]

In addition, dpa is considered an important chelate because of its ability to form hydrogen-bonded networks through the amine function group, [174, 167(a)] and to luminescence [173(c)] through  $\pi$ - $\pi^*$  transitions. [174] In other words, it have been shown as potential emitting compounds for electroluminescent (EL) devices. [173(b)]

Dpa and its derivatives play a vital role as high-performance group including molecular flexibility, and as strong chelating ability for transition metal ions. Therefore, their coordination chemistry received a great attention to be used for synthesis of new compounds in metal complexes. For example, Pd(II) and Pt(II) complexes of such dpa derivatives have been researched as potential anticancer agents because their structure is similar to cisplatin ions. While, the dpa with other metals as Ag(I), Zn(II), Cd(II) and Hg(II) have been researched as potential luminescent and molecular recognition materials, in which their potential applications in optoelectronic devices, fluorescent sensors and probe. [168, 173(d-e)]

However, dpa worked as a chelating ligand mostly formed mono- or dinuclear Zn<sup>II</sup> complexes, in which that support using them as building blocks in the construction of crystal structures represent in one-, two-, or three- dimensional structures through both intermolecular hydrogen bonds and  $\pi$ - $\pi$  interactions. [175, 173(f)]

Whereas, the dpa with metals as Mn(II), Cu(II), Co(II), Ni(II), Cr(II) and Ru(II) works as potential molecular wires and magnetic materials. [173(e), 168] Dpa, its derivatives, and their metal complexes also used in blue emitters in electroluminescent devices and used as function as chemical sensors for specific organic molecules, and as building blocks for nano engineering. [176, 176(a)]

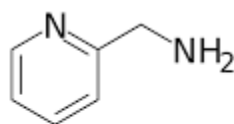
In addition, dpa is preferred to use as ligand in comparison with 2,2'-bipyridine, because the bridging nitrogen atoms in dpa is attainable to control the electronic, and steric characteristics of dpa-based ligands. Also, nitrogen atom is as a critical point for associate catalysts or for the design of task specific ligands. Beside to that, the presence of a bridging N-H group may display an important part in substrate orientation/activation, and product release through H-bonding. [177]

### **1.6 2-(Aminomethyl)pyridine ligand**

Pyridine based ligands have a significant role in the area of metal-complexes catalyzed asymmetric transformations, or to make a new generation of catalysts with high performances. Due to their ability to form complexes with various metals in different

oxidation states. Therefore, that contributes to obtain new active compounds in good yields and with high stereoselectivity. [178, 179]

2-(aminomethyl)pyridine or 2-picolyamine (ampy) ligand, is one of the most pyridine ligands common. It is commercially available, an unsymmetrical N,N'-bidentate, weakly basic chelating ligand; containing both aromatic pyridine (pyridyl group) and aliphatic amine donor function (flexible alkylamine side chain), as what shown in scheme 1.5. The ampy can behave as monodentate ligands, in which its nitrogen of the ring coordinate toward the metal ions. It can act also as a bridging ligand, and the high incidence of pharmacological activity among heteroaromatic amines. These characteristics encourage researchers to use it in diverse studies. Thus, different results clarified its successful coordination chemistry with different metals, one of them is the complexation of mercury to this ligand. [180 – 185]



**Scheme 1.5** View the structure of 2-(aminomethyl)pyridine or 2-picolyamine (ampy) ligand. <sup>[180]</sup>

The stable metal complexes are formed by Lewis acid/base interactions. [181] In addition, one of ruthenium(II) studies with ampy in combination with various phosphines show that ampy plays as a particularly high ligand acceleration effect in the transfer hydrogenation catalyzed by ruthenium(II) complexes. [182] Also, ampy is an asymmetrical ligand which usually coordinates as chelating bidentate, forming five member rings. [185(c), 186]

On one hand, ampy has different uses. One of them is used in trying to improve the silica gel plate; owing to its ability to attach onto a silica gel surface and so an easily adsorbing metal ions from water. [187] Second, it is used in the chemically modified cellulose, in which it deals as pendant function chain, in which a covalently bound to the polymeric framework. That adding support material to apply in the cations removal from aqueous solution in a heterogeneous system. [188] At least, ampy introduce a vital electronic tuning property. [189]

At the consequence, ampy and its derivatives are usually utilized in several ways. First, it is used as synthetic intermediates to obtain novel compound in chemical synthesis. Second, it is applied as ligands in coordination chemistry; due to existing of flexible alkylamine side chain and so that support its ability to interact with a number of metals ions. For instance, the  $[\text{Cu}(\text{di-(2-picolyl)amine})(\text{NO}_3)_2]$  complex, has distorted square-pyramidal geometry, where Cu(II) center around by three nitrogen atoms of di-(2-picolyl)amine ligand with nitrate anions via their two oxygen atoms. [190]

Third is that they have various applications in different fields, such as the chromatographic separation of the metallic ions, antibacterial, antifungal magnetism properties. 2-(aminomethyl pyridine) $\text{SbI}_5$ , for example, is an ideal material for a lead-free organic–inorganic hybrid photocatalyst, as its showing a ferroelectric property. [183, 191, 192] Also, chelating resins with functional groups of 2-aminomethylpyridine was applied to remove copper from simulated nickel electrolyte. [193, 194]

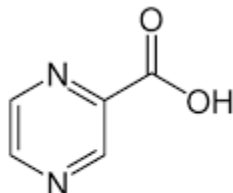
Addition to that, one of experimental observations showed that bis(2-picolyl)amine  $\text{Cu}(\text{Cl})_2$  complex active as anticancer, in which it has an ability to cleave the genomic DNA and so it is easily solubilized in water. These properties make complex promising as anticancer drug. [195] Also, studies notice that the combination of the 2-picolylamine and 1,1-cyclobutanedicarboxylate chelate ligands on the square-planar Pd(II)center displays unique properties for the evolution of antitumor drugs. [189]

### **1.7 pyrazine-2-carboxylate ligand**

The studies on ligands that containing heterocyclic carboxylic acids derived from pyrazine, and their complexation exposes an interesting trend. Due to their varied properties, including bonding, electrochemical, spectroscopic, thermal, magnetic behavior, catalytic and photocatalytic activities. [196, 197]

Pyrazine-2-carboxylic acid (pcaH) and its anion pyrazine-2-carboxylate or 2-pyrazinecarboxylate (pca) is one of pyrazine derivatives (scheme 1.6). It combines two rich donor groups in the form of ring two nitrogen atoms and the two carboxylic oxygen atoms. [198, 199] The integration of both functions support the abilities of different complexes and polymers, thus, high-dimensional heterometallic frameworks are made. [198, 201(a-b)] For example, creating of monomeric components, forming of heteromeric complexes

like bi-metallic, multi-valent organic–inorganic hybrid substances with diverse divalent ions and 3d transition metal atoms. [198 – 202]



**Scheme 1.6** View the structure of pyrazine-2-carboxylic acid (pcaH).<sup>[198]</sup>

In addition, pca does not only act as monodentate ligand through a carboxylate oxygen, but also it is considered as one of multidentate N-/O-donor [203] used as linking in building coordination polymers. Meaning that, pca has ability to link metal ions into polymeric compounds. [199, 201(c), 204, 205] and so different supramolecular architectures formed with different magnetic properties. [199, 205, 206] That's because of its dual functionality can react as donor atoms, potent to participate in strong coordinative bonds, oriented in versatile directions. Beside to the oxygen and the nitrogen atoms role in hydrogen-bonding acceptors. [198, 201(a, d), 207] In short, pca is able to react as potential bridging or chelating ligand producing extended metal-organic networks. [197, 198, 208, 209]

On one hand, pca has proved to be a multi-using ligand. [205] The variety usages of pca is returned to the arrangement of nitrogen and oxygen atoms enables the ligand to occupy in different binding modes, which is clarified in figure 1.2 [198, 201(c), 210] In phase (I), the reason for utilizing of pca as bidentate chelating is that the oxygen atom of carboxylate group and neighboring pyrazine nitrogen coordinate to metal ion. [199, 205, 210]

However, phase (II) clarified that pca can be act as a tridentate bridging ligand through bidentate/N-monodentate bridge, where metal ion (M') links with the other nitrogen of pyrazine ring, whereas phase (III) exhibited another coordination mode which is that pca acted as bidentate/O-monodentate bridge, the metal ion joins with the second oxygen of the carboxylate group, in phase (IV) pca employed as tetradentate ligand through bidentate/O,N-monodentate bridge. At least, in phase (V) pca plays as N-monodentate

terminal pcaH ligand, where the metal ion binds with the other nitrogen atom of pyrazine without needing to deprotonate the carboxylic group. [210, 211]

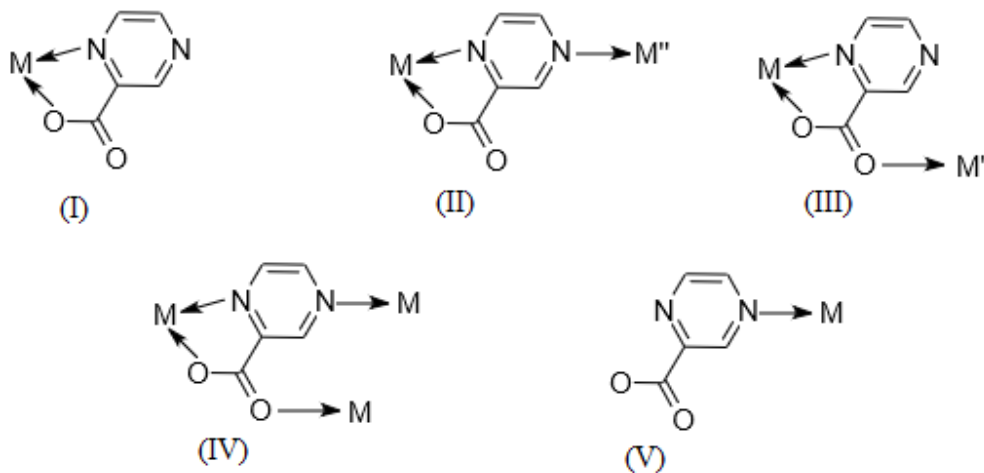


**Figure 1.2** pca ligand has various coordination modes. (I) bidentate terminal. (II) bidentate/N-monodentate bridge. (III) bidentate/O-monodentate bridge. (IV) bidentate/O,N-monodentate bridge. (V) N-monodentate terminal pcaH ligand. [210-211]

On other perspective, not only pyrazine-2-carboxylate offered diverse coordination nodes, but also its substituted derivatives have proven multipurpose for synthesis of new framework structures. Due to their ability to involve many coordination modes. Meaning that, the ability of pca substituted derivatives resulted in construction a stable metal-containing building blocks, in which that facilitate the coordinating with other metal centers. Therefore, many mixed metal coordination polymers are developed, whose bridging roles are summarized in figure 1.3 [198]

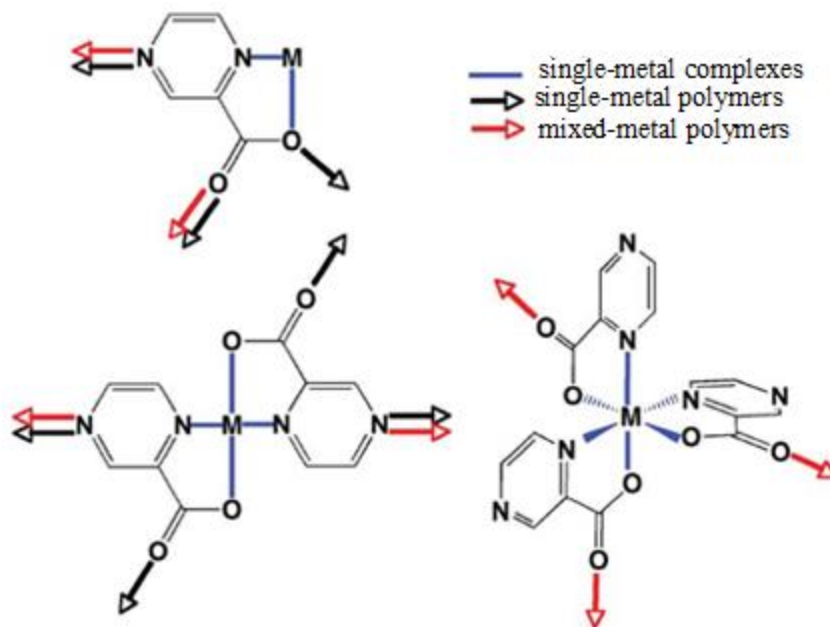


**Figure 1.3** View different coordination modes of pca-metal complexes and polymers. <sup>[198]</sup>

Pyrazine-2-carboxylate and its derivatives show biological characteristics through antimicrobial and antifungal. [197, 212] Consequently, many searches used it as a ligand; in trying to mimic the coordination environment of the metal site, like Mn in manganese enzymes owing to its biological significance. [211] In addition to that, pca also have ability to build many of mixed-metal framework structures, because of their facility to bind in different coordination modes. [213] As a result, these complexes are useful in different applications as functional, magnetic materials and gas storage; because of their diversity physical properties, for instance, catalytic activity, microporosity, electrical conductivity, non-linear optical activity. [214(a-b), 215, 216]

Copper(II) complexes is an example of multi compounds that show different coordination modes, when pyrazine-2-carboxylate used as ligand, since molecular chains consisting of Cu(II) coordinated by two ligand molecules via their N, O bonding moiety. [217] Furthermore, other studies predicted to favor a stable five-member ring with Cu(II) ions to create diverse coordination environments for the two metal ions connected through the bridge. [201(c)]

## **1.8 The role of mixed ligands in producing of new complexes**

Mixed ligand complexes are defined as that their metal ion is linked with at least two different types of ligands. Their ability of linking with many ligands lead to increases chances of variation in properties expected for the complex. The preparation and characterization of mixed ligand complexes is earning importance day by day. The increased interest in area of this research has prompted many researchers to get engaged in this field. In recent years many publications are dedicated to synthesis and characterization of mixed ligand complexes. [218(a-b), 219] Mixed ligands have a vital role in many chemical and biological systems as water softening, ion exchange resin. Numerous of these metal complexes displayed good biological activity against pathogenic microorganisms. [219]

In addition to that, the importance of mixed ligand complexes have different perspectives. They are considered as the most general form of the presence of the elements in a solution. And studies of formation them facilitate the evaluation the characteristics of intermediate and final forms of the complexes, thus, understanding the mechanism and kinetics of reactions. Also, there are certain property of elements are more notable in mixed ligand complexes, as well as physical phenomena accompanying the process of their formation. That expand the improvement of methods for determination, separation and concentration of element. [220]

The structural diversity of mixed ligands does not only limit in having a significant role in coordination chemistry, but also that lead to expand their application [221]. They are known to be attention in multi-areas as biological, clinical, analytical, magneto chemistry, photochemistry, electronic spectra, industrial, and flexidentate behavior of polydentate ligands, spectrochemical equilibrium. Adding to that, they have critical roles in catalysis and organic synthesis. [218(a, c), 222] For example, nickel(II) is one of metallic ions that most widely studied for the synthesis of mixed ligand complexes. Because it formed low molecular weight complexes that are proved to be more efficient against many diseases. [218(c)]

In more details, there are different examples that appear the important role of mixed ligands in numerous chemical and biological systems electroplating, dyeing, antioxidant,

[219, 223] photosynthesis in plants, removal of undesirable and harmful metals from living organisms. [223] Also, they displayed good biological activity [224] against pathogenic microorganisms, [219] antimicrobial, antiviral, anticonvulsant, anticancer, anti-mycobacterial, antimalarial, herbicidal and anti-inflammatory. [218(a), 225] The antibacterial and anti-fungal properties of a many of copper(II) complexes have been estimated against a number of pathogenic bacteria and fungi. [225]

Mixed ligand complexes used as therapeutic or tumor preserving agent in different medical and cosmetic field. [226] Their biological activates based on two factors: type of metal ion and nature of ligand. [227] Mixed-ligand copper(II) complexes, for example, have been found as excellent anticancer agents because of their effective DNA binding/cleaving ability and has a significance cytotoxic toward cancer cells. [228, 229] Also, they show antimicrobial activities against bacteria, yeast, and fungi. [230] For example, although Cu(II) mixed-ligand that contain 2,2-bipyridine and other bidentate ligand used as antineoplastic agents, [231] they acted as bactericidal agent and bacteriostatic toward many gram positive bacteria . [231(b)]

Sometimes metal complexes of ligands that have biologically important more effective than free ligands. Mixed ligand complexes show a significant role in biological chemistry, for this reason that the mixed chelation occurs generally in biological fluids as many of potential ligands are probable to compete for metal ions in vivo. These formed specific structures and have been involved in the storage and carry of active substances through membranes. [218(d), 223, 232] On other view, in many cases in which enzymes are known to be activated by metal ions. [223, 233, 234(a-c), 235]

For example, glycine amino acid presents in vary mixed-metal ligand compounds, where its role is to act like bidentate ligand coordinating with octahedral geometry for metal chelates, amino acids have special significance, and they considered as cornerstones of living organisms. [233, 234(b)]

At least, in many cases, the metal complexes of drugs are more active than the parent compound and they used in fighting microbial infections, antibacterial, anticancer, antifungal, and antimalarial activities. [218(a), 234(a)] Mixed ligand compounds seem that

have related in biological fluids, form particular structures and appear themselves as enzyme-metal ion-substrate complexes. [236]

In this work we synthesized simple compounds as started materials to construction of larger aggregates complexes. In addition, we report the synthesis, properties and crystal structures of mononuclear copper(II) complexes in order to better understand some aspects of different molecular topologies, and we report the synthesis, properties and crystal structure of mononuclear nickel(II) complex.

## **1.9 Literature review**

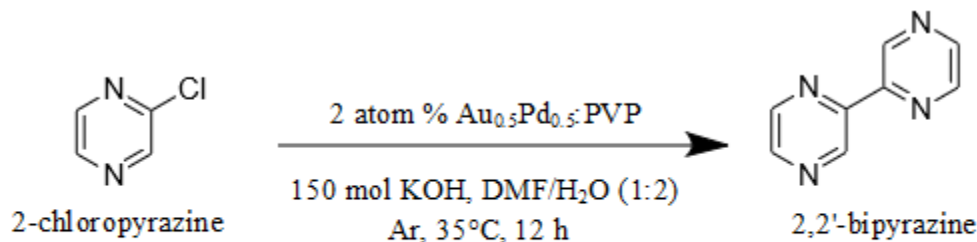
The synthesis of the coordination compounds focused on specific metals as platinum, palladium and rhenium with common ligands like 2,2'-bipyridine and 2,2'-bipyrimidine. However, few searches turn to examine the synthesis of metal complexes with 2,2'-bipyrazine ligand. As a results, the attentions today start to study the synthesis of complex using 2,2'-bipyrazine ligand with various metals as nickel(II) and copper(II) due to their important properties that utilizing in different applications as biological studies, solar energy and transition metals catalysts, etc.

### **1.9.1 Synthesis of 2,2'-bipyrazine ligand**

The synthesis of 2,2'-bipyrazine (bpz) started in 1967 by J. J. Lafferty and F. H. Cas, where their way was using pyrolysis of the copper(II) salt of pyrazine-2-carboxylic acid. Pyrolysis of the salt proceed at atmospheric pressure in short-way resulting in 7% of bpz crystallizing from hexane. [237] On other way, R. J. Crutchley and A. B. P. Lever in 1982 reported that their method in the preparation of bpz is simplified; due to generating an improvement yield without decreasing the purity of the product. Their method began with Bis(2-pyrazinecarboxylato)copper(II) in Pyrex boat was placed into a Pyrex tube, in which it exposed to heat under nitrogen atmosphere with a Meker burner leading to pyrolysis of the copper complex. The chloroform is used to wash the produced bipyrazine, and then it underwent to recrystallize using toluene resulting in 21% of bpz. [238]

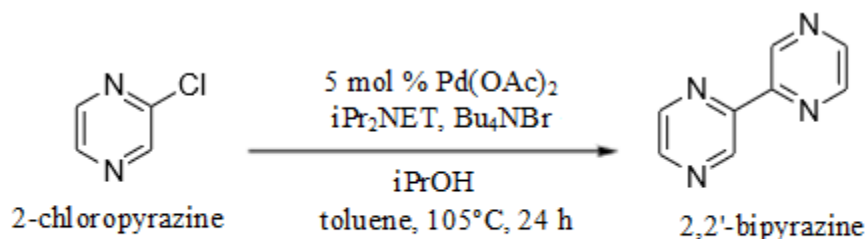
By the time, R. Dhital et al, in 2013 were their protocol led to produce about 94% of bpz, where 2-chloropyrazine used as starting material catalyzed by poly(N-

vinylpyrrolidone)(PVP)-stabilized bimetallic Au–Pd alloy nanoclusters (NCs) under ambient conditions (scheme 1.7). [239]



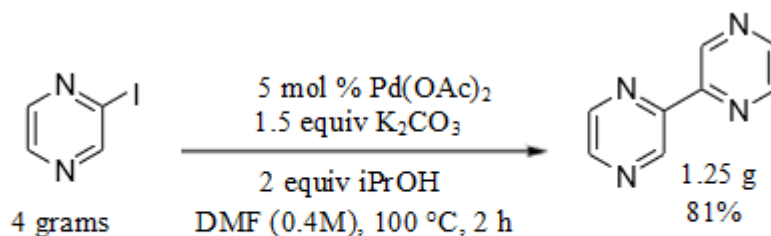
**Scheme 1.7** View the synthesis of 2,2'-bipyrazine ligand, using 2-chloropyrazine as starting material. [239]

Later on, D. Schultz et al, in 2015 mentioned that there are diverse methods for the synthesis of bpz. The most general one is that comprised transition metal-catalyzed reductive homocouplings of halopyrazine electrophile. Plé reported that 40% yield of bpz is get due to using Pd-catalyzed procedure (scheme 1.8). [138(d)]



**Scheme 1.8** View of that Pd-catalyzed reductive of 2-chloropyrazine to produce 40% of bpz. [138(d)]

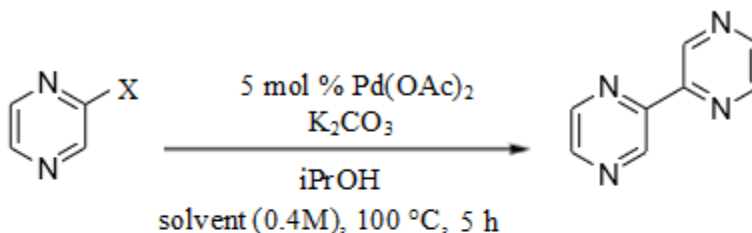
On one hand, D. Schultz et al, also reported that the exposing of 2-iodopyrazine to optimized conditions lead to produce about 81% yield of bpz (scheme 1.9). [138(d)]



**Scheme 1.9** View of that exposing of 2-iodopyrazine to optimized conditions to form 81% of bpz. [138(d)]

Consequently, D. Schultz et al, summarized their methodologies in producing bpz utilizing 2-halopyrazines as a substrate. Poor yields of bpz resulted according to use organic or inorganic bases (table 1.1, entries 1 and 2). Then, it replaced with more reactive aryl iodides beside to applying several solvents in Pd-catalyzed cross coupling reactions. As a result, DMF solvent offered the highest yields of bpz (table 1.1, entries 3 – 5). [138(d)]

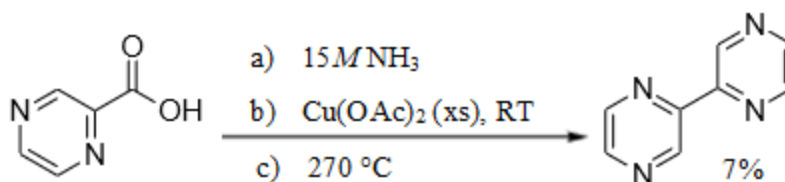
**Table 1.1** View of optimization of Pd-catalyzed reductive homocoupling of 2-halopyrazines<sup>[138(d)]</sup>



entry	X	solvent	equiv iPrOH	yield
1 <sup>a</sup>	Cl	toluene	3	3%
2	Cl	toluene	3	3%
3	I	toluene	3	4%
4	I	dioxane	3	10%
5	I	DMF	3	85%

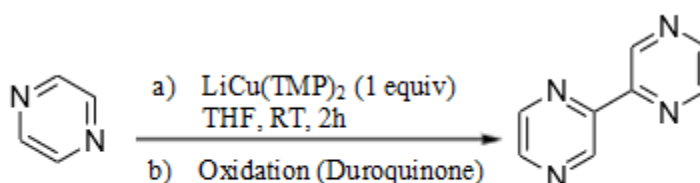
<sup>a</sup>Reaction conducted using 1.5 equiv  $i\text{Pr}_2\text{NEt}$  instead of  $\text{K}_2\text{CO}_3$

On one hand, M. Graaf et al, in 2015 reviewed that the protocol of Lafferty and coworkers in producing bpz needs an elevated temperature and using Cu-based aryl – aryl coupling reaction to generate 7% yield of bpz ligand (scheme 1.10). [138(g)] M. Graaf et al, also reported that Lipshutz and coworkers strategy to produce bpz is using a mixed copper catalyst system, which made from an aryl lithium. It formed by altering metal halogen with the corresponding aryl halide. However, this strategy failed to prove its feasibility to manufacture bpz from pyrazine halide. [138(g)]



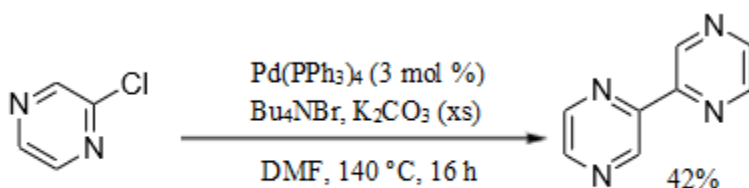
**Scheme 1.10** View of synthesis of 2,2'-bipyrazine ligand by starting with pyrazinecarboxylic acid. [138(g)]

In addition, Graaf et al, pointed to that raising up the percent yield of bpz to 76% is succeed due to using cuprate, stronger oxidant and accelerating the period of sonication/oxidation step to 60 minutes (scheme 1.11). [138(g)]



**Scheme 1.11** View of conditions that used to raise the yield % of 2,2'-bipyrazine ligand. [138(g)]

M. Graaf et al, in 2015 reported about Yoon and coworkers that their protocol leads to produce 42% of bpz (scheme 1.12). [138(g)]



**Scheme 1.12** View of conditions that used to get 42% yield of 2,2'-bipyrazine ligand [138(g)]

Afterward, Kom Reddy et al, in 2019 also noted that bpz firstly was produced by Lafferty and Case, applying a copper catalyzed solid-state method. As well as its limitation is that needs high temperatures (270°C) and low yields of bpz resulted (7%). Kom Reddy et al, also reported that Yoon and co-workers showed the producing of bpz ligand is done by palladium catalysis using conventional methods. [138(a)]

### 1.9.2 Copper complexes

W. Qing et al, in 2003 were prepared  $\text{Cu}(\text{AMP})_2(\text{NO}_3)_2$ , using copper nitrate ( $\text{Cu}(\text{NO}_3)_2$ ) with 2-amino-4,6-dimethoxypyrimidine (AMP) in the mole ratio of 1:2 via reflux in alcohol. The characterization of its structure were investigated by IR, XPS, and  $^1\text{H}$  NMR. The analysis explained that the ligand in the complex is bidentate, according to both nitrogens of amino group and of pyrimidine are coordinated toward  $\text{Cu}(\text{II})$  metal. [240]

Meanwhile, J. Carranza et al, in 2004 were made copper(II) complex of formula  $[\text{Cu}_2(\text{dpp})_2(\text{H}_2\text{O})_2(\text{NO}_3)_2(\text{ox})].4\text{H}_2\text{O}$ , where  $\text{dpp} = 2,3\text{-bis}(2\text{-pyridyl})\text{pyrazine}$ ;  $\text{ox} = \text{oxalate}$ , and X-ray diffraction was used to determine the structure of complex. The results appeared the significance of structural knowledge is for understanding the magnetic properties. The compound is constructed from of symmetrical oxalato-bridged copper(II) dinuclear complex and water of hydration. Ox and dpp implemented as bis-bidentate and bidentate ligands, respectively. The geometry of complex is elongated octahedral, where nitrogen atom of heterocyclic and oxygen of oxalate occupied the equatorial positions. Whilst, the water molecule located in one axial position and the oxygen of nitrate complete the coordination sphere. Antiferromagnetic interactions between the copper(II) atoms were detected between the copper(II) atoms bridging oxalato, in compatible with the  $\sigma$  in-plane as what shown in figure 1.4 [241]

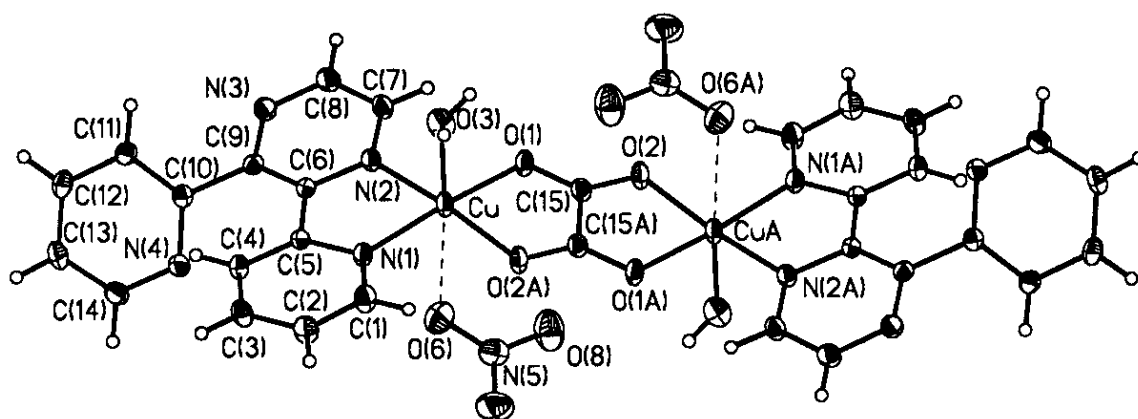


**Figure 1.4** View of the complex unit  $[\text{Cu}_2(\text{dpp})_2(\text{H}_2\text{O})_2(\text{NO}_3)_2(\text{ox})].4\text{H}_2\text{O}$  with the atomic numbering. [241]

Moreover, J. Carranza and coworkers were also synthesized another copper complex in which its formula is  $[\text{Cu}(\text{bpz})(\text{ox})]_n$ , where bpz = 2,2'-biprazine and ox = oxalate. The structure of the complex was detected by X-ray diffraction. The building blocks of the complex are neutral units. The copper atoms have elongated octahedral geometry. Oxalate and 2,2'-biprazine both are bidentate ligands and surround the copper(II) atom, where the two nitrogen atoms of heterocyclic and two oxalate-oxygen atoms locate in the equatorial positions. Nevertheless, the creation of a series with double out-of-plane oxalato bridges as a result of the existing of two weak axial connections oxygen of oxalate. The magnetic susceptibility measurements identifies that there is weak antiferromagnetic interactions between the copper(II) atoms in agreement with the out-of-plane exchange pathways involved, figure 1.5 [241]

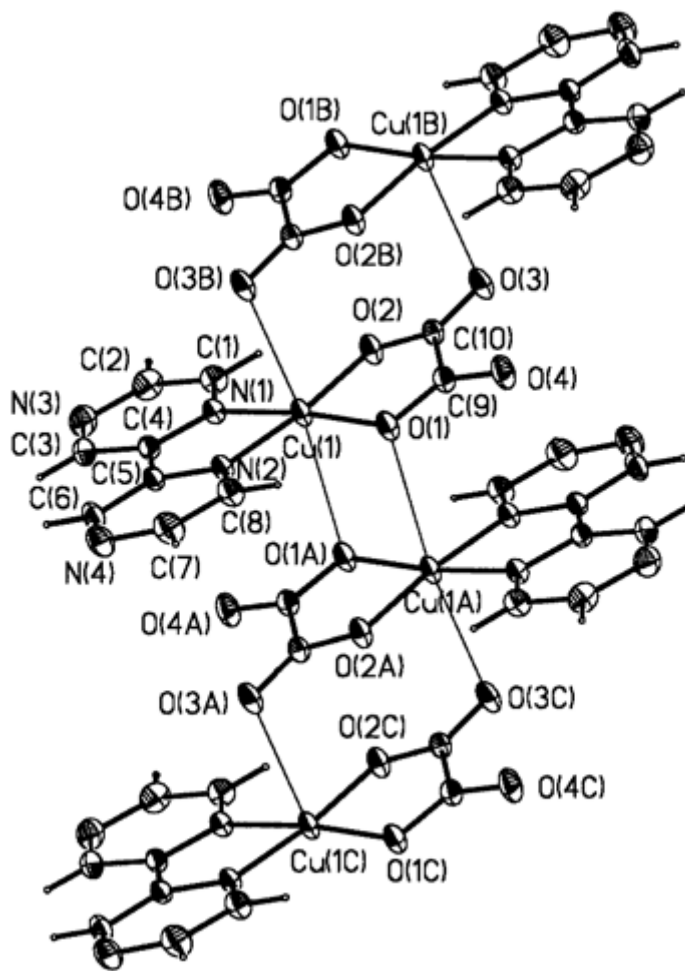


**Figure 1.5** View the section of the chain in  $[\text{Cu}(\text{bpz})(\text{ox})]_n$  with the atomic numbering.<sup>[241]</sup>

By the time, H. Wang et al, in 2006 were synthesized Cu(II) complex which is formulated  $[\text{Cu}(\text{dpa})_2(\text{dca})_2]$  where dpa = 2,2'-dipyridylamine and dca = sodium dicyanamide. X-ray crystallographic analyses showed that Cu(II) atom is an octahedral (CuN6) environment, where six nitrogen atoms (from two dpa and two dca) are coordinated toward it. The equatorial plane are occupied by two dpa the end-cap N atom of the two dca, respectively (N3, N3A, N4, N4A), while the axial plane are provided by two nitrogen atoms (N1, N1A) from two dpa, see the figure 1.6 [242]

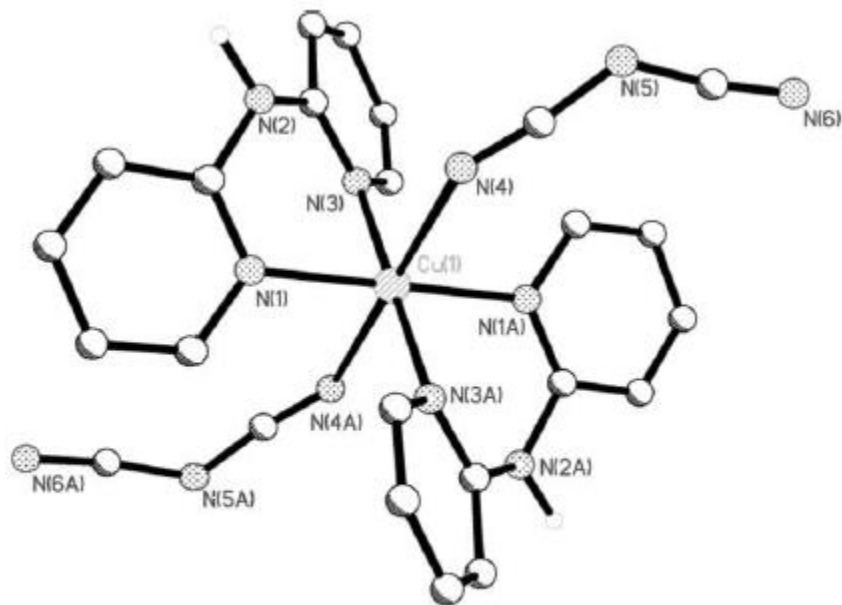


**Figure 1.6** View of X-ray crystal structure for  $[\text{Cu}(\text{dpa})_2(\text{dca})_2]$  showing the structure unit (pyridine rings of hydration not shown).<sup>[242]</sup>

The year later, P. Subramanian et al, in 2007 were prepared a ternary Cu(II) complex, which its formula is  $[\text{Cu}(\text{D,L-phe})(\text{bpy})] \cdot (\text{ClO}_4)$  (bpy = 2,2'-bipyridine, phen = 1,10-phenanthroline). The X-ray structural analysis assumed the helical structure for the complex. The outcome of the analysis showed that Cu(II) ions has a distorted square-pyramidal geometry. It formed from the pyridyl nitrogen atoms of the heterocyclic diamines and the  $\text{NH}_2$  and  $\text{CO}_2$  molecules of the amino acids (D-,L-phe). The fifth axial ligand consists of a carboxylate oxygen atom. On other side, the two helical of the complex which is resulting from the L- and D-phe have opposite chirality. Therefore, the crystalline sample is racemic, see the figure 1.7 [243]

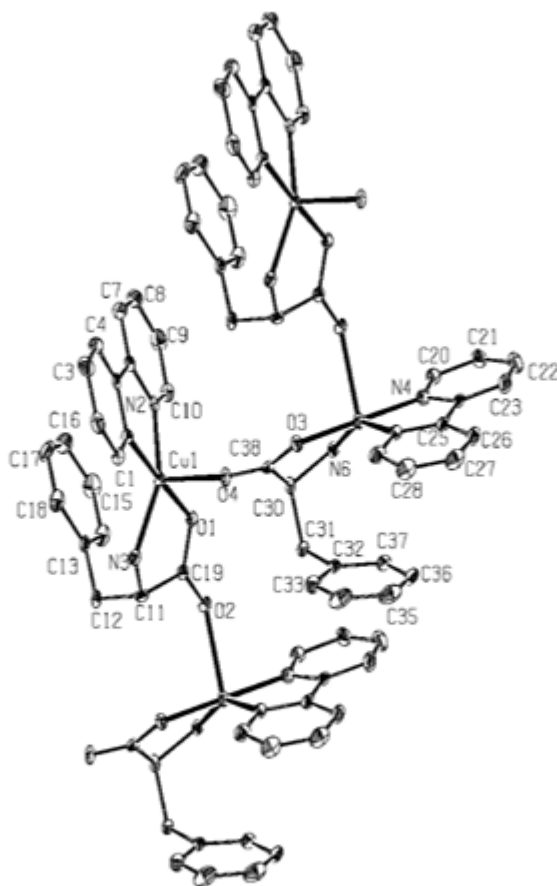


**Figure 1.7** View the X-ray crystal structure of [Cu(D,L-phe)(bpy)].(ClO<sub>4</sub>) complex. with showing the structure unit (pyridine rings of hydration not shown) <sup>[243]</sup>

Until that time, V. P. Singh, in 2008 were prepared Cu(II) complexes, formulation as [Cu(iinh)<sub>2</sub>(NO<sub>3</sub>)<sub>2</sub>] & [Cu(ibh)<sub>2</sub>(H<sub>2</sub>O)<sub>2</sub>](NO<sub>3</sub>)<sub>2</sub>, iinh = isopropanoneisonicotinoylhydrazone, and ibh = isopropanone benzoyl hydrazone, as what shown in figure 1.8. The description of compounds are done via different techniques like elemental analyses, molar conductances, dehydration studies, ESR, IR and electronic spectral studies. The electronic and ESR spectra clarified that two compounds have a six-coordinate tetragonally distorted octahedral geometry. Adding to that, ESR spectra indicated to [Cu(iinh)<sub>2</sub>(NO<sub>3</sub>)<sub>2</sub>] has an axial signals at 77K in DMSO solution. Whereas in the same conditions, ESR spectra of [Cu(ibh)<sub>2</sub>(H<sub>2</sub>O)<sub>2</sub>](NO<sub>3</sub>)<sub>2</sub> displays isotropic type. [244]

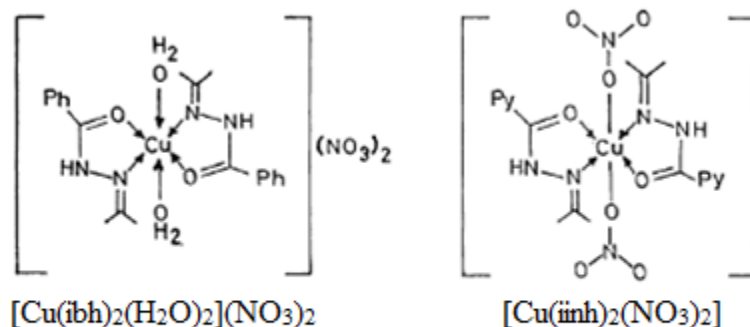


**Figure 1.8** View the structure of the compounds. [244]

At the same year, C. Yuste et al, in 2008 were synthesized, characterized structures and magnetic properties of  $[\text{Cu}(\text{bpy})(\text{tcm})_2]_n$ ,  $[\text{Cu}_4(\text{bpz})_4(\text{tcm})_8]$  tcm= tricyanomethanide, bpy = 2,2'-bipyridine, bpz = 2,2'-bipyrazine, see figure 1.9. The Cu(II) atoms of the  $[\text{Cu}(\text{bpy})(\text{tcm})_2]_n$  compound has six coordination with two nitrogen atoms of bpy ligands [N(1) and N(2)], and nitrile-nitrogen atoms of bridging tcm groups [N(4a), N(6), N(3) and N(8b)] building as an elongated octahedral surrounding. [245]

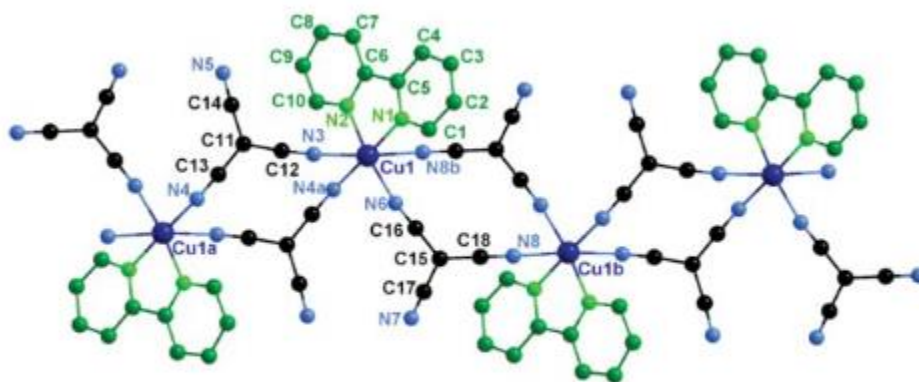


**Figure 1.9** View a section of neutral  $[\text{Cu}(\text{bpy})(\text{tcm})_2]_n$  chain with displaying the atomic numbering. [245]

Nevertheless, the  $[\text{Cu}_4(\text{bpz})_4(\text{tcm})_8]$  complex is built up of rectangular shape of discrete cyclic tetracopper(II), (2,2'-bipyrazine)copper(II) units at the corners, with single- and double- $\mu$ -1,5- tcm bridges alternating at the edges. The coordination of Cu(1) and Cu(2) atoms are noted by X- ray diffraction, as what clarified in figure 1.10. The analysis displayed that there are five and six coordinated copper atoms with Cu(1) has a distorted square pyramidal geometry and Cu(2) has an elongated octahedral geometry. The magnetic

studies show that  $[\text{Cu}(\text{bpy})(\text{tcm})_2]_n$  has weak ferromagnetic, while  $[\text{Cu}_4(\text{bpz})_4(\text{tcm})_8]$  has antiferromagnetic interactions. [245]

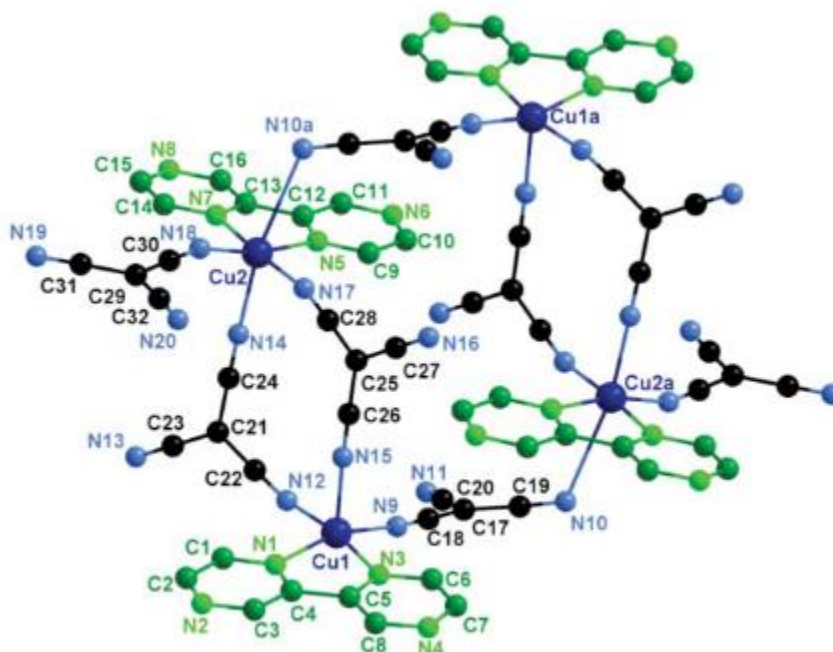


**Figure 1.10** View the tetranuclear  $[\text{Cu}(\text{bpz})_4(\text{tcm})_8]$  complex with showing the atom numbering. [245]

In the next year, K. N. Lazarou et al, in 2009 were prepared copper(II) complex which is expressed as  $[\text{Cu}_2(\text{HL})_2(\text{bpy})_2(\text{H}_2\text{O})_2](\text{ClO}_4)_2 \cdot 2\text{H}_2\text{O}$ , where HL is maleamic acid and bpy is 2,2'-bipyridine, as what shown in figure 1.11. Characteristic IR bands of the complexes are discussed in terms of the known structures and the coordination modes of the ligands. The structure of complex contains two copper(II) atoms bridged by the carboxylate groups of the two HL ligands. The copper atoms have five coordinated with chelating bpy and water molecules in which that completing the square pyramidal coordination. The amide group of the HL ligands is uncoordinated. Consequently, the coordination geometry of each metal is known as square pyramidal with the bridging carboxylate oxygen atoms. [246]

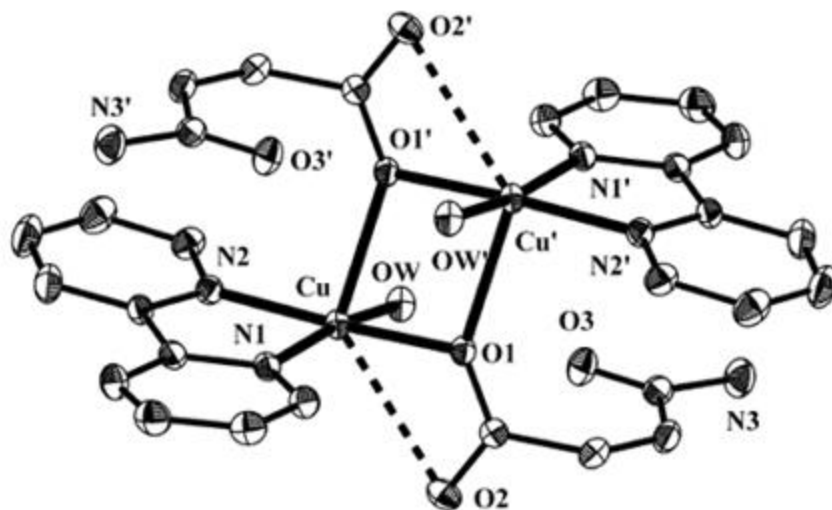


**Figure 1.11** View the structure of  $[\text{Cu}_2(\text{HL})_2(\text{bpy})_2(\text{H}_2\text{O})](\text{ClO}_4)_2 \cdot 2\text{H}_2\text{O}$  compound. [246]

Until that time, M.O. Agwara et al, in 2010 were prepared copper(II) mixed-ligand complex containing 1,10-phenanthroline (phen) and 2,2'-bipyridine (bpy) as ligands. It is formulated as  $[\text{Cu}(\text{bpy})(\text{phen})\text{H}_2\text{O}]_2\text{Cl}_2 \cdot 2\text{H}_2\text{O}$ . The synthesized complex is described by elemental, IR and visible spectroscopic analyses. The results showed that both ligands are coordinated toward copper(II) ion causing an octahedral complex. Moreover, antimicrobial studies discovered that the antimicrobial activity of the metal atoms raised on coordination to the ligands. Where copper complex has highest activity compared with others as Co and Zn complexes. That encouraged further studied to examine it for the treatment of infections which caused by organisms. [247]

At next year, M. P. Yutkin et al, in 2011 were prepared copper complexes which are formulated  $[\text{Cu}(\text{bpy})_2(\text{H}_2\text{O})_2](\text{NO}_3)_2 \cdot 4.5\text{C}_2\text{H}_5\text{OH}$  where bpy = 4,4'-bipyridyl. By slow evaporation of an aqueous alcoholic solution of copper nitrate, L-phenylalanine, and 4,4'-bipyridyl. The structure and component of the complex is characterized by using single crystal diffraction technique, XRD. The structure of  $[\text{Cu}(\text{bpy})_2(\text{H}_2\text{O})_2](\text{NO}_3)_2 \cdot 4.5\text{C}_2\text{H}_5\text{OH}$  constructs two types of crossing channels. In more details, the copper coordination links with two 4,4'-bipyridyl ligands via four nitrogen atoms and with water molecules via oxygen atoms. [248]

Later, A. Draksharapu et al, in 2015 were tested the interaction of Cu(II) polypyridyl complexes with st-DNA (Salmon testes DNA), one of them is

[Cu(bpy)(NO<sub>3</sub>)<sub>2</sub>], where bpy = 2,2'-bipyridine, see figure 1.12. It described by utilizing many means as elemental analysis, FTIR, EPR, Raman and resonance Raman. The results, for example spectroscopic data, detected that its interaction can characterized as groove binding. Meaning that, the complex is flexible in binding to DNA and so be the best catalyst DNA based asymmetric Diels-Alder reaction. While, the result of Roman spectroscopy appeared that nitrate ligands are moved by water solvent. [249]

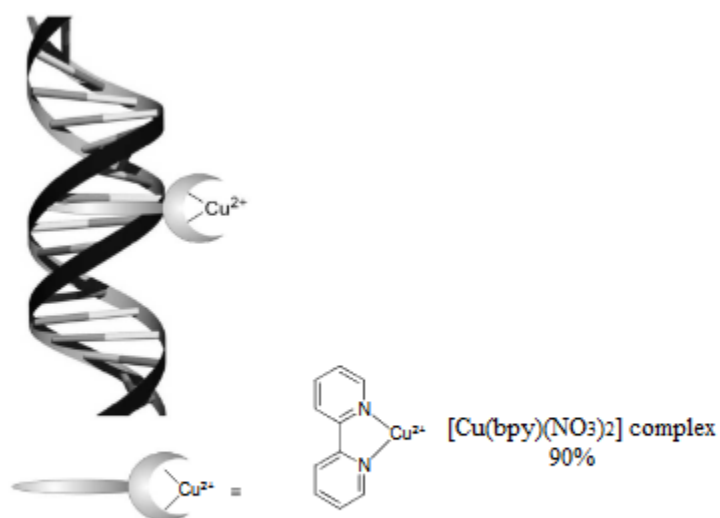


**Figure 1.12** View of [Cu(bpy)(NO<sub>3</sub>)<sub>2</sub>] complex that used as a hybrid catalyst by placing it in proximity to DNA via non covalent interactions.<sup>[249]</sup>

After couple years, J. H. Kwon et al, in 2014 were prepared [Cu(dpa)<sub>2</sub>(NO<sub>3</sub>)<sub>2</sub>] and [Cu(2,2'-bipyridine)<sub>2</sub>(NO<sub>3</sub>)]NO<sub>3</sub> where dpa = 2,2'-dipyridylamine. The complexes were studied due to determine their efficiency in oxidative DNA cleavage, utilizing electrophoresis and linear dichroism (LD). The results displayed that [Cu(2,2'-bipyridine)<sub>2</sub>(NO<sub>3</sub>)]NO<sub>3</sub> complex has the highest efficiency of DNA cleavage. [250]

At the same period, R. F. Brissos et al, in 2014 were synthesized copper(II) complex with different nuclearities which is worded as [Cu<sub>2</sub>(L4)(ClO<sub>4</sub>)(OH)(CH<sub>3</sub>OH)](ClO<sub>4</sub>), where L4 is 4-tert-butyl-2,6-bis-(quinoline-2-ylhydrazonomethyl)phenol, figure 1.13. It was determined by single-crystal X-ray diffraction. Cu1 is triply linked to Cu2 which displayed an octahedral geometry. The equatorial plane is established by the atoms N4, N6, O1 (from ligand L4), and the bridging hydroxide atom O2. The axial positions are employed

by a methanol molecule O3 and the oxygen atom O4 from the perchlorate anion that bridges Cu2 to Cu1. Adding to that, phenoxide and hydroxide bridges. The complex has an effective DNA-interacting activity, where it has been prepared to rise the DNA-oxidative-cleaving abilities of the corresponding copper systems. [251]

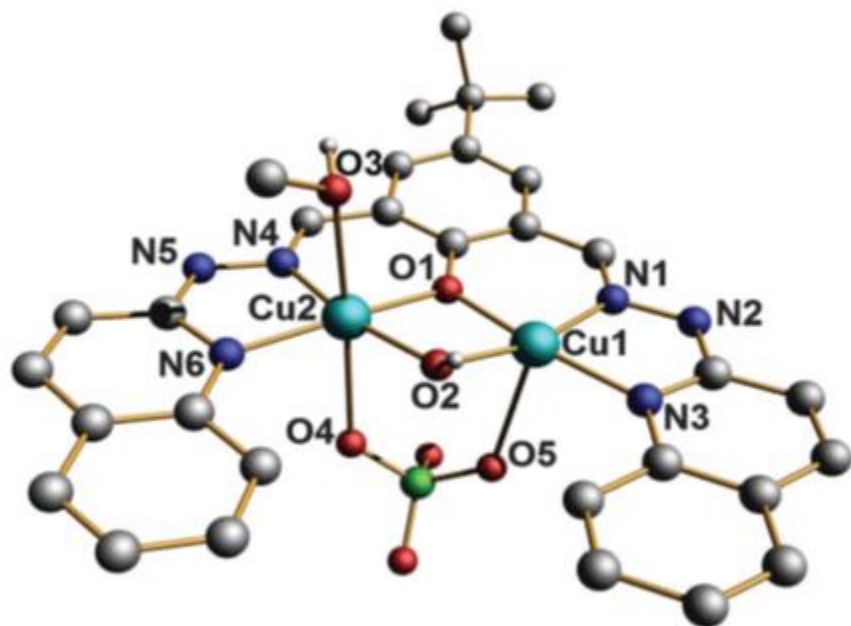


**Figure 1.13** View the structure of  $[\text{Cu}_2(\text{L4})(\text{ClO}_4)(\text{OH})(\text{CH}_3\text{OH})](\text{ClO}_4)$  complex. [251]

In addition to that, R. F Brissos and coworkers, in 2014 were prepared  $[\text{Cu}(\text{L2})\text{NO}_3]$  complex, where L2 is 2-tert-butyl-6-(quinoline-2-ylhydrazonomethyl)phenol, figure 1.14. The structure is revealed by using single-crystal X-ray diffraction. The coordination geometry around copper atom is nearly a square planar, where the coordination of copper is done by N, N, O atoms of ligand and O2 atom of the nitrate. The studies show that the metal of complex has an efficient DNA binders. [251]

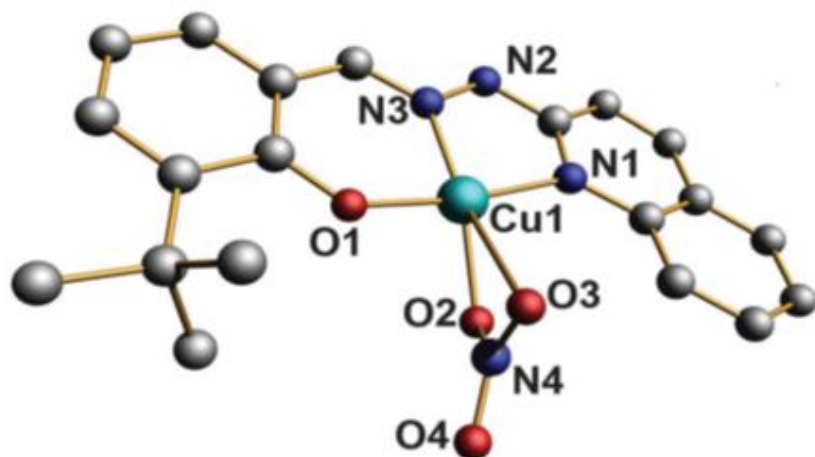


**Figure 1.14** View the structure of  $[\text{Cu}(\text{L}2)(\text{NO}_3)]$  complex, showing partial atom numbering. <sup>[251]</sup>

Also, in 2014 M. Puchoňová et al, were prepared different Cu(II) complexes in which its general formula is  $\text{Cu}(\text{XSal})_2(\text{ampy})$ , where  $\text{ampy} = 2\text{-aminomethylpyridine}$  and  $\text{XSal} = 3\text{-methylsalicylate}, 4\text{-methylsalicylate}$  or  $5\text{-methylsalicylate}$ . The supposing structure of the complexes are examined by elemental analysis and spectra data as EPR, electronic and infrared. The two nitrogen atoms of bidentate  $\text{ampy}$  contributed to coordinated the Cu(II) atom of all compounds as well as monodentate and/or highly asymmetrically chelating salicylate anions. Based on that analysis, the structures of the complexes could be similar to  $[\text{Cu}(\text{HCOO})_2(\text{ampy})]$ , or  $[\text{Cu}(\text{CH}_3\text{COO})_2(\text{ampy})]$  that are reported in the literature. [252]

Subsequently, M. M. Ibrahim et al, in 2017 were synthesized  $[\text{Cu}(\text{BPy})(\text{Gly})]\text{ClO}_4$ , where  $\text{Bpy} = \text{bipyridine}$  and  $\text{Gly} = \text{glycine}$  (fig. 1.15), and identified by elemental analysis, spectroscopic (FT-IR, UV-Vis and ESR), thermal analysis, and magnetic moment measurements. The structure of the complex is square planar geometry, in which that determined by single crystal X-ray diffraction. It offered four coordinated copper center with nitrogens of two bipyridyl and glycine, and oxygen of glycine. The antioxidant (*superoxide dismutase and catalase*) appeared that complex might be used as dual functional mimic enzyme to assist of reactive oxygen species (ROS) detoxification, both with regard to the superoxide radicals and the related peroxides. [253]

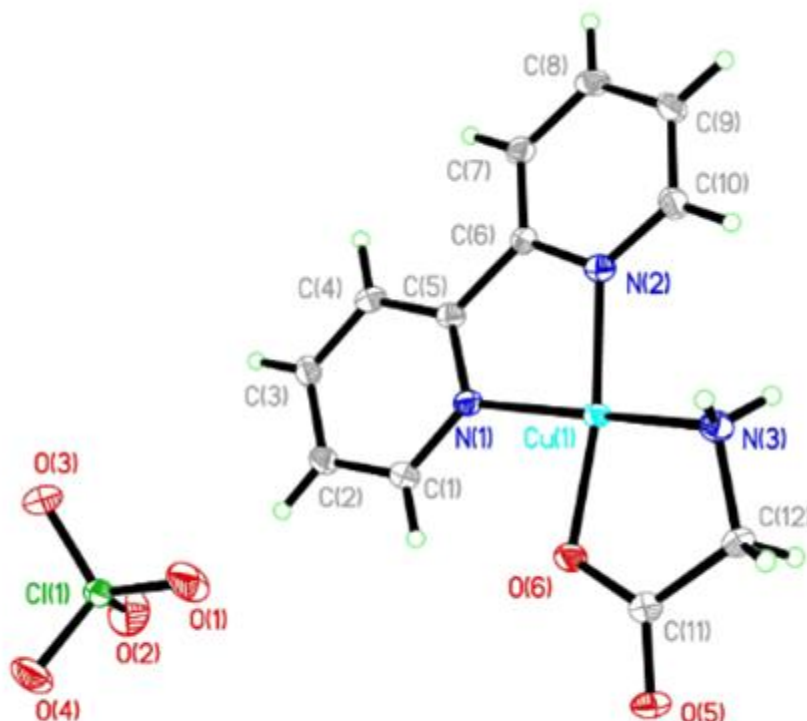


**Figure 1.15** View of X-ray structure for [Cu(BPy)(Gly)]ClO<sub>4</sub> complex, with showing the atomic numbering<sup>[253]</sup>

After year, C. E. Knapp et al, in 2018 was synthesized monomeric copper complexes of the type [Cu(NH<sub>2</sub>CH<sub>2</sub>CH(R)Y)<sub>2</sub>(NO<sub>3</sub>)<sub>2</sub>] (1, R=H, Y= NH<sub>2</sub>; 2, R=H, Y=OH; 3, R=Me, Y=OH) characterized by elemental analysis, mass spectrometry, infrared spectroscopy, thermal gravimetric analysis, and single crystal X-ray diffraction. They found that, the use of isolated copper coordination complexes provided a convenient approach to avoid the dissociation of the inks. Additionally, plasma assisted inkjet printing evidenced that compounds are an functional alternative for thermal sintering, see figure 1.16 a and figure 1.16 b [254]

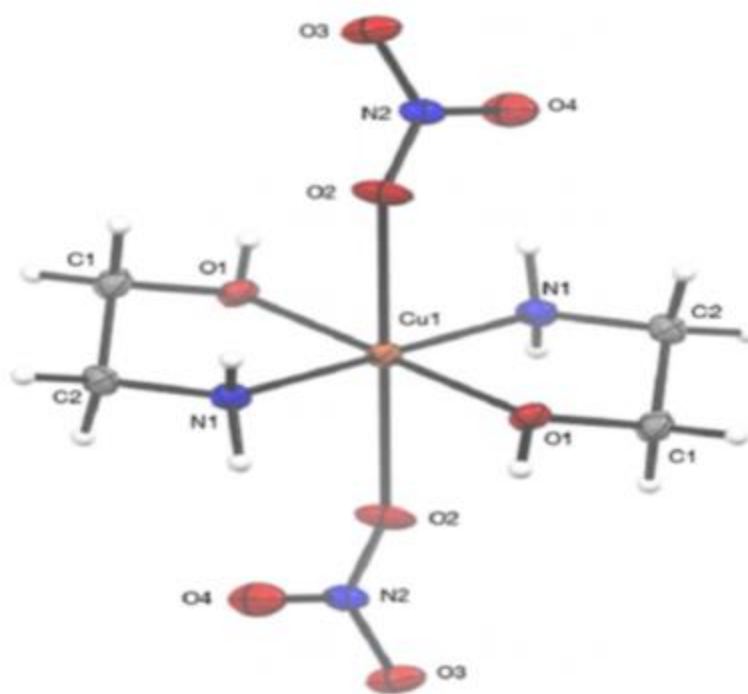


**Figure 1.16 a** View of the structure for  $[\text{Cu}(\text{NH}_2\text{CH}_2\text{CH}_2\text{OH})_2(\text{NO}_3)_2]$  complex. <sup>[254]</sup>

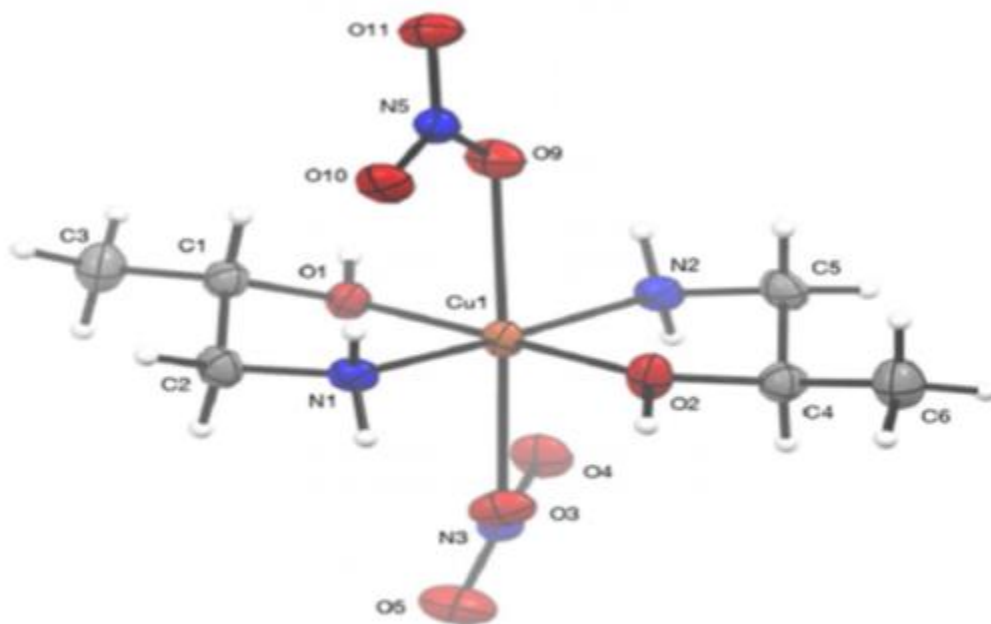


**Figure 1.16 b** View of the structure for  $[\text{Cu}(\text{NH}_2\text{CH}_2\text{CH}(\text{CH}_3)\text{OH})_2(\text{NO}_3)_2]$  complex. <sup>[254]</sup>

Furthermore, M. Mangoli et al, in 2020 was used 2-aminopyrimide with tartaric acid for synthesis of a mixed ligand complex of copper(II), in which it formula is  $\text{asm}(\text{C}_2\text{O}_4)\text{-bis}([\text{Cu}(\text{amp})(\text{NO}_3)(\text{H}_2\text{O})_2]\cdot\text{H}_2\text{O}$ . The characterization of complex studied according to different methods as elemental analyses, spectroscopic methods (IR, UV/Vis), thermal analysis and X-ray diffraction (XRD). Cu(II) atom of the complex has six coordination, where O,O'-bidentate oxalate ion, two water molecules and one nitrogen atom of 2-aminopyrimide are coordinated towered it. [255]

After that, M. L. Nisbet et al, in 2021 were made many copper complexes with different ligands, in which expressed as  $[\text{Cu}(\text{bpy})_2(\text{TaF}_6)_2]$  and  $[\text{Cu}(\text{bpy})_3][\text{TaF}_6]_2$  where  $\text{bpy} = 2,2'$ -bipyridine,  $\text{TaF}_6 =$  hexafluoridotantalate(V). Each copper atom of Cu(II)  $[\text{Cu}(\text{bpy})_2(\text{TaF}_6)_2]$  complex is coordinated by two bpy ligands in an equatorial plane, and by two  $\text{TaF}_6^-$  groups in an axial plane figure 1.17. [256]

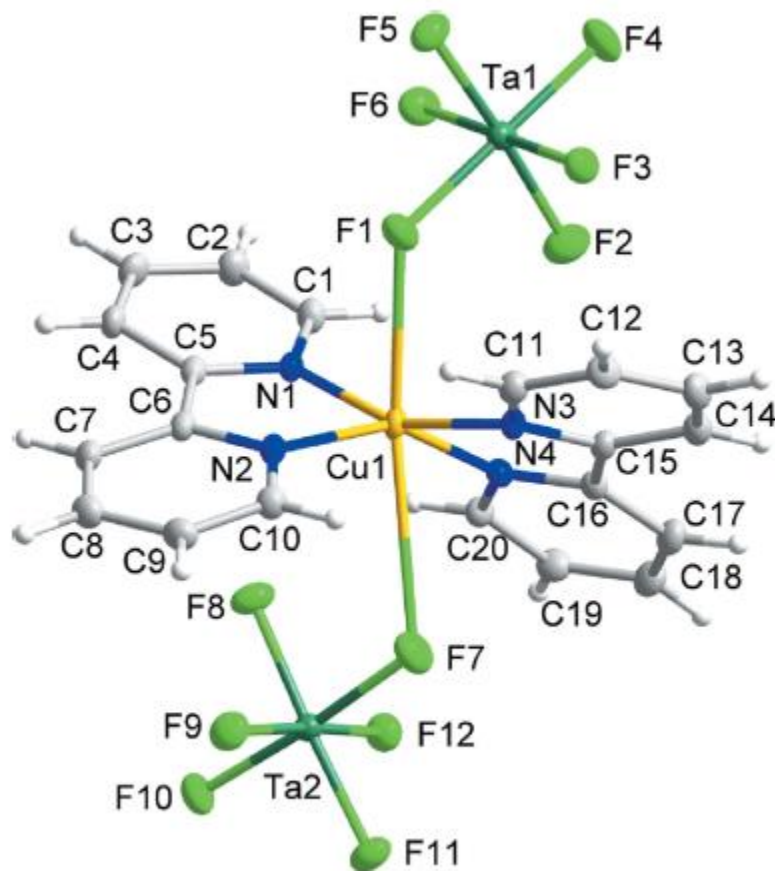


**Figure 1.17** View the structure of  $[\text{Cu}(\text{bpy})_2(\text{TaF}_6)_2]$  complex. [256]

Whereas, the  $\text{Cu}(\text{bpy})_3^{2+}$  cations of  $[\text{Cu}(\text{bpy})_3][\text{TaF}_6]_2$  complex with Cu(II) atom is in an octahedral  $\text{CuN}_6$  coordination environment, as what clarified in figure 1.18. [256]

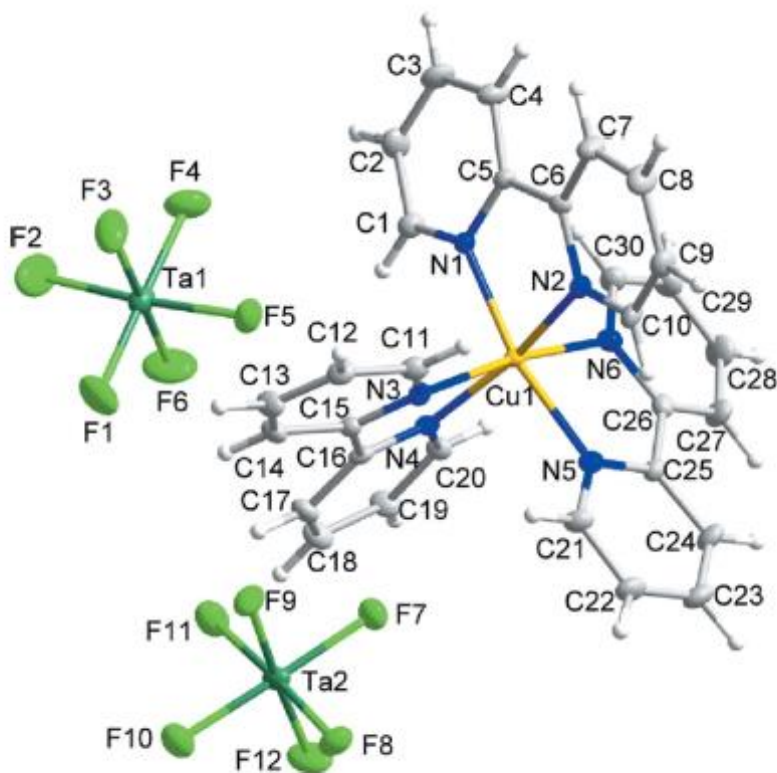


**Figure 1.18** View the structure of  $[\text{Cu}(\text{bpy})_3][\text{TaF}_6]_2$  complex. [256]

In addition to that, S. Gao et al, in 2021 were synthesized a copper(II) complex  $[\text{Cu}(\text{bpy})(\text{C}_4\text{H}_4\text{O}_6)]$ . The complex composed a synthetic 2-(hydroxymethyl)tartronate ( $\text{C}_4\text{H}_4\text{O}_6$ ) is unusual anionic chelating ligand. The structural of the complex is studied using X-ray diffraction. The results showed that the structure of the complex has square pyramidal geometry, where two bpy (via nitrogen atoms) and 2-(hydroxymethyl)tartronate anion ( $\text{C}_4\text{H}_4\text{O}_6^{-2}$ ) (via three oxygen atoms) are coordinated toward Cu(II) center atom. [257]

### 1.9.3 Nickel complexes

S. Tanase et al, in 2000 was synthesized  $\text{trans-[Ni(ampy)}_2(\text{NO}_3)_2]$  where  $\text{ampy} = 2\text{-aminomethylpyridine}$ , figure 1.19. The complex composed of nickel atom placed on an inversion center in which it linked with neutral mononuclear entities. The crystal structure found that Ni(II) atom of the complex has distorted octahedral geometry, in which the four nitrogen atoms of ampy ligands and two oxygen atoms of nitrate groups are surrounded the Ni(II) center atom. The cryomagnetic studies showed that complex has ferromagnetic as well as there is a  $\pi\text{-}\pi$  stacking interactions between mononuclear units. [258]

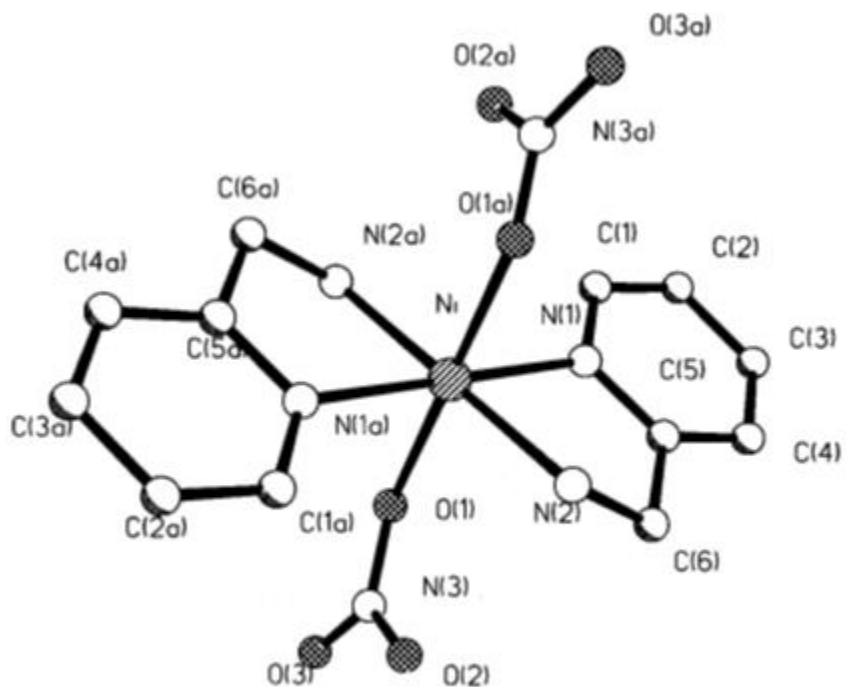


**Figure 1.19** View the structure of  $[\text{Ni(ampy)}_2(\text{NO}_3)_2]$  complex [258]

After few years, Y. Lin et al, in 2003 were prepared Ni(II) complex that composed of tetradentate ligand, 2,2',2''-triaminotriethylamine (tren), and the bidentate ligand 2,2'-bipyridine (bpy), see figure 1.20. The X-ray analysis clarified that the Ni(II) atom center of the complex has a distorted six coordinated octahedron, where two nitrogen atoms of

bpy ligand tetradentate tren ligands coordinated toward Ni(II) center atom via its four nitrogen atoms. [259]

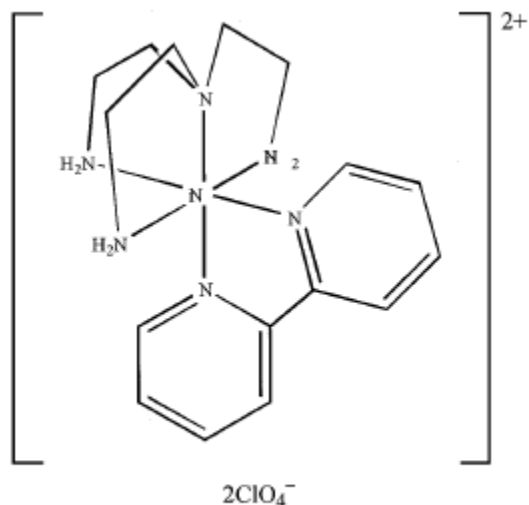


**Figure 1.20** View the structure of Ni(II) complex. [259]

In the same year, Y. Zhou et al, in 2003 were prepared Ni(II) complex, which its formula  $[\text{Ni}(\text{C}_{10}\text{H}_8\text{N}_2)_3](\text{ClO}_4)$ , where  $\text{C}_{10}\text{H}_8\text{N}_2$  is 2,2'-bipyridine (bpy), figure 1.21. The characterization of the complex is done by elemental and single-crystal diffraction analysis. The coordination of complex is a highly distorted octahedral geometry, where Ni(II) metal is surrounded by six nitrogen atoms of three chelating bpy ligands. [260]

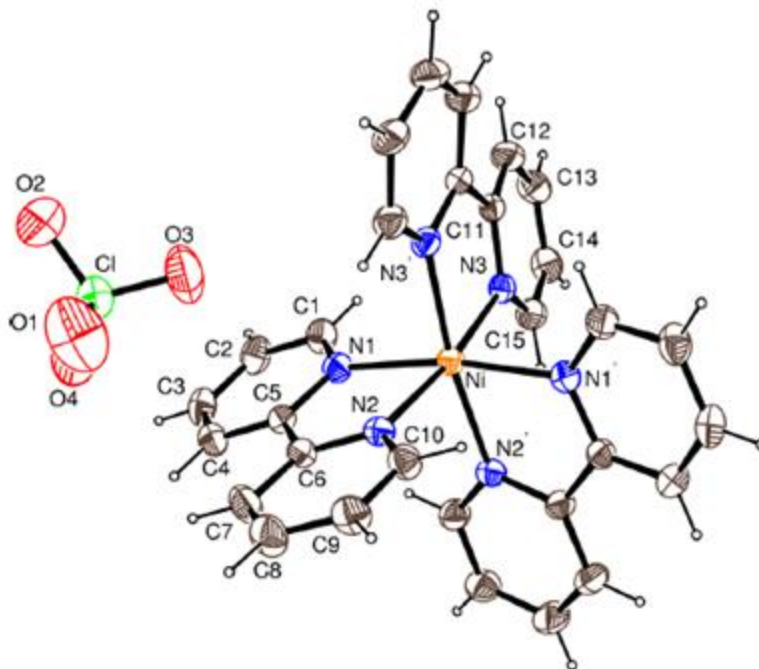


**Figure 1.21** View the structure of  $[\text{Ni}(\text{C}_{10}\text{H}_8\text{N}_2)_3](\text{ClO}_4)$  complex, showing the atomic labelling. [260]

Afterward, S. H. Rahaman et al, in 2005 were prepared  $[\text{M}(\text{dpa})_2(\text{N}_3)_2]\cdot\text{H}_2\text{O}$ , where  $\text{M} = \text{Ni}(\text{II})$  and 2,2'-dipyridylamine, as what shown in figure 1.22. The structure of the complex characterized by X-ray crystallographic. The results clarified that distorted octahedral formed according to that polyhedron, round the  $\text{Ni}(\text{II})$  atom center, with a  $\text{MN}_6$  coordinated by the four nitrogen atoms of dpa (N1, N3, N4, N6) and two nitrogen atom of two azide (N7, N10) as terminal ligands. The equatorial plane around the center of the  $\text{Ni}(\text{II})$  metal is occupied by three nitrogen atoms (N1, N4, N6) of dpa group beside to one nitrogen atom (N7) of azido unit. The trans axial sites are exploited by the remaining nitrogen (N3) of dpa and one nitrogen (N10) of other pendant azido ligand. Dpa is expected to produce hydrogen bonds via the hydrogen of amine, that resulting  $\pi\cdots\pi$  and/or  $\text{C}-\text{H}\cdots\pi$  interactions by pyridyl planes. Therefore, various crystalline aggregates with luminescence merits. [261]

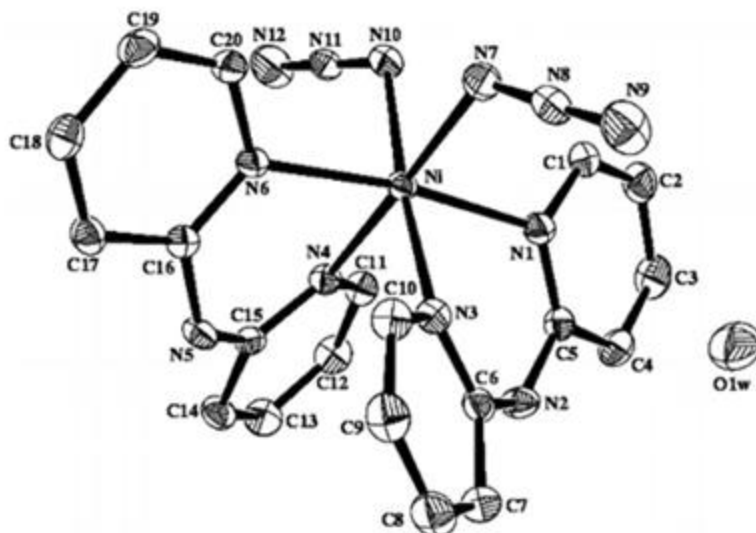


**Figure 1.22** View the structure of  $[\text{Ni}(\text{dpa})_2(\text{N}_3)_2] \cdot \text{H}_2\text{O}$  complex, showing the atomic labelling.<sup>[261]</sup>

After year, V. R. Pedireddi et al, in 2006 were prepared  $[\text{Ni}(\text{bpy})_2(\text{NO}_3)](\text{NO}_3)$  where bpy is 2,2'-bipyridine, figure 1.23. The characterization of complex is determined through single crystal X-ray diffraction methods. The Ni(II) atom is a hexacoordination, in which two bpy ligands and one nitrate group are linked toward it in a chelating mode. [262]

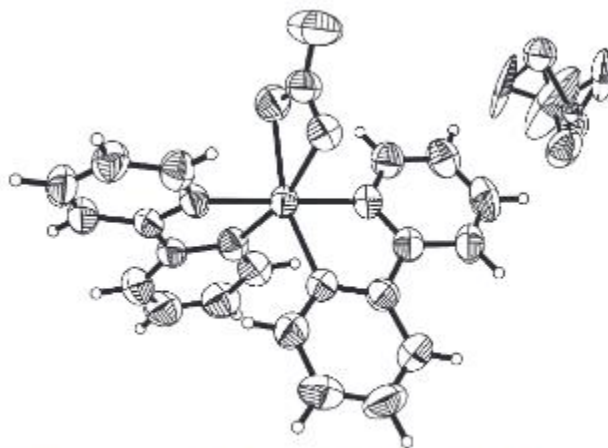


**Figure 1.23** View the structure of  $[\text{Ni}(\text{bpy})_2(\text{NO}_3)](\text{NO}_3)$  complex.<sup>[262]</sup>

Then, S. Bruda et al, in 2006 were formed a Ni(II) complex  $[\text{Ni}(\text{ampy})_2(\text{tcm})_2]$ , where ampy is 2-aminomethylpyridine and tcm is tricyanomethanide (tcm), as what shown



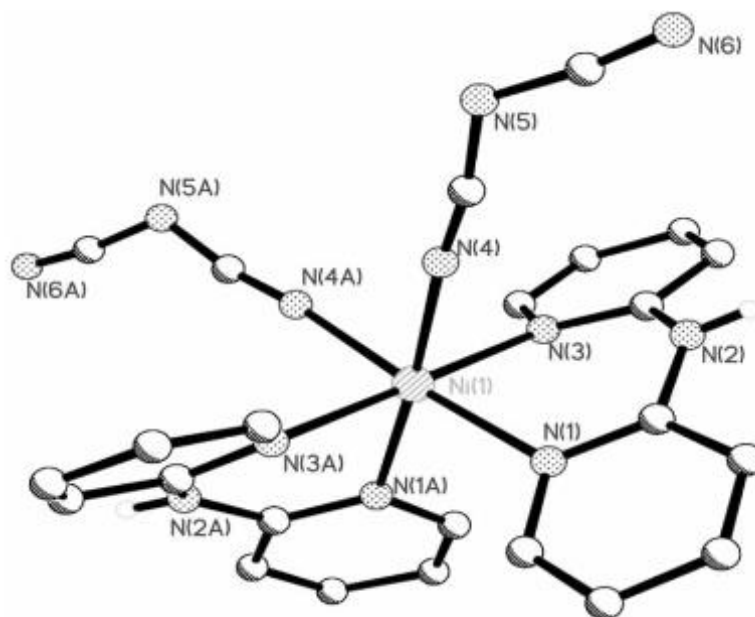


**Figure 1.25** View the structure of  $[\text{Ni}(\text{dpa})_2(\text{dca})_2]$  complex. [242]

After couple years, B.J. Wang et al, in 2008 were formed  $[\text{Ni}(\text{C}_8\text{H}_7\text{O}_3)(\text{C}_{10}\text{H}_8\text{N}_2)]\text{ClO}_4$  where  $\text{C}_{10}\text{H}_8\text{N}_2$  is 2,2'-bipyridine and  $\text{C}_8\text{H}_7\text{O}_3$  is 2-formyl-6-methoxyphenolate (mbd), see figure 1.26. The X-ray crystal structure analyzed that Ni(II) atom has a slightly distorted square coordination geometry, in which the bipy ligand (via its two nitrogen atoms) and protonated mbd ligand (via its two oxygen atoms) are coordinated toward it. A weak interaction are noticed between the Ni atom and one of the oxygen of the perchlorate. [264]

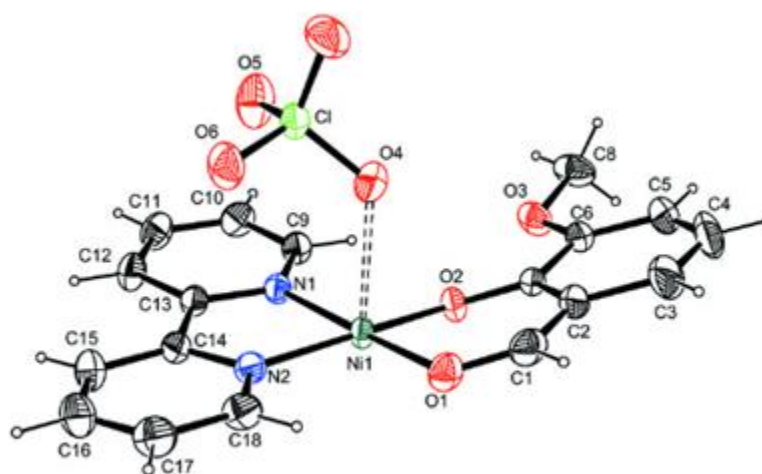
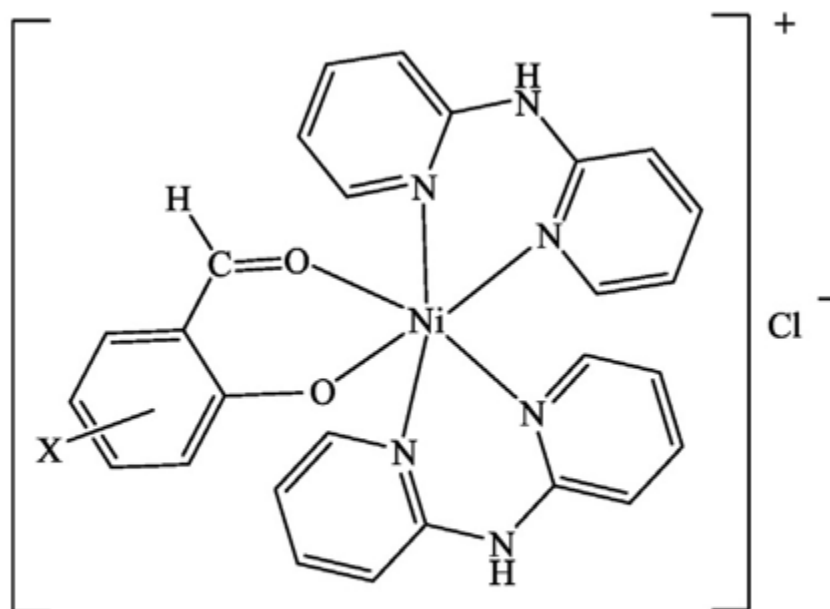


**Figure 1.26** View the structure of  $[\text{Ni}(\text{C}_8\text{H}_7\text{O}_3)(\text{C}_{10}\text{H}_8\text{N}_2)]\text{ClO}_4$  complex, with showing the atomic labelling. [264]

Later, A. Zianna et al, in 2016 were synthesized several Ni(II) complexes with general formula  $[\text{Ni}(\text{dpamH})_2(\text{X-salo})]\text{Cl}$ , where X-salo is 5-Cl-salo, 5-Br-salo and 5-CH<sub>3</sub>-salo, using 2,2'-dipyridylamine (dpamH) and substituted salicylaldehydes (X-saloH) as starting materials, scheme 1.13. The X-ray crystallography method characterized that the nickel(II) metal is an octahedral coordination by nitrogen atoms of two dpamH ligand and X-salo ligand via its oxygen atoms of carbonyl and phenolic groups. The biological studies concluded to that complexes could use as potential metallo-therapeutic agents. [265]



**Scheme 1.13** View the structures of cationic  $[\text{Ni}(\text{dpamH})_2(\text{X-salo})]\text{Cl}$  complexes (X=5-Cl, 5-Br, 5-CH<sub>3</sub> or 3-OCH<sub>3</sub>)<sup>[265]</sup>

After that, R. Carballo et al, in 2017 were synthesized Ni(II) complex in which it formulated as  $[\text{Ni}(\text{bz})(\text{dipyam})_2](\text{bz}) \cdot 2\text{MeOH}$ , where bz = benzilato and dipyam = 2,2'-dipyridylamine, figure 1.27. The characterization of the complex is done by using elemental analysis, IR and electronic absorption spectroscopy, magnetic measurements, thermo gravimetric analysis and single crystal X-ray diffraction. The structure of the nickel(II) ion complex is hexacoordinated through four nitrogen atoms of dipyam ligands and one carboxylate and one hydroxyl oxygen atoms of benzilato ligand and the geometry is a distorted octahedron due to the presence of three chelate rings. [266]

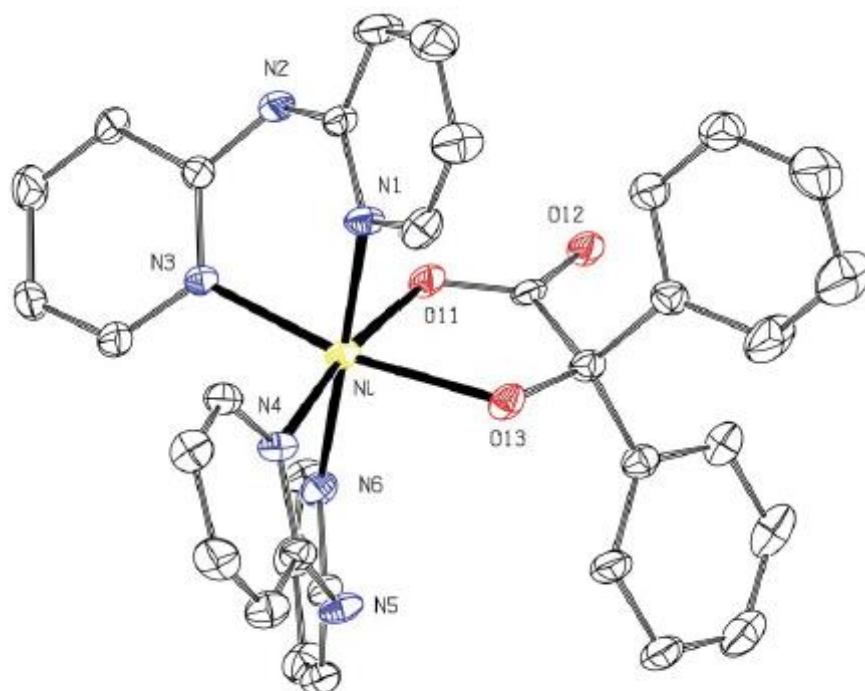


**Figure 1.27** View the structure of cationic  $[\text{Ni}(\text{bz})(\text{dipyam})_2]^+$  complex. [266]

At least, L. Krešáková et al, in 2021 were produced many nickel complex which is formed as  $[\text{Ni}(\text{bpy})(\text{Bz})_2]$  and  $[\text{Ni}(\text{bpy})_2(\text{Bz})](\text{NO}_3) \cdot 1.25\text{H}_2\text{O}$  where (bpy = 2,2'-bipyridine and Bz = benzoate anion), see figure 1.28. The structures of the complexes were analyzed via single-crystal X-ray crystallography. The Ni(II) atom of  $[\text{Ni}(\text{bpy})(\text{Bz})_2]$  complex is a hexacoordinated through two benzoate group and one bpy ligand. While, the Ni(II) atom of  $[\text{Ni}(\text{bpy})_2(\text{Bz})](\text{NO}_3) \cdot 1.25\text{H}_2\text{O}$  complex is a hexacoordinated via two bpy and one Bz ligands. [267]

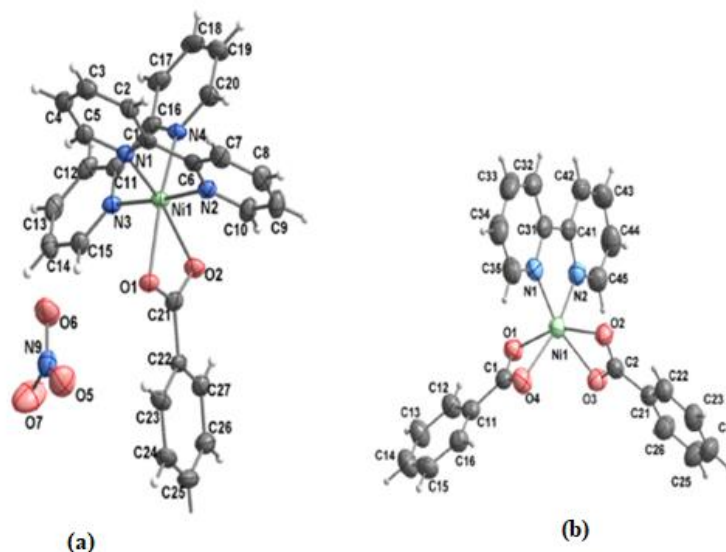


**Figure 1.28** View the structure of (a)  $[\text{Ni}(\text{bpy})_2(\text{Bz})]\text{NO}_3 \cdot 1.25\text{H}_2\text{O}$  complex and (b)  $[\text{Ni}(\text{Bz})_2(\text{bpy})]$  complex <sup>[267]</sup>

#### 1.9.4 Other metals complexes

S.S. Tandon et al, in 2000 were synthesized Zn(II) complex with formula  $[\text{Zn}(\text{AMP})_2(\text{NO}_3)_2]$  where AMP is 2-aminomethylpyridine, figure 1.29. The characterization of complex is explained via different techniques as IR,  $^1\text{H}$ ,  $^{13}\text{C}$ , 2-D NMR spectroscopy and X-ray crystallography. The geometry of the complex is octahedron, the zinc(II) atom coordinate with two pyridine nitrogens and two amino nitrogen atoms from bidentate 2-aminomethylpyridine ligands in an equatorial plane, and with two oxygen atoms from two monodentate nitrate molecules in an axial plane. [268]

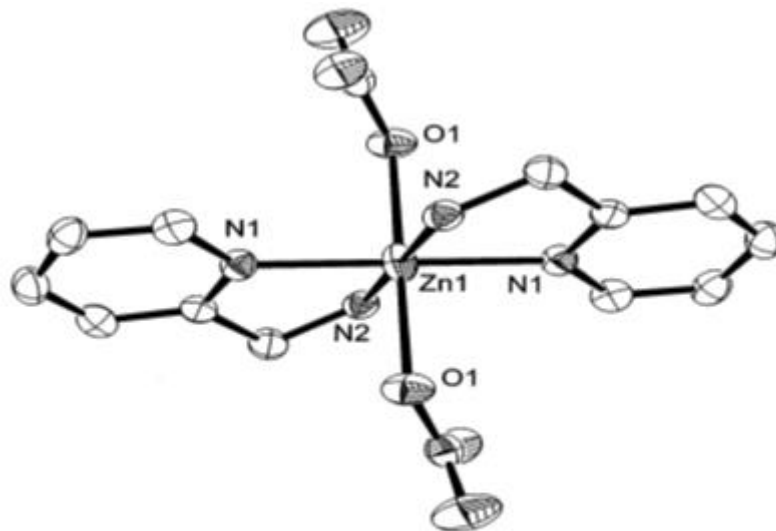


**Figure 1.29** View the structure of  $[Zn(AMP)_2(NO_3)_2]$  complex. [268]

In other research, T. Sunahara et al, in 2004 were prepared  $[Zn(bpp)(pca)(MeOH)]ClO_4$  where 1,3-bis(4-pyridyl)propane (bpp), pyrazine-2-carboxylate (pca), see figure 1.30. Its structure is established by single-crystal X-ray diffraction. The results showed that complex exhibit distorted octahedral skeletons around the Zn ions. MeOH could be took out without destruction of the parental superstructure. There are two methods to prepare the complex. First, using pyrazine-2-carbonitrile (pcn), bis(pyridine) ligands, and zinc perchlorate. The successful of the synthesis is done by hydrolysis of the CN group of pcn to  $CO_2$  during the reaction with explosion to air for couple days, thus a multidentate ligand is formed. Second, it could easily obtained by mixing of pca, bpp, and  $Zn(ClO_4)_2 \cdot 6H_2O$  in EtOH/ $H_2O$  at room temperature resulting in similar. [269]

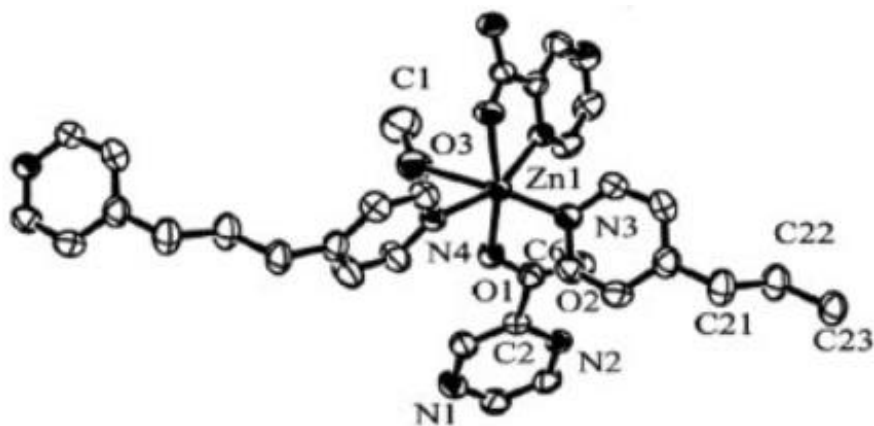


**Figure 1.30** View the structure of  $[Zn(bpp)(pca)(MeOH)]ClO_4$  complex. <sup>[269]</sup>

It should be noticed that Kopelet et al, in 2004 were synthesized  $[Fe(bpy)_3](ttcH).2bpy.7H_2O$  complex, where ttcH is trithiocyanuric acid, figure 1.31. The elemental analysis, IR and UV-Vis spectroscopies have been used to analyze the complex. Its coordination structure is distorted octahedral arrangement, in which Fe(II) atoms with monoanionic leads to located trithiocyanurate outside the internal coordination sphere. <sup>[270]</sup>

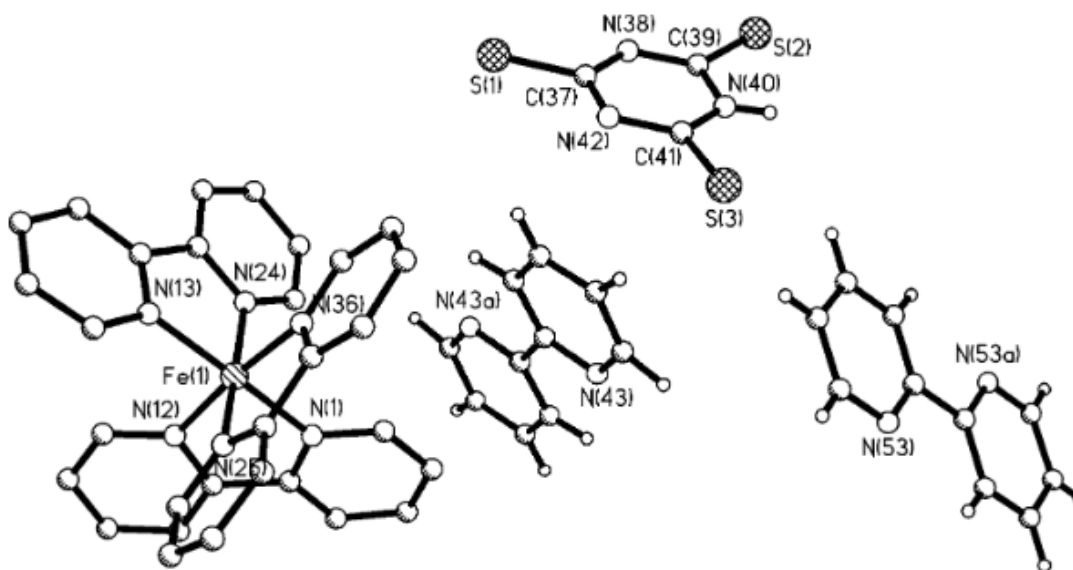


**Figure 1.31** View the structure of  $[Fe(bpy)_3](ttcH).2bpy.7H_2O$  complex. The water molecules and hydrogen atoms of coordinated bpy are deleted for clarity. <sup>[270]</sup>

Other researchers as S. Hamamcia et al, in 2005 were synthesized new Ag(I) complex in which its formula is  $[Ag(sac)(ampy)]$  where sac is saccharinate and ampy is 2-(aminomethyl)pyridine, figure 1.32. The structure analyzed using many methods like

elemental analysis, IR spectroscopy, thermal analysis and single crystal X-ray diffraction. The Ag(I) atom in compound display a distorted T-shaped  $\text{AgN}_3$  coordination geometry, where ampy and sac ligands coordinated toward it. [271]

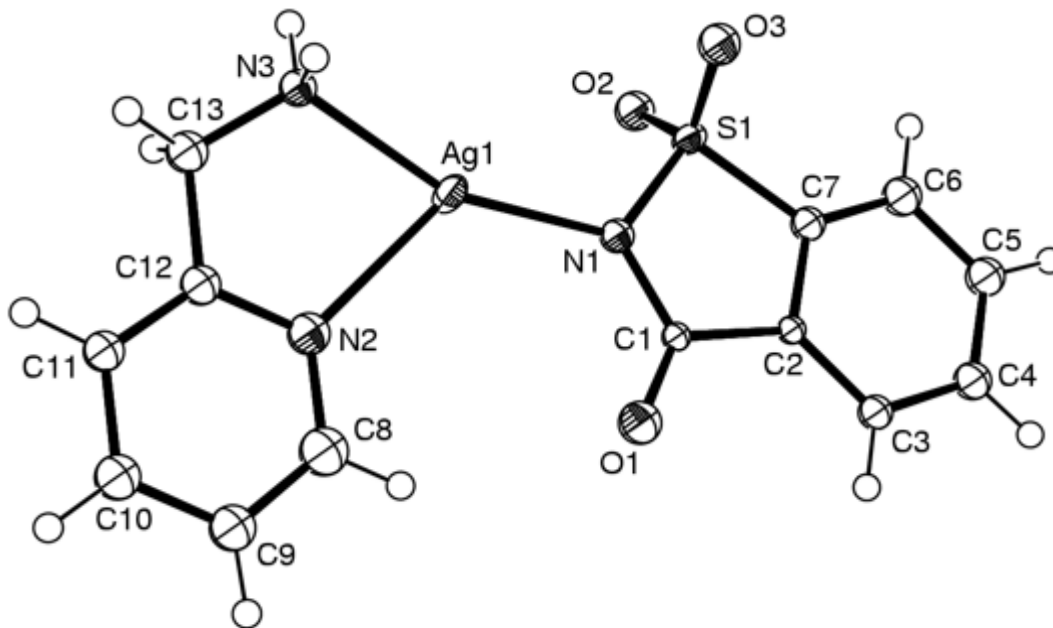


**Figure 1.32** View the structure of  $[\text{Ag}(\text{sac})(\text{ampy})]$  complex.[271]

Whereas, J.C. Yao et al, in 2005 were synthesized  $[\text{Co}(\text{bipy})_3](\text{ClO}_4)_2$  complex, using cobalt(II) perchlorate hexahydrate  $\text{Co}(\text{ClO}_4)_2 \cdot 6\text{H}_2\text{O}$  and 2,2'-bipyridine, figure 1.33. X-ray single-crystal diffraction is used to study the structure of complex. The Co(II) is coordinated by six nitrogen atoms of three bipy ligands. The description for the coordination of polyhedron surrounds the Co(II) atoms is a distorted octahedron. [272]

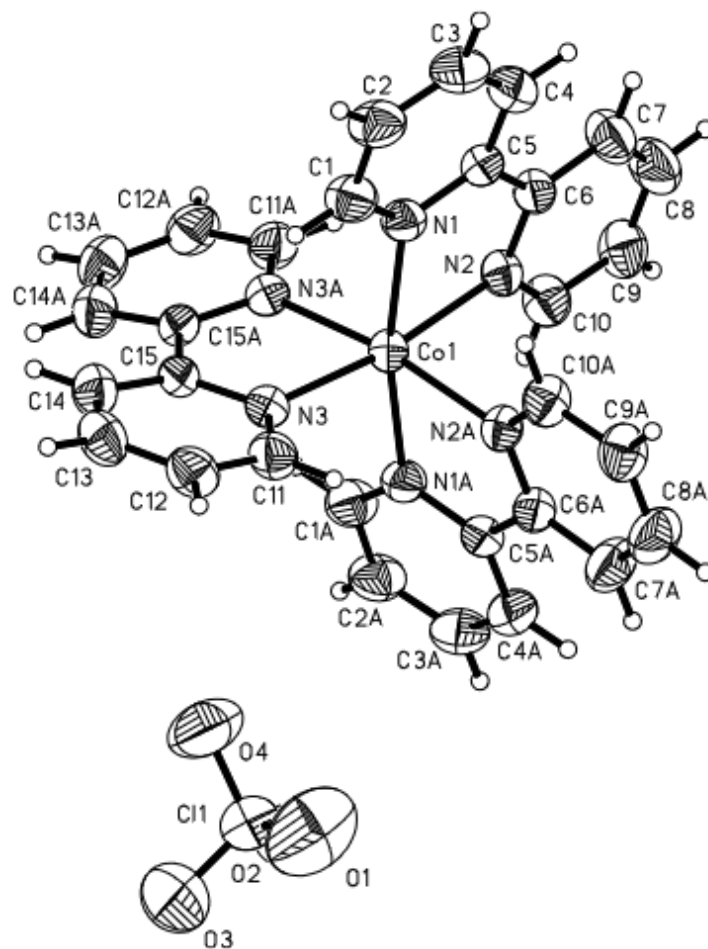


**Figure 1.33** View the structure of  $[\text{Co}(\text{bipy})_3](\text{ClO}_4)_2$  complex. [272]

However, A. Malassa et al, in 2006 were used 2-Pyridylmethylamine ligand (amp) with Iron halides as  $\text{FeCl}_2$  and  $\text{FeBr}_2$ , methanol employed as solvent to form bis(amp) complexes as  $[(\text{amp})_2\text{FeCl}_2]$  and  $[(\text{amp})_2\text{FeBr}_2]$ , figure 1.34. Their structures were investigated by crystallographic, where the coordination of iron is distorted octahedral geometry. [273]

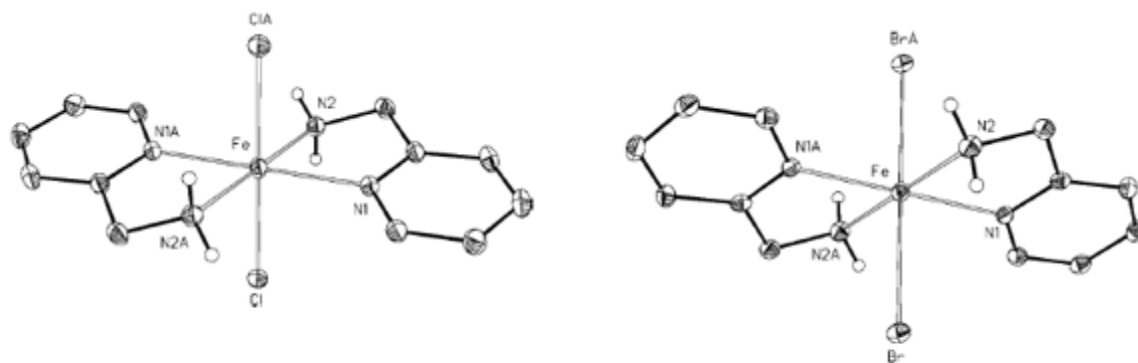


**Figure 1.34** View the structure of (a)  $[(amp)_2FeCl_2]$  complex and (b)  $[(amp)_2FeBr_2]$  complex.<sup>[273]</sup>

On the other hand, Z. Talaei et al, in 2006 were used other metal as zinc(II) with 2,2'-bipyridine and  $CH_3COO^-$  is acetate anion to form  $[Zn(bpy)_2(CH_3COO)](ClO_4) \cdot H_2O$  complex. The characterization of the structure is done by utilizing elemental analysis, IR,  $^1H$  NMR and  $^{13}C$  NMR spectroscopy. The result of the analysis displayed that Zn(II) atom is surrounded by N atoms of bpy ligands and two O atoms of acetate group. Thus, the coordination of Zn(II) is distorted octahedral geometry, as what shown in the figure 1.35 [274]

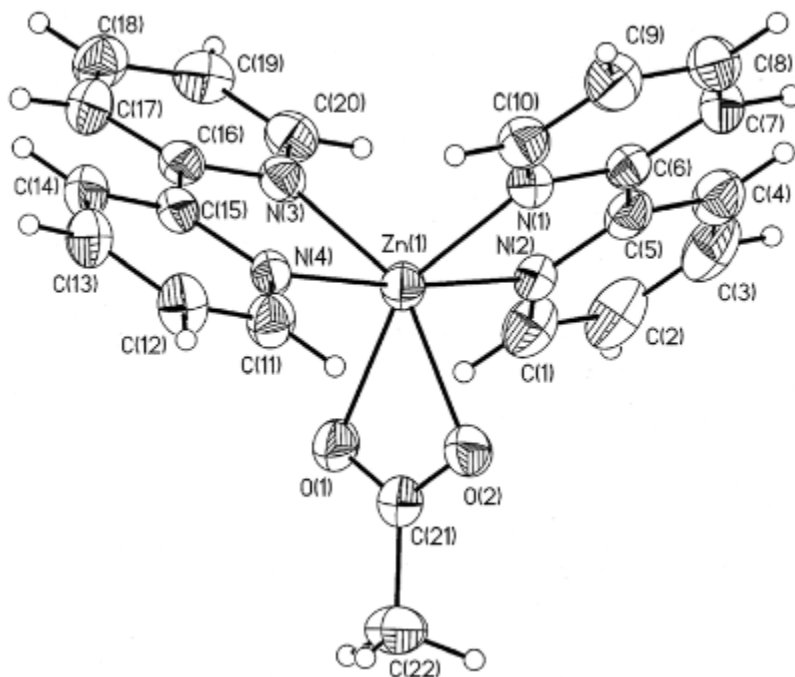


**Figure 1.35** View the structure of  $[Zn(bpy)_2(CH_3COO)](ClO_4) \cdot H_2O$  complex.<sup>[274]</sup>

In other view, W. Z. Shen, in 2007 was produced Pt(II) complex in formula  $[\{cis-Pt(NH_3)_2(2,2'-bpz-N4,N4')\}_4](NO_3)_8 \cdot 4H_2O$  by uniting two groups of  $[\{Pt(en)(2,2'-bpz-N4,N4')\}_3](NO_3)_6$ , see figure 1.36. The  $^1H$  NMR and X-ray crystallography are used to analyze the structure of the complex. The coordination for complex is square planar geometry. [275]

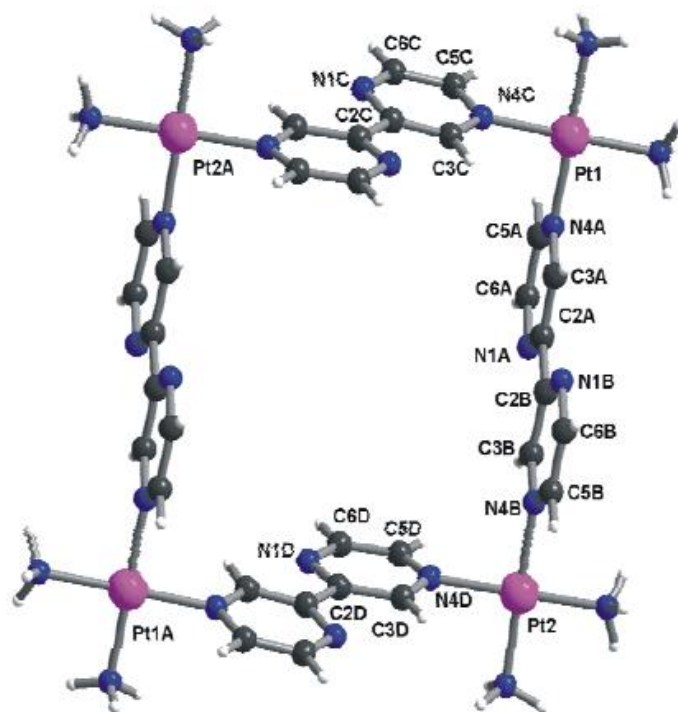


**Figure 1.36** View the structure of tetranuclear cation  $[\{cis-Pt(NH_3)_2(2,2'-bpz-N4,N4')\}_4]^{8+}$  complex. [275]

In addition to that, the figure below explained that the structure has been as open box two nitrate anions and four water molecules combined in the inside, as what shown in figure 1.37 [275]

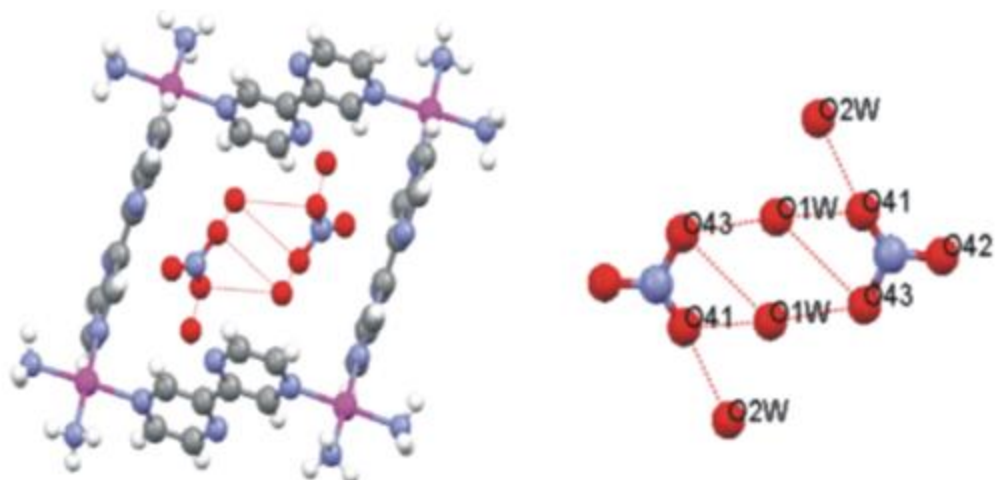


**Figure 1.37** View the structure of  $[\{\text{cis-Pt}(\text{NH}_3)_2(2,2'\text{-bpz-N}4,\text{N}4')\}_4](\text{NO}_3)_8 \cdot 4\text{H}_2\text{O}$  complex with two nitrate anions and four water molecules cluster encapsulated. [275]

Same year, M. G. B. Drew et al, in 2007 were prepared  $[\text{Ru}(2,2'\text{-bipyridine})_2(\text{Hdpa})](\text{BF}_4)_2 \cdot 2\text{H}_2\text{O}$  complex, where Hdpa is 2,2'-dipyridylamine, figure 1.38. The structure of complex is analyzed using X-ray crystal structure. The geometry of Ru metal is octahedral  $\text{N}_6$  coordination sphere, where Hdpa ligands linked with Ru atom via the two nitrogen atoms (N51 and N63) of two pyridyl groups. [276]

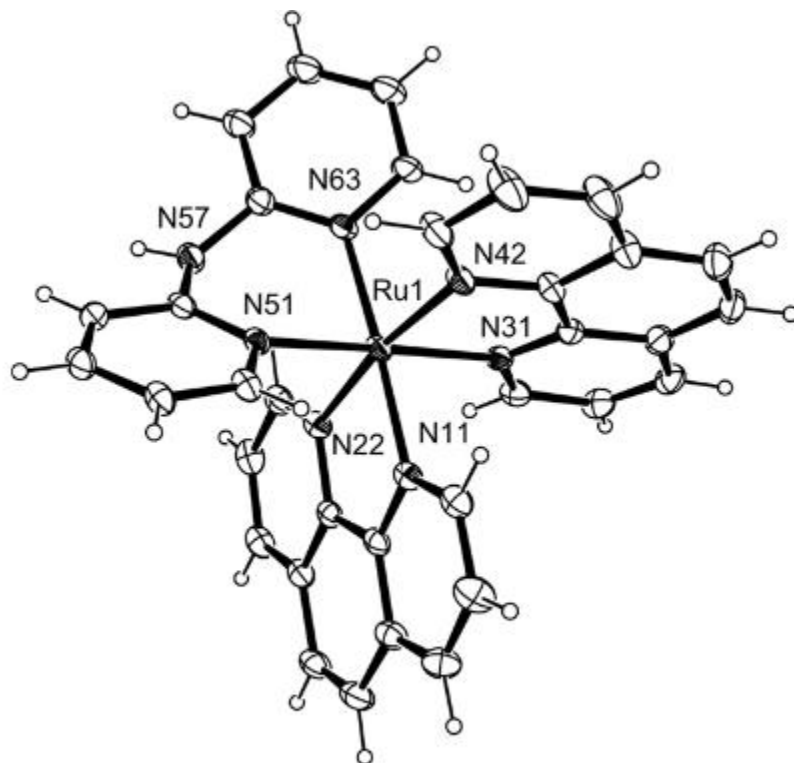


**Figure 1.38** View the structure of cation  $[\text{Ru}(2,2'\text{-bipyridine})_2(\text{Hdpa})]^{2+}$  complex. <sup>[276]</sup>

Thereafter, K. K Kpogo et al, in 2017 were prepared  $[\text{Co}^{\text{II}}_2(\text{L}^1)(\text{bpy})_2]\text{ClO}_4$ , where  $\text{L}^1$  is triply deprotonated ligand as what is shown in the figure 1.39. The structure of complex is clarified by using means of electrochemical, spectroscopic, and computational methods. The figure 1.39 below shows that there are two phenolic groups and one amidic protons are lost from ligand  $(\text{L}^1)^{-3}$  due to supporting of dicobalt(II) atoms. [277]

Moreover, both of five coordinate  $\text{Co}(\text{II})$  is linked with azomethine via nitrogen atom (N1 or N2), phenolate through oxygen atom (O1 or O2) and with bipyridine (bpy), in which the coordination sphere is completed. The role of single counter ion  $\text{ClO}_4^-$  contributed in neutralizing of mono- cationic unit. [277]

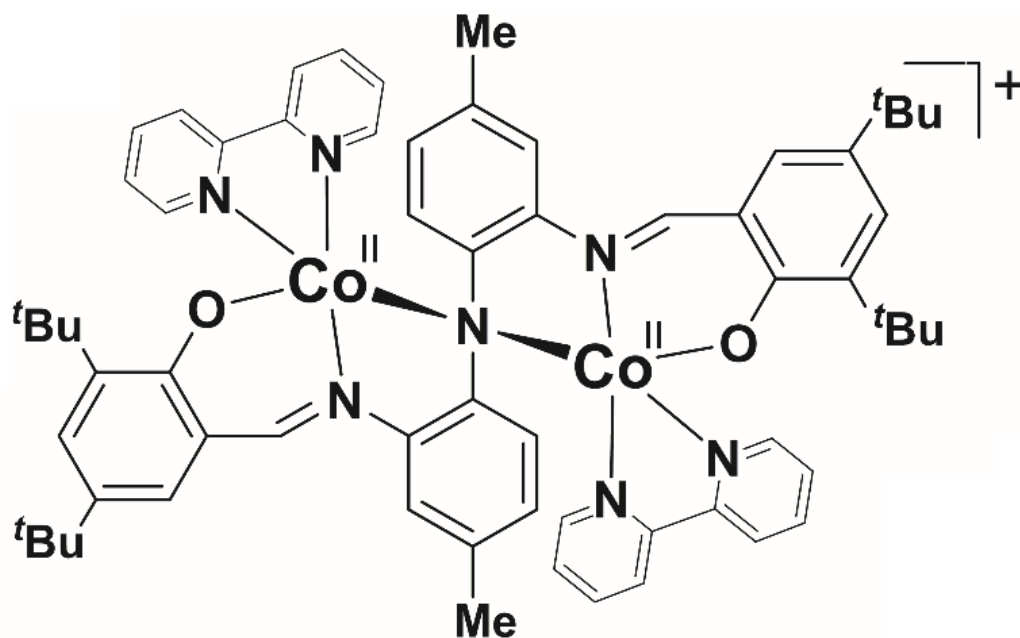
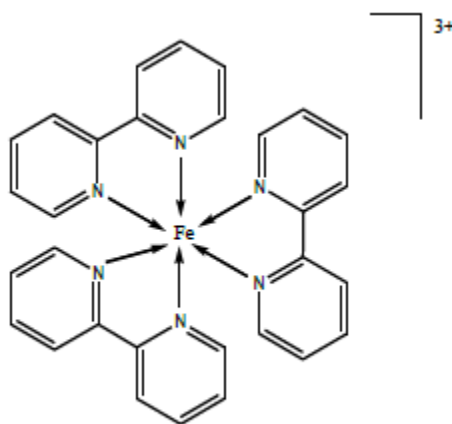


**Figure 1.39** View the structure of cation  $[\text{Co}^{\text{II}}_2(\text{L}^1)(\text{bpy})_2]^+$  complex. [277]

In addition to that, A. S. Priyal et al, in 2017 we synthesized  $[\text{Fe}(\text{bpy})_3]\text{Cl}_2$  complex, where bpy is 2,2'-bipyridine ligand (scheme 1.14). The preparation is done by converting the Iron(II)-polypyridyl complex through putting ammonium hexanitrate cerium(IV) in  $\text{HClO}_4$  or  $\text{PbO}_2$  solution in ice bath. After half an hour, sodium perchlorate solution is added. The resulted precipitate is filtered and washed by mixture of ethanol and ice cold water, then dehydrated by vacuum. It synthesized as model compounds and applied as electron acceptors. [278]



**Scheme 1.14** View the structure of cationic  $[\text{Fe}(\text{bpy})_3]^{2+}$  complex. [278]

At least, N. A. Annana et al, in 2020 were prepared  $[\text{Zn}(\text{bpy})_3]\text{Cl}_2$  complex where bpy is a 2,2'-bipyridyl ligand, figure 1.40. The study of the complex's structure is determined via X-ray crystal structure. The two nitrogen atoms of bpy coordinated around Zn(II) atom, therefore, the geometry of complex is a distorted octahedral. [279]

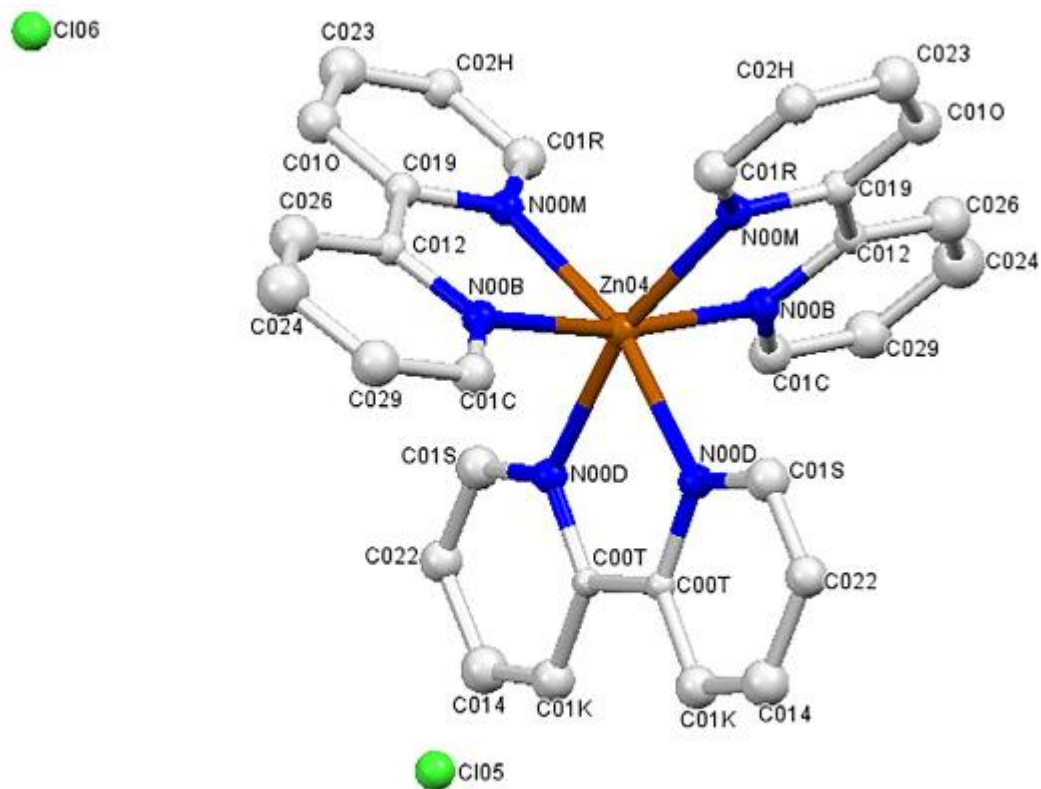


**Figure 1.40** View the structure of  $[\text{Zn}(\text{bpy})_3]\text{Cl}_2$  complex [279]

### **1.10 Research Objectives:**

- 1- Synthesis of new coordination compounds containing copper(II) ion and homoleptic ligands.
- 2- Synthesis a new mixed ligand complexes containing nickel(II) and copper(II) with 2,2'-bipyrazine, 2,2'-dipyridylamine and other Lewis bases.
- 3- Study the influence of different solvent and counter ions on the structure of the new complexes.
- 4- Synthesis a new mixed ligand complexes of copper(II) with new ligand different of the initial ligands.
- 5- Preparation single crystals suitable for X-ray single crystal analysis.
- 6- Characterization of the new complexes using X-ray, FTIR spectroscopy and thermal analysis by differential scanning calorimetry (DSC).
- 7- Study the structurally properties of the new complexes.

## Chapter Two

### Experimental

#### (Materials and methods)

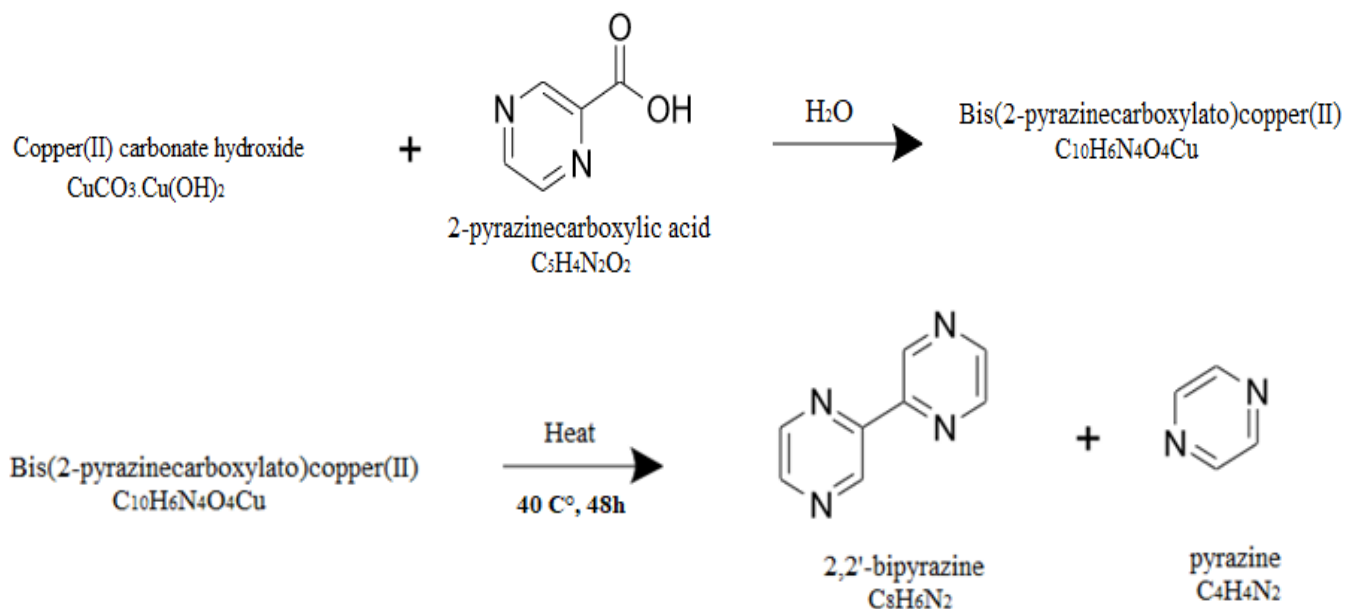
#### 2.1 Materials:

Metal salt copper(II) perchlorate hexahydrate  $\text{Cu}(\text{ClO}_4)_2 \cdot 6\text{H}_2\text{O}$ , copper(II) nitrate trihydrate  $\text{Cu}(\text{NO}_3)_2 \cdot 3\text{H}_2\text{O}$ , nickel(II) perchlorate hexahydrate  $\text{Ni}(\text{ClO}_4)_2 \cdot 6\text{H}_2\text{O}$ , 2,2'-dipyridylamine ( $\text{C}_{10}\text{H}_9\text{N}_3$ ), 2-(aminomethyl)pyridine ( $\text{C}_6\text{H}_8\text{N}_2$ ), N,N-diethylenediamine ( $\text{C}_6\text{H}_{16}\text{N}_2$ ), tricyclohexylphosphine ( $\text{C}_{18}\text{H}_{33}\text{P}$ ), copper(II) carbonate hydroxide  $\text{Cu}_2(\text{OH})_2\text{CO}_3$ , 2-pyrazinecarboxylic acid ( $\text{C}_5\text{H}_4\text{N}_2\text{O}_2$ ),  $\text{H}_2\text{O}$ , chloroform, toluene, methanol, acetonitrile were purchased from sigma Aldrich. And used as received.

#### 2.2 Methods:

##### 2.2.1 Synthesis of 2,2'-bipyrazine (bpz) ( $\text{C}_8\text{H}_6\text{N}_4$ ):

The synthesis of 2,2'-bipyrazine (bpz) illustrated according to the following scheme 2.1



**Scheme 2.1** View the synthesis of 2,2'-bipyrazine ligand. <sup>[238,280]</sup>

The synthesis was prepared according to previous described procedure, where 4.1 gram (0.0185) mole of copper(II) carbonate hydroxide reacted with 9.2 gram (0.074) mole 2-pyrazinecarboxylic acid in 150 ml of water. Then, the mixture stirred about 16.5 hours at room temperature. A blue Bis(2-pyrazinecarboxylato)copper(II) precipitate was formed by filtering and washing with little amount of water. After that, Bis(2-pyrazinecarboxylato)copper(II) was dried using oven at 40 C° about 48 hours and then was putted in a Pyrex boat that placed in Pyrex tube. At least, the Pyrex boat was heated using Bunsen burner under argon atmosphere to pyrolysis the copper complex. [238,280(a)]

During the pyrolysis, 2,2'-bipyrazine and pyrazine raised to the side of the Pyrex tube. The burning process is completed after 20 minutes, therefore, the color of copper complex turned to black. While the cooling was done at room temperature, the boat was taken away and the pyrazine impurity was removed according to air that passed the tube. The remaining solid in the Pyrex was washed using 50 ml of chloroform, in which it evaporated at room temperature. The product was recrystallized by 80 ml of toluene, and it evaporated at room temperature. A yellow pale crystal collected as 2,2'-bipyrazine in which it characterized by FTIR spectroscopy. [280(a)]

## 2.2.2 *Synthesis of coordination complexes:*

### 2.2.2.1 *Synthesis of [Cu(amp)<sub>2</sub>(NO<sub>3</sub>)<sub>2</sub>]:*

#### 2.2.2.1.1 *Preparations:*

The [Cu(amp)<sub>2</sub>(NO<sub>3</sub>)<sub>2</sub>] complex was prepared by dissolved 48.4 mg (0.2 mmol) of copper(II) nitrate trihydrate (Cu(NO<sub>3</sub>)<sub>2</sub>·3H<sub>2</sub>O) in 5 ml of methanol with stirring for twenty minutes at room temperature, then 21.7 mg (0.2 mmol) of 2-(aminomethyl)pyridine (C<sub>6</sub>H<sub>8</sub>N<sub>2</sub>) is dissolved in 11 ml methanol and added to the clear solution of the metal. Immediately afterwards, 55 ml of methanol is also added with continuous stirring for 35 hours and heat under reflux for one and half hour until a clear solution occurred. Hence, 30.7 mg (0.192 mmol) of 2,2'-bipyrazine (C<sub>8</sub>H<sub>6</sub>N<sub>4</sub>) is dissolved in 8 ml of methanol and added to the mixture with continuous stirring and reflux at temperature 60 C° for 26 hours. A clear turquoise solution was filtrated and left to evaporate at room temperature until most

of the solvent was evaporated. A yellow brown single crystals suitable to X-ray analysis was filtered off and air dried. The percentage yield of this complex is 42.80 %.

#### 2.2.2.1.2 Crystal Data:

A summary of the key crystallographic information is given in (table 2.1) for the [Cu(amp)<sub>2</sub>(NO<sub>3</sub>)<sub>2</sub>] complex. [281-287]

**Table 2.1:** Crystal Data and Structure Refinement Parameters for [Cu(amp)<sub>2</sub>(NO<sub>3</sub>)<sub>2</sub>] complex.

Molecular formula	C <sub>12</sub> H <sub>16</sub> CuN <sub>6</sub> O <sub>6</sub>
Molecular weight	403.84
Crystal system, space group	Monoclinic, P2 1 /c
Temperature (K)	295
a, b, c (Å)	8.6377 (7), 8.9833 (6), 9.9958 (8)
β (°)	99.430
V (Å <sup>3</sup> )	765.14 (10)
Z	2
Radiation type	Mo Kα
μ (mm <sup>-1</sup> )	1.47
Crystal size (mm)	0.23 × 0.22 × 0.15
Data collection	
Diffractometer	Bruker Kappa Apex2
Absorption correction	Numerical Analytical Absorption (De Meulenaer & Tompa, 1965)
T <sub>min</sub> , T <sub>max</sub>	0.72, 0.80
No. of measured, independent and observed [I > 2.0σ(I)] reflections	7044, 1470, 1248
R <sub>int</sub>	0.021
(sin θ/λ) <sub>max</sub> (Å <sup>-1</sup> )	0.612
Refinement	
R[F <sup>2</sup> > 2σ(F <sup>2</sup> )], wR(F <sup>2</sup> ), S	0.025, 0.044, 1.00
No. of reflections	1 248
No. of parameters	115
No. of restraints	1
H-atom treatment	H-atom parameters constrained
Δρ <sub>max</sub> , Δρ <sub>min</sub> (e Å <sup>-3</sup> )	0.36, -0.24

### 2.2.2.2 Synthesis of $[Cu(dipyam)(H_2O)(pca)]ClO_4$ :

#### 2.2.2.2.1 Preparations:

The complex of  $[Cu(dipyam)(H_2O)(pca)]ClO_4$  was prepared by dissolving of 74.2 mg (0.2 mmol) of copper(II) perchlorate hexahydrate ( $Cu(ClO_4)_2 \cdot 6H_2O$ ) in 10 ml of water with stirring at room temperature for 15 minutes. Then, a dissolved 34.4 mg (0.2 mmol) of 2,2'-dipyridylamine ( $(C_5H_4N)_2NH$ ) in 8 ml of water is added to the solution with continuous stirring for 45 minutes and then the reflux turned on at temperature  $70\text{ }^\circ\text{C}$  for 20 minutes. Consequently, 30.4 mg (0.192 mmol) of dissolved 2,2'-bipyrazine ( $C_8H_6N_4$ ) in 10 ml of water was added to the clear solution, the stirring and reflux was continuous for ten minutes. A clear green solution was filtrated and left to evaporate at room temperature until most of the solvent was vaporized. A green single crystal suitable to X-ray analysis was filtrated off and air dried. The percentage yield of this complex is 65.13 %.

#### 2.2.2.2.2 Crystal Data:

A summary of the key crystallographic information is given in (table 2.2) for the  $[Cu(dipyam)(H_2O)(pca)]ClO_4$  complex. [281-287]

**Table 2.2:** Crystal Data and Structure Refinement Parameters for  $[Cu(dipyam)(H_2O)(pca)]ClO_4$  complex.

Molecular formula	$C_{15}H_{14}ClCuN_5O_7$
Molecular weight	475.30
Crystal system, space group	Triclinic, P-1
Temperature (K)	295
a, b, c (Å)	7.8943 (10), 9.9511 (14), 13.412 (2)
$\alpha, \beta, \gamma$ ( $^\circ$ )	98.908 (9), 106.079 (8), 112.715 (7)
V (Å <sup>3</sup> )	892.2 (2)
Z	2
Radiation type	Mo Ka
$\mu$ (mm <sup>-1</sup> )	1.43
Crystal size (mm)	0.28 × 0.27 × 0.16
Data collection	
Diffractionmeter	Bruker Kappa Apex2
Absorption correction	Numerical Analytical Absorption (De Meulenaer & Tompa, 1965)
$T_{min}, T_{max}$	0.68, 0.80
No. of measured, independent and observed [ $I > 2.0\sigma(I)$ ] reflections	10729, 3391, 2648

$R_{\text{int}}$	0.017
$(\sin \theta/\lambda)_{\text{max}}$ ( $\text{\AA}^{-1}$ )	0.613
Refinement	
$R[F^2 > 2\sigma(F^2)], wR(F^2), S$	0.055, 0.148, 1.00
No. of reflections	2648
No. of parameters	262
H-atom treatment	H-atom parameters constrained
$\Delta\rho_{\text{max}}, \Delta\rho_{\text{min}}$ ( $e \text{\AA}^{-3}$ )	0.50, -1.28

### 2.2.2.3 Synthesis of $[\text{Cu}(\text{bpz})_2(\text{H}_2\text{O})](\text{NO}_3)_2$ :

#### 2.2.2.3.1 Preparations:

The complex of  $[\text{Cu}(\text{bpz})_2(\text{H}_2\text{O})](\text{NO}_3)_2$  was prepared by adding 31.8 mg (0.2 mmol) 2,2'-bipyrazine ( $\text{C}_8\text{H}_6\text{N}_4$ ) in two equally portions, in which is dissolved in 12 ml, 20 ml of water respectively, to 10 ml of light turquoise solution of 24.4 mg (0.1 mmol) of copper(II) nitrate trihydrate ( $\text{Cu}(\text{NO}_3)_2 \cdot 3\text{H}_2\text{O}$ ) under stirring for an hour at room temperature until the solid dissolved. A green single crystal suitable to X-ray analysis was filtrated off and air dried. The percentage yield of this complex is 77.80 %.

#### 2.2.2.3.2 Crystal Data:

A summary of the key crystallographic information is given in (table 2.3) for the  $[\text{Cu}(\text{bpz})_2(\text{H}_2\text{O})](\text{NO}_3)_2$  complex. [281-287]

**Table 2.3:** Crystal Data and Structure Refinement Parameters for  $[\text{Cu}(\text{bpz})_2(\text{H}_2\text{O})](\text{NO}_3)_2$  complex.

Molecular formula	$\text{C}_{16}\text{H}_{14}\text{CuN}_{10}\text{O}_7$
Molecular weight	521.90
Crystal system, space group	Monoclinic, C2/c
Temperature (K)	295
a, b, c ( $\text{\AA}$ )	15.886 (6), 7.208 (4), 18.016 (7)
$\beta$ ( $^\circ$ )	107.07 (4)
V ( $\text{\AA}^3$ )	1972.2 (17)
Z	4
Radiation type	Mo K $\alpha$
$\mu$ ( $\text{mm}^{-1}$ )	1.18
Crystal size (mm)	$0.29 \times 0.17 \times 0.14$
Data collection	
Diffractometer	Bruker Kappa Apex2

Absorption correction	Numerical Analytical Absorption (De Meulenaer & Tompa, 1965)
$T_{\min}, T_{\max}$	0.82, 0.85
No. of measured, independent and observed [ $I > 2.0\sigma(I)$ ] reflections	11601, 1935, 1755
$R_{\text{int}}$	0.018
$(\sin \theta/\lambda)_{\text{max}}$ ( $\text{\AA}^{-1}$ )	0.621
Refinement	
$R[F^2 > 2\sigma(F^2)], wR(F^2), S$	0.059, 0.122, 1.00
No. of reflections	1755
No. of parameters	157
No. of restraints	2
H-atom treatment	H-atom parameters constrained
$\Delta\rho_{\text{max}}, \Delta\rho_{\text{min}}$ ( $\text{e \AA}^{-3}$ )	0.69, -1.13

#### 2.2.2.4 Synthesis of [(bpz)Cu(OH)(ClO<sub>4</sub>)(H<sub>2</sub>O)]<sub>2</sub>.2H<sub>2</sub>O:

##### 2.2.2.4.1 Preparations:

The [(bpz)Cu(OH)(ClO<sub>4</sub>)(H<sub>2</sub>O)]<sub>2</sub>.2H<sub>2</sub>O complex is prepared by dissolve 37.3 mg (0.1 mmol) copper(II) perchlorate hexahydrate (Cu(ClO<sub>4</sub>)<sub>2</sub>.6H<sub>2</sub>O) in 8 ml of methanol with stirring for five minutes at room temperature, then 15.9 mg (0.1 mmol) of 2,2'-bipyrazine is dissolved in 4 ml of methanol and then adding to the light green solution with continuous stirring for half hour. After that, 11.62 mg (0.1 mmol) of N,N-diethylethylenediamine (C<sub>6</sub>H<sub>16</sub>N<sub>2</sub>), which it dissolved in 6 ml of methanol, was added to the clear solution with continuous stirring for also about half hour. A clear green solution was filtered and left until the most of solvent evaporated at room temperature. A blue black single crystal suitable to X-ray analysis was filtrated off and air dried.

##### 2.2.2.4.2 Crystal Data:

A summary of the key crystallographic information is given in (table 2.4) for the [(bpz)Cu(OH)(ClO<sub>4</sub>)(H<sub>2</sub>O)]<sub>2</sub>.2H<sub>2</sub>O complex. [281-287]

**Table 2.4:** Crystal Data and Structure Refinement Parameters for [(bpz)Cu(OH)(ClO<sub>4</sub>)(H<sub>2</sub>O)]<sub>2</sub>.2H<sub>2</sub>O complex.

Molecular formula	C <sub>16</sub> H <sub>22</sub> Cl <sub>2</sub> Cu <sub>2</sub> N <sub>8</sub> O <sub>14</sub>
Molecular weight	748.39

Crystal system, space group	Triclinic, P-1
Temperature (K)	295
Unit cell dimension	
a, b, c (Å)	8.0391 (10), 8.1718 (9), 10.5662 (14)
$\alpha, \beta, \gamma$ (°)	77.973 (5), 80.465 (6), 84.271 (5)
V (Å <sup>3</sup> )	667.98 (14)
Z	1
Radiation type	Mo Ka
$\mu$ (mm <sup>-1</sup> )	1.88
Crystal size (mm)	0.22 × 0.19 × 0.12
Data collection	
Diffractometer	Bruker Kappa Apex2
Absorption correction	Numerical Analytical Absorption (De Meulenaer & Tompa, 1965)
$T_{\min}, T_{\max}$	0.70, 0.80
No. of measured, independent and observed [ $I > 2.0\sigma(I)$ ] reflections	10260, 2590, 2096
$R_{\text{int}}$	0.032
$(\sin \theta/\lambda)_{\text{max}}$ (Å <sup>-1</sup> )	0.617
Refinement	
$R[F^2 > 2\sigma(F^2)], wR(F^2), S$	0.051, 0.112, 1.00
No. of reflections	2096
No. of parameters	187
No. of restraints	3
H-atom treatment	H-atom parameters constrained
$\Delta\rho_{\text{max}}, \Delta\rho_{\text{min}}$ (e Å <sup>-3</sup> )	0.97, -0.85

### 2.2.2.5 Synthesis of $[\text{Ni}(\text{dipyam})_2(\text{bpz})](\text{ClO}_4)_2$

#### 2.2.2.5.1 Preparations:

The  $[\text{Ni}(\text{dipyam})_2(\text{bpz})](\text{ClO}_4)_2$  complex is prepared by dissolve 73.1 mg (0.2 mmol) nickel(II) perchlorate hexahydrate ( $\text{Ni}(\text{ClO}_4)_2 \cdot 6\text{H}_2\text{O}$ ) in 5 ml of methanol with stirring for twenty minutes at room temperature, then 33.9 mg (0.2 mmol) of 2,2'-dipyridylamine ( $\text{C}_{10}\text{H}_9\text{N}_3$ ) dissolved in 6 ml of methanol and adding to the clear solution of metal with continuous stirring for 17.5 hours. After that, 30.5 mg (0.192 mmol) of 2,2'-bipyrazine is dissolved in 5 ml of methanol and added to the mixture with continues stirring for extra four hours. After that, 10 ml of methanol is added to the solution with continuous stirring and the reflux turned on at temperature 60 C° for 17.5 hours. Subsequently, to the hot clear solution, 10 ml of water is added with continuous stirring and reflux for two and

half hours. A clear yellow solution was filtered and left until the most of solvent evaporated at room temperature. An orange single crystal suitable to X-ray analysis was filtrated off and air dried. The percentage yield of this complex is 30.40 %.

#### 2.2.2.5.2 Crystal Data:

A summary of the key crystallographic information is given in (table 2.5) for the [Ni(dipyam)<sub>2</sub>(bpz)](ClO<sub>4</sub>)<sub>2</sub> complex. [281-287]

**Table 2.5:** Crystal Data and Structure Refinement Parameters for [Ni(dipyam)<sub>2</sub>(bpz)](ClO<sub>4</sub>)<sub>2</sub> complex

Molecular formula	C <sub>28</sub> H <sub>24</sub> Cl <sub>2</sub> N <sub>10</sub> NiO <sub>8</sub>
Molecular weight	758.18
Crystal system, space group	Monoclinic, C2/c
Temperature (K)	295
a, b, c (Å)	16.919 (3), 11.2635 (18), 17.588 (4)
β (°)	113.037 (4)
V (Å <sup>3</sup> )	3084.4 (10)
Z	4
Radiation type	Mo Kα
μ (mm <sup>-1</sup> )	0.87
Crystal size (mm)	0.16 × 0.14 × 0.07
Data collection	
Diffractometer	Bruker Kappa Apex2
Absorption correction	Numerical Analytical Absorption (De Meulenaer & Tompa, 1965)
T <sub>min</sub> , T <sub>max</sub>	0.89, 0.94
No. of measured, independent and observed [I > 2.0σ(I)] reflections	14457, 2926, 2238
R <sub>int</sub>	0.020
(sin θ/λ) <sub>max</sub> (Å <sup>-1</sup> )	0.612
Refinement	
R[F <sup>2</sup> > 2σ(F <sup>2</sup> )], wR(F <sup>2</sup> ), S	0.041, 0.064, 1.00
No. of reflections	2238
No. of parameters	222
H-atom treatment	H-atom parameters constrained
Δρ <sub>max</sub> , Δρ <sub>min</sub> (e Å <sup>-3</sup> )	0.25, -0.26

### 2.2.2.6 Synthesis of [Cu(bpz)<sub>3</sub>](ClO<sub>4</sub>)<sub>2</sub>.2CH<sub>3</sub>CN:

#### 2.2.2.6.1 Preparations:

The [Cu(bpz)<sub>3</sub>](ClO<sub>4</sub>)<sub>2</sub>.2CH<sub>3</sub>CN complex was prepared by dissolve 37.5 mg (0.1 mmol) of copper(II) perchlorate hexahydrate (Cu(ClO<sub>4</sub>)<sub>2</sub>.6H<sub>2</sub>O) in 11 ml of acetonitrile with stirring at room temperature for five minutes, then 30.8 mg (0.192 mmol) of 2,2'-bipyrazine is dissolved in 4 ml of acetonitrile with continuous stirring for half hour, After that, 56.2 mg (0.2 mmol) of tricyclohexylphosphine (C<sub>18</sub>H<sub>33</sub>P) is dissolved in 4 ml of acetonitrile and added to the solution with stirring for half hour. After that while stirring continuous, the reflux turned on at temperature 70 C° for 21.5 hours. A clear green solution was filtered and left until the most of solvent evaporated at room temperature. A green single crystal suitable to X-ray analysis was filtrated off and air dried. The percentage yield of this complex is 82.77 %.

#### 2.2.2.6.2 Crystal Data:

A summary of the key crystallographic information is given in (table 2.6) for the [Cu(bpz)<sub>3</sub>](ClO<sub>4</sub>)<sub>2</sub>.2CH<sub>3</sub>CN complex. [281-287]

**Table 2.6:** Crystal Data and Structure Refinement Parameters for [Cu(bpz)<sub>3</sub>](ClO<sub>4</sub>)<sub>2</sub>.2CH<sub>3</sub>CN complex.

Molecular formula	C <sub>28</sub> H <sub>24</sub> C <sub>12</sub> CuN <sub>14</sub> O <sub>8</sub>
Molecular weight	819.05
Crystal system, space group	Monoclinic, P 21/n
Wavelength	0.71073 Å
Temperature (K)	173 (2)
Unit cell dimensions	
a, b, c (Å)	11.2508(6), 22.1602(12), 13.6980(8)
A, b, g (°)	90°, 90.302(5)°, 90°
V (Å <sup>3</sup> )	3415.1(3)
Z	4
Density calculated (Mg/m <sup>3</sup> )	1.593
Absorption coefficient (mm <sup>-1</sup> )	0.868
F (000)	1668
Crystal size (mm <sup>3</sup> )	0.090 x 0.020 x 0.020
Theta range for data collection	3.497 to 25.645°
Index ranges	-13<=h<=13, -26<=k<=26, -16<=l<=16
Reflections collected	28424
Independent reflections	6401 [R(int) = 0.1298]

Completeness to theta = 25.000°	99.7 %
Absorption correction	Semi-empirical from equivalents
Max. and min. transmission	1.000 and 0.678
Refinement method	Full-matrix least-squares on F <sup>2</sup>
Data / restraints / parameters	6401 / 78 / 517
Goodness-of-fit on F <sup>2</sup>	1.402
Final R indices [I>2sigma(I)]	R1 = 0.1502, wR2 = 0.2690
R indices (all data)	R1 = 0.1896, wR2 = 0.2855
Extinction coefficient	n/a
Largest diff. peak and hole	0.900 and -0.859 e.Å <sup>-3</sup>

## Chapter Three

---

### *Result and Discussion*

Series of copper(II) complexes are prepared and structurally characterized, in which they are containing different nitrogen donor ligands as 2,2'-bipyrazine (bpz), 2-(aminomethyl)pyridine (amp), 2,2'-dipyridylamine (dipyam), and/or containing coordinated nitrate and water molecules. Beside to preparing a nickel(II) complex that contained dipyam and bpz ligands. It found that the copper atom is both five and six-coordinated in these complexes, and ligands are bidentately bonded only through N atom or chelated through H and O atoms of counter ions as water and nitrate molecules. Where some of their counter ions are coordinated toward center metal atom and other neutralized the charge of the complex. Additionally to that, solvent as water also participated and coordinated. Majority of the prepared complexes are mononuclear that having mixed ligands which is the aiming of this work, but there are not. At least, some of these observations are noticed by other researches. [270]

The X-ray diffraction analysis for  $[(bpz)Cu(OH)(ClO_4)(H_2O)]_2 \cdot H_2O$ ,  $[Cu(amp)_2(NO_3)_2]$ ,  $[Cu(dipyam)(H_2O)(pca)]ClO_4$ , and  $[Cu(bpz)_2(H_2O)](NO_3)_2$   $[Ni(dipyam)_2(bpz)](ClO_4)_2$  complexes are done by Professor Dr. Antonios Hatzidimitriou, laboratory of Inorganic Chemistry, Faculty of Chemistry, Aristotle University of Thessaloniki from Greece, while  $[Cu(bpz)_3](ClO_4)_2 \cdot 2CH_3CN$  complex is done by Prof. Dr. Matthias Wagner, Institut für Anorganische und Analytische Chemie, Goethe-Universität Frankfurt, and Dr. Michael Bolte, Institut fuer Anorganische und Analytische Chemie, J.-W.-Goethe-Universitaet from Germany.

#### **3.1 $[(bpz)Cu(OH)(ClO_4)(H_2O)]_2 \cdot H_2O$ complex:**

Hydroxo-bridged metal complexes, where metals bonded through hydroxobridge, are worthy spread wide in material, coordination and supramolecular chemistry fields. [280(a)] Hydroxo bridged copper complexes, for example, played an important role in different applications as bioinorganic chemistry, magneto-chemistry, materials science, multi-metal center catalysis, superconductivity and multielectron redox chemistry. [288] In more details, biological studies, for instance, found that hydroxo-bridged dicopper(II)

complex has special affinity for a tyrosinase inhibitor, which is used for prevention of skin disease, via an unsymmetrical binding. [289(a-b)] Furthermore, the interest turned to study the hydroxo-bridged copper(II) complexes due to their active catalytically for oxidative coupling reactions. [290(a-b)]

On one hand, their magnetically is simple, where every metal ion has one unpaired electron; in which they could be ferro- or antiferromagnetically arrangement based on their molecular geometry. [280(a-b), 291(a-j), 292(a-b), 293(a-d), 294(a)] In other words, the hydroxo-bridged Cu(II) binuclear complexes have a huge attention in research area due to their condensed-phase magnetic properties, in which they illustrate the relationship between the analysis of single crystal structure and the interpretation of the magnetic results. Furthermore, because Cu(II) has one active unpaired electron in d orbital ( $d^9$ ), their data analysis could employ in the improving of empirical correlations of strength of magnetic coupling in super exchange-coupled compounds referring to Cu–OH–Cu bridging unit. [280(a, c), 291(a-c, f), 293(a-e), 294(a-b), 295(a, c)]

At the same point, the characterization of their magneto-structural property have got a lot of attention. [292(a-b), 293(a), 294(a), 295(a)] Hatfield and Hodgson derived an equation to consume the J value of dihydroxo-bridged copper(II) complexes according to Cu–O–Cu bridging angle ( $\alpha$ ) and the singlet–triplet energy gap, in which the theoretical result are justified by Hoffmann and co-workers. If the value of bridging angle ( $\alpha$ )  $> 97.5^\circ$ , an antiferromagnetic interaction will be expected. While, the ferromagnetic interaction is found, if  $\alpha < 97.5^\circ$ . The study of magnetic behavior extends to analogous parameters via bending of  $\text{Cu}_2\text{O}_2$ , distance of the Cu–O and Cu–Cu and the location of hydrogen atom of hydroxide ligand. [291(a-j), 293(a), 294(a-d), 295(a-c)]

At least, the role of dihydroxo-bridged copper(II) complexes is not only to know the magnetic properties but also to probability of metal–metal interaction returned to the rather small bridging ligands. And also, they considered as model compounds for spin-coupling phenomena. [296]

In this work, the synthesis complex was prepared based on how Khaled prepared except using methanol solvent instead of water. In trying to get less angle and distance between Cu center atoms than what Khaled got.

### 3.1.1 Crystal structure for $[(bpz)Cu(OH)(ClO_4)(H_2O)]_2 \cdot H_2O$ complex:

The structure of complex  $[(bpz)Cu(OH)(ClO_4)(H_2O)]_2 \cdot H_2O$  is built up of two separate centrosymmetric  $\mu$ -hydroxy copper(II) dimers, with two terminal 2,2'-bipyrazine ligands in equatorial position, while two molecules of water and two perchlorate ions located in axial position with trans arrangement, and one water molecule. The depicted complex is showed in figure 3.1 with the atom numbering.

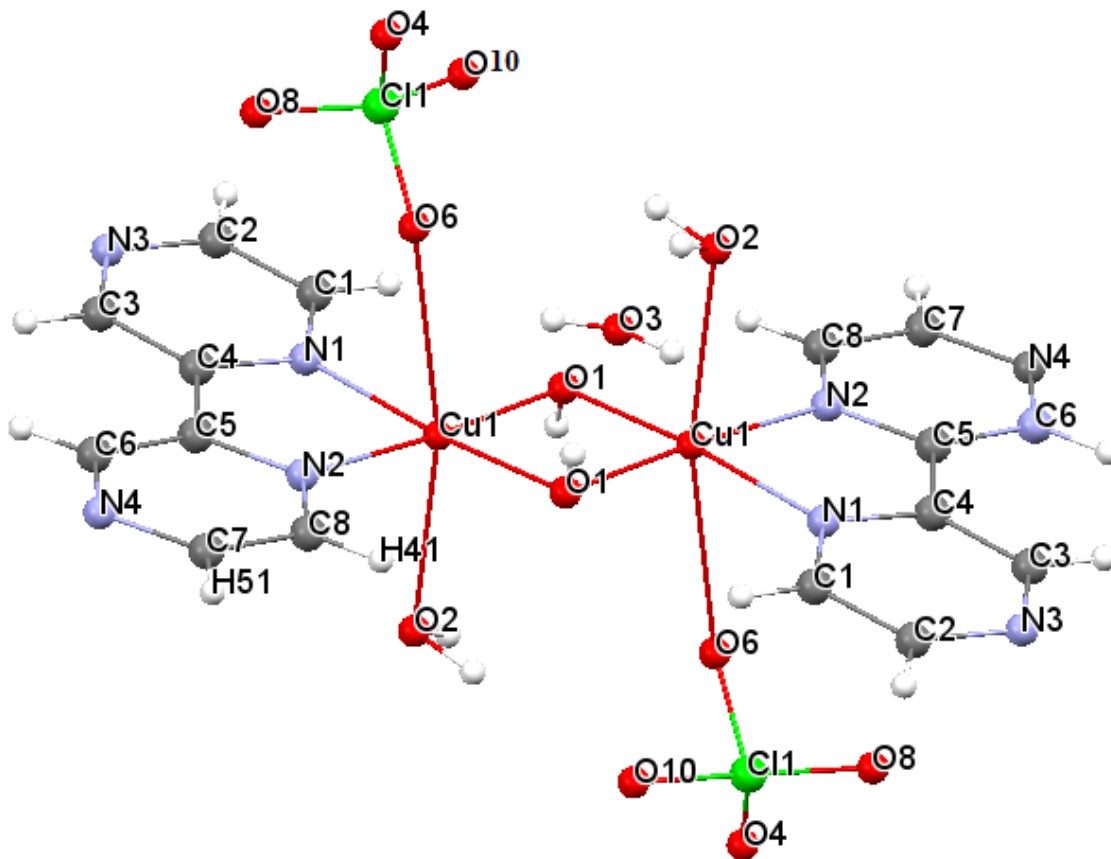


**Figure 3.1** View the structure of  $[(bpz)Cu(OH)(ClO_4)(H_2O)]_2 \cdot H_2O$  complex with showing the numbering.

Each copper(II) atom of complex is a distorted elongated tetragonal octahedral geometry,  $CuN_2O_4$ , in which the axial positions are occupied by oxygen atoms of water and perchlorate particles, while two nitrogen atoms of 2,2'-bipyrazine ligand and two oxygen of the bridging hydroxo groups are located in equatorial sites. The Cu-N distances are for Cu(1)-N(1) is 1.994 Å and for Cu(1)-N(2) is 2.012 Å, see figure 3.2. The values are rather closed to 2,2'-dipyridylamine, 2,2'-bipyridine and 2,2'-bipyrimidine- copper(II) complexes.

[280(d-i)]. The Cu-O (hydroxo bridge) distances are 1.931 and 1.923 Å, are slightly shorter in 2,2'-bipyrimidine-containing copper(II) complexes.[280(d,g)] The bond distance of Cu1-O6 and Cu1-O2 at axial site is longer compared to the distance bond of Cu metal with ligand at equatorial position, where their distance's value is 2.742, 2.486 Å respectively (table 3.1, fig. 3.2).

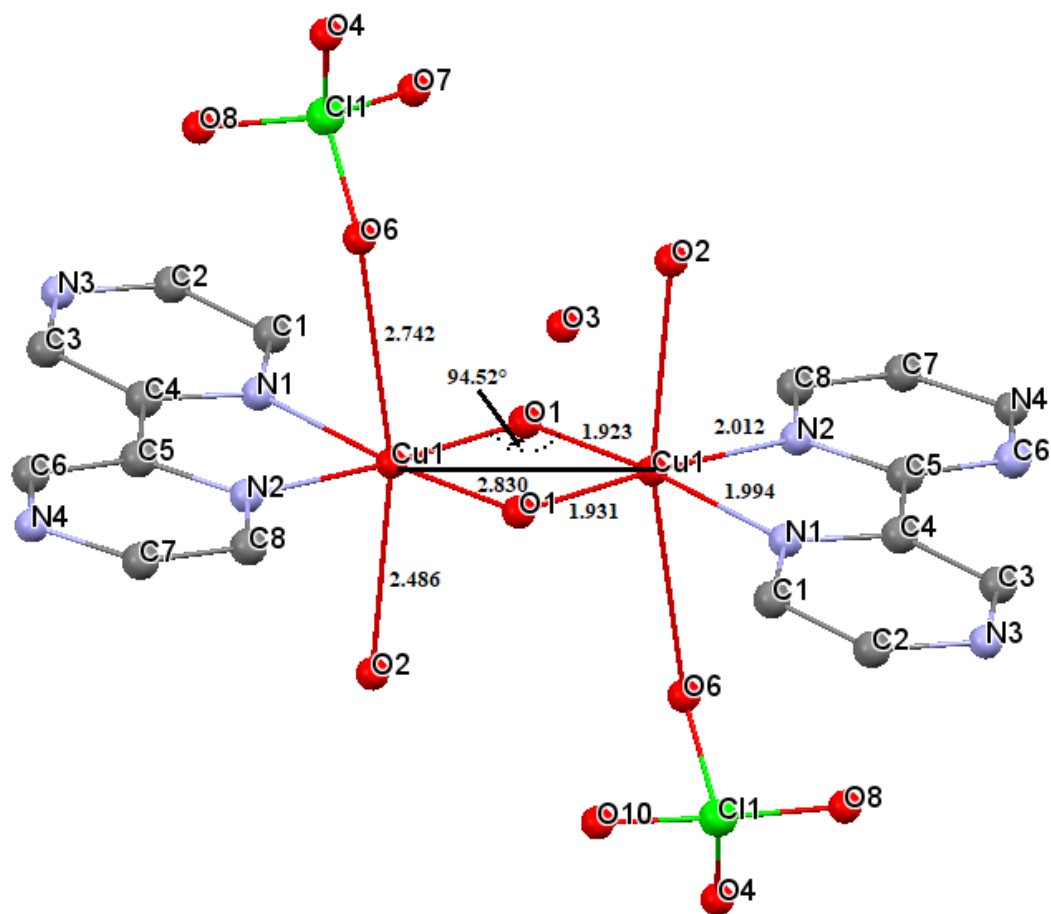


**Figure 3.2** View the distance between Cu-ligand and the angle between Cu1-O-Cu1 of the  $[(bpz)Cu(OH)(ClO_4)(H_2O)]_2 \cdot H_2O$  complex according to the X-ray analysis.

In the  $CuN_2O_4$  coordination environment, the two axial Cu1-O6 and Cu1-O2 distances are different ( $\Delta d = 0.256 \text{ \AA}$ ), resulting in a six-coordination environment (fig. 3.2). Distortion of the regular octahedral geometry is noticed for the  $CuN_2O_4$  coordination environment, with a cis X-Cu1-X angle range (N1-Cu1-O6, O6-Cu1-O1) 80.11–92.90° and a trans X-Cu1-X angle range (O2-Cu1-O6, N2-Cu1-O1) 167.57–176.30° (table 3.2).

The Cu–Cu distance within the dinuclear unit is 2.830 Å, while the Cu1–O1–Cu1 angle is 94.52° as in (table 3.1 and table 3.2, fig.3.2). By comparing with the results of Khaled thesis, the difference between the distance of Cu-Cu and the angle of Cu1–O1–Cu1 are little bit, where the distance is 2.826 Å and the angle is 94.40°. As a result, the complex that Khaled synthesized is only had the shortest distance and smallest angle comparable with others [280(a)]. The exchange interaction of the complex should be ferromagnetic due to the value of Cu–O–Cu angle is smaller than 97.5°. [280(k)]

**Table 3.1:** Bond length [Å] of [(bpz)Cu(OH)(ClO<sub>4</sub>)(H<sub>2</sub>O)]<sub>2</sub>.H<sub>2</sub>O complex

Atom 1	Atom 2	Length	Atom 1	Atom 2	Length
Cu1	Cu1	2.830(1)	N2	C5	1.338(6)
Cu1	O6	2.74(1)	N3	C2	1.333(8)
Cu1	O6	2.74(1)	N3	C2	1.333(8)
Cu1	O2	2.486(5)	N4	C6	1.332(7)
Cu1	O2	2.486(5)	N4	C6	1.332(7)
Cu1	N2	2.012(5)	N2	C8	1.330(7)
Cu1	N2	2.012(5)	N2	C8	1.330(7)
Cu1	N1	1.994(4)	N1	C1	1.329(7)
Cu1	N1	1.994(4)	N1	C1	1.329(7)
Cu1	O1	1.931(4)	N4	C7	1.327(7)
O1	Cu1	1.931(4)	N4	C7	1.327(7)
Cu1	O1	1.923(3)	N3	C3	1.323(7)
Cu1	O1	1.923(3)	N3	C3	1.323(7)
C4	C5	1.475(7)	C2	H121	0.925
C4	C5	1.475(7)	C2	H121	0.925
O8	C11	1.45(2)	C3	H141	0.923
O8	C11	1.45(2)	C3	H141	0.923
O6	C11	1.44(1)	C6	H71	0.922
O6	C11	1.44(1)	C6	H71	0.922
O10	C11	1.41(1)	C8	H41	0.921
O10	C11	1.41(1)	C8	H41	0.921
O4	C11	1.405(5)	C1	H111	0.917
O4	C1	1.405(5)	C1	H111	0.917
C5	C6	1.392(8)	C7	H51	0.916
C5	C6	1.392(8)	C7	H51	0.916
C7	C8	1.381(8)	O3	H12	0.823
C7	C8	1.381(8)	O2	H151	0.821
C3	C4	1.378(7)	O2	H151	0.821
C3	C4	1.378(7)	O3	H11	0.821
C1	C2	1.374(7)	O2	H1	0.810

C1	C2	1.374(7)	O2	H1	0.810
N1	C4	1.351(7)	O1	H21	0.800
N1	C4	1.351(7)	O1	H21	0.800
N2	C5	1.338(6)	O3	H11	0.821
			O3	H12	0.823

**Table 3.2:** Bond angle [deg.] of [(bpz)Cu(OH)(ClO<sub>4</sub>)(H<sub>2</sub>O)]<sub>2</sub>.H<sub>2</sub>O complex

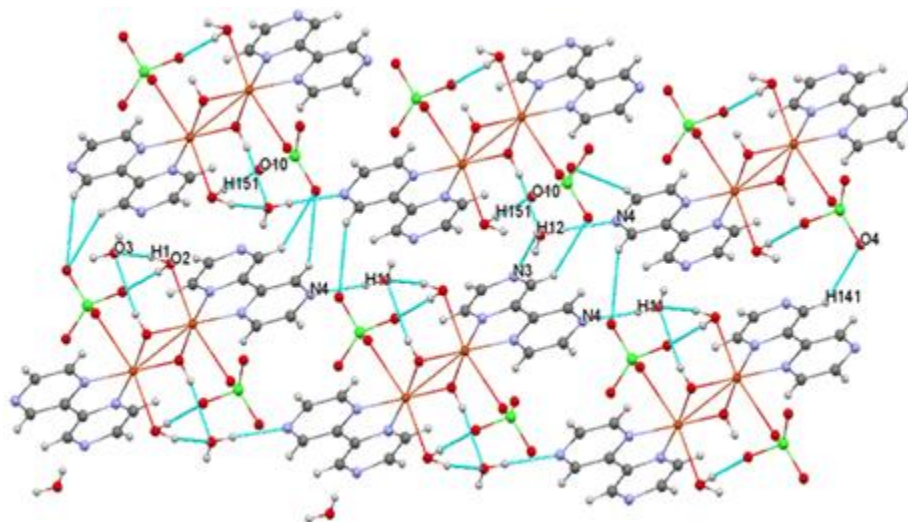
O1 <sup>i</sup> —Cu1—O1	85.47 (14)	C5—N2—C8	118.5 (4)
O1 <sup>i</sup> —Cu1—O2	91.72 (18)	C2—N3—C3	116.6 (4)
O1—Cu1—O2	93.37 (19)	C6—N4—C7	117.2 (4)
O1 <sup>i</sup> —Cu1—O6	99.5 (3)	N1—C1—C2	121.0 (4)
O1—Cu1—O6	92.9 (3)	C1—C2—N3	122.1 (5)
O2—Cu1—O6	167.6 (3)	N3—C3—C4	122.8 (4)
O1 <sup>i</sup> —Cu1—N1	95.72 (14)	C3—C4—N1	119.7 (4)
O1—Cu1—N1	173.00 (16)	C3—C4—C5	125.9 (4)
O2—Cu1—N1	93.48 (19)	N1—C4—C5	114.4 (4)
O6—Cu1—N1	80.1 (3)	C4—C5—N2	115.5 (4)
O1 <sup>i</sup> —Cu1—N2	176.29 (15)	C4—C5—C6	124.4 (4)
O1—Cu1—N2	97.29 (14)	N2—C5—C6	120.1 (4)
O2—Cu1—N2	90.59 (18)	C5—C6—N4	121.6 (4)
O6—Cu1—N2	78.0 (3)	N4—C7—C8	122.2 (5)
N1—Cu1—N2	81.25 (15)	C7—C8—N2	120.4 (5)
Cu1 <sup>i</sup> —O1—Cu1	94.53 (14)	O8—C11—O6	105.4 (8)
Cu1—O6—C11	134.8 (7)	O8—C11—O10	139.5 (9)
Cu1—N1—C1	127.1 (3)	O6—C11—O10	85.3 (9)
Cu1—N1—C4	114.8 (3)	O8—C11—O4	107.5 (6)
C1—N1—C4	117.8 (4)	O6—C11—O4	109.2 (5)
Cu1—N2—C5	114.1 (3)	O10—C11—O4	105.3 (8)
Cu1—N2—C8	127.4 (3)		

The hydrogen bond are formed according to the nitrogens of pyrazine ligands, oxygen of perchlorate, hydroxide groups of coordinated water and crystallization water molecule, as what figure 3.3 showed [280(l)]. The table 3.3 below displays the corresponding D-H, H···A and D···A bond distances and D-H···A bond angles, where D: donor, A: acceptor.

**Table 3.3:** Hydrogen geometry (Å, °) of [(bpz)Cu(OH)(ClO<sub>4</sub>)(H<sub>2</sub>O)]<sub>2</sub>.H<sub>2</sub>O complex

D—H...A	D—H (Å)	H...A (Å)	D...A (Å)	D—H...A (°)
O2—H1...O3	0.81	2.02	2.745 (7)	149
O3—H11...N4 <sup>ii</sup>	0.82	2.13	2.943 (7)	170
O3—H12...N3 <sup>iii</sup>	0.82	2.13	2.934 (7)	167
O1—H21...O3 <sup>i</sup>	0.80	2.19	2.982 (7)	168
C1—H111...O10 <sup>vi</sup>	0.92	2.59	3.239 (7)	129
C2—H121...O2 <sup>vii</sup>	0.93	2.52	3.436 (7)	171
C3—H141...O4 <sup>viii</sup>	0.92	2.53	3.299 (7)	141
C3—H141...O4 <sup>ix</sup>	0.92	2.52	3.232 (7)	134
O2—H151...O10 <sup>i</sup>	0.82	2.21	3.027 (7)	176

As what the table 3.3 shown, the following atoms act as hydrogen bond acceptor, including nitrogens of 2,2'-bipyrazine ligand with crystallization water molecules [O3—H11...N4] and [O3—H12...N3], crystallization water molecules with hydroxo bridge [O1—H21...O3], coordinated water molecule with different site of chain [O1—H21...O2], and perchlorate group [O2—H151...O10].

**Figure 3.3a** View the crystal packing of [(bpz)Cu(OH)(ClO<sub>4</sub>)(H<sub>2</sub>O)]<sub>2</sub>.H<sub>2</sub>O complex with showing the inter-intrachain H-bonds.

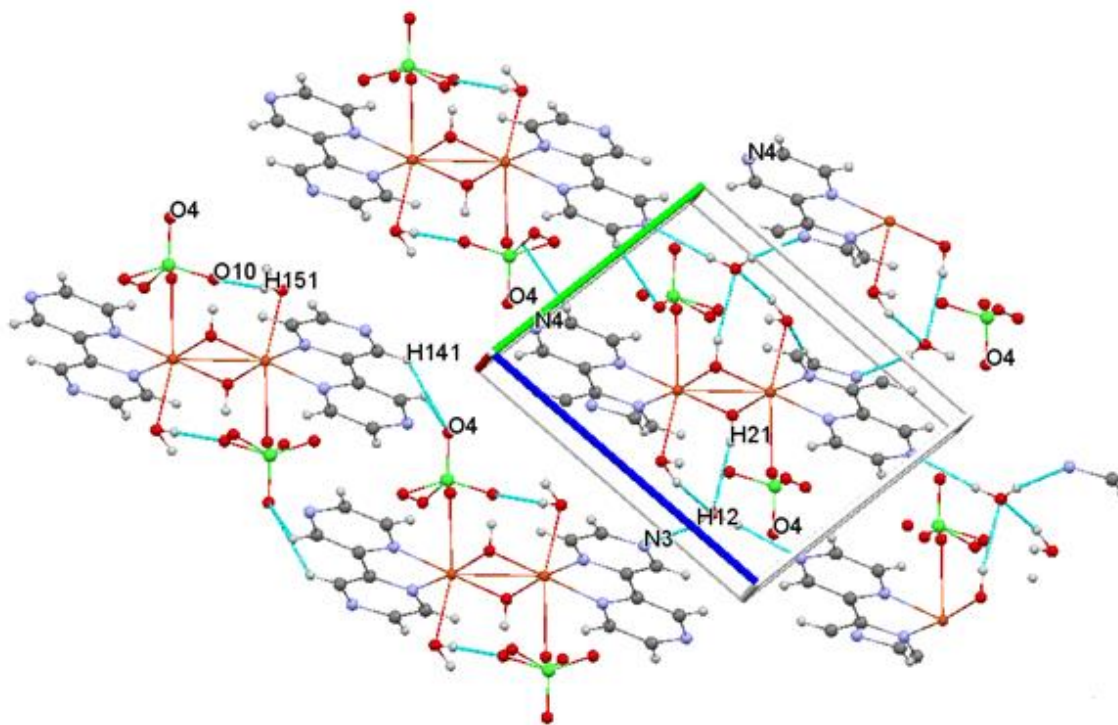


**Figure 3.3b** View the crystal packing of the complex with showing inter-interchain H-bonds within the unit cell.

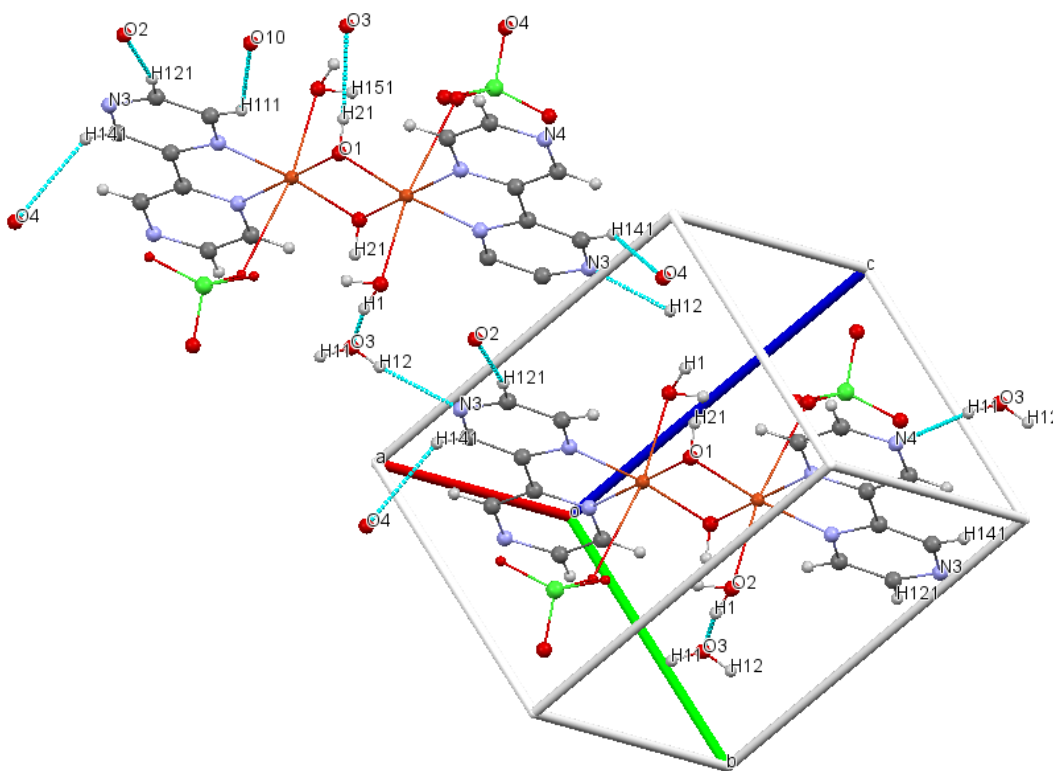


**Figure 3.3c** View the inter-intrachain H-bonds within unit cell.

The structure of the complex is filled with hydrogen bond interactions including water molecules and compound lead to form two-dimensional sheet. These sheets linked with others into three dimensional (fig. 3.4) via the oxygen atoms of perchlorate with C-H bond of 2,2'-bipyrazine in distance range between 2.530 – 2.663 Å with C $\cdots$ O, which its distance is 3.127 Å, and nitrogen atom of 2,2'-bipyrazine with hydrogen of water molecule with distance value 2.934 Å. Adjacent Cu chains overlapping with others by  $\pi$ - $\pi$  stacking interactions connecting each 2,2'-bipyrazine ligand at 3.484 Å closest connection, resulting in forming of 2D sheets.

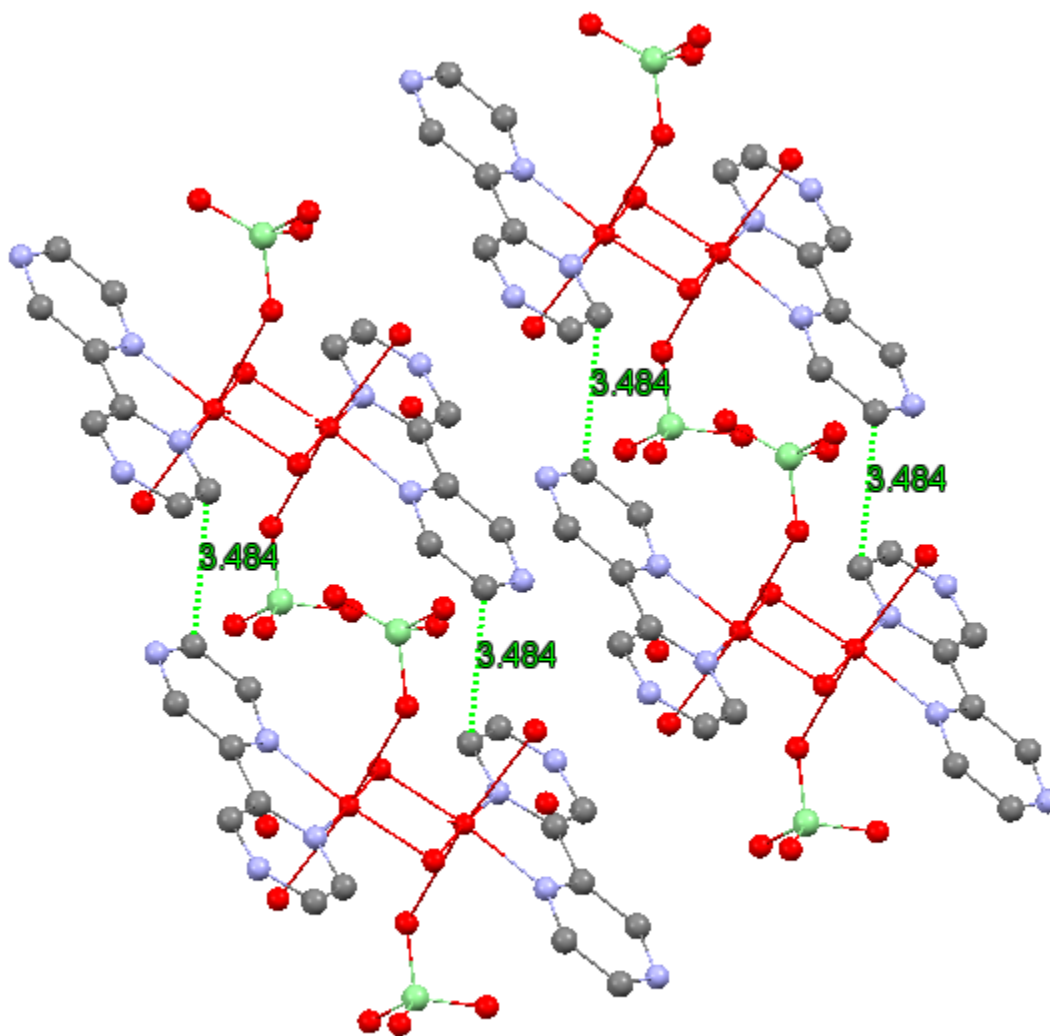


**Figure 3.4:** View the distance of  $\pi$ - $\pi$  stacking interaction between the 2,2'-bipyrazine ligand in the  $[(\text{bpz})\text{Cu}(\text{OH})(\text{ClO}_4)(\text{H}_2\text{O})]_2 \cdot \text{H}_2\text{O}$  complex.

### 3.2 [Cu(bpz)<sub>2</sub>(H<sub>2</sub>O)](NO<sub>3</sub>)<sub>2</sub> complex:

The [Cu(bpz)<sub>2</sub>(H<sub>2</sub>O)](NO<sub>3</sub>)<sub>2</sub> complex in this work was synthesized by new method, characterized by IR analysis, thermal analysis using differential scanning calorimetry (DSC) and X-ray diffraction analysis. This complex is resemble in some kind of to many produced complexes, for example, [Cu(ibh)<sub>2</sub>(H<sub>2</sub>O)<sub>2</sub>](NO<sub>3</sub>)<sub>2</sub>, ibh = isopropanone benzoyl hydrazone (C<sub>6</sub>H<sub>5</sub>CONHN=C(CH<sub>3</sub>)<sub>2</sub>) [244], [Cu(bpy)<sub>2</sub>(H<sub>2</sub>O)<sub>2</sub>](NO<sub>3</sub>)<sub>2</sub>·4.5C<sub>2</sub>H<sub>5</sub>OH, bpy = 4,4'-bipyridyl. [248], [M(bpy)<sub>2</sub>(NO<sub>3</sub>)](NO<sub>3</sub>) where bpy = 2,2'-bipyridine, M = Cu(I)/(II) or Ni(II), etc. [262] With agreement with previous studies of these complexes, this work aims to form new Cu(II) complexes using 2,2'-bipyridine ligand.

Analysis data indicated to that copper(II) complexes have variability in stereochemistry obtained by copper(II). That caused to expand their usage in different applications. For example, they considered as one of the most active complexes in proteins due to their responsibility of storage and transport of molecules, moreover, having a role in inhibition of tumor growth, as what studies concluded about [Cu(ibh)<sub>2</sub>(H<sub>2</sub>O)<sub>2</sub>](NO<sub>3</sub>)<sub>2</sub> [244]

On other perspective, other researchers used 4,4'-bipyridyl (bpy) instead of ibh = isopropanone benzoyl hydrazone ligand using Cu(II) metal and so synthesize [Cu(bpy)<sub>2</sub>(H<sub>2</sub>O)<sub>2</sub>](NO<sub>3</sub>)<sub>2</sub>·4.5C<sub>2</sub>H<sub>5</sub>OH, in trying to produce new metal-organic coordination polymers, in which their functions include gas storage, catalysis, etc. [248] On one hand, [Cu(bpy)<sub>2</sub>(NO<sub>3</sub>)]NO<sub>3</sub>, bpy = 2,2'-bipyridine complex has highest efficiency in the DNA cleavage during manipulation genetic process as what biological studies reported. [250] In addition, others found that Cu(I) and Ni(II) coordination polymers with ligands as 4,4'-bipyridine and 2,2'-bipyridine, forming [M(bpy)<sub>2</sub>(NO<sub>3</sub>)](NO<sub>3</sub>) complex lead to form many coordination environment and supramolecular networks. [262]

### 3.2.1 Infrared Spectroscopy

#### 3.2.1.1 2,2'-bipyrazine (bpz) ligand

The infrared absorption frequencies obtained for the free 2,2'-bipyrazine are listed in (table 3.4), and spectrum is given in (fig. 3.5).

**Table 3.4:** Infrared frequencies ( $\text{cm}^{-1}$ ) for the free 2,2'-bipyrazine and assignments.

Assignment	Frequencies ( $\text{cm}^{-1}$ )
$\nu$ C-H	3078vw, 3050vw, 2972s, 2988s and 2901s
$\nu$ C $\equiv$ N	1592m, 1564m and 1528m
$\nu$ C $\equiv$ C	1433m, 1413m, 1394m and 1341m and 1311w
$\delta$ ring	1460s
$\beta$ CH	1251m and 1230m
$\beta$ ring, breathing	1149s and 1076vs and 991vs
Ring bending	670vw, 645vw and 621vw
ring-H in-plane binding vibrations	1028s, 1018s and 846s and 813w
out-of-plane ring-H bending and $\tau$ ring	881w, 780vw, 756w, 733w 594vw and 520vw

The FTIR spectra of 2,2'-bipyrazine have various characteristic bands including,  $\nu$  C-H,  $\nu$  C $\equiv$ C,  $\nu$  C $\equiv$ N,  $\delta$  ring,  $\beta$  CH,  $\beta$  ring, ring bending, ring-H in-plane binding vibrations, out-of-plane ring-H bending and torsion ( $\tau$ ) ring. Both very weak peaks at 3078 and 3050  $\text{cm}^{-1}$ , and the strong bands at 2972, 2988, 2901  $\text{cm}^{-1}$  related to  $\nu$  C-H. The three medium bands at 1592, 1564 and 1528  $\text{cm}^{-1}$  contributed to  $\nu$  C $\equiv$ N, while the medium bands at 1433, 1413, 1394, 1341 and 1311  $\text{cm}^{-1}$  correlated to  $\nu$  C $\equiv$ C, and the strong band at 1460  $\text{cm}^{-1}$  vibration essentially deformed the ring. In addition, the medium peaks at 1251 and 1230  $\text{cm}^{-1}$  are related to  $\beta$  CH, while the strong peak at 1149  $\text{cm}^{-1}$  and the very strong peaks at 1076, 991  $\text{cm}^{-1}$  are for  $\beta$  ring. Furthermore, the weak peaks at 670, 645 and 621  $\text{cm}^{-1}$  are related to ring bending. Moreover, the strong bands 1028, 1018, 846  $\text{cm}^{-1}$  and the weak band at 813  $\text{cm}^{-1}$  are referred to ring-H in-plane binding vibrations, whereas the weak bands at 881, 780, 756, 733  $\text{cm}^{-1}$  and the weak peaks at 594, 520  $\text{cm}^{-1}$  are mostly out-of-plane ring-H bending and vibration torsion ring. The very weak peak at 1726  $\text{cm}^{-1}$  could be considered as overtone. The assignment vibration of 2,2'-bipyrazine ligand is done with taking the analysis of 2,2'-bipyridine. [280 (a, j)] It would be worth to mention that the

peaks at 3685, 3675 and 3663  $\text{cm}^{-1}$  may be attributed to CH bond, since the CH bond beside the nitrogen varies from the CH bond that far the nitrogen atom in the ring, therefore, the two different peaks are formed. Also, Nakamoto indicated to that the highest frequencies ranges from 3700 – 2500  $\text{cm}^{-1}$ ; returns to X-H stretching, in which the intramolecular hydrogen bonds indicates the presence of exchangeable protons, within nitrogen and hydrogen atom of one single molecule. [297]

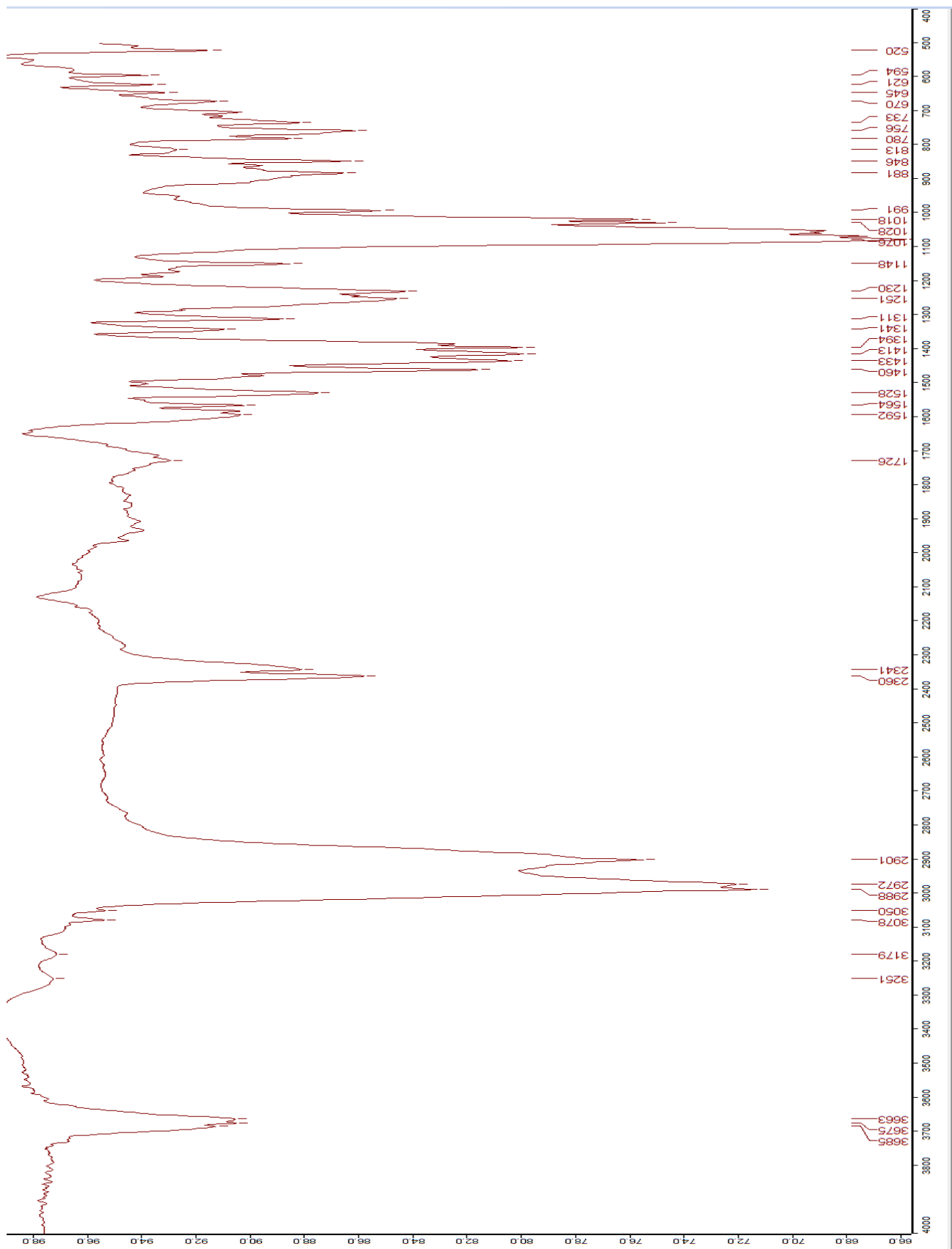


Figure 3.5 FTIR for 2,2'-bipyrazine ligand.

### 3.2.1.2 Infrared spectroscopy for $[\text{Cu}(\text{bpz})_2(\text{H}_2\text{O})](\text{NO}_3)_2$

The infrared absorption frequencies obtained for  $[\text{Cu}(\text{bpz})_2(\text{H}_2\text{O})](\text{NO}_3)_2$  complex are listed in (table 3.5), and spectra are given in (fig. 3.6).

**Table 3.5:** Comparison Infrared frequencies ( $\text{cm}^{-1}$ ) of 2,2'-bipyrazine ligand of  $[\text{Cu}(\text{bpz})_2(\text{H}_2\text{O})](\text{NO}_3)_2$  complex with the free 2,2'-bipyrazine ligand.

$[\text{Cu}(\text{bpz})_2(\text{H}_2\text{O})](\text{NO}_3)_2$ complex	Assignment	Frequencies ( $\text{cm}^{-1}$ ) for 2,2'-bipyrazine
3094 m, 3065 m and 3041 m	$\nu$ C-H	3078vw, 3050vw, 2972s, 2988 and 2901s
1593m, 1639m and 1621m	$\nu$ C=N	1592m, 1564m and 1528m,
1493w, 1379s and 1313vs	$\nu$ C=C	1394m and 1341m, 1311w, 1413m and 1433m
1479w and 1463m	$\delta$ ring	1460s
1146s, 1089m	$\beta$ ring, breathing	1148s and 1076vs and 991vs
1054s, 1029s and 1018s, 845s	ring-H in-plane binding vibrations	1028s, 1018s and 846s and 813w
717m	out-of-plane ring-H bending and $\tau$ ring	881w, 780vw, 756w, 733w 594vw and 520vw
1107m, 1041s and 826s	$\text{NO}_3^-$	-----

The IR spectrum of the  $[\text{Cu}(\text{bpz})_2(\text{H}_2\text{O})](\text{NO}_3)_2$  complex was compared with that of the free 2,2'-bipyrazine ligand (fig. 3.6). The shifting of bands to lower or higher wave number because of the coordinated metal or crystal packing. [280 (a)] It should be noticed that the peak  $1528 \text{ cm}^{-1}$  in 2,2'-bipyrazine ligand spectra shifted about  $45 \text{ cm}^{-1}$  and be in  $1639 \text{ cm}^{-1}$  in the spectra of the complex. This observation is strong evidence for the 2,2'-bipyrazine ligand is coordinated. The path of nitrate ion's vibration in the IR spectrum of  $[\text{Cu}(\text{bpz})_2(\text{H}_2\text{O})](\text{NO}_3)_2$  complex, displays a strong absorption at  $1107 \text{ cm}^{-1}$  related to N-O stretching, a weak intensity peak at  $826 \text{ cm}^{-1}$  owing to  $\text{NO}_3^-$  stretching, and a medium intensity peak at  $1041 \text{ cm}^{-1}$  is characteristic of the presence of uncoordinated  $\text{NO}_3$  and did not appear in free ligand. [298,299,300] for the broad peak that begin from  $3650-2600 \text{ cm}^{-1}$ , it contains an interfering absorption. The vibration the OH of water and the vibration C-H of bpz has a shoulder peak at  $3300-3400 \text{ cm}^{-1}$ . Compared with the FTIR of the ligand, there is no peak at  $3300-3500 \text{ cm}^{-1}$ , that is an evidence for no water molecule exists in the ligand, but there is a water molecule coordinated in the complex.

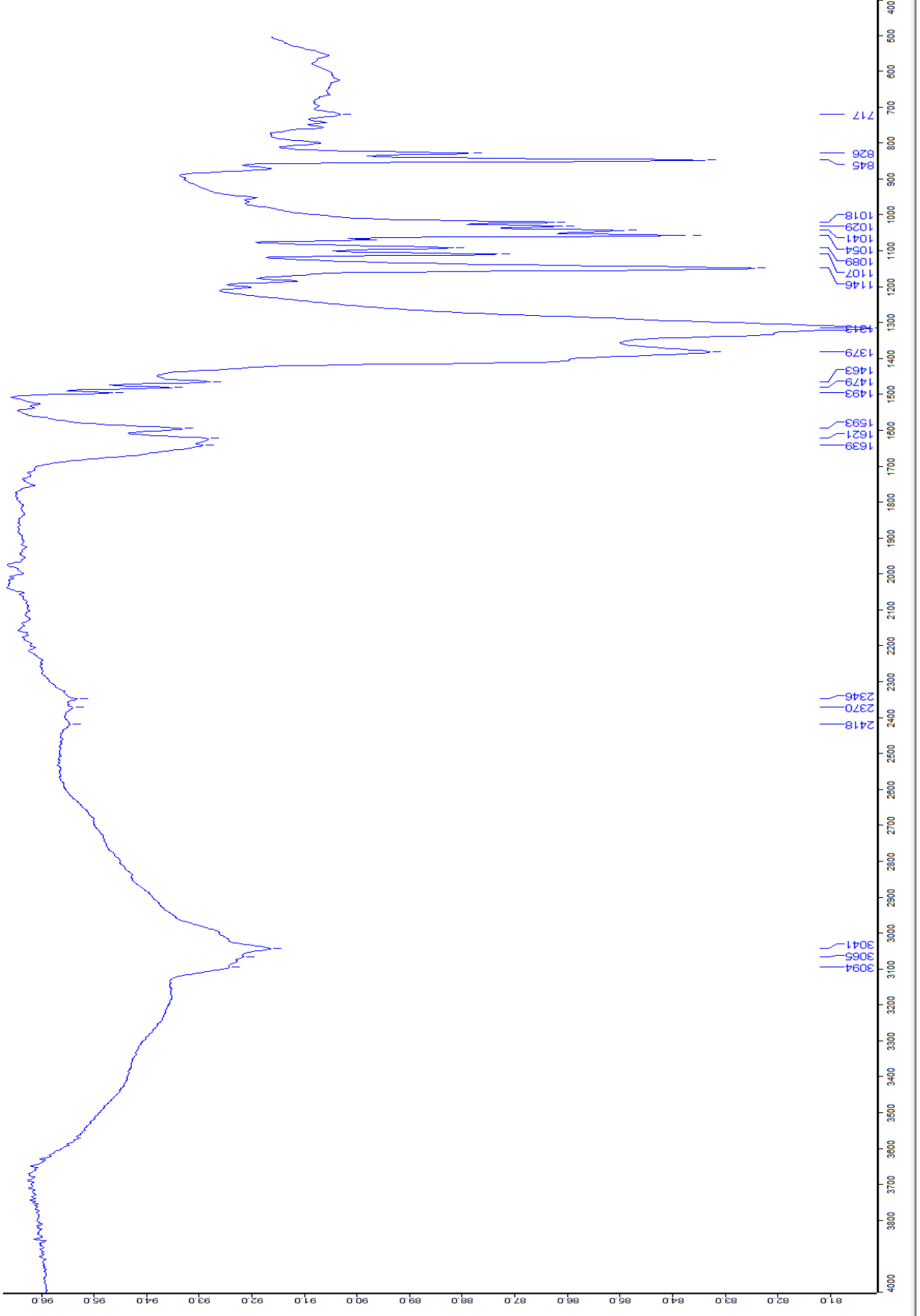
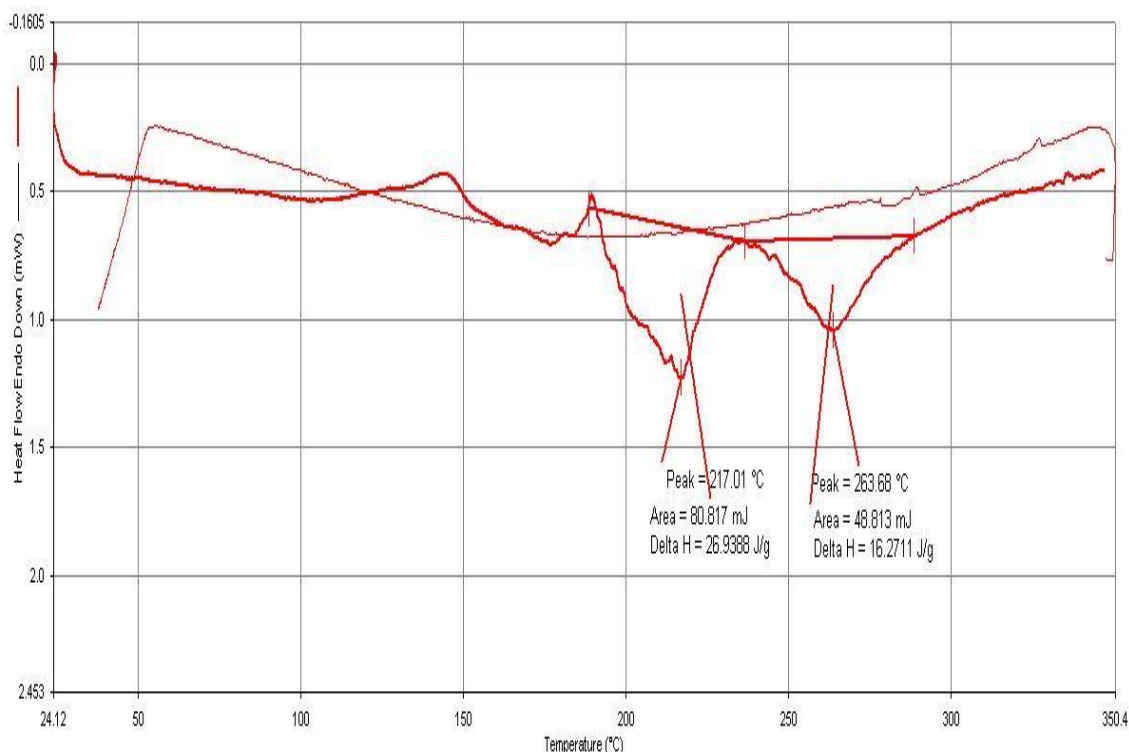


Figure 3.6 The infrared spectra of the [Cu(bpz)<sub>2</sub>(H<sub>2</sub>O)](NO<sub>3</sub>)<sub>2</sub> complex

### 3.2.2 Thermal analysis

The Differential Scanning Calorimetry (DSC) thermal analysis for the  $[\text{Cu}(\text{bpz})_2(\text{H}_2\text{O})](\text{NO}_3)_2$  complex were performed using Perkin Elmer DSC equipment. Samples about 6 mg of complex with aluminum pans, nitrogen gas flow and a scan rate  $5^\circ\text{C}/\text{min}$  from 25 up to  $350^\circ\text{C}$ , and then the cooling was done in the same range. The DSC curve (fig. 3.7) displayed an endothermic peak associated with enthalpy of  $26.9388 \text{ J/g}$  at  $T_{\text{max}} = 217.01^\circ\text{C}$ , followed by another endothermic peak associated with enthalpy of  $16.2711 \text{ J/g}$  at  $T_{\text{max}} = 263.68^\circ\text{C}$  which predict to melting point process. Also, two peaks are indicators to that there are two single components are formed, where 2,2'-bipyrazine ligand has possibility to form more than one single crystal compound.



**Figure 3.7** Differential Scanning Calorimetry (DSC) of  $[\text{Cu}(\text{bpz})_2(\text{H}_2\text{O})](\text{NO}_3)_2$  complex.

### 3.2.3 Crystal structure for $[\text{Cu}(\text{bpz})_2(\text{H}_2\text{O})](\text{NO}_3)_2$ :

The structure of complex  $[\text{Cu}(\text{bpz})_2(\text{H}_2\text{O})](\text{NO}_3)_2$  consists of, first, Cu(II) center, in which it is five coordinated with four nitrogen atoms of 2,2'-bipyrazine ligands, and

with one oxygen atom of the water molecule and, second, two nitrate molecules as counter ion, as what shown in the figure 3.8 below:

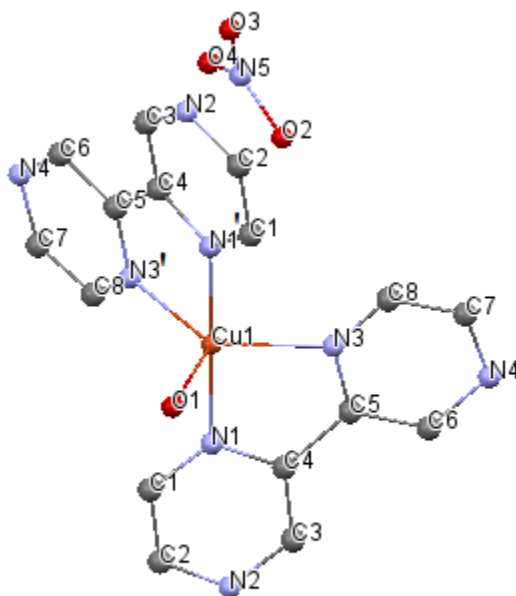


**Figure 3.8** View the structure of  $[\text{Cu}(\text{bpz})_2(\text{H}_2\text{O})](\text{NO}_3)_2$  complex, with showing the atomic numbering

Since the complex is an ionic structure that comprised chemically identical four cations  $[\text{Cu}(\text{bpz})_2(\text{H}_2\text{O})]^{+2}$  along with eight uncoordinated nitrate anions  $\text{NO}_3^-$  per unit cell, the relative arrangement of the constituents units in the unit cell are shown in figure 3.9 [298]

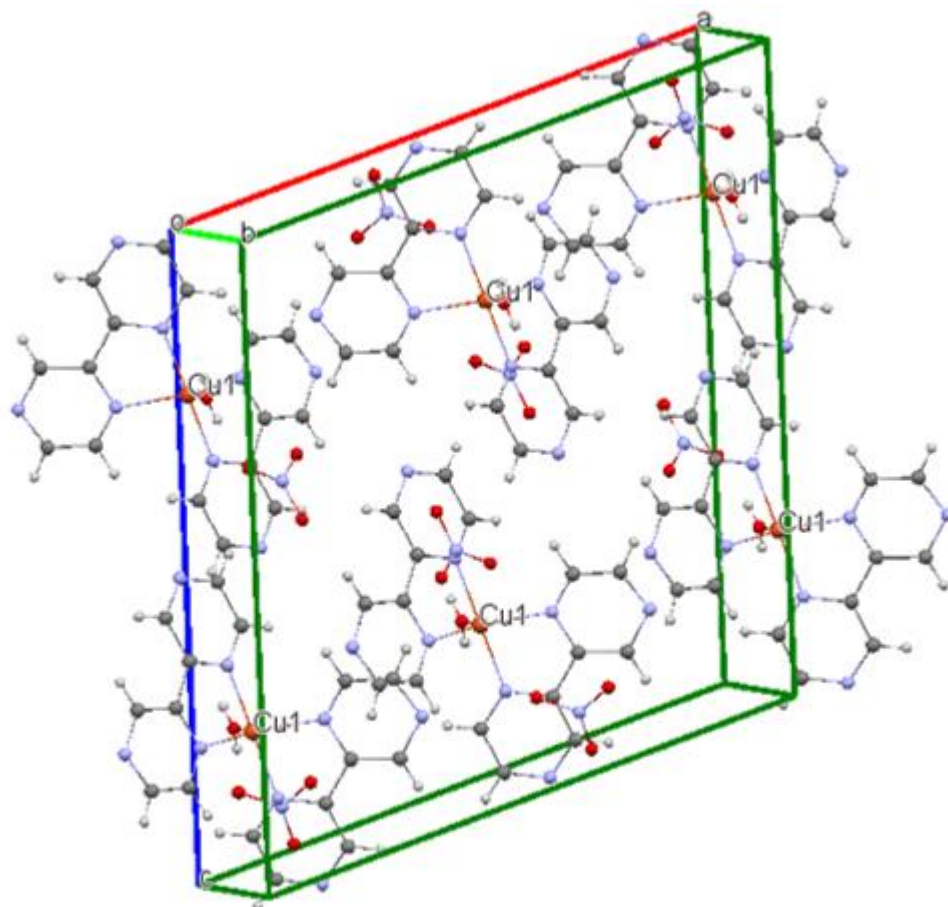


**Figure 3.9** View the structure packing of  $[\text{Cu}(\text{bpz})_2(\text{H}_2\text{O})](\text{NO}_3)_2$  complex within the unit cell.

The nitrate anions link the cations to form a chain structure through  $\text{O}-\text{H}\cdots\text{N}$  close contacts and  $\text{O}-\text{H}\cdots\text{O}$  hydrogen bonds, as what shown in the figure 3.10 below:

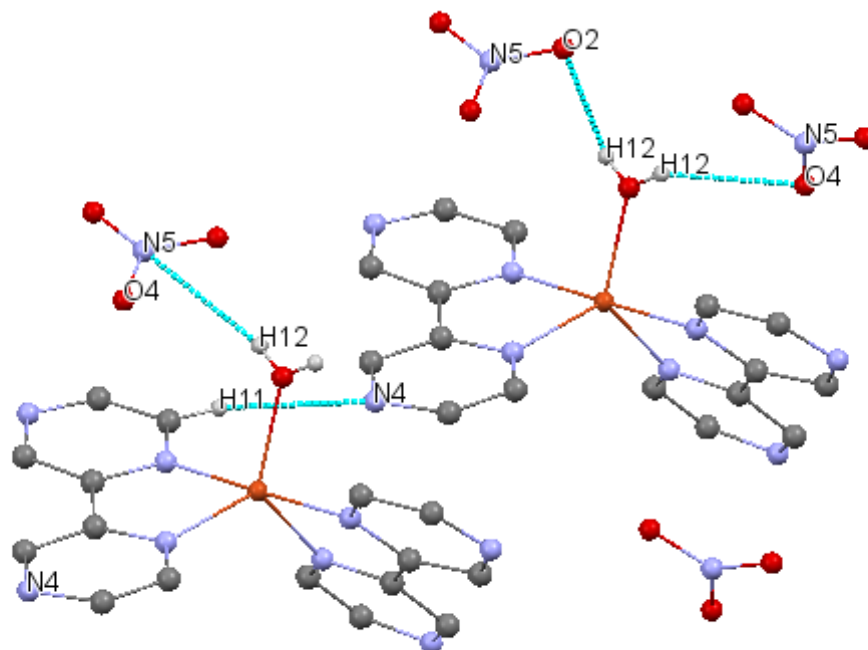


**Figure 3.10** View the inter-intrachain H-bonds of the  $[\text{Cu}(\text{bpz})_2(\text{H}_2\text{O})](\text{NO}_3)_2$  complex

The crystal structure reveals that the Cu atom of the complex has a distorted trigonal bipyramidal geometry. The Cu-N (where N is N1, N1<sup>i</sup>) bond lengths are 1.965(3), 1.965(3) Å respectively (table 3.6, fig. 3.11a) lie in the axial positions (fig. 3.8). While, the Cu-N (where N is N3, N3<sup>i</sup>) bond lengths are 2.067(4), 2.067(4) Å respectively (table 3.6, fig. 3.11a) lie in the equatorial positions (fig. 3.8). While, Cu–O1 bond located in the equatorial position and its length is 1.931(6) Å. These results are nearly equivalent to the value of the similar complexes. [280 (a, m, n)] They involve bite angle [N3<sup>i</sup>—Cu1—N1<sup>i</sup>] of 82.02° somewhat less than 90° (table 3.7, fig. 3.11a).

**Table 3.6:** Bond length [Å] of  $[\text{Cu}(\text{bpz})_2(\text{H}_2\text{O})](\text{NO}_3)_2$  complex

Atom 1	Atom 2	Length	Atom 1	Atom 2	Length
Cu1	N3 <sup>i</sup>	2.067 (4)	N4	C6	1.360 (7)
Cu1	N1 <sup>i</sup>	1.965 (3)	N4	C7	1.313 (7)
Cu1	N1	1.965 (3)	N5	O2	1.247 (6)
Cu1	N3	2.067 (4)	N5	O3	1.200 (6)
Cu1	O1	1.931 (6)	N5	O4	1.213 (6)

N1	C1	1.304 (6)	C1	C2	1.378 (7)
N1	C4	1.334 (5)	C3	C4	1.362 (6)
N2	C2	1.278 (7)	C4	C5	1.473 (6)
N2	C3	1.328 (7)	C5	C6	1.370 (6)
N3	C5	1.327 (5)	C7	C8	1.323 (7)
N3	C8	1.242 (6)			

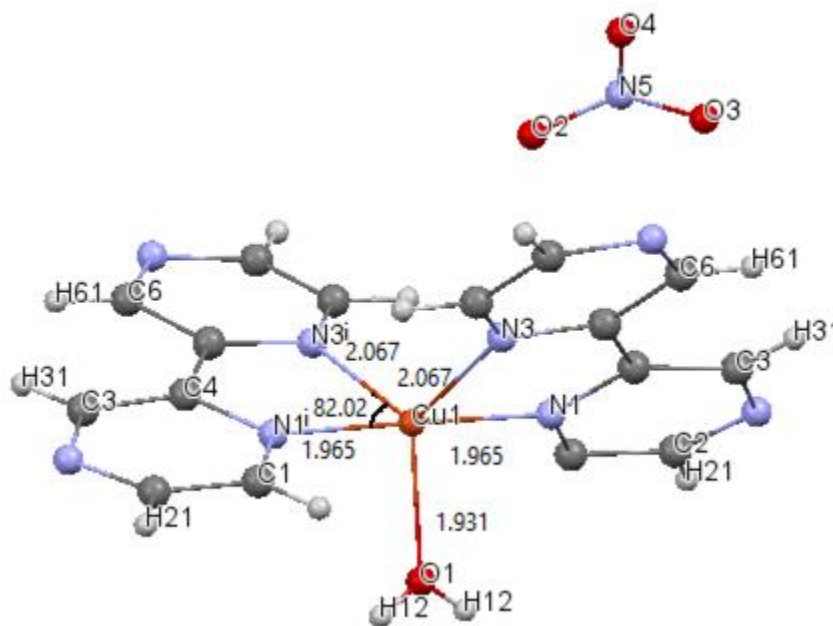


**Figure 3.11a** View the distance between the Cu-ligand and the angle between N3<sup>i</sup>-Cu1-N1<sup>i</sup> of the [Cu(bpz)<sub>2</sub>(H<sub>2</sub>O)](NO<sub>3</sub>)<sub>2</sub> according to the X-ray complex

As what noticed from (table 3.7, fig. 3.11b) the angle between N1<sup>i</sup>-Cu1-N1 is 179.0°(2) on the axial position and it is near to 180°. The angle between N3<sup>i</sup>-Cu1-N3 is 121.5°(2) on the equatorial position and it is near to 120°. Also, the angle between N3-Cu1-O1 is 119.26°(11) on the equatorial position and it is near to 120°. Therefore, these values are strong evidence to that the geometry of the complex is a distorted trigonal bipyramidal.

**Table 3.7:** Bond angle [deg.] of [Cu(bpz)<sub>2</sub>(H<sub>2</sub>O)](NO<sub>3</sub>)<sub>2</sub> complex

N3 <sup>i</sup> -Cu1-N1 <sup>i</sup>	82.02 (15)	C6-N4-C7	114.8 (5)
N3 <sup>i</sup> -Cu1-N1	98.47 (15)	O2-N5-O3	119.8 (5)

N1 <sup>i</sup> —Cu1—N1	179.0 (2)	O2—N5—O4	119.6 (5)
N3 <sup>i</sup> —Cu1—N3	121.5 (2)	O3—N5—O4	120.6 (5)
N1 <sup>i</sup> —Cu1—N3	98.47 (14)	N1—C1—C2	121.1 (5)
N1—Cu1—N3	82.02 (15)	C1—C2—N2	122.1 (5)
N3 <sup>i</sup> —Cu1—O1	119.26 (11)	N2—C3—C4	121.5 (5)
N1 <sup>i</sup> —Cu1—O1	89.50 (13)	C3—C4—N1	120.3 (4)
N1—Cu1—O1	89.50 (13)	C3—C4—C5	125.6 (4)
N3—Cu1—O1	119.26 (11)	N1—C4—C5	114.0 (4)
Cu1—N1—C1	127.0 (3)	C4—C5—N3	118.4 (4)
Cu1—N1—C4	115.5 (3)	C4—C5—C6	121.2 (4)
C1—N1—C4	117.4 (4)	N3—C5—C6	120.4 (4)
C2—N2—C3	117.4 (4)	C5—C6—N4	119.8 (5)
Cu1—N3—C5	110.0 (3)	N4—C7—C8	123.8 (5)
Cu1—N3—C8	130.9 (3)	C7—C8—N3	122.2 (5)
C5—N3—C8	119.0 (4)		
Trigonality index, $\tau$ 0.801			

Furthermore, the distortion of the polyhedron is obviously observable and confirmed by the values of the Trigonality  $\tau$ <sup>1</sup> (table 3.7) That's because the non-planarity of 2,2'-bipyrazine ligand and the formation of the six membered ring which is more demanding when coordinating. [300 (a-c), 301] One of the best examples about the distortion of the polyhedron is noticed in copper–quinolonato complexes with square–pyramidal geometry and N<sub>2</sub>O<sub>2</sub>Cl coordination sphere mentioned thus far. [300 (a, d)]

---

<sup>1</sup> Trigonality is defined based on bond angles in the coordination sphere.  $\tau = (\varphi_1 - \varphi_2) / 60$ , where  $\varphi_1$  and  $\varphi_2$  are the largest angles in the coordination sphere. The values are ranged between 0 and 1, in which 0 corresponds to a perfect square pyramid, while 1 corresponds to a perfect trigonal bipyramidal. [300 (a, c)]

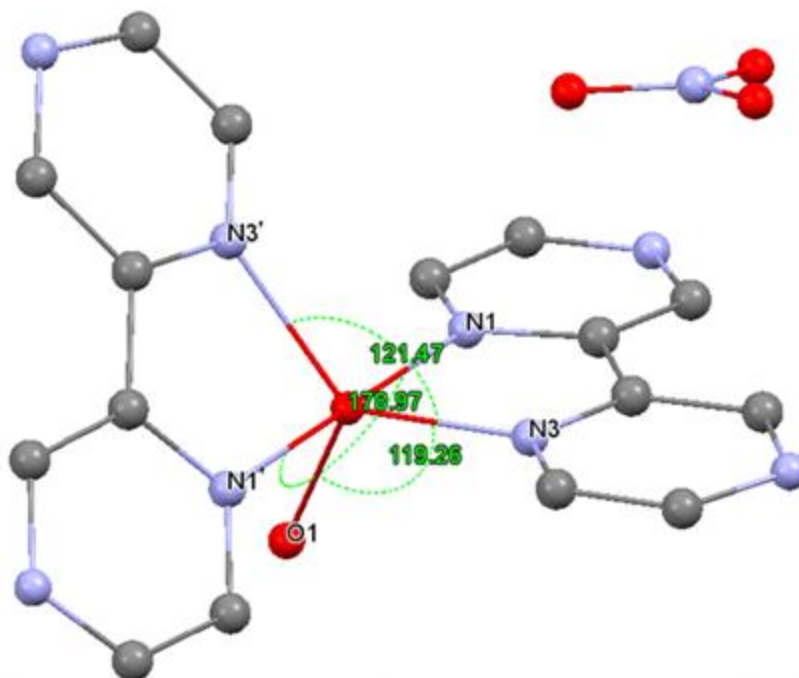


**Figure 3.11b** View the angles between the Cu-ligand of the  $[\text{Cu}(\text{bpz})_2(\text{H}_2\text{O})](\text{NO}_3)_2$  complex according to the X-ray analysis.

The hydrogen bond are formed according to nitrogen and the oxygen atoms of nitrate molecule. The strength of hydrogen bond would be weak or moderate, as what figure 3.12 showed. [280(a)] The table below displays the corresponding D-H, H $\cdots$ A and D $\cdots$ A bond distances and D-H $\cdots$ A bond angles, where D: donor, A: acceptor. As what the table 3.8 shown, the following atoms act as hydrogen bond acceptor, including nitrogen of nitrate group with coordinated water molecules [O1—H12 $\cdots$ N5], oxygen atoms of nitrate molecule with hydrogen atoms of coordinated water [O1—H12 $\cdots$ O2] and [O1—H12 $\cdots$ O4]. Also, the oxygen atoms of nitrate molecule with the hydrogen atom of 2,2'-bipyrazne ligand [C2—H21 $\cdots$ O3], [C3—H31 $\cdots$ O4] and [C6—H61 $\cdots$ O3]

**Table 3.8:** Hydrogen geometry ( $\text{\AA}$ ,  $^\circ$ ) of  $[\text{Cu}(\text{bpz})_2(\text{H}_2\text{O})](\text{NO}_3)_2$  complex

D—H $\cdots$ A	D—H ( $\text{\AA}$ )	H $\cdots$ A ( $\text{\AA}$ )	D $\cdots$ A ( $\text{\AA}$ )	D—H $\cdots$ A ( $^\circ$ )
O1—H12 $\cdots$ N5 <sup>ii</sup>	0.73	2.51	3.194 (7)	157
O1—H12 $\cdots$ O2 <sup>ii</sup>	0.73	2.02	2.726 (7)	164
O1—H12 $\cdots$ O4 <sup>ii</sup>	0.73	2.39	2.908 (7)	129
C2—H21 $\cdots$ O2 <sup>iii</sup>	0.93	2.46	3.349 (7)	162

C2—H21...O3 <sup>iii</sup>	0.93	2.46	3.236 (7)	141
C3—H31...O4 <sup>iv</sup>	0.92	2.59	3.389 (7)	145
C6—H61...O3 <sup>iv</sup>	0.92	2.17	3.071 (7)	167

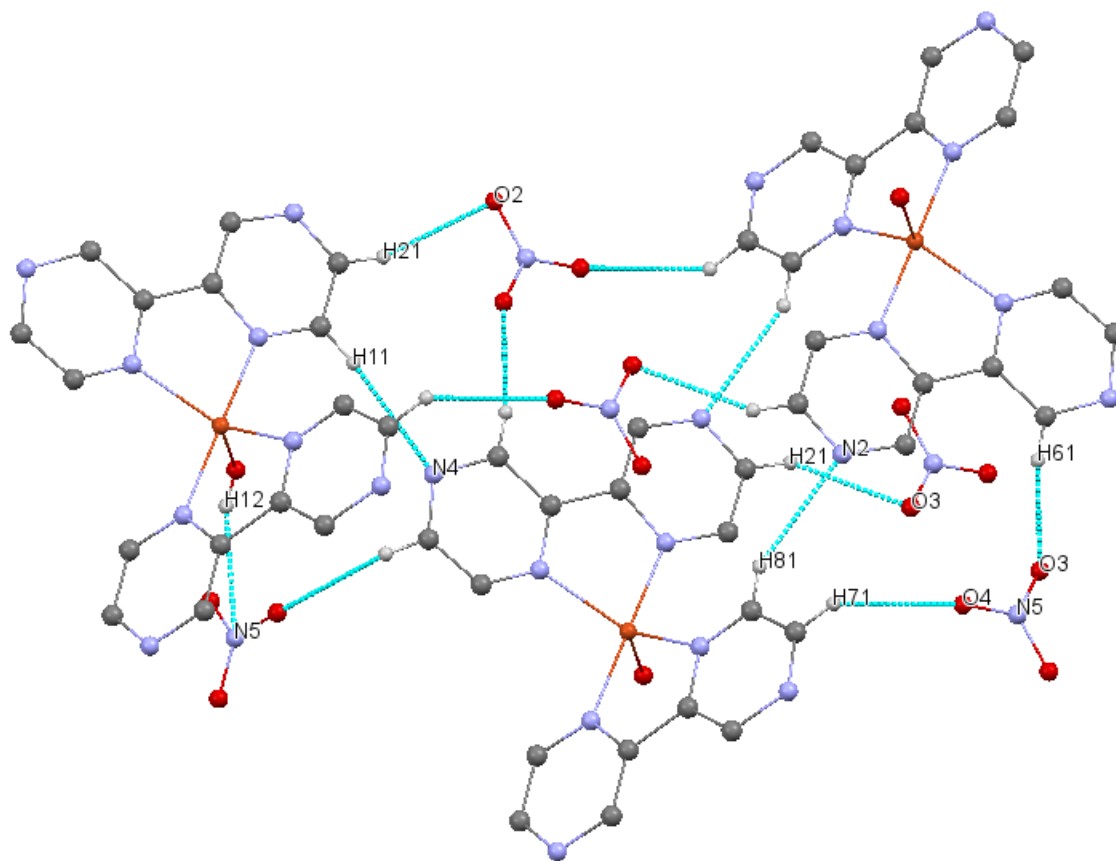


**Figure 3.12** View the crystal packing of  $[\text{Cu}(\text{bpz})_2(\text{H}_2\text{O})](\text{NO}_3)_2$  complex with showing the inter-intrachain H-bonds.

The role of nitrate anions is acting as bridges to bond with the cations of the complex via  $\text{O}-\text{H}\cdots\text{N}$  and  $\text{O}-\text{H}\cdots\text{O}$  hydrogen bonds and  $\text{C}-\text{H}\cdots\text{O}$  closed contacts forming three-dimensional sheet, the figure 3.13 shown. Moreover, the complex cations of  $[\text{Cu}(\text{bpz})_2(\text{H}_2\text{O})](\text{NO}_3)_2$  are stacked in the closest approach between the 2,2'-bipyrazine rings of  $4.990 \text{ \AA}$ , indicating no significant  $\pi\cdots\pi$  stacking interactions, figure 3.14

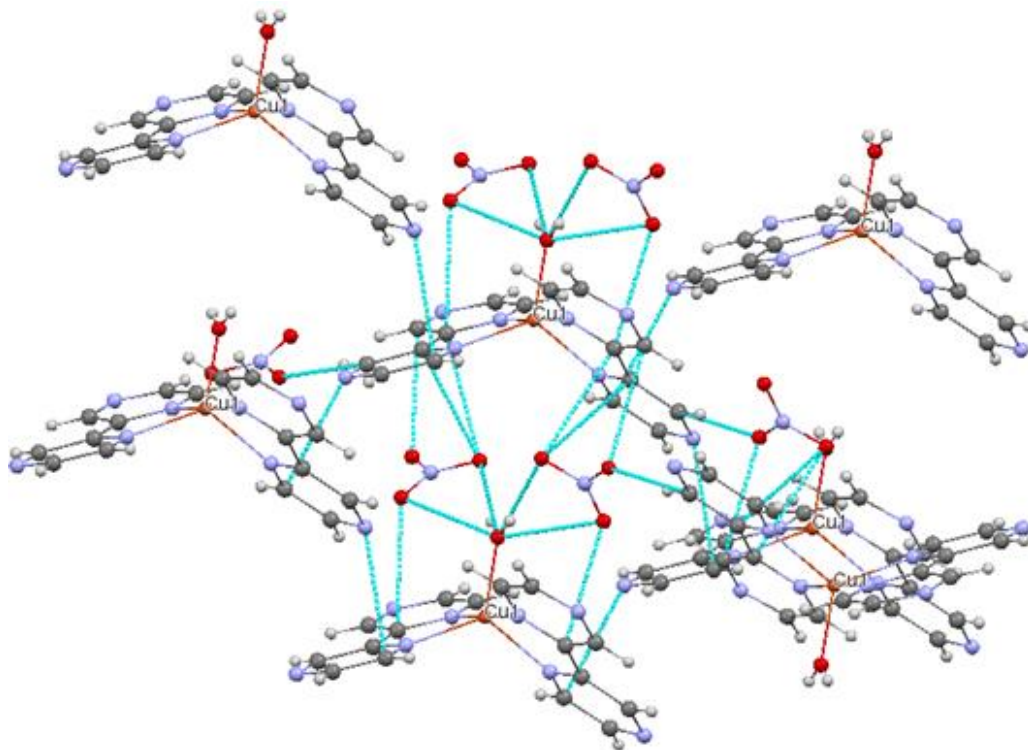


**Figure 3.13** View of the network around coordination water of the  $[\text{Cu}(\text{bpz})_2(\text{H}_2\text{O})](\text{NO}_3)_2$  complex and nitrate anion.

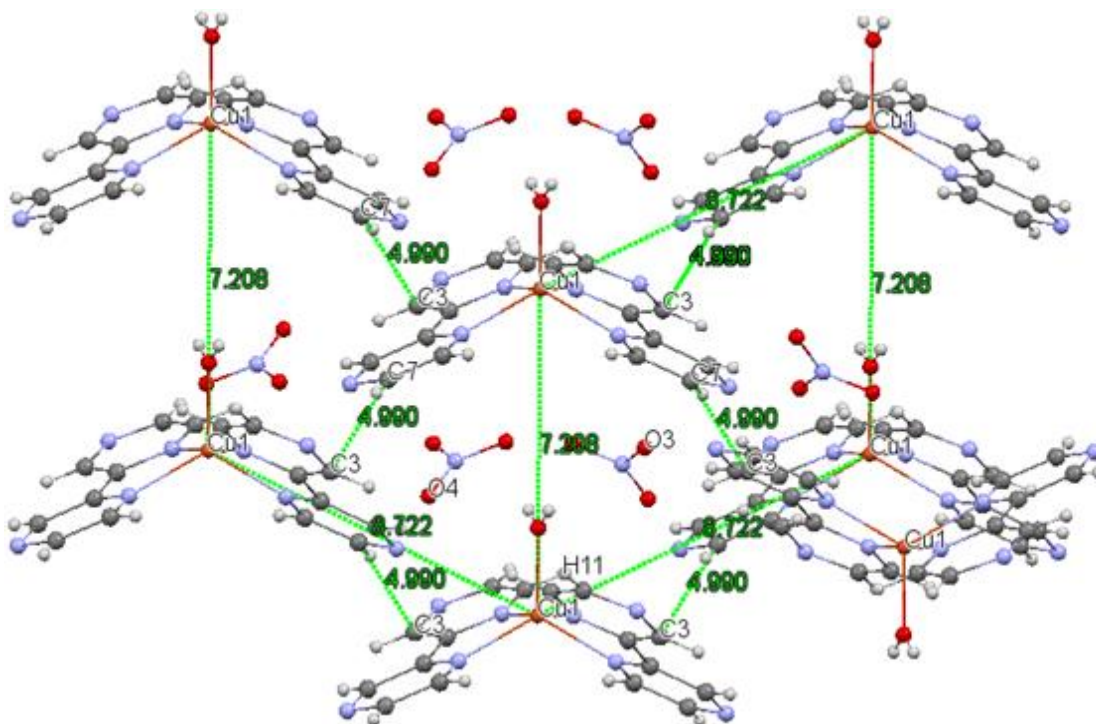


**Figure 3.14** View the View the  $\pi$ - $\pi$  stacking interactions distance between the 2,2'-bipyrazine ligand in  $[\text{Cu}(\text{bpz})_2(\text{H}_2\text{O})](\text{NO}_3)_2$  complex.

In each typical sheet, the adjacent coordination spheres are held together through C–H···O hydrogen bonds formed between the H-atoms on bpz and O-atoms on nitrate anion. [262] The NO<sub>3</sub><sup>-</sup> counter anion engaged the H-bonding with coordinated water molecule and with C-H bond of 2,2'-bipyrazine ring of the adjacent positively charged tetramers, reinforced by NO<sub>3</sub><sup>-</sup> anions at the periphery of the boxes, all of which are involved in multiple H bonding interactions with water ligands. [275] The packing in the crystal structure of the complex is caused by NO<sub>3</sub><sup>-</sup> anion which acts as linkers between the building blocks of the complex via the oxygen atoms of water and hydrogen atoms of 2,2'-bipyrazine ligands. Two disordered positions of the 2,2'-bipyrazine molecules are related by an inversion center. [267]

### **3.3 [Cu(dipyam)(H<sub>2</sub>O)(pca)]ClO<sub>4</sub> complex**

Bi and tridentate ligands have attracted caring in the studies which focused in supramolecular architectures studies. These kinds of ligands, especially that contain pyridine rings as 2-pyrazinecarboxylate (pca) and 2,2'-dipyridylamine, have ability to build network by both hydrogen bond via NH group and  $\pi$ - $\pi$  interaction through pyridine ring.[242] Beside to that, the variety coordination modes of pca and its derivatives encouraged chemists attend them toward projects of the construction of molecular structures. [303]

2-Pyrazinecarboxylic acid and its metal complexes also are important organic–inorganic hybrid material. In addition, they are used in different applications as development of selective catalysis, molecular recognition, electro-optic materials, semiconductor materials and magnetic materials. [209, 304 (a-d)] For example, the researchers investigated that Cu complexes like [Cu(pzca)<sub>2</sub>(H<sub>2</sub>O)], pzca = pyrazine-2-carboxamide, used as friendly environment catalysts, high quality, generality, simplicity, mild conditions reaction as needing short time and low temperature, easy to isolate the product, the yield of desired products ranges from good to excellent. [303, 305]

On one hand, the new interest of supermolecule studies is to trap the small gaseous molecules as CO<sub>2</sub> into channel-like structure and converted into more benefits substances. For example, the Zn complexes like [Zn(bpp)(pca)(MeOH)]ClO<sub>4</sub>, bpp = 1,3-bis(4-pyridyl)propane, prepared by construct cage-like nanostructure composing pyrazine-2-

carboxylate used as linker; because of its potential multidentate coordination ability. That facilitates the catching of CO<sub>2</sub> molecule and converted to organic derivatives. [269]

[Cu<sub>2</sub>(2-pac)<sub>2</sub>(4,4'-bpy)<sub>2</sub>].7H<sub>2</sub>O compound, 4,4'-bpy = 4,4'-bipyridine, is also used to understand the interactions among water clusters as they contributed in the stability of the crystal host. [306] Beside to that, the studies on [M(2-PCA)<sub>2</sub>(H<sub>2</sub>O)<sub>2</sub>] complex, where 2-PCA is a pyrazine-2-carboxylic acid ligand, show that the five membered chelate ring has a significant role in the stabilization of the aromatic system in the complexes. [307]

Pyrazinecarboxylic acid and its derivatives have essential role in biological properties as antimicrobial, antifungal and mimic the metal sites in enzymes. [211, 307]

### **3.3.1 Infrared Spectroscopy**

#### **3.3.1.1 2,2'-dipyridylamine (dipyam) ligand**

The infrared absorption frequencies obtained for the 2,2'-dipyridylamine are listed in (table 3.9), and spectra are given in (fig. 3.15)

**Table 3.9:** Infrared frequencies (cm<sup>-1</sup>) data for the 2,2'-dipyridylamine ligand and assignments.[168a, 297, 308, 319]

<b>Assignment</b>	<b>Frequencies (cm<sup>-1</sup>)</b>
νN-H	3252(w), 3684(w), 3663(w)
νC-H	3178(w), 3101(w), 2988(m), 2901(m), 1146(m), 1076(m), 1049(m), 910(m), 880(m), 858(m)
νCC,CN	1591(s), 1564(s), 1529(s), 1477(s), 1478, 1459(s), 1432(vs), 1414(vs), 1340(s), 1310(s), 1229(s)
αCCC	621(m), 762(vs), 672(m), 593(m)
Ring breathing	991(s)
Φ <sub>ring</sub>	732(s), 520(s)

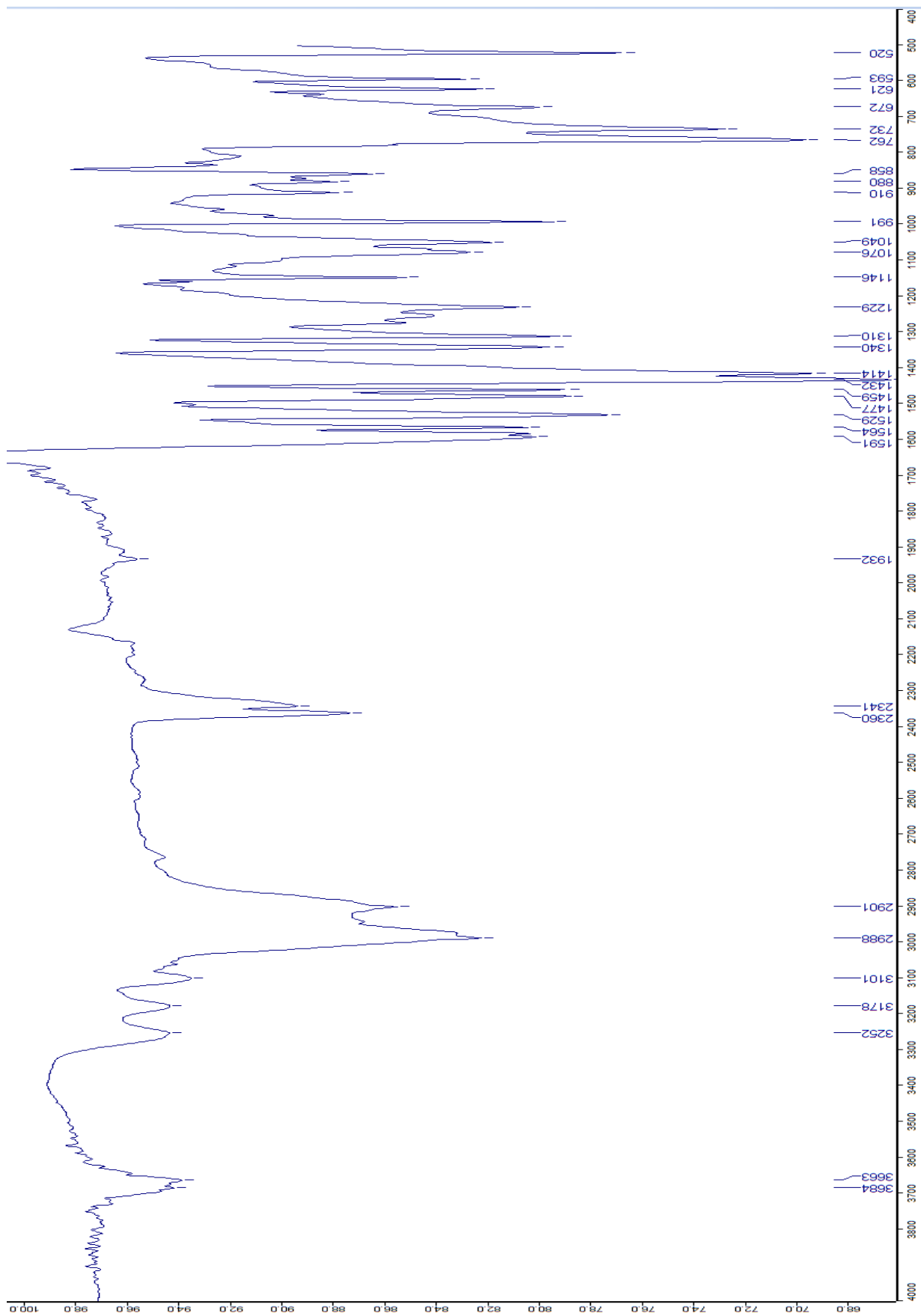


Figure 3.15 FTIR for 2,2'-dipyridylamine ligand

### 3.3.1.2 Infrared spectroscopy for [Cu(dipyam)(H<sub>2</sub>O)(pca)]ClO<sub>4</sub>

The infrared absorption frequencies obtained for [Cu(dipyam)(H<sub>2</sub>O)(pca)]ClO<sub>4</sub> complex via its spectra (fig.3.16), and the infrared absorption frequencies for 2-pyrazinecarboxylate ligand are got from (table 3.10).

**Table 3.10:** Infrared frequencies (cm<sup>-1</sup>) data for the 2-pyrazinecarboxylate ligand and assignments. [212]

Assignment	Frequencies (cm <sup>-1</sup> )
v(CH) <sub>ar</sub>	3066vw, 3068w, 3011vw, 2934vw
v(COO <sup>-</sup> ) <sub>ar</sub>	1616vs, 1384vs, 1619vs, 1381 vs
v(CC) <sub>ar</sub> , v(CN) <sub>ar</sub>	1575vw, 1527m, 1185s, 1163s, 1571s, 1520w, 1180sh, 1157m
v(CC) <sub>ar</sub> , v(CN) <sub>ar</sub> , β(CH) <sub>ar</sub>	1483m 1422s, 1293w, 1055s, 1464w, 1405s, 1245 w, 1051m
β(CH) <sub>ar</sub>	1030s, 1018m
β(COO <sup>-</sup> )	855m, 538 w, 848 m, 517w
γ(COO <sup>-</sup> )	807m, 795m
φ(CC) <sub>ar</sub> , γ(CH) <sub>ar</sub>	767vw
α(CCC)	727m, 633m, 734m, 673w
φ(CC) <sub>ar</sub>	432m
γ(CH) <sub>ar</sub>	990vw
γ(CH) <sub>ar</sub> , γ(NH) <sub>ar</sub>	889m, 874w
φ(CC) <sub>ar</sub>	433m

FTIR spectrum for [Cu(dipyam)(H<sub>2</sub>O)(pca)]ClO<sub>4</sub> complex (fig. 3.16) shows the bands of 2,2'-dipyridylamine ligand was moved to lower or to higher wave number according to metal coordination and crystal packing. The very weak bands at 3324, 3262, 3221, 3154 and 3120 cm<sup>-1</sup> which attributed to v(C-H) and v(N-H), the medium peaks at 1591, 1527 and 1415 cm<sup>-1</sup> beside to the strong band in 1482 cm<sup>-1</sup> composite to CC and CN vibrations. [280a, 309, 310, 314] The coordinated water molecules generally show characteristic peaks around 768 cm<sup>-1</sup> due to r(H<sub>2</sub>O) and 659 cm<sup>-1</sup> w(H<sub>2</sub>O). [311] IR spectrum of the complex, the bands of 2-pyrazinecarboxylate ligand show a weak band at 2360 cm<sup>-1</sup> to v(OH), the medium band at 1643 cm<sup>-1</sup> for v(C=O), there are two bands for v(CC), v(CN) of aromatic ring one is medium at 1591 cm<sup>-1</sup> and the other is medium peak at 1527 cm<sup>-1</sup>. The v(CC)<sub>ar</sub>, v(CN)<sub>ar</sub>, β(CH)<sub>ar</sub> groups has medium bands at 1415, 1273 and 1234 cm<sup>-1</sup>. The medium band at 1164 cm<sup>-1</sup> returns to v(CC)<sub>ar</sub>, v(CN)<sub>ar</sub>, and medium band at 1016 cm<sup>-1</sup> β(CH)<sub>ar</sub>. The weak band at 839 cm<sup>-1</sup> is for α(CCC) and medium band at 528 cm<sup>-1</sup> is for γ(CO), γ(OH). [212] The pattern vibration of the perchlorate counter ion shows very strong

vibration for Cl–O stretch vibration absorbance at  $1072\text{ cm}^{-1}$  is characteristic of the presence of uncoordinated perchlorate, a medium intensity peak at  $910\text{ cm}^{-1}$  owing to  $\text{ClO}_4^-$  stretching, and a very strong intensity peak at  $619\text{ cm}^{-1}$  [312 - 314]

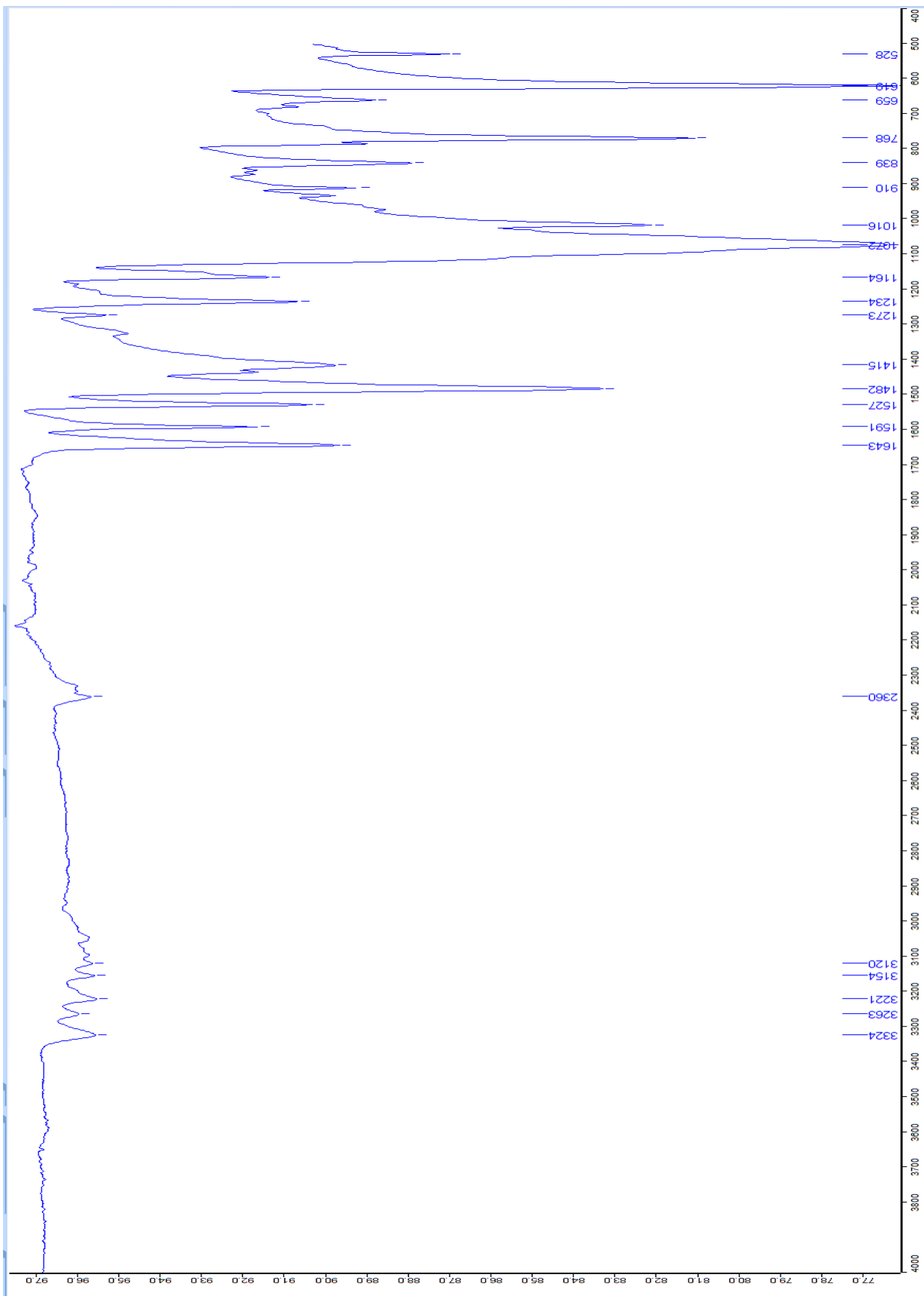
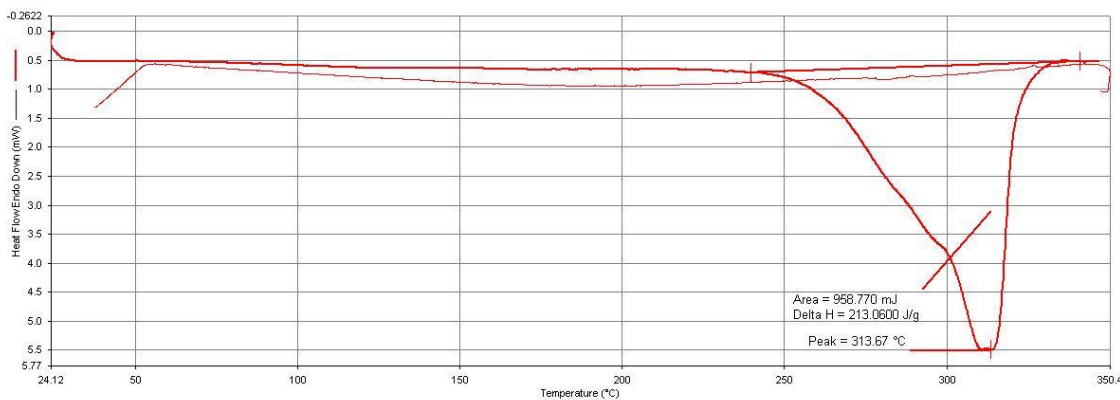


Figure 3.16 The infrared spectra of the [Cu(dipym)(H<sub>2</sub>O)(pca)]ClO<sub>4</sub> complex

### 3.3.2 Thermal analysis:

The Differential Scanning Calorimetry (DSC) thermal analysis for the [Cu(dipyam)(H<sub>2</sub>O)(pca)]ClO<sub>4</sub> complex. The complex was set for heating in the DSC instrument at a rate of 5°C/min, from 20 to 450°C in nitrogen gas flowing at a rate of 25ml/min, and then the cooling was done in the same range. The DSC curve (fig. 3.17) displayed an endothermic peak associated with enthalpy of 213.060 J/g at T<sub>max</sub> = 313.67°C which nearly corresponds to melting point.



**Figure 3.17** Differential Scanning Calorimetry (DSC) of [Cu(dipyam)(H<sub>2</sub>O)(pca)]ClO<sub>4</sub> complex

### 3.3.3 Crystal structure for [Cu(dipyam)(H<sub>2</sub>O)(pca)]ClO<sub>4</sub>:

The structure of complex [Cu(dipyam)(H<sub>2</sub>O)(pca)]ClO<sub>4</sub> consists of ,first, Cu(II) center, in which it is five coordinated by two nitrogen atoms of 2,2'-dipyridylamine, one nitrogen and one oxygen atom of 2-pyrazinecarboxylate ligand, one oxygen atom of coordinated water. The perchlorate molecule is a counter ion, as what shown in the figure 3.18 below:

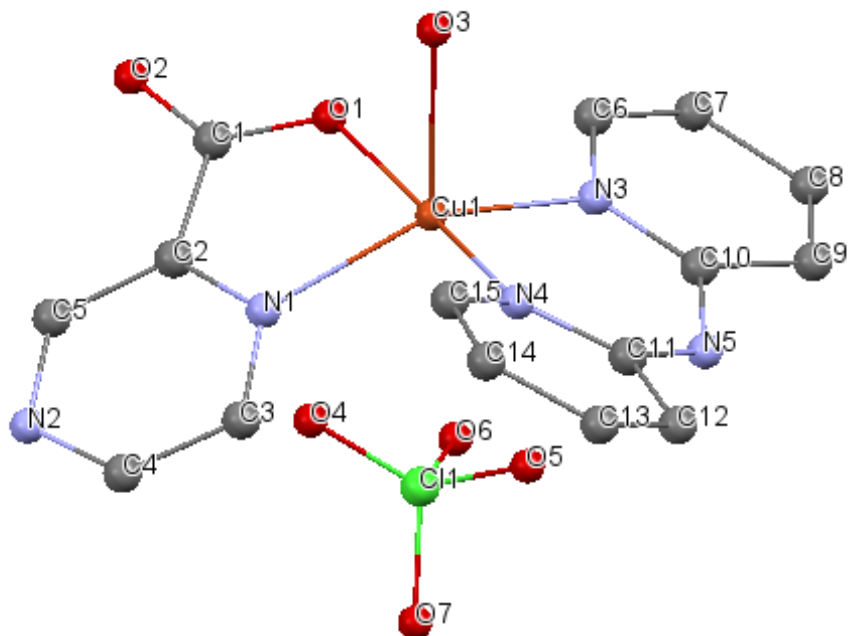


**Figure 3.18** View the structure of  $[\text{Cu}(\text{dipyam})(\text{H}_2\text{O})(\text{pca})]\text{ClO}_4$  complex, with showing the atomic numbering

The complex is an ionic structure that comprised chemically identical complex two cation  $[\text{Cu}(\text{dipyam})(\text{H}_2\text{O})(\text{pca})]^+$  along with two uncoordinated perchlorate anions  $\text{ClO}_4^-$  per unit cell. The relative arrangement of the constituents units in the unit cell are shown in figure 3.19

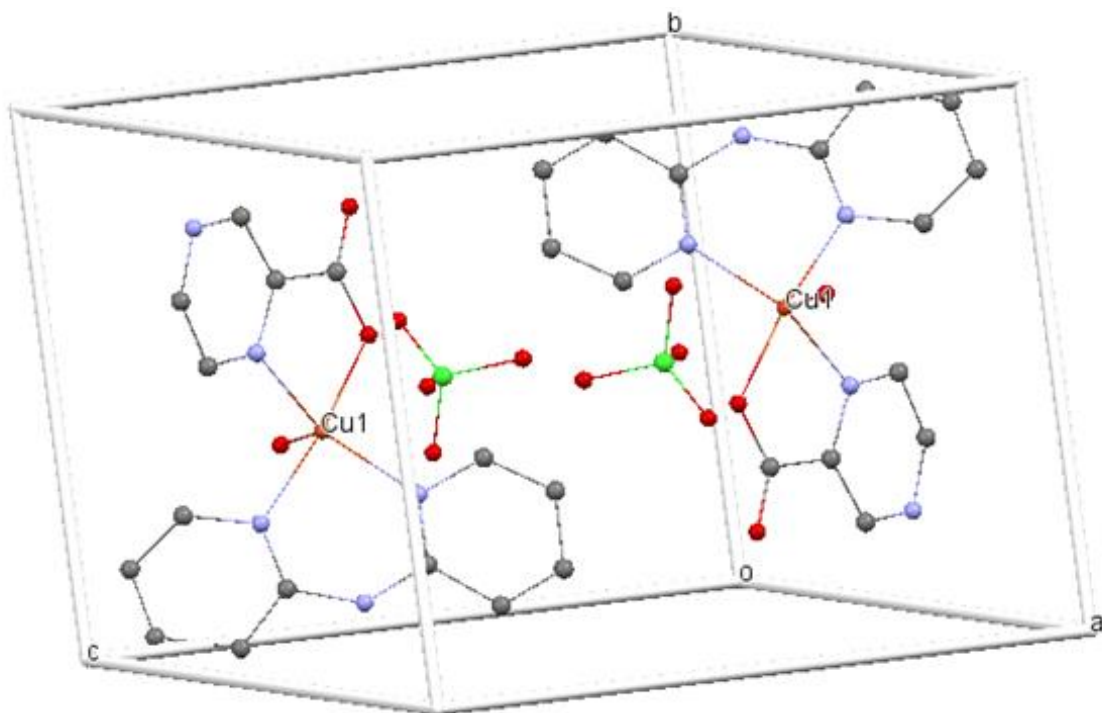


**Figure 3.19** View the structure packing of  $[\text{Cu}(\text{dipyam})(\text{H}_2\text{O})(\text{pca})]\text{ClO}_4$  complex within unit cell

On one hand, The crystal structure of  $[\text{Cu}(\text{dipyam})(\text{H}_2\text{O})(\text{pca})]\text{ClO}_4$  complex exposed that Cu atom has a distorted square pyramid geometry as what detected from table 3.11 where the angle between N4-Cu1-O1 is  $171.04(6)$  and it is near to 180, therefore, it will be located on axial position. The angle between N1-Cu1-O3  $112.64(15)$  and its value near to 150. The angle between N3-Cu1-O3 is  $99.79(16)$  and its value is near to 90. The angle between N4-Cu1-O3  $89.71(16)$  and N1-Cu1-O1 is  $81.02$  which their value also near to 90.

The crystal structure reveals that the Cu atom of the complex has a distorted square pyramid. The four equatorial positions are occupied by N1, N3 of dipyam ligand, N4, O1 of pca ligand. While the axial position is located by O4 atom of coordinated water. The bond length of Cu-N (where N is N1, N3, N4) are  $2.035(4)$ ,  $1.979(4)$ ,  $1.960(4)$  Å respectively, and the bond length of Cu-O (where O is O1, O3) are  $1.946(3)$ ,  $2.279(4)$  Å respectively (table 3.12, fig. 3.20a).

It could be noticed that the distance of Cu-N and Cu-O atoms of pca is less than the general distance compared with other studies as  $[\text{Zn}(\text{bpp})(\text{pca})(\text{MeOH})]\text{ClO}_4$  complex, the

bond lengths between Zn-N and Zn-O of pca are 2.082 - 2.190 and 2.028 - 2.166 Å. [5, 14] Therefore, this results could be used as an evidence for that pca is produced according to break the two rings of 2,2'-bipyrazine and CO<sub>2</sub> gas reacted with the rings of 2,2'-bipyrazine to form 2-pyrazine carboxylate.

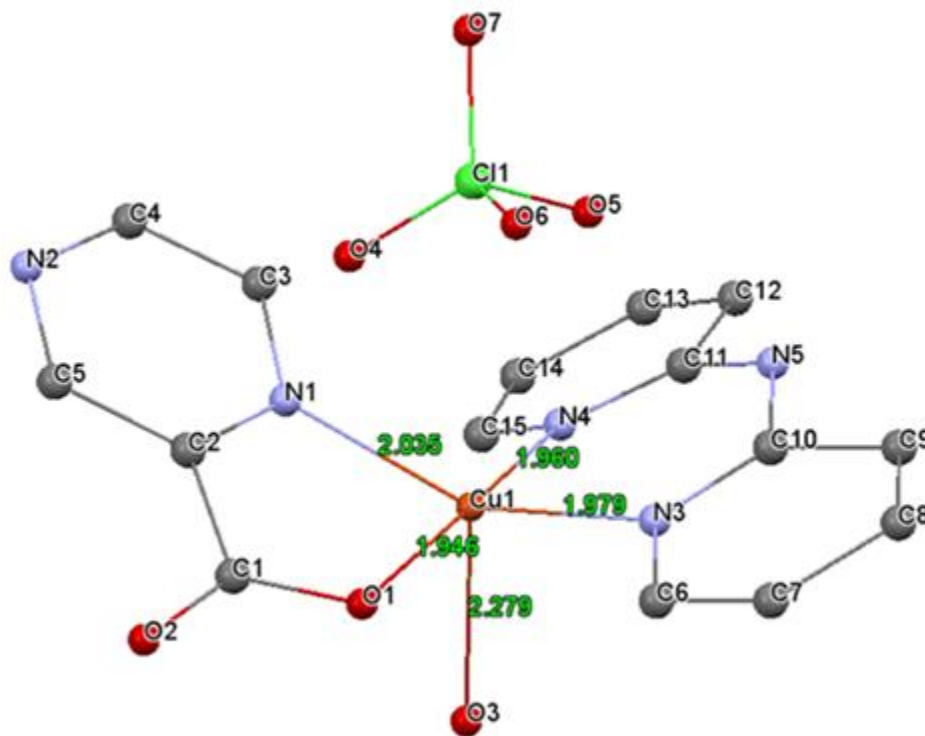


**Figure 3.20a** View the distance between the Cu-ligand of the [Cu(dipyam)(H<sub>2</sub>O)(pca)]ClO<sub>4</sub> complex according to the X-ray complex.

**Table 3.11:** Bond angle [deg.] of [Cu(dipyam)(H<sub>2</sub>O)(pca)]ClO<sub>4</sub> complex

N1—Cu1—N3	146.80 (16)	C1—C2—C5	124.7 (4)
N1—Cu1—N4	95.78 (15)	N1—C2—C5	120.1 (4)
N3—Cu1—N4	91.11 (15)	N1—C3—C4	116.2 (5)
N1—Cu1—O1	81.02 (15)	C3—C4—N2	127.8 (5)
N3—Cu1—O1	96.13 (15)	C2—C5—N2	121.6 (5)
N4—Cu1—O1	171.04 (16)	N3—C6—C7	121.0 (5)
N1—Cu1—O3	112.64 (15)	C6—C7—C8	119.0 (5)
N3—Cu1—O3	99.79 (16)	C7—C8—C9	120.5 (4)
N4—Cu1—O3	89.71 (16)	C8—C9—C10	116.8 (4)
O1—Cu1—O3	83.87 (16)	C9—C10—N5	115.4 (4)
Cu1—N1—C2	111.3 (3)	C9—C10—N3	123.4 (4)
Cu1—N1—C3	128.5 (3)	N5—C10—N3	121.2 (4)
C2—N1—C3	119.5 (4)	N5—C11—N4	121.4 (4)

C4—N2—C5	114.6 (5)	N5—C11—C12	113.6 (5)
Cu1—N3—C6	115.9 (3)	N4—C11—C12	125.0 (5)
Cu1—N3—C10	124.6 (3)	C11—C12—C13	114.9 (5)
C6—N3—C10	119.1 (4)	C12—C13—C14	118.4 (5)
Cu1—N4—C11	127.4 (3)	C13—C14—C15	118.9 (6)
Cu1—N4—C15	113.9 (3)	N4—C15—C14	123.8 (6)
C11—N4—C15	118.6 (4)	O7—C11—O6	110.9 (4)
C10—N5—C11	128.8 (4)	O7—C11—O4	117.8 (4)
Cu1—O1—C1	117.6 (3)	O6—C11—O4	107.2 (4)
O1—C1—O2	127.1 (5)	O7—C11—O5	100.9 (4)
O1—C1—C2	114.0 (4)	O6—C11—O5	104.8 (4)
O2—C1—C2	118.9 (4)	O4—C11—O5	114.6 (4)
C1—C2—N1	115.1 (4)		

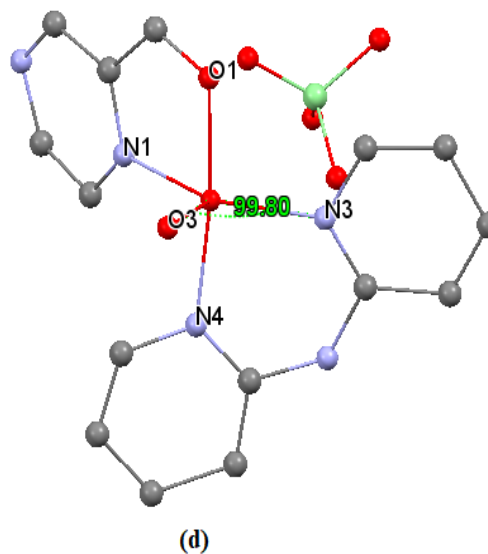
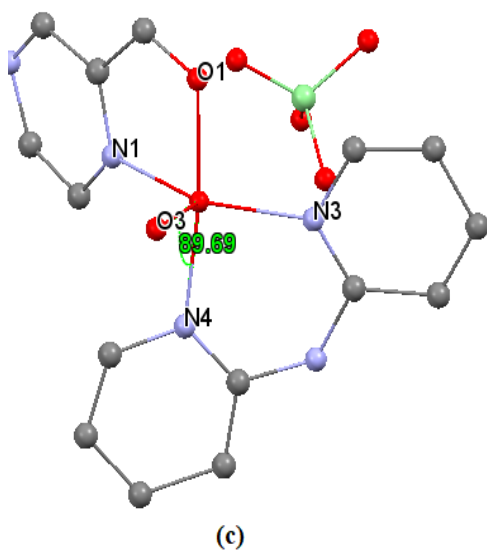
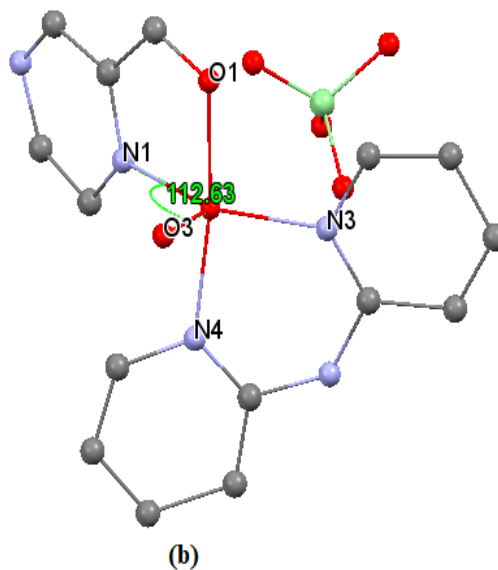
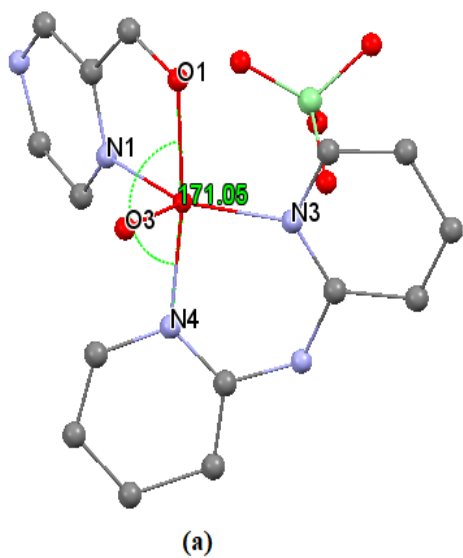
**Table 3.12:** Bond length [Å°] of [Cu(dipyam)(H<sub>2</sub>O)(pca)]ClO<sub>4</sub> complex

Atom 1	Atom 2	Length	Atom 1	Atom 2	Length
Cu1	N1	2.035 (4)	O2	Cl	1.225 (6)
Cu1	N3	1.979 (4)	O4	C11	1.405 (7)
Cu1	N4	1.960 (4)	O5	C11	1.398 (7)
Cu1	O1	1.946 (3)	O6	C11	1.427 (6)
Cu1	O3	2.279 (4)	O7	C11	1.429 (6)
N1	C2	1.326 (6)	C1	C2	1.506 (6)
N1	C3	1.326 (6)	C2	C5	1.424 (7)
N2	C4	1.303 (8)	C3	C4	1.383 (8)
N2	C5	1.303 (8)	C6	C7	1.359 (7)
N3	C6	1.401 (6)	C7	C8	1.476 (8)
N3	C10	1.343 (6)	C8	C9	1.355 (8)
N4	C11	1.300 (6)	C9	C10	1.445 (7)
N4	C15	1.355 (7)	C11	C12	1.354 (7)
N5	C10	1.408 (6)	C12	C13	1.504 (9)
N5	C11	1.366 (6)	C13	C14	1.365 (10)
O1	C1	1.254 (6)	C14	C15	1.337 (8)
Trigonality index, $\tau$		0.404			
<sup>2</sup> Tetragonality, T <sup>5</sup>		0.870			

The distortion of the polyhedron is obviously observable and confirmed by the values of the Trigonality  $\tau$  and tetragonality T<sup>5</sup>, respectively, (table 3.11, fig. 3.20b). The reason of distortion returns to non-planarity of 2,2'-dipyridylamine ligand which is formed six membered ring with metal center and the formation of the 2-pyrazinecarboxylate five

<sup>2</sup> The tetragonality T<sup>5</sup> is determined based on the M-ligand bond lengths. T<sup>5</sup> = (mean in-plane distance M-L)/(mean out-of-plane distance M-L). [301(a,c)]

membered ring which is more demanding when coordinating. [301(a-c)] In other words, the non-planarity of 2,2'-dipyridylamine ligand returns to that the angle of N3-Cu-O3 angle is not 90 and N4-Cu-O3 angle is not 90. The angle for N3-Cu1-N1 and N4-Cu-O1 are not 180 because one of the 2,2'-bipyrazine rings broke and become five membered ring.



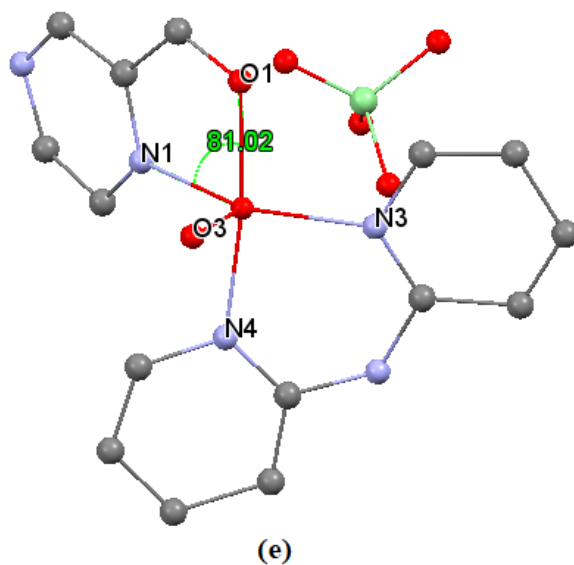


**Figure 3.20b** View the angles between the Cu-ligand of the  $[\text{Cu}(\text{dipyam})(\text{pca})(\text{H}_2\text{O})]\text{ClO}_4$  complex, (a) the angle between N4-Cu1-O1 (b) the angle between the N-Cu1-O3 (c) the angle between N4-Cu1-O3 (d) the angle between N3-Cu1-O3 (e) the angle between N1-Cu1-O1

The hydrogen bond are formed according to nitrogen and oxygen atoms of perchlorate ions and 2-pyrazinecarboxylate ligand, as what figure 3.21 showed.

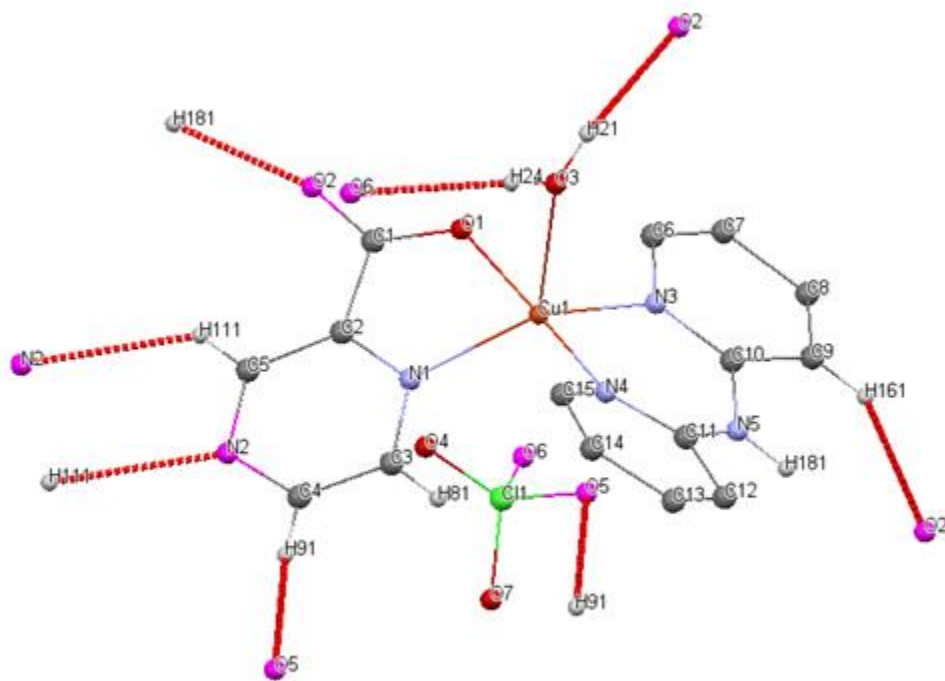


**Figure 3.21** View the inter-intrachain H-bonds of the  $[\text{Cu}(\text{dipyam})(\text{H}_2\text{O})(\text{pca})]\text{ClO}_4$  complex

The table 3.13 below shows the corresponding D-H, H...A and D...A bond distances and D—H...A bond angles, where D: donor, A: acceptor. As what the table shown, the following atoms act as hydrogen bond acceptor, including, first, nitrogen and oxygen atoms of 2-pyrazinecarboxylate ligand [C5—H111...N2<sup>iv</sup>], [O3—H21...O2<sup>i</sup>] and [C9—H161...O2<sup>v</sup>]. Second, the oxygen atoms of perchlorate [O3—H24...O6<sup>ii</sup>] and [C4—H91...O5<sup>iii</sup>]

**Table 3.13:** Hydrogen geometry (Å, °) of [Cu(dipyam)(H<sub>2</sub>O)(pca)]ClO<sub>4</sub> complex

D—H...A	D—H (Å)	H...A (Å)	D...A (Å)	D—H...A (°)
O3—H21...O2 <sup>i</sup>	0.83	2.24	3.020 (9)	156
O3—H24...O6 <sup>ii</sup>	0.83	2.27	2.986 (9)	144
C4—H91...O5 <sup>iii</sup>	0.92	2.54	3.386 (9)	153
C5—H111...N2 <sup>iv</sup>	0.94	2.54	3.206 (9)	128
C9—H161...O2 <sup>v</sup>	0.93	2.59	3.353 (9)	140
N5—H181...O2 <sup>v</sup>	0.87	2.15	3.002 (9)	166

The complex cations are connected and formed network structure through binding with perchlorate anions via O—H...O close contacts and C—H...O hydrogen bonds. Beside to 2-pyrazinecarboxylate ligand links through C—H...N and C—O...H with other cation unit as what shown in the figure 3.22 below

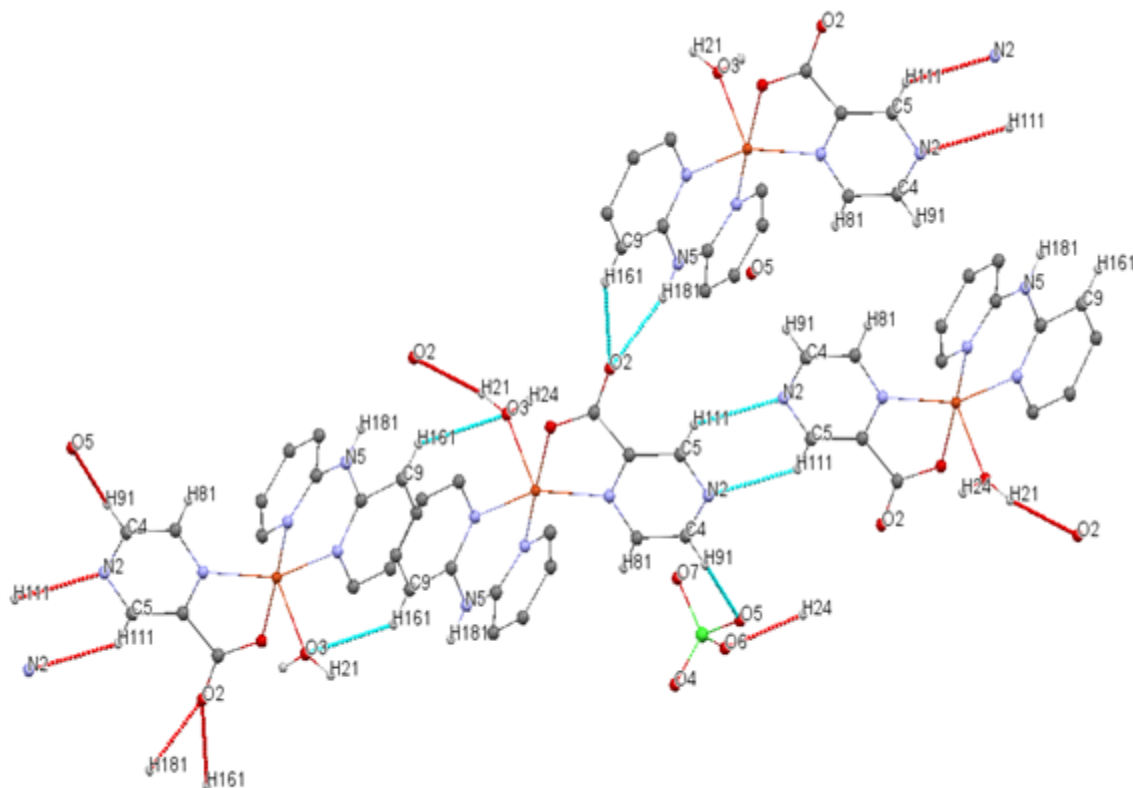


**Figure 3.22** View the network structure of  $[\text{Cu}(\text{dipyam})(\text{H}_2\text{O})(\text{pca})]\text{ClO}_4$  complex with showing the inter intrachain H-bonds.

In addition, the crystal packing of the  $[\text{Cu}(\text{dipyam})(\text{H}_2\text{O})(\text{pca})]\text{ClO}_4$  complex are fixed closed to each other by  $\pi$ - $\pi$  stacking interactions between 2-pyrazincarboxylate ligand at 3.635 - 3.812 Å and between the 2,2'-dipyridylamine ligand at 4.002 Å (fig. 3.23). The forming of 3D sheets are resulted due to hydrogen bond, the  $\pi$ ••• $\pi$  and/or C-H••• $\pi$  interactions. [242, 261, 266]

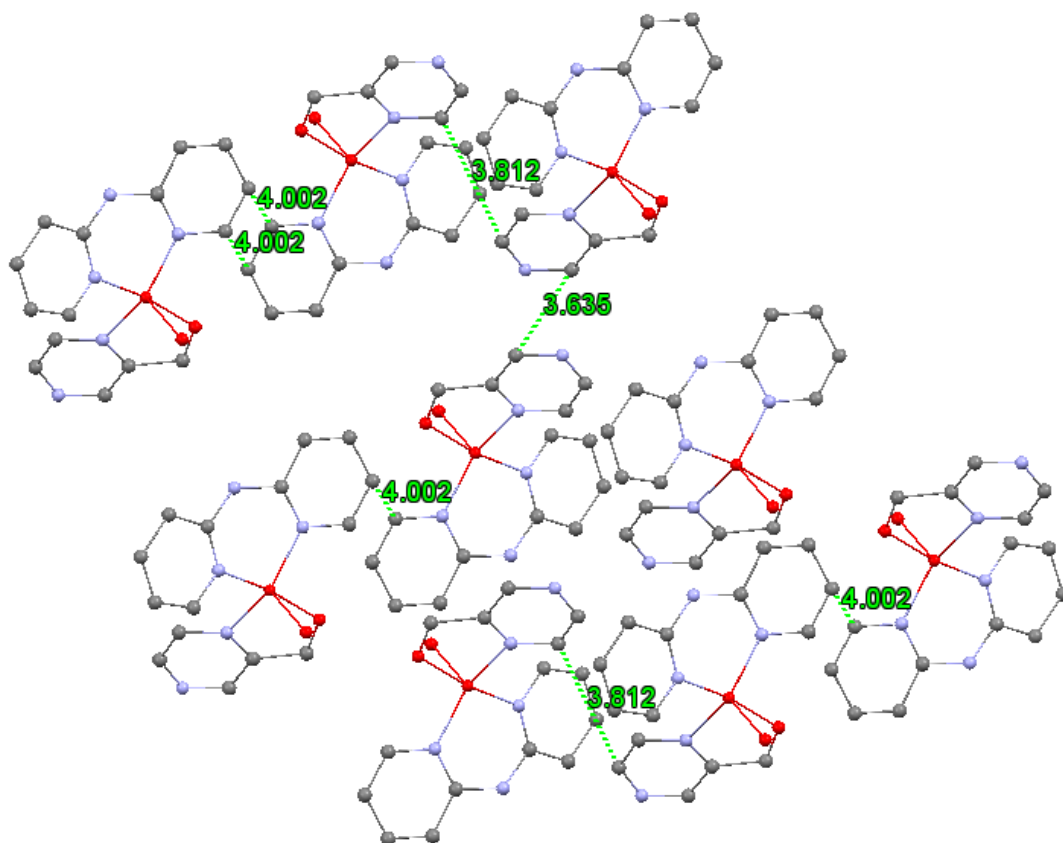


**Figure 3.23** View the distance of  $\pi$ - $\pi$  interaction 2-pyrazinecarboxylate ligand at 3.635-3.812 Å and between the 2,2'-dipyridylamine ligand at 4.002 Å in the [Cu(dipyam)(H<sub>2</sub>O)(pca)]ClO<sub>4</sub> complex

The units of sheets also connected via weak interaction between N atom and C-H group of 2-pyrazinecarboxylate ligand of other sheet with distance value 2.540 Å (fig. 3.24) and the distance between the NH group of 2,2'-dipyridylamine ligand and OH group of 2-pyrazinecarboxylate ring in adjacent structure unit is 2.585 Å and between the NH group of 2,2'-dipyridylamine ligand and oxygen (O3) of coordinated water is 2.618 Å (fig. 3.25) which are in the normal range of the weak interactions. [211, 253, 315-318]

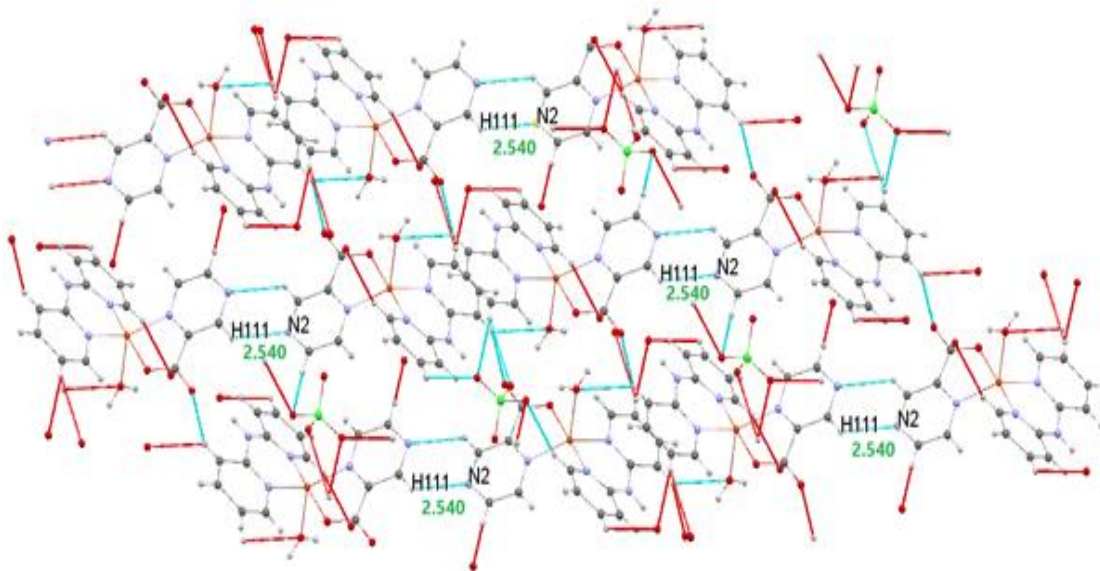


**Figure 3.24** View the weak interaction between N atom & C-H group of pca ligand of other sheet with distance 2.54 Å in the  $[\text{Cu}(\text{dipyam})(\text{H}_2\text{O})(\text{pca})]\text{ClO}_4$  complex.

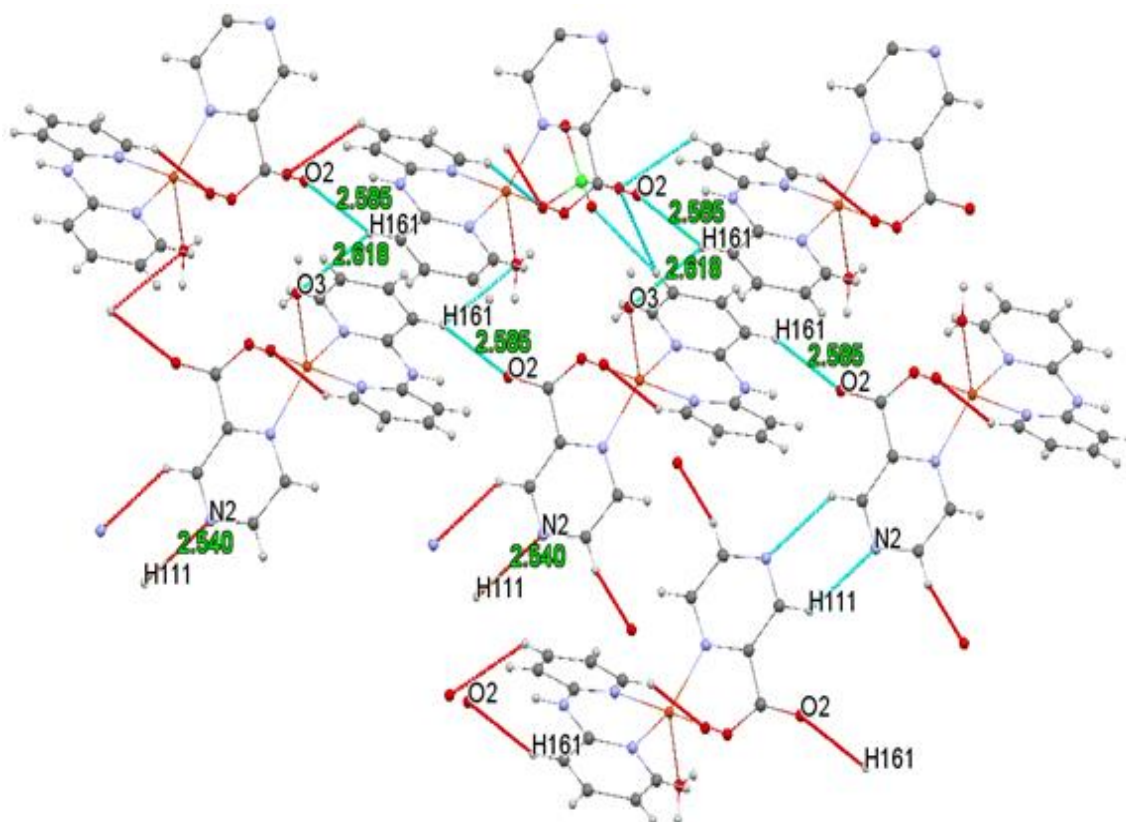


**Figure 3.25** View the weak interaction between the NH group of 2,2'-dipyridylamine ligand and OH group of 2-pyrazine carboxylate ring in adjacent structure unit is 2.585 Å and between the NH group of 2,2'-dipyridylamine ligand and oxygen (O3) of coordinated water is 2.618 Å in the  $[\text{Cu}(\text{dipyam})(\text{H}_2\text{O})(\text{pca})]\text{ClO}_4$  complex.

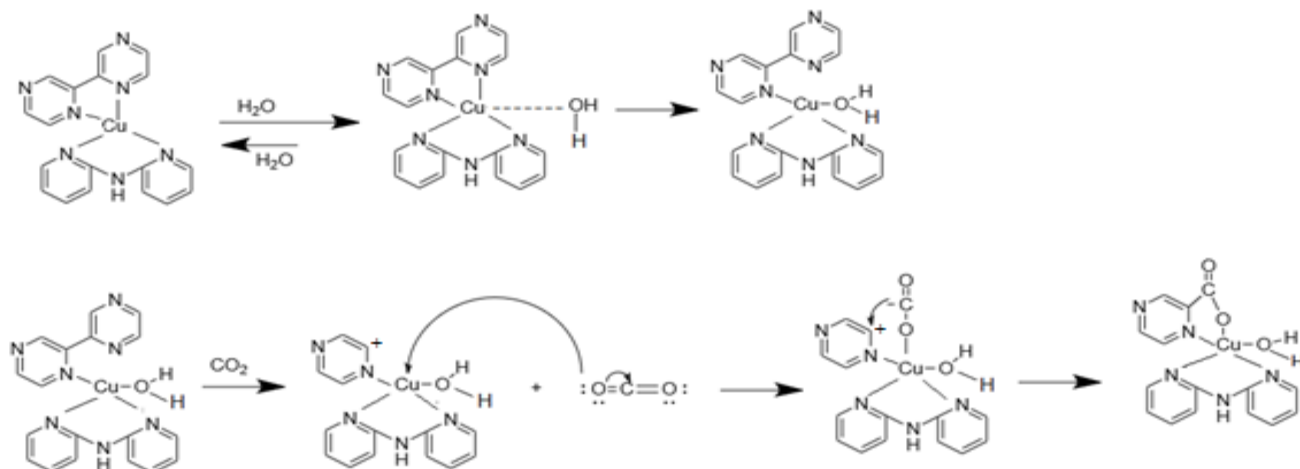
### 3.3.4 Cleavage of 2,2'-bipyrazine Ring

The assumed suggestion expected to prepare the complex in which its formula is  $[\text{Cu}(\text{dipyam})(\text{bpz})](\text{ClO}_4)_2$ , however, the produced compound's formula is  $[\text{Cu}(\text{dipyam})(\text{H}_2\text{O})(\text{pca})]\text{ClO}_4$ , where pca is 2-pyrazinecarboxylate ligand which does not use during synthesis process.

The unsaturated heterocycles could undergo aromatic substitution on reaction with electrophiles.[319] This merit considered as encouraged step for developing a new proposing on dearomatization of six-membered N-heterocycles hypothesis (methodology for their C-N / C-C bond cleavage), especially this kind of cleavage is relatively rare. [320] Also, it will provide new routes for synthesis new functionalized molecules exist in numerous natural and pharmaceuticals products. [321]

The supposed mechanism for the reaction of  $[\text{Cu}(\text{dipyam})(\text{H}_2\text{O})(\text{pca})]\text{ClO}_4$  complex is that the nucleophile attack the ligand by  $\text{OH}^-$  or  $\text{H}_2\text{O}$  takes place. A decomposition caused for the bpz ligand during the preparation of complex, in which its supposed molecular formula was  $[\text{Cu}(\text{dipyam})(\text{bpz})](\text{ClO}_4)_2$  when the addition of dipyam to the aqueous metal solution, a green solution is obtained after short time at room temperature with stirring, followed by appearing a purple precipitate. This suggested explanation is mentioned according to that 2,2'-bipyraizne belongs to pyrazines family, in which quaternized pyrazines and pyridazines are also known to form pseudo-bases and covalent hydrates in aqueous solution. [322]

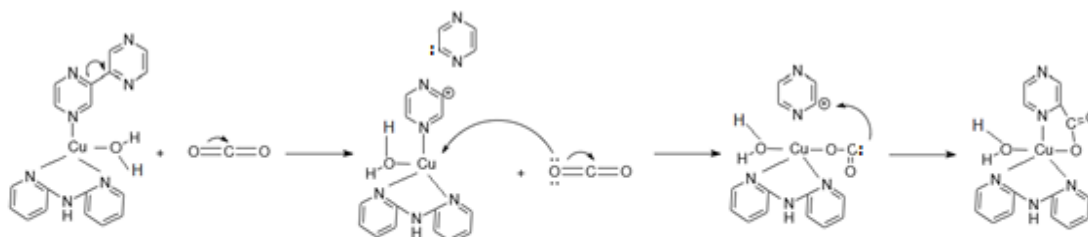
On one hand, the proposed reaction mechanism using the reaction with  $\text{OH}^-/\text{H}_2\text{O}$  for our complex is that first preassociation step, involving anion recognition by Cu complex forming an ion pair in solution. The dashed line indicates an interaction happens between the Cu complex and the oxygen of  $\text{H}_2\text{O}$ . Substitution occurs in step two forming a bond between the metal center and the  $\text{H}_2\text{O}$ , while simultaneously breaking one of the Cu nitrogen bonds resulting in a monodentate bipyrazine ligand (scheme 3.1). [323]



**Scheme 3.1** View the proposed mechanism for the reaction of  $[Cu(dipyam)(H_2O)(pca)]ClO_4$

In other view, some studies showed that the C-C cleavage could happen according to hydrogenolysis process because of existing  $H_2$  (available form atmosphere) and water. [324] While, others suggested that the protonation of the carbon of bpz rather than at nitrogen, (this process could offer an entry to aromatic C-C bond cleavage), weakening an aromatic C-C bond and providing a dihydropyridyl. This analysis is taken in mind the detailed examination is done for 2,2'-bipyridine. [321] At least, the open ringing will be happened by the rupture of the C-C bond between the pyrazine rings of the bipyrazine ligand and so  $CO_2$  is caught. [323]

However, the breakage of the bond would be a high energy process that results to the presence of free radical in solution. The mechanism looks unusual, specifically the rapid disassociation of the compound in water. [323] [Note: the scheme 3.2 below is just a personal suggestion for the mechanism of breaking bond of bpz, where more studies showed that this type of broken is rare and unknown explanation].



**Scheme 3.2** View the personal suggestion for the mechanism of breaking bond of 2,2'-bipyrazine ligand during the forming of  $[Cu(dipyam)(H_2O)(pca)]ClO_4$  complex.

Nevertheless, other inorganic studies on  $[\text{Ir}(\text{bpy})_3]^{+3}$  complex supposed description in which the complex contain bpy ligands as monodentate and coordinated water molecule. [325] Finally, these predicted views take place in recent searches that suggest an amine-based  $\text{CO}_2$  capture systems, in which it depends on chemical reactions between  $\text{CO}_2$  and an aqueous amine solution at low temperature and atmospheric pressure. [304a]

### **3.4 $[\text{Cu}(\text{bpz})_3](\text{ClO}_4)_2 \cdot 2\text{CH}_3\text{CN}$ complex**

The  $[\text{Cu}(\text{bpz})_3](\text{ClO}_4)_2 \cdot 2\text{CH}_3\text{CN}$  complex in this work was produced by distinguish approaches, characterized using different methods. It is one of polypyridyl complexes that they have special interest in research areas. They mostly utilized in the synthetic applications as visible light-absorbing photocatalysts. For example,  $[\text{Ru}(\text{bpz})_3]^{2+}$  complex, in which is similar to  $[\text{Cu}(\text{bpz})_3](\text{ClO}_4)_2 \cdot 2\text{CH}_3\text{CN}$  complex, is one of the most useful photooxidant that has been shown to be uniquely suited to oxidant-induced phototoxic transformations [138d] On one hand,  $[\text{Ni}(\text{bpz})_3](\text{ClO}_4)_2 \cdot \text{H}_2\text{O}$  is another similar compound that has potential biological applicability such as antiepileptic, anticonvulsant, antibacterial, antifungal, antimicrobial, and anticancer/antiproliferative activities. [280a] Moreover,  $[\text{Co}(\text{bpy})_3]^{3+/2+}$  /  $[\text{Co}(\text{phen})_3]^{3+/2+}$  where bpy = 2,2-bipyridine and phen = 1,10-phenanthroline, redox couples play role as an electron mediator visible-light-driven photocatalyst systems. [326] At least,  $[\text{Ru}(\text{bpy})_3]^{2+}$  complex also has huge role in various areas as energy storage, hydrogen and oxygen evolution from water, and methane production from carbon dioxide. [327]

#### **3.4.1 Infrared Spectroscopy**

The infrared absorption frequencies obtained for  $[\text{Cu}(\text{bpz})_3](\text{ClO}_4)_2 \cdot 2\text{CH}_3\text{CN}$  complex are listed in (table 3.14), and spectra are given in (fig. 3.26).

**Table 3.14:** Comparison Infrared frequencies ( $\text{cm}^{-1}$ ) of 2,2'-bipyrazine ligand of  $[\text{Cu}(\text{bpz})_3](\text{ClO}_4)_2 \cdot 2\text{CH}_3\text{CN}$  complex with the free 2,2'-bipyrazine ligand.

$[\text{Cu}(\text{bpz})_3](\text{ClO}_4)_2 \cdot 2\text{CH}_3\text{CN}$	Assignment	Frequencies ( $\text{cm}^{-1}$ ) for 2,2'-bipyrazine
3095m, 3078m, 3042m, 2930w and 2850w	$\nu$ C-H	3078vw, 3050vw, 2972s, 2988s and 2901s
1637m 1590w and 1526vw	$\nu$ C $\equiv$ N	1592m, 1564m and 1528m
1314vs and 1379vs	$\nu$ C $\equiv$ C	1433m, 1413m, 1394m and 1341m and 1311w
1464m, 1478m	$\delta$ ring	1460s
1147vs and 1055vs	$\beta$ ring, breathing	1148s and 1076vs and 991vs
1029vs, 1018vs and 845vs	ring-H in-plane binding vibrations	1028s, 1018s and 846s and 813w
769m	out-of-plane ring-H bending and $\tau$ ring	881w, 780vw, 756w, 733w 594vw and 520vw
1107vs, 1089 vs, 1067vs, 826s and 621s	$\text{ClO}_4^-$	-----

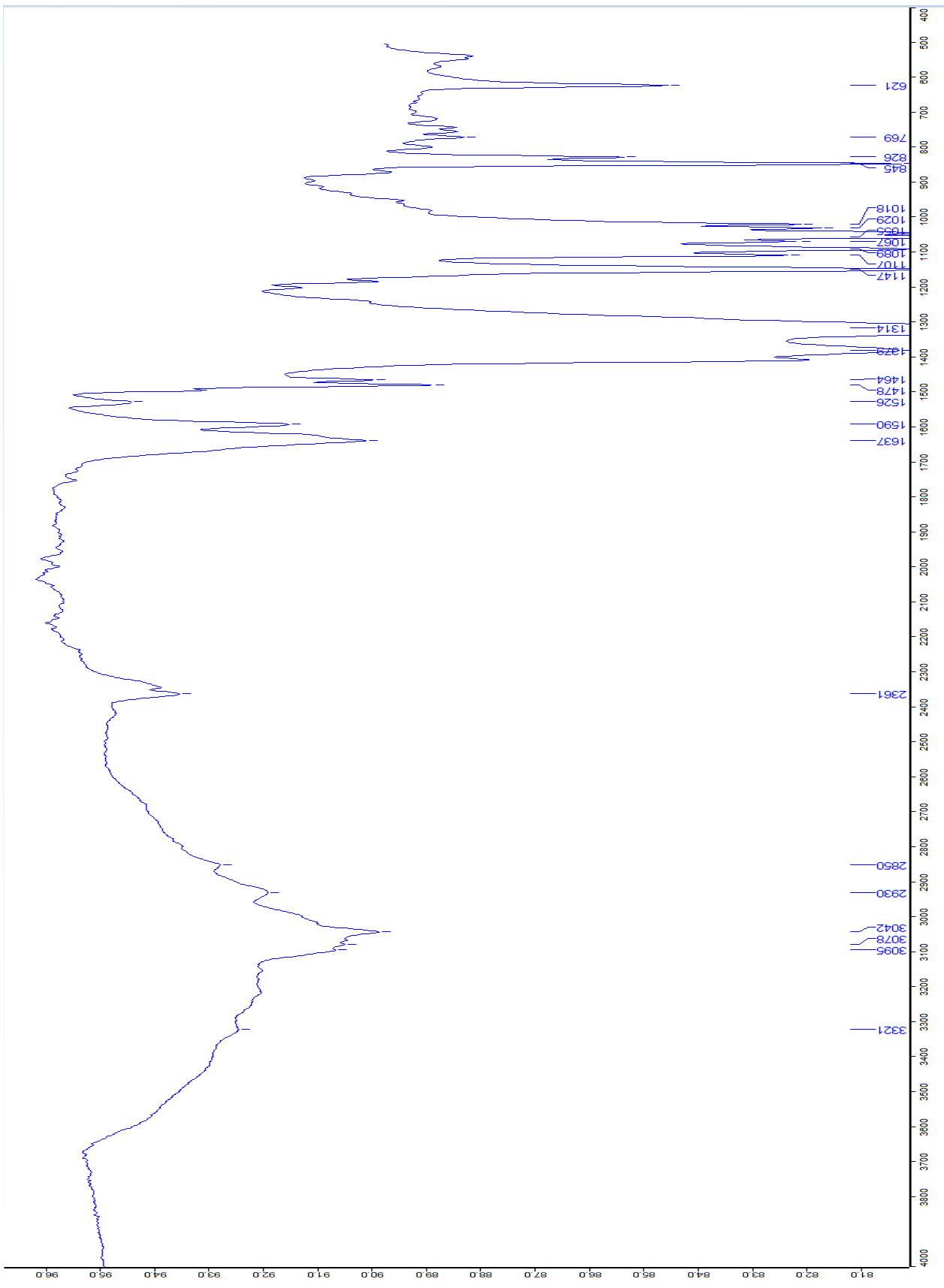


Figure 3.26 The infrared spectra of the [Cu(bpz)<sub>3</sub>](ClO<sub>4</sub>)·2CH<sub>3</sub>CN complex

IR spectrum of the  $[\text{Cu}(\text{bpz})_3](\text{ClO}_4)_2 \cdot 2\text{CH}_3\text{CN}$  complex was compared with that of the free 2,2'-bipyrazine ligand (fig. 3.26). The FTIR spectra of 2,2'-bipyrazine have characteristic bands which are  $\nu \text{ C-H}$ ,  $\nu \text{ C}\equiv\text{C}$ ,  $\nu \text{ C}\equiv\text{N}$ ,  $\delta$  ring,  $\beta$  ring, ring bending, ring-H in-plane binding vibrations, out-of-plane ring-H bending and torsion ( $\tau$ ) ring. The medium bands at 3095, 3078, 3042  $\text{cm}^{-1}$  and weak bands at 2930 and 2850  $\text{cm}^{-1}$  are related to  $\nu \text{ C-H}$ . The medium band at 1637  $\text{cm}^{-1}$ , weak band at 1590 and the very weak band at 1526  $\text{cm}^{-1}$  are contributed to  $\nu \text{ C}\equiv\text{N}$ , while the very strong bands at 1314 and 1379  $\text{cm}^{-1}$  correlated to  $\nu \text{ C}\equiv\text{C}$ , and the medium bands at 1464 and 1478  $\text{cm}^{-1}$  vibrations essentially deformed the ring. In addition, the very strong bands at 1147 and 1055  $\text{cm}^{-1}$  are installed for  $\beta$  ring, the very strong bands at 1029, 1018 and 845  $\text{cm}^{-1}$  are referred to ring-H in-plane binding vibrations, whereas the medium band at 769  $\text{cm}^{-1}$  is mostly out-of-plane ring-H bending and vibration torsion ring. The medium peak at 3321  $\text{cm}^{-1}$  referred to the intramolecular hydrogen bond between bpz ring. Nakamoto indicated to that the highest frequencies ranges from 3700 – 2500  $\text{cm}^{-1}$ ; returns to X-H stretching, in which the intramolecular hydrogen bonds indicates the presence of exchangeable protons, within nitrogen and hydrogen atom of one single molecule. [297]

The pattern vibration of the perchlorate counter ion displays a very strong sharp absorption at 1089  $\text{cm}^{-1}$  and two strong peaks at 826 and 621  $\text{cm}^{-1}$ . The vibration of the Cl–O stretch vibration absorbance at 1107 and 1067  $\text{cm}^{-1}$  is characteristic of the presence of uncoordinated perchlorate [280a, 298, 314]

### **3.4.2 Thermal analysis**

The Differential Scanning Calorimetry (DSC) thermal analysis for the  $[\text{Cu}(\text{bpz})_3](\text{ClO}_4)_2 \cdot 2\text{CH}_3\text{CN}$  complex were performed using Perkin Elmer DSC equipment. Samples about 6 mg of complex with aluminum pans, nitrogen gas flow and a scan rate 5°C/min from 25 up to 350°C, and then the cooling was done in the same range. The DSC curve (fig. 3.27) displayed an endothermic peak associated with enthalpy of 189.898 J/g at  $T_{\text{max}}=274.78^\circ\text{C}$  which corresponds to melting point process.

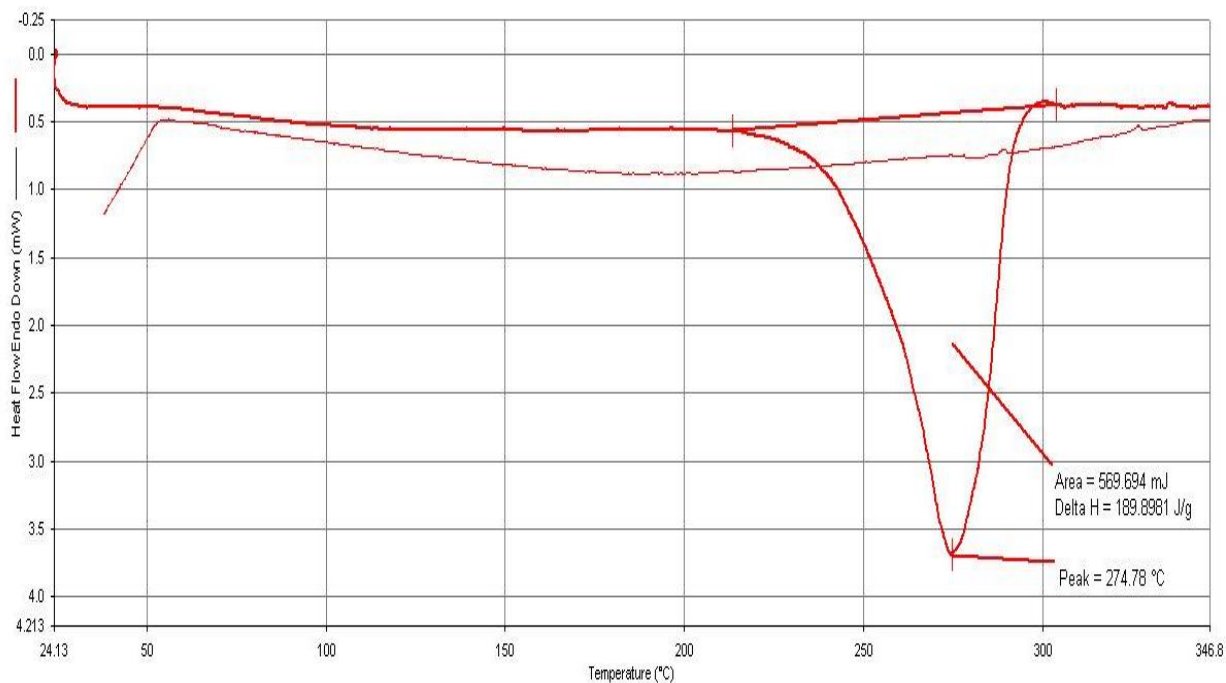


**Figure 3.27** Differential Scanning Calorimetry (DSC) of  $[\text{Cu}(\text{bpz})_3](\text{ClO}_4)_2 \cdot 2\text{CH}_3\text{CN}$

### 3.4.3 Crystal structure for $[\text{Cu}(\text{bpz})_3](\text{ClO}_4)_2 \cdot 2\text{CH}_3\text{CN}$ :

The structure of the copper(II) compound is made up of discrete  $[\text{Cu}(\text{bpz})_3]^{+2}$  cations, four uncoordinated molecules that are two perchlorate anions and two acetonitrile, figure 3.28 They are bonded through electrostatic interactions, Van der Waals forces and hydrogen bonds. There are four molecules per unit cell, as what shown in the figure 3.29

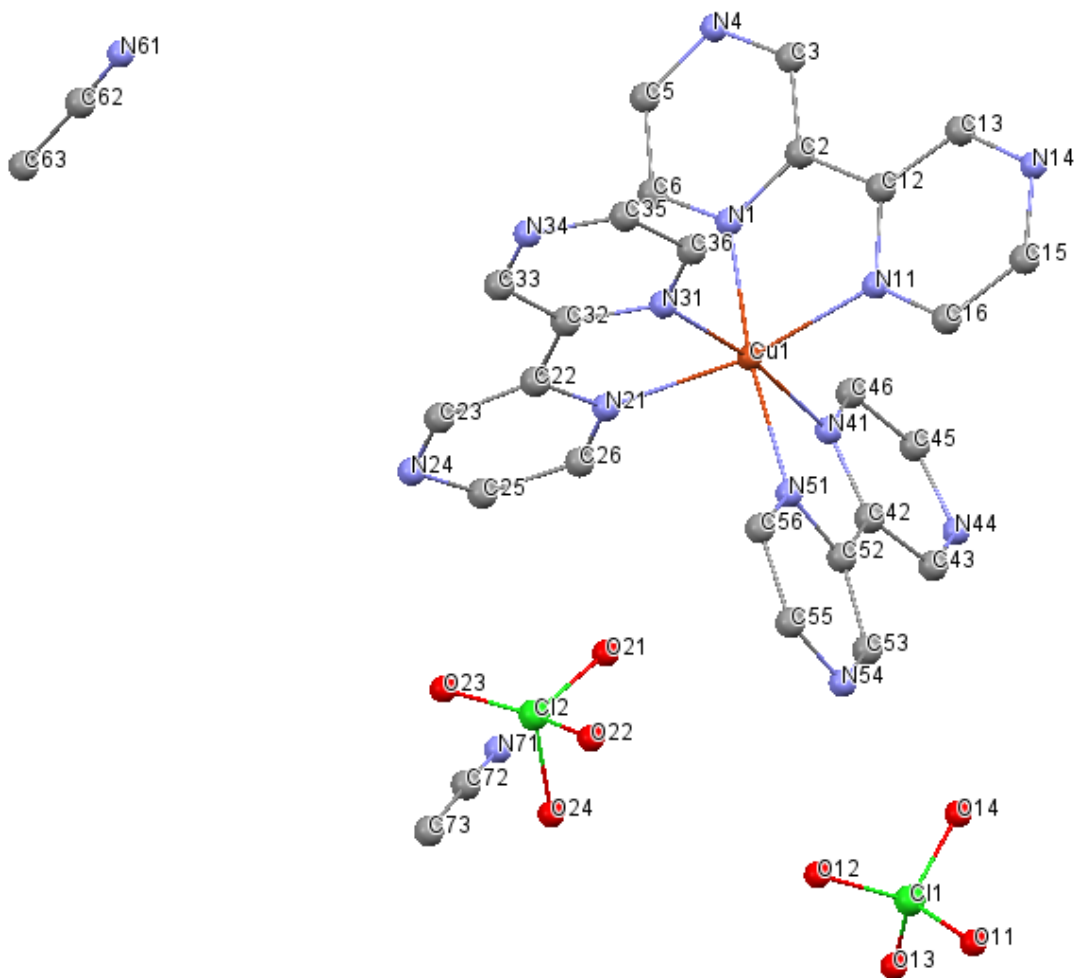


**Figure 3.28** View the structure of [Cu(bpz)<sub>3</sub>](ClO<sub>4</sub>)<sub>2</sub>·2CH<sub>3</sub>CN complex, with showing the atomic numbering

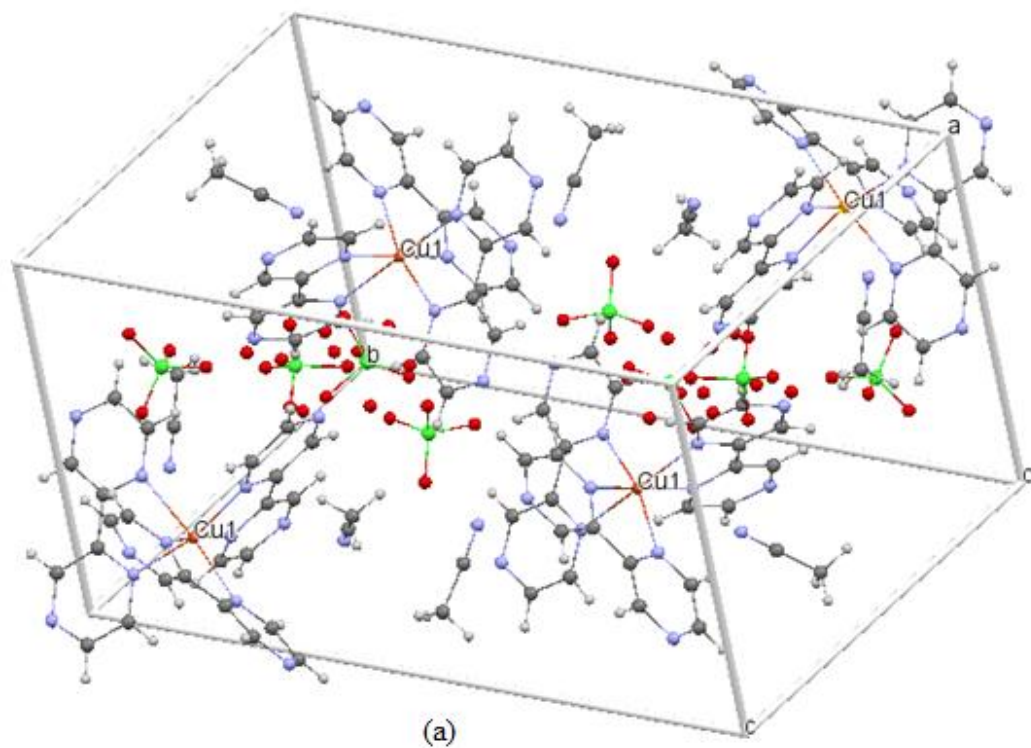


**Figure 3.29 a** View the structure packing of  $[\text{Cu}(\text{bpz})_3](\text{ClO}_4)_2 \cdot 2\text{CH}_3\text{CN}$  complex within the unit cell.

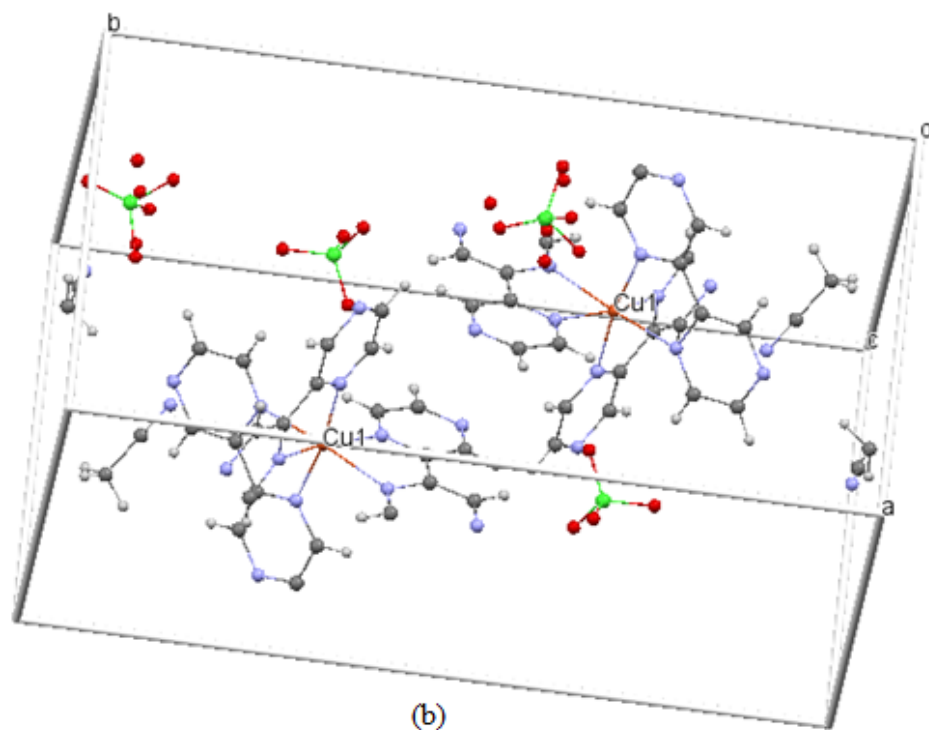


**Figure 3.29 b** View a part of unit cell for the  $[\text{Cu}(\text{bpz})_3](\text{ClO}_4)_2 \cdot 2\text{CH}_3\text{CN}$  complex

The three bidentate bpz ligands are nearly to form a propeller-like trigonal arrangement around the Cu(II) atom. The copper(II) ion is coordinated by six nitrogen atoms of three chelating bpz ligands in a distorted octahedral geometry, where the bite distance of the ligand is too short to fit identical octahedron. The N41 and N31 in the axial positions with distance Cu1-N41 2.290 Å, Cu1-N31 2.330 Å which is longest Cu-N and the angle N41-Cu-N31 is 172.6°. Also the largest angle, the N1, N11, N21 and N5 at equatorial positions forming elongated octahedral geometry. Four distinct CH<sub>3</sub>CN and ClO<sub>4</sub><sup>-</sup> molecules are present in the crystal lattices. The bonding of N atoms of three bpz ligands with the copper metal lead to forming five-member chelate rings, in which the distance bond of Cu-N is range between 2.024(8) – 2.330(10) Å with an average of 2.137 Å (table 3.15, fig. 3.30) [256, 260, 272, 280(a)]

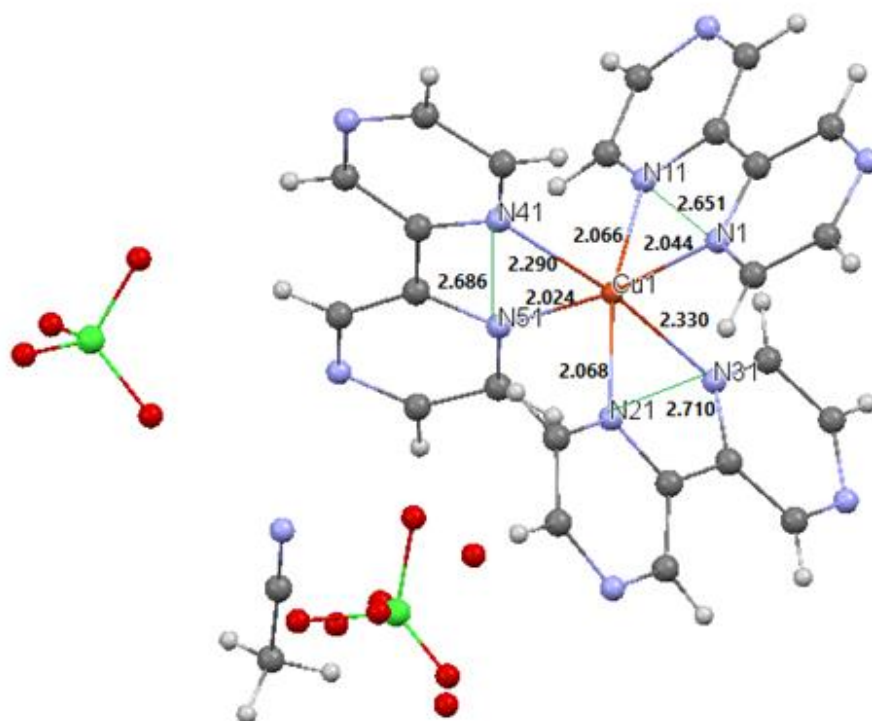


**Figure 3.30** View the bite distance and the distance between the Cu-ligand of the [Cu(bpz)<sub>3</sub>](ClO<sub>4</sub>)<sub>2</sub>·2CH<sub>3</sub>CN complex according to the X-ray complex

**Table 3.15:** Bond length [Å°] of [Cu(bpz)<sub>3</sub>](ClO<sub>4</sub>)<sub>2</sub>.2CH<sub>3</sub>CN complex

Atom 1	Atom 2	Length	Atom 1	Atom 2	Length	Atom 1	Atom 2	Length
Cu(1)	N(51)	2.024(8)	C(23)	N(24)	1.323(17)	Cl(1)	O(11)	1.401(11)
Cu(1)	N(1)	2.044(9)	C(23)	H(23)	0.9500	Cl(1)	O(12)	1.421(9)
Cu(1)	N(21)	2.067(9)	N(24)	C(25)	1.317(17)	Cl(1)	O(14)	1.429(10)
Cu(1)	N(11)	2.067(8)	C(25)	C(26)	1.382(17)	Cl(2)	O(22')	1.23(3)
Cu(1)	N(41)	2.290(10)	C(25)	H(25)	0.9500	Cl(2)	O(23)	1.27(4)
Cu(1)	N(31)	2.330(10)	C(26)	H(26)	0.9500	Cl(2)	O(24')	1.36(3)
N(1)	C(6)	1.317(14)	N(31)	C(36)	1.332(15)	Cl(2)-	O(23')	1.43(3)
N(1)	C(2)	1.356(14)	N(31)	C(32)	1.336(15)	Cl(2)-	O(21)	1.46(2)
C(2)	C(3)	1.387(15)	C(32)	C(33)	1.383(16)	Cl(2)-	O(24)	1.51(3)
C(2)	C(12)	1.450(16)	C(33)	N(34)	1.314(17)	Cl(2)-	O(22)	1.53(2)
C(3)	N(4)	1.337(17)	C(33)	H(33)	0.9500	Cl(2)-	O(21')	1.54(5)
C(3)	H(3)	0.9500	N(34)	C(35)	1.335(18)	N(61)-	C(62)	1.14(2)
N(4)	C(5)	1.341(17)	C(35)	C(36)	1.376(18)	C(62)-	C(63)	1.44(3)
C(5)	C(6)	1.371(17)	C(35)	H(35)	0.9500	C(63)-	H(63A)	0.9800
C(5)	H(5)	0.9500	C(36)	H(36)	0.9500	C(63)-	H(63B)	0.9800
C(6)	H(6)	0.9500	N(41)	C(46)	1.330(14)	C(63)-	H(63C)	0.9800
N(11)	C(16)	1.323(14)	N(41)	C(42)	1.350(14)	N(71)-	C(72)	1.15(3)
N(11)	C(12)	1.369(13)	C(42)	C(43)	1.372(17)	C(72)-	C(73)	1.42(3)
C(12)	C(13)	1.373(16)	C(42)	C(52)	1.474(16)	C(73)-	H(73A)	0.9800
C(13)	N(14)	1.347(16)	C(43)	N(44)	1.337(17)	C(73)-	H(73B)	0.9800
C(13)	H(13)	0.9500	C(43)	H(43)	0.9500	C(73)-	H(73C)	0.9800
N(14)	C(15)	1.335(16)	N(44)	C(45)	1.318(16)			
C(15)	C(16)	1.382(17)	C(45)	C(46)	1.403(18)			
C(15)	H(15)	0.9500	C(45)	H(45)	0.9500			
C(16)	H(16)	0.9500	C(46)	H(46)	0.9500			
N(21)	C(26)	1.318(15)	N(51)	C(56)	1.342(14)			
N(21)	C(22)	1.364(14)	N(51)	C(52)	1.369(14)			
C(22)-	C(23)	1.393(17)	C(52)	C(53)	1.374(15)			
C(22)	C(32)	1.480(16)	C(53)	N(54)	1.323(16)			
C(15)	H(15)	0.9500	C(53)	H(53)	0.9500			
C(16)	H(16)	0.9500	N(54)	C(55)	1.308(16)			
N(21)	C(26)	1.318(15)	C(55)	C(56)	1.398(15)			
N(21)	C(22)	1.364(14)	C(55)	H(55)	0.9500			
C(22)	C(23)	1.393(17)	C(56)	H(56)	0.9500			
C(22)	C(32)	1.480(16)	Cl(1)	O(13)	1.384(12)			

Beside to that, the distortion of octahedral geometry is confirmed because of the values of angles between N atom of bpz ligands and Cu metal ( $80.32^\circ(3)$ ,  $76.74^\circ(3)$  and  $75.80^\circ(3)$ ) for N(11)–Cu–N(1), N(41)–Cu– N(51) and N(21)–Cu–N(31) respectively, (table 3.16, fig. 3.31) [272] The theoretical study expect a deformation towards the trigonal- prismatic geometry for tris(bidentate chelate) compounds, that correspond to angles less than  $90^\circ$  at the coordination metal atom. [280a]

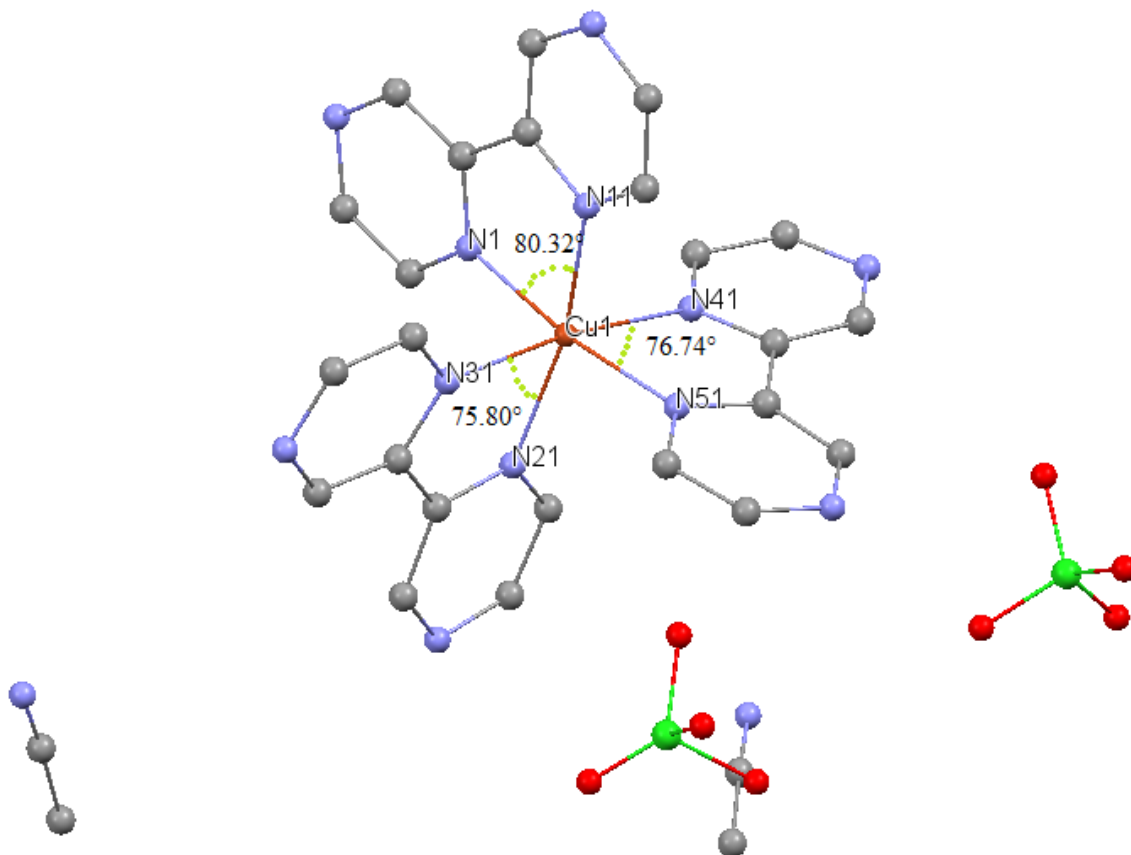


**Figure 3.31** View the bite angles between N atom of bpz ligands and Cu metal of  $[\text{Cu}(\text{bpz})_3](\text{ClO}_4)_2 \cdot 2\text{CH}_3\text{CN}$  complex.

**Table 3.16:** Bond angle [deg.] of  $[\text{Cu}(\text{bpz})_3](\text{ClO}_4)_2 \cdot 2\text{CH}_3\text{CN}$  complex

N(51)–Cu(1)–N(1)	171.4(4)	C(6)–C(5)–H(5)	118.9
N(51)–Cu(1)–N(21)	90.6(3)	N(1)–C(6)–C(5)	121.6(12)
N(1)–Cu(1)–N(21)	95.5(4)	N(1)–C(6)–H(6)	119.2
N(51)–Cu(1)–N(11)	95.3(3)	C(5)–C(6)–H(6)	119.2

N(1)-Cu(1)-N(11)	80.3(3)	C(16)-N(11)-C(12)	118.1(9)
N(21)-Cu(1)-N(11)	165.5(4)	C(16)-N(11)-Cu(1)	128.6(7)
N(51)-Cu(1)-N(41)	76.7(3)	C(12)-N(11)-Cu(1)	113.2(7)
N(1)-Cu(1)-N(41)	96.1(3)	N(11)-C(12)-C(13)	118.8(11)
N(21)-Cu(1)-N(41)	100.3(3)	N(11)-C(12)-C(2)	115.7(10)
N(11)-Cu(1)-N(41)	94.1(3)	C(13)-C(12)-C(2)	125.5(11)
N(51)-Cu(1)-N(31)	96.9(3)	N(14)-C(13)-C(12)	123.7(11)
N(1)-Cu(1)-N(31)	90.6(3)	N(14)-C(13)-H(13)	118.2
N(21)-Cu(1)-N(31)	75.8(3)	C(12)-C(13)-H(13)	118.2
N(11)-Cu(1)-N(31)	90.2(3)	C(15)-N(14)-C(13)	116.0(10)
N(41)-Cu(1)-N(31)	172.6(3)	N(14)-C(15)-C(16)	121.7(11)
C(6)-N(1)-C(2)	118.7(10)	N(14)-C(15)-H(15)	119.1
C(6)-N(1)-Cu(1)	127.1(8)	C(16)-C(15)-H(15)	119.1
C(2)-N(1)-Cu(1)	114.0(7)	N(11)-C(16)-C(15)	121.7(11)
N(1)-C(2)-C(3)	118.3(10)	N(11)-C(16)-H(16)	119.2
N(1)-C(2)-C(12)	116.6(9)	C(15)-C(16)-H(16)	119.2
C(3)-C(2)-C(12)	125.1(10)	C(26)-N(21)-C(22)	118.6(10)
N(4)-C(3)-C(2)	123.7(12)	C(26)-N(21)-Cu(1)	123.3(8)
N(4)-C(3)-H(3)	118.1	C(22)-N(21)-Cu(1)	118.0(8)
C(2)-C(3)-H(3)	118.1	N(21)-C(22)-C(23)	117.3(11)
C(3)-N(4)-C(5)	115.6(11)	N(21)-C(22)-C(32)	118.3(10)
N(4)-C(5)-C(6)	122.1(12)	C(23)-C(22)-C(32)	124.3(11)
N(4)-C(5)-H(5)	118.9	N(24)-C(23)-C(22)	124.7(12)

The Cu-N bond length indicated to that Cu(II) atom is displaced from the central of the octahedral, the coordination environment has some kind of flexible and could be fit within certain limits to suit packing requirements, the (Cu-N31) is the longest bond distance 2.330 Å, that may the reason for that returned to Jahn-teller effect and maybe the bite distance of the ligand or the ligand is pushed away as a result of existing of ClO<sub>4</sub> and CH<sub>3</sub>CN counter ions neighboring to the complex. [280a, 328]

There are different hydrogen bonds are formed between atoms (fig. 3.32), where there are hydrogen bond between hydrogen atoms of acetonitrile and nitrogen atom of bpz ligands which are [3.591 Å for C73—H73A···N4] and [3.538 Å for C63—H63B···N44].

Moreover, according to table 3.17, there are two hydrogen bonds made up between the oxygen atoms of perchlorate molecules and hydrogen atom of bpz ligands, first, the hydrogen bond is between [2.917 Å for C56—H56···O13], [3.232 Å for C36—H36···O14] and between [2.977 Å for C26—H26···O11]. Second, hydrogen bond is between [3.334 Å for C33—H33···O13], [3.411 Å for C23—H23···O11], [3.384 Å for C15—H15···O21], [3.470 Å for C45—H45···O22] and between [3.473 Å for C3—H3···O12]. Furthermore, returned to table 3.17, another hydrogen bond formed between hydrogen atom of acetonitrile and oxygen atom of perchlorate [3.177 Å for C63—H63C···O22] and [3.605 Å for C73—H73B···O23]. At least, the interaction of the C-H of bpz with O atom of ClO<sub>4</sub> could display a Van Der Waal force. [280a]

On one hand, based on table 3.17, it could be noticed that there are different types of hydrogen bonds depend on the bond angles. The majority of hydrogen bonds between atoms classified as moderate hydrogen bond because the values of bond angles ranged between. While, there are weak and moderate hydrogen bonds between the hydrogen atoms of bpz ligand and oxygen atoms of perchlorate, which are [169.25° C3—H3···O12 (nearly to be strong)] and [96.48° C56—H56···O13 (weak)] [280(1)]

**Table 3.17:** Hydrogen geometry (Å, °) of [Cu(bpz)<sub>3</sub>](ClO<sub>4</sub>)<sub>2</sub>.2CH<sub>3</sub>CN complex

D—H···A	D—H (Å°)	H···A (Å°)	D···A (Å°)	D—H···A (°)
C73—H73A···N4	0.978	2.693	3.591	152.80
C3—H3···O12	0.951	2.535	3.473	169.25
C36—H36···O14	0.949	2.608	3.232	123.69
C26—H26···N14	0.951	2.533	3.318	139.94
C15—H15···O21	0.950	2.658	3.384	133.64
C46—H46···N54	0.950	2.387	3.222	146.52
C45—H45···O22	0.951	2.705	3.470	138.68
C63—H63B···N44	0.980	2.587	3.538	163.82
C56—H56···N34	0.950	2.481	3.263	139.64
C26—H26···O11	0.951	2.506	2.977	110.61
C6—H6···N24	0.950	2.502	3.225	132.96
C23—H23···O11	0.950	2.586	3.411	145.41
C33—H33···O13	0.951	2.509	3.334	145.26
C56—H56···O13	0.950	2.653	2.917	96.48
C73—H73B···O23	0.981	2.638	3.605	168.28
C63—H63C···O22	0.980	2.327	3.177	144.64

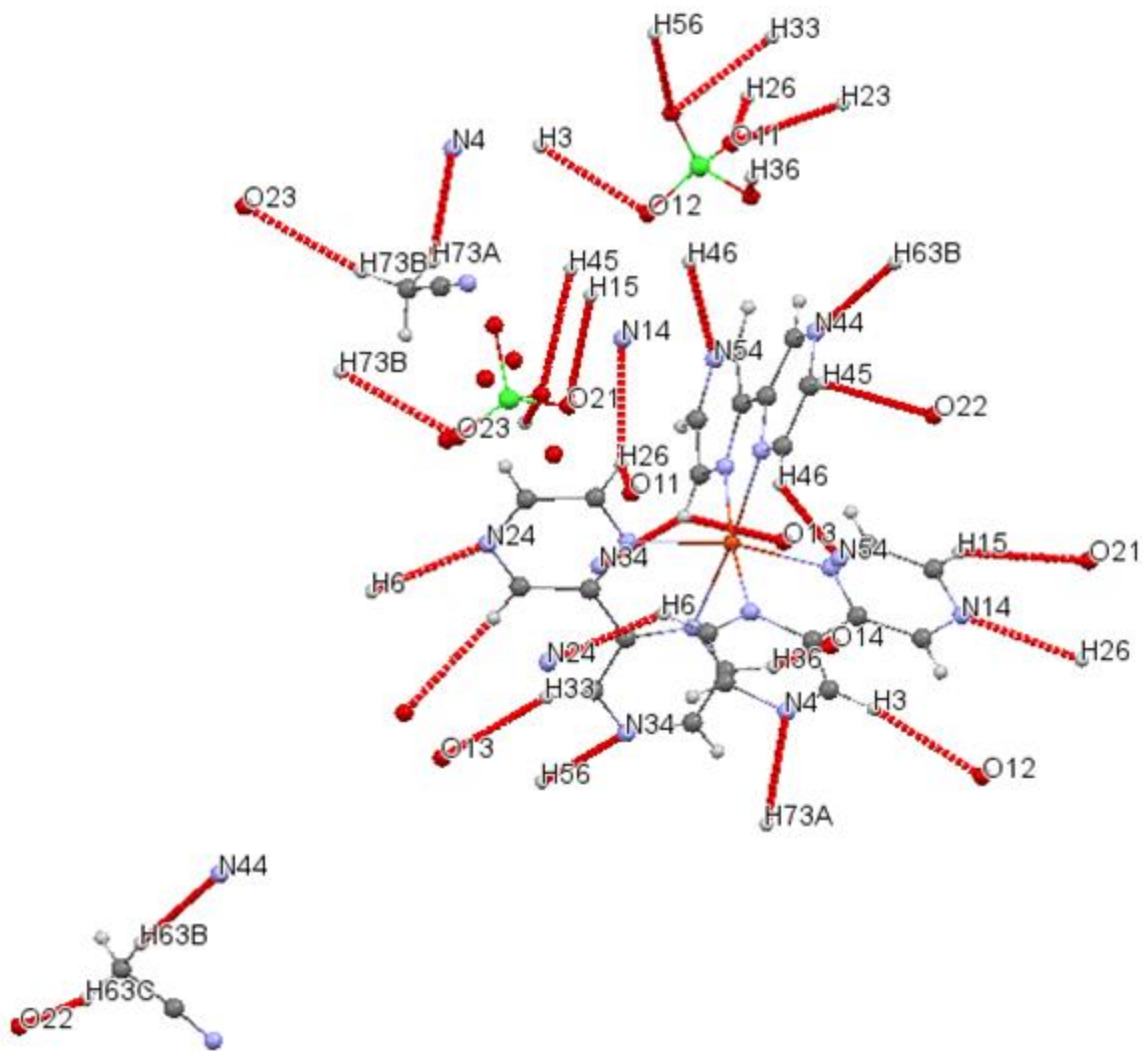


**Figure 3.32** View the inter-interaction H-bonds of the  $[\text{Cu}(\text{bpz})_3](\text{ClO}_4)_2 \cdot 2\text{CH}_3\text{CN}$

On one hand, not only the hydrogen bond contributed in construction of the supramolecular in the crystal packing (fig. 3.33), but also the  $\pi$ - $\pi$  interaction has a role (fig. 3.34); because the distance between the aromatic rings, which is larger than  $3.0 \text{ \AA}$ , is an evidence for their occurring. [280(a)]

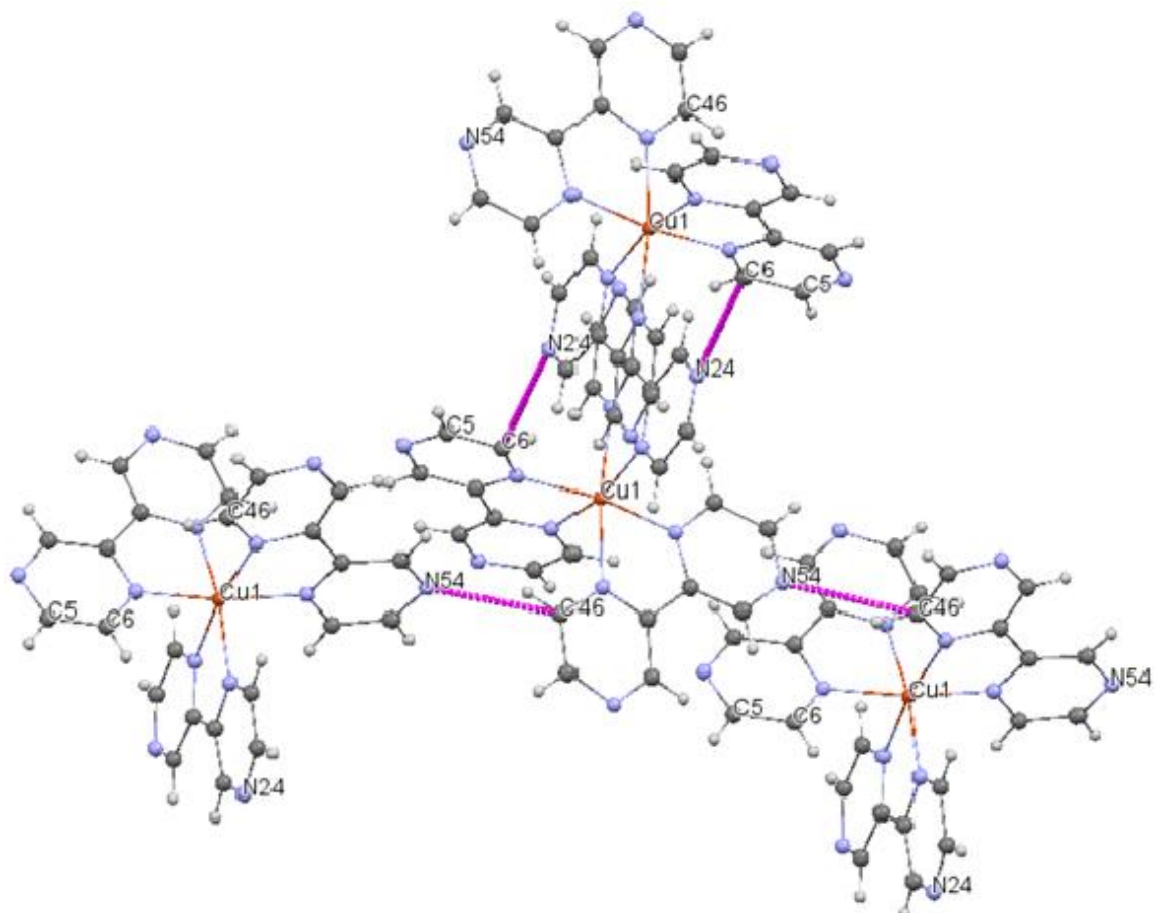


**Figure 3.33** View the crystal packing of  $[\text{Cu}(\text{bpz})_3](\text{ClO}_4)_2 \cdot 2\text{CH}_3\text{CN}$  complex with showing the inter-interaction H-bonds.

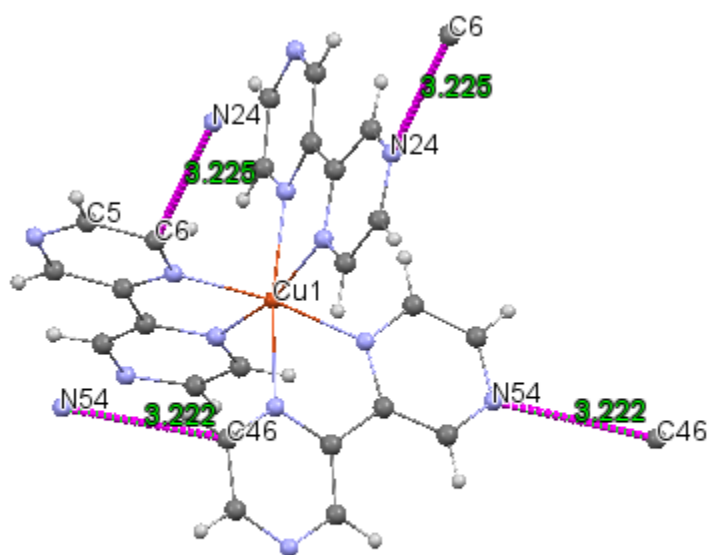


**Figure 3.34** View the  $\pi$ - $\pi$  interaction distance between the atomic rings of the  $[\text{Cu}(\text{bpz})_3](\text{ClO}_4)_2 \cdot 2\text{CH}_3\text{CN}$  complex

The packing of the  $[\text{Cu}(\text{bpz})_3](\text{ClO}_4)_2 \cdot 2\text{CH}_3\text{CN}$  complex is appeared that the polypyridyl ligands are fixed in one set between the bpz ligands with parallel displacement shaped interaction, figure 3.35. [280a]

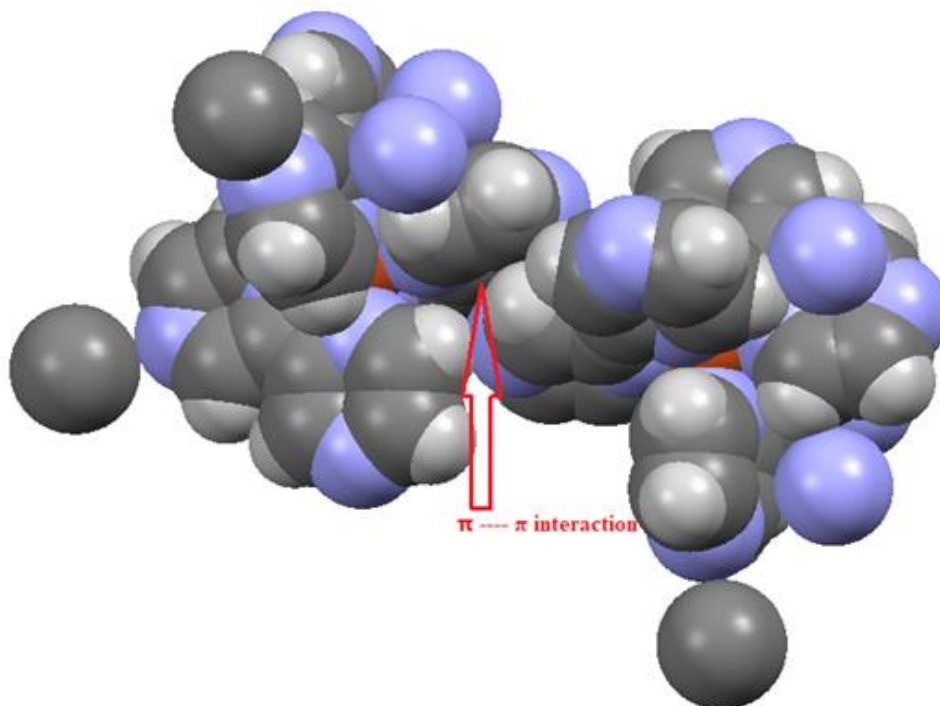


**Figure 3.35** View the space-filling packing diagram of  $[\text{Cu}(\text{bpz})_3](\text{ClO}_4)_2 \cdot 2\text{CH}_3\text{CN}$  complex, showing the interactions of adjacent chains.

According to the comparison between the  $[\text{Cu}(\text{bpz})_3](\text{ClO}_4)_2 \cdot 2\text{CH}_3\text{CN}$  complex and the isomorphous compounds, its ligand bite and M-N distance (its values :  $2.137 \text{ \AA}$ ) is the highest one. Where the value of M-N distance for the  $[\text{Ni}(\text{bpz})_3](\text{ClO}_4)_2 \cdot \text{H}_2\text{O}$ ,  $[\text{Fe}(\text{bpz})_3](\text{ClO}_4)_2 \cdot \text{H}_2\text{O}$ ,  $[\text{Ru}(\text{bpz})_3](\text{PF}_6)_2$  and  $[\text{Ni}(\text{bpy})_3](\text{PF}_6)_2$  are  $2.081$ ,  $1.961$ ,  $2.051$  and  $2.094 \text{ \AA}$  respectively. Because of Johan-Teller effect on  $\text{Cu}^{+2}$  ( $d^9$ ) complex and this is confirmed the elongated octahedral geometry. And because the ligands are similar that support to exist the John Teller effect. [138(h), 280(a)].

#### **3.4.4 Synthesis for [Cu(bpz)<sub>3</sub>](ClO<sub>4</sub>)<sub>2</sub>.2CH<sub>3</sub>CN complex**

While trying to prepare the Cu(II) complex containing 2,2'-bipyrazine and tricyclohexylphosphine (C<sub>18</sub>H<sub>33</sub>P) ligands by using acetonitrile solvent. The expected complex did not get, instead of that, green crystals of tris(2,2'-bipyrazine)copper(II) perchlorate, and two molecules of acetonitrile in the lattice. The novel complex has been characterized via single-crystal diffraction analysis, IR analysis and thermal analysis. The single crystal X-ray diffraction showed that tricyclohexylphosphine (C<sub>18</sub>H<sub>33</sub>P) does not appear neither coordination and nor uncoordination region. The role of tricyclohexylphosphine could be facilitate to bind the tris bpz ligands with Cu(II) metal beside to existing of acetonitrile, where when used other solvents as water and methanol failed to get [Cu(bpz)<sub>3</sub>]<sup>+2</sup> complex.

#### **3.5 [Ni(dipyam)<sub>2</sub>(bpz)](ClO<sub>4</sub>)<sub>2</sub> complex**

Nickel complexes, in general, are gaining huge cared in the bioinorganic research. In this regard, nickel compounds have been able to performance as antiepileptic and anticonvulsant agents and others possess antibacterial, antifungal, antimicrobial and antiproliferative activity. Beside to that, the studies that about DNA-binding explored that nickel complexes are considered as a potential alternative to cis-platin [280a, 265]

The [Ni(dipyam)<sub>2</sub>(bpz)](ClO<sub>4</sub>)<sub>2</sub> complex in this work may have attention in the future researches because it consists bidentate ligands. The idea about bidentate ligands that they have ability to build the supramolecular architectures via covalent bonding or hydrogen bonding and  $\pi$ - $\pi$  interactions in organic-inorganic hybrid molecules since they have possibility to utilize as function materials. [167b, 242, 261]

This expectation is resulted as there are some complexes are similar in their structure to the [Ni(dipyam)<sub>2</sub>(bpz)](ClO<sub>4</sub>)<sub>2</sub> complex, including [Ni(dpa)<sub>2</sub>(dca)<sub>2</sub>] [242], [Cu(2,2'-dipyridylamine)<sub>2</sub>(NO<sub>3</sub>)<sub>2</sub>] [250], [M(dpa)<sub>2</sub>(N<sub>3</sub>)<sub>2</sub>].H<sub>2</sub>O, where M= Ni [261], [Ni(bz)(dipyam)<sub>2</sub>](bz).2MeOH complex [266], [Ru(2,2'-bipyridine)<sub>2</sub>(Hdpa)](BF<sub>4</sub>)<sub>2</sub>.2H<sub>2</sub>O complex, where dpa= 2,2'-dipyridylamine, dca = sodium dicyanamide, dipyam= 2,2'-dipyridylamine, bz= benzilato, Hdpa= 2,2'-dipyridylamine [276].

These resemble complexes have different using. For example, [Cu(2,2'-dipyridylamine)<sub>2</sub>(NO<sub>3</sub>)<sub>2</sub>] has an efficiency in the DNA cleavage [250], [M(dpa)<sub>2</sub>(N<sub>3</sub>)<sub>2</sub>] . H<sub>2</sub>O acts as luminous materials, in which can be attached to their supramolecular networks, [261] and [Ni(dpamH)<sub>2</sub>(X-salo)]Cl complex and its derivatives are promising to use as potential metallo-therapeutic agents (where dpamH= 2,2'-dipyridylamine, and X-salo= substituted salicylaldehydes). [265]

### 3.5.1. Infrared Spectroscopy

The infrared absorption frequencies obtained for the 2,2'-bipyrazine ligand listed in (table 3.4), for 2,2'-dipyridylamine are listed in (table 3.9), and for [Ni(dipyam)<sub>2</sub>(bpz)](ClO<sub>4</sub>)<sub>2</sub> complex are listed in table 3.18 below, and spectra are given in figure 3.36.

**Table 3.18:** Infrared frequencies (cm<sup>-1</sup>) for [Ni(dipyam)<sub>2</sub>(bpz)](ClO<sub>4</sub>)<sub>2</sub> complex and assignments.

[Ni(dipyam) <sub>2</sub> (bpz)](ClO <sub>4</sub> ) <sub>2</sub>	Assignment
3320w, 3246w, 3215w,	ν N-H
3095m, 3042m	ν C-H
1635m, 1587w, 1528w	ν C≡N
1406s, 1371vs, 1314vs	ν C≡C
1477m	δ ring
1238m	β CH
1148vs	β ring
1018s, 1054vs, 845s	ring-H in-plane bending vibrations
767s, 739s, 537m	out-of-plane ring-H bending and τ ring
1089vs, 619s, m908, s1106	ClO <sub>4</sub> <sup>-</sup>

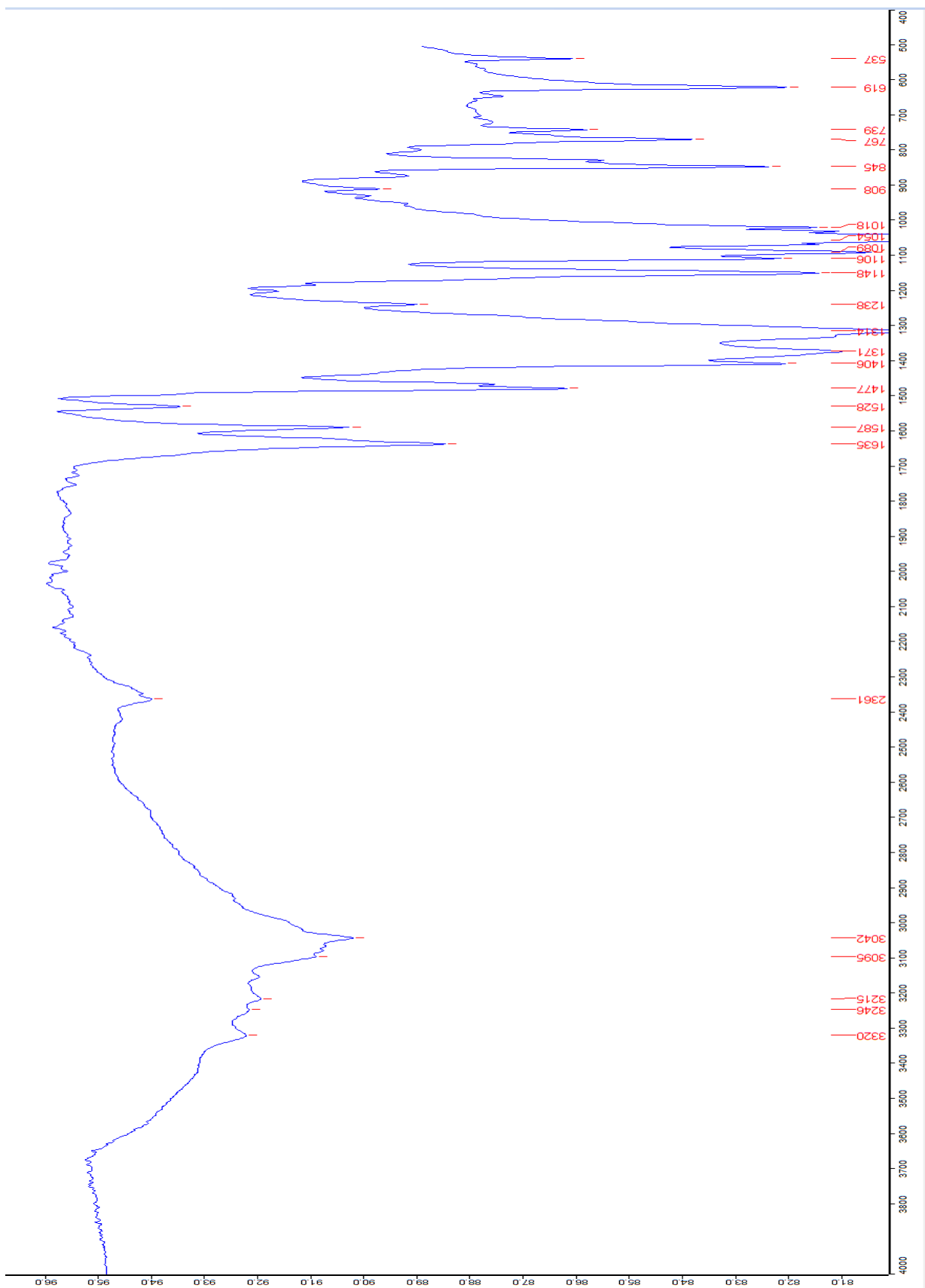
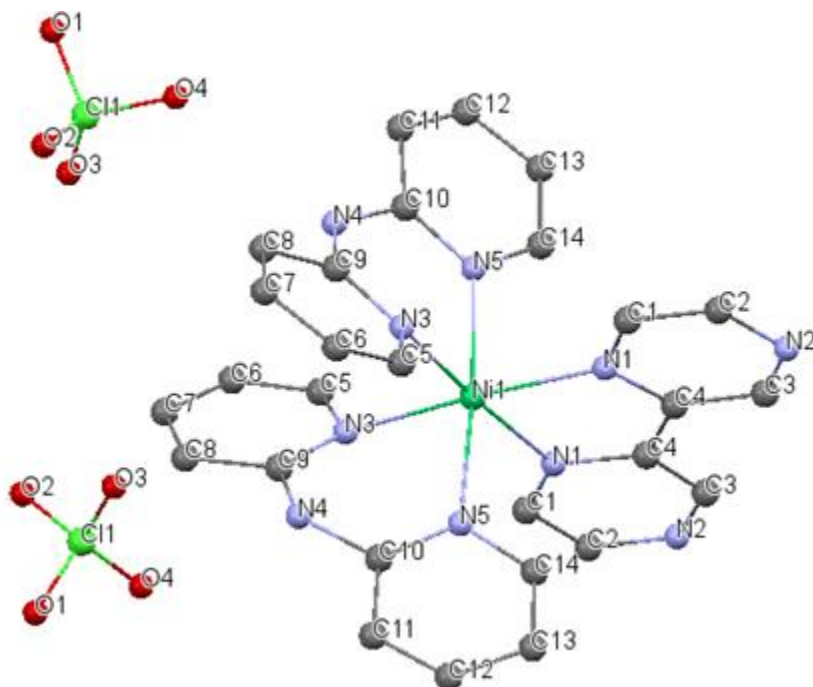


Figure 3.36 The infrared spectra of the [Ni(dipyam)2(bpz)](ClO4)2 complex

The IR spectrum of the  $[\text{Ni}(\text{dipyam})_2(\text{bpz})](\text{ClO}_4)_2$  complex was compared with that of the free 2,2'-bipyrazine and 2,2'-dipyridylamine ligands (table. 3.18, fig. 3.15). The bands in IR spectra of the complex related of 2,2'-bipyrazine ligand have characteristic bands, including medium bands at 3095, 3042  $\text{cm}^{-1}$  related to  $\nu$  C–H. The medium band at 1635  $\text{cm}^{-1}$  and two weak bands at 1587 and 1528  $\text{cm}^{-1}$  contributed to  $\nu$   $\text{C}\equiv\text{N}$ , while the strong bands at 1406, 1371 and 1314  $\text{cm}^{-1}$  correlated to  $\nu$   $\text{C}\equiv\text{C}$ , and the medium band at 1477  $\text{cm}^{-1}$  vibrations essentially deformed the ring. In addition, the medium band at 1238  $\text{cm}^{-1}$  related to  $\beta$  CH, while the very strong band at 1148  $\text{cm}^{-1}$  related to  $\beta$  ring. The strong bands at 1018 and 845  $\text{cm}^{-1}$  and the very strong band at 1054  $\text{cm}^{-1}$  are referred to ring-H in-plane binding vibrations. Whereas the medium band at 537  $\text{cm}^{-1}$  and strong bands at 767 and 739  $\text{cm}^{-1}$  are mostly out-of-plane ring-H bending and vibration torsion ring. Also, in the IR spectrum of the complex, the bands related to 2,2'-dipyridylamine ligand was moved to lower or to higher wavenumber according to metal coordination and crystal packing. Where, the medium bands at 3246 and 3215  $\text{cm}^{-1}$  assigned to N-H stretching [280a, 309,310]. The pattern vibration of the perchlorate counter ion displays a very strong sharp absorption at 1089  $\text{cm}^{-1}$ , strong peak at 619  $\text{cm}^{-1}$  and a medium intensity peak at 908  $\text{cm}^{-1}$ . The vibration of the Cl–O stretch vibration absorbance at 1106  $\text{cm}^{-1}$  is characteristic of the presence of uncoordinated perchlorate. [280a, 298, 312-314]

### **3.5.2 Crystal structure for $[\text{Ni}(\text{dipyam})_2(\text{bpz})](\text{ClO}_4)_2$ :**

The structure of complex  $[\text{Ni}(\text{dipyam})_2(\text{bpz})](\text{ClO}_4)_2$  consists of ,first, Ni(II) center, in which it is hexacoordinated by two nitrogen atoms of 2,2'-bipyrazine ligand, and four nitrogen atoms of two 2,2'-dipyridylamine ligands. The two perchlorate ions are a counter ion, as what shown in the figure 3.37 below:



**Figure 3.37** The ball and stick model represents the structure of the  $[\text{Ni}(\text{dipyam})_2(\text{bpz})]-(\text{ClO}_4)_2$  complex with the atom numbering.

Since the complex is an ionic structure that comprised chemically identical complex cation  $[\text{Ni}(\text{dipyam})_2(\text{bpz})]^{2+}$  and two uncoordinated perchlorate anions  $\text{ClO}_4^-$ , the unit cell contains two complete cations with four anions, and four half cations with four anions. The relative arrangement of the constituents units in the unit cell are shown in figure 3.38

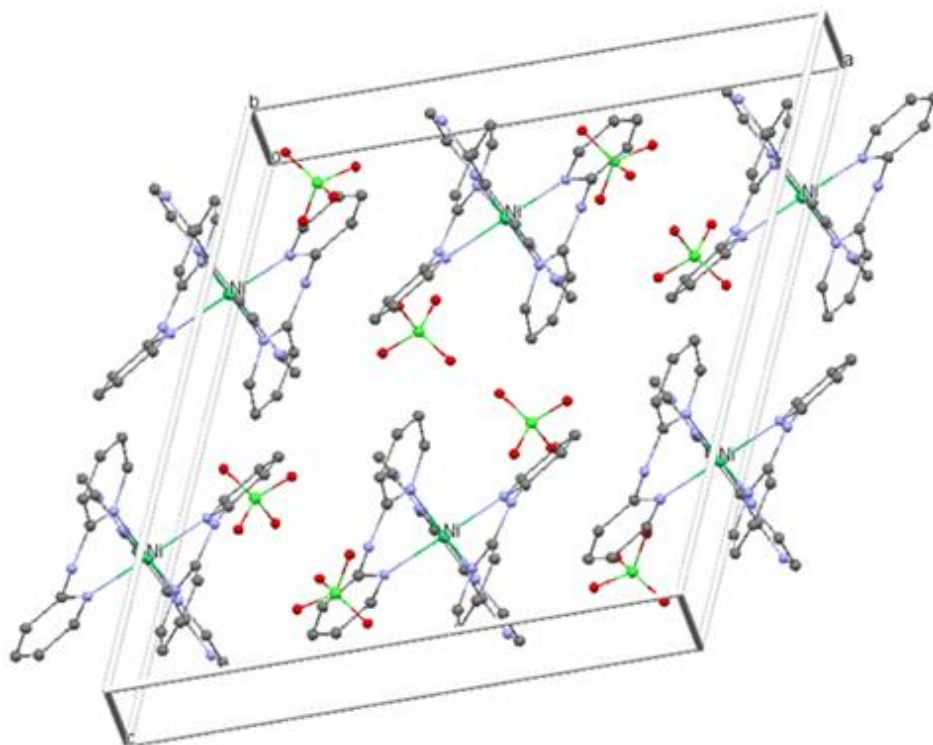


**Figure 3.38** View the structure packing of  $[\text{Ni}(\text{dipyam})_2(\text{bpz})](\text{ClO}_4)_2$  complex within unit

The complex cation possesses a distorted octahedral geometry because of existing the three chelate rings binds with Ni(II) metal, including two (dipyam), one 2,2'-bipyrazine ligands, each 2,2'-dipyridylamine located at equatorial plane N3 and at axial position N5, and bipyrazine ligands located at equatorial positions N1, N1. The geometry is proven via value of angles between nitrogen that bonded with Ni(II) metal, including  $\text{N}3^i - \text{Ni}1 - \text{N}3$  [89.31 (11)],  $\text{N}5^i - \text{Ni}1 - \text{N}3$  [91.53 (8)],  $\text{N}1^i - \text{Ni}1 - \text{N}5$  [88.70 (8)],  $\text{N}5^i - \text{Ni}1 - \text{N}5$  [175.22° (11)],  $\text{N}3^i - \text{Ni}1 - \text{N}1^i$  [175.13 (9)],  $\text{N}1 - \text{Ni}1 - \text{N}3$  [175.13 (9)]. These values deviate from the perfect bond angles of 90° and 180°. The figures 3.39 (a+b) below clarify the bond angles [329] and the table 3.19 shows the angle between atoms.

**Table 3.19:** Bond angle [deg.] of  $[\text{Ni}(\text{dipyam})_2(\text{bpz})](\text{ClO}_4)_2$  complex

$\text{N}3^i - \text{Ni}1 - \text{N}5^i$	85.06 (8)	$\text{N}1 - \text{C}1 - \text{C}2$	121.8 (3)
$\text{N}3^i - \text{Ni}1 - \text{N}1^i$	175.13 (9)	$\text{C}1 - \text{C}2 - \text{N}2$	121.7 (3)
$\text{N}5^i - \text{Ni}1 - \text{N}1^i$	94.98 (8)	$\text{N}2 - \text{C}3 - \text{C}4$	123.7 (3)
$\text{N}3^i - \text{Ni}1 - \text{N}1$	95.55 (7)	$\text{C}4^i - \text{C}4 - \text{C}3$	126.07 (19)
$\text{N}5^i - \text{Ni}1 - \text{N}1$	88.70 (8)	$\text{C}4^i - \text{C}4 - \text{N}1$	116.12 (14)
$\text{N}1^i - \text{Ni}1 - \text{N}1$	79.58 (12)	$\text{C}3 - \text{C}4 - \text{N}1$	117.8 (3)
$\text{N}3^i - \text{Ni}1 - \text{N}3$	89.31 (11)	$\text{N}3 - \text{C}5 - \text{C}6$	126.1 (3)

N5 <sup>i</sup> —Ni1—N3	91.53 (8)	C5—C6—C7	114.6 (3)
N1 <sup>i</sup> —Ni1—N3	95.55 (7)	C6—C7—C8	122.3 (3)
N1—Ni1—N3	175.13 (9)	C7—C8—C9	117.1 (3)
N3 <sup>i</sup> —Ni1—N5	91.53 (8)	C8—C9—N4	116.2 (2)
N5 <sup>i</sup> —Ni1—N5	175.22 (11)	C8—C9—N3	123.2 (3)
N1 <sup>i</sup> —Ni1—N5	88.70 (8)	N4—C9—N3	120.6 (2)
N1—Ni1—N5	94.98 (8)	N4—C10—N5	120.2 (2)
N3—Ni1—N5	85.06 (8)	N4—C10—C11	118.1 (2)
Ni1—N1—C1	128.23 (17)	N5—C10—C11	121.7 (3)
Ni1—N1—C4	114.05 (17)	C10—C11—C12	119.4 (3)
C1—N1—C4	117.7 (2)	C11—C12—C13	121.1 (3)
C2—N2—C3	117.1 (3)	C12—C13—C14	117.1 (3)
Ni1—N3—C5	119.42 (18)	C13—C14—N5	124.6 (3)
Ni1—N3—C9	120.96 (17)	O4—C11—O1	102.7 (3)
C5—N3—C9	116.2 (2)	O4—C11—O2	105.5 (3)
C9—N4—C10	129.4 (2)	O1—C11—O2	109.2 (3)
Ni1—N5—C10	122.74 (17)	O4—C11—O3	119.8 (3)
Ni1—N5—C14	121.31 (17)	O1—C11—O3	110.0 (3)
C10—N5—C14	115.8 (2)	O2—C11—O3	109.2 (3)

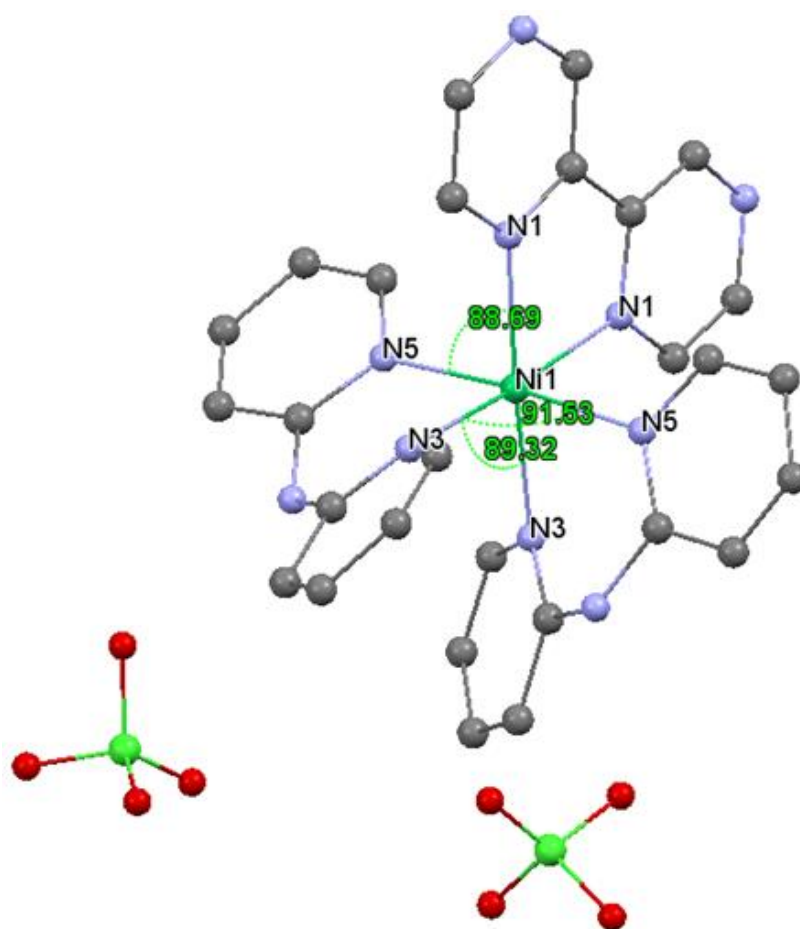


**Figure 3.39a** The angles between N atoms of ligands & Ni metal of  $[\text{Ni}(\text{dipyam})_2(\text{bpz})]\text{-(ClO}_4)_2$  complex according to the X-ray complex

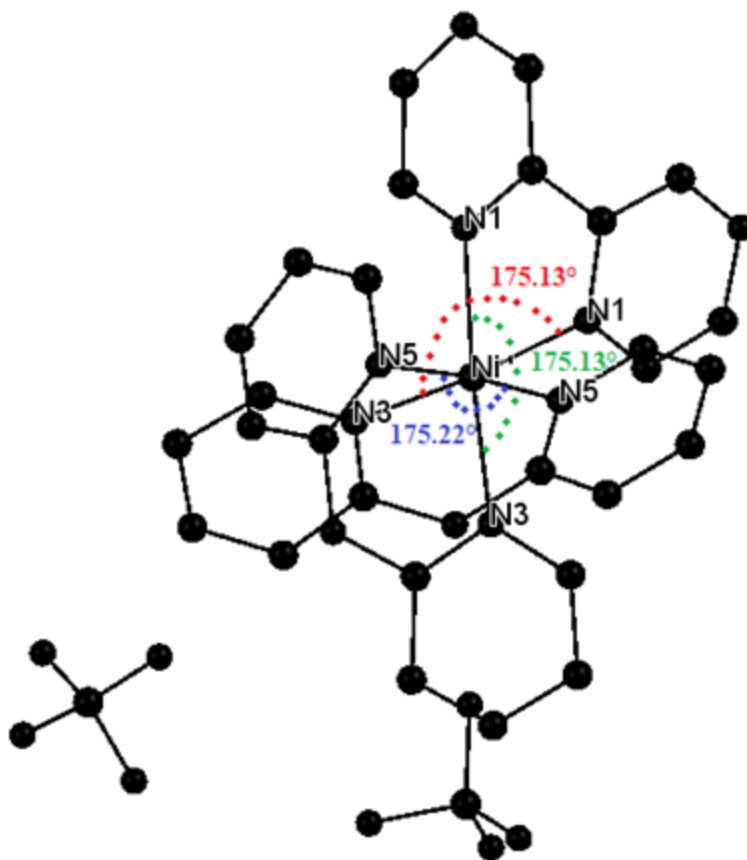


**Figure 3.39b** View the value of angles between nitrogen that bonded with Ni(II) metal of  $[\text{Ni}(\text{dipyam})_2(\text{bpz})](\text{ClO}_4)_2$  complex, color used to distinguish between them.

They involve bite angle  $[\text{N}3^i\text{—Ni1—N}5^i]$  of  $85.06^\circ$  (table 3.20, fig. 3.40(a+b)), slightly less than  $90^\circ$ . This reflect the degrees of distortion from the perfect octahedral geometry. [261] The  $\text{N}(3^i) \dots \text{N}(5^i)$  bite distances  $2.826 \text{ \AA}$  (fig. 3.40(a+b)) are remarkably raised with respect to the bite value of the uncoordinated 2,2'-dipyridylamine ( $2.6 \text{ \AA}$ ) which assessed by A. N. Chernyshev et al. [280a+o)]

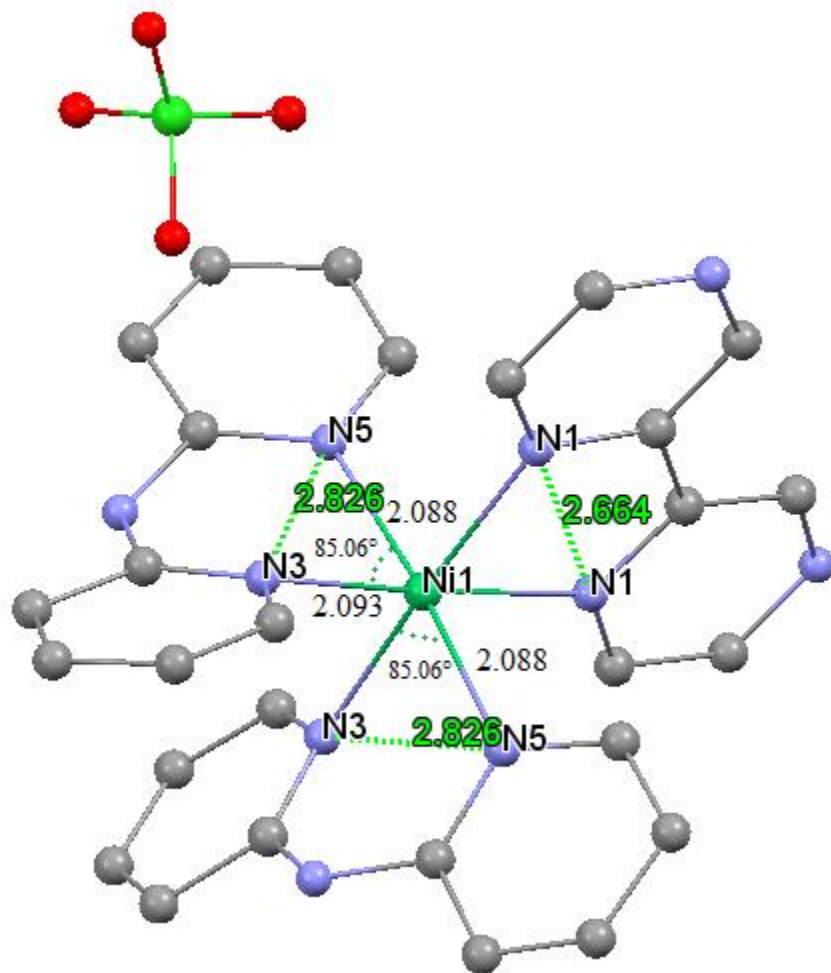


**Figure 3.40a** View the bite distance and the bite angles between N atoms of ligands & Ni metal of  $[\text{Ni}(\text{dipyam})_2(\text{bpz})](\text{ClO}_4)_2$  complex according to the X-ray.

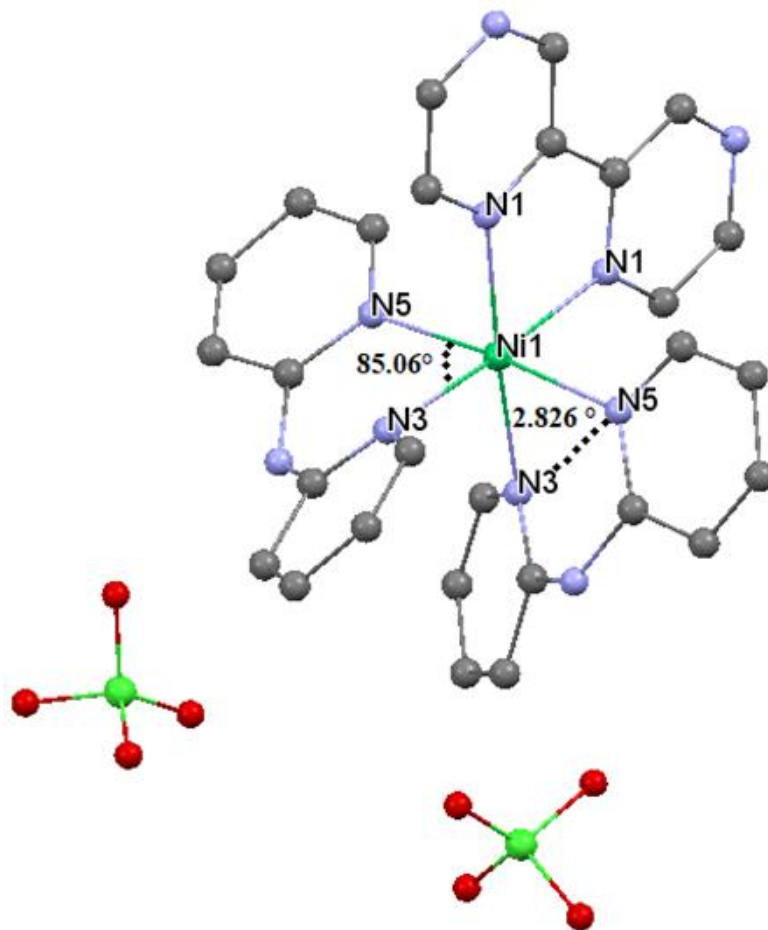


**Figure 3.40b** View the value of bite angle between  $N3^i-Ni1-N5^i$  and bite distance between  $N(3^i)\dots N(5^i)$  of  $[Ni(dipyam)_2(bpz)](ClO_4)_2$  complex.

The distance between Ni metal and nitrogen atoms range between 2.081 – 2.093 Å. The dipyam ligands binds Ni metal via the two pyridine ends without losing the dissociable proton on N4 atom. The Ni–dipyam bond distances are very similar to those observed in other dipyam complexes. [276, 329] The Ni–N bond distances (table 3.20, fig. 3.41) are 2.088 and 2.093 Å for Ni–N5, Ni–N3 respectively, which are so similar to the dpa analogous complexes with Ni–N systems. [167b, 242, 261, 280(a, m), 309]

**Table 3.20:** Bond length [Å] of  $[Ni(dipyam)_2(bpz)](ClO_4)_2$  complex

Atom 1	Atom 2	Length	Atom 1	Atom 2	Length
Ni1	N3 <sup>i</sup>	2.093 (2)	O1	Cl1	1.355 (4)
Ni1	N5 <sup>i</sup>	2.0881 (19)	O2	Cl1	1.352 (4)
Ni1	N1 <sup>i</sup>	2.081 (2)	O3	Cl1	1.283 (4)

Ni1	N1	2.081 (2)	O4	C11	1.374 (4)
Ni1	N3	2.093 (2)	C1	C2	1.379 (4)
Ni1	N5	2.0881 (19)	C3	C4	1.393 (4)
N1	C1	1.309 (3)	C4	C4 <sup>i</sup>	1.466 (5)
N1	C4	1.360 (3)	C5	C6	1.361 (4)
N2	C2	1.301 (4)	C6	C7	1.370 (4)
N2	C3	1.302 (4)	C7	C8	1.351 (4)
N3	C5	1.340 (3)	C8	C9	1.394 (4)
N3	C9	1.303 (3)	C10	C11	1.390 (4)
N4	C9	1.371 (3)	C11	C12	1.305 (4)
N4	C10	1.370 (3)	C12	C13	1.346 (4)
N5	C10	1.329 (3)	C13	C14	1.359 (4)
N5	C14	1.331 (3)			

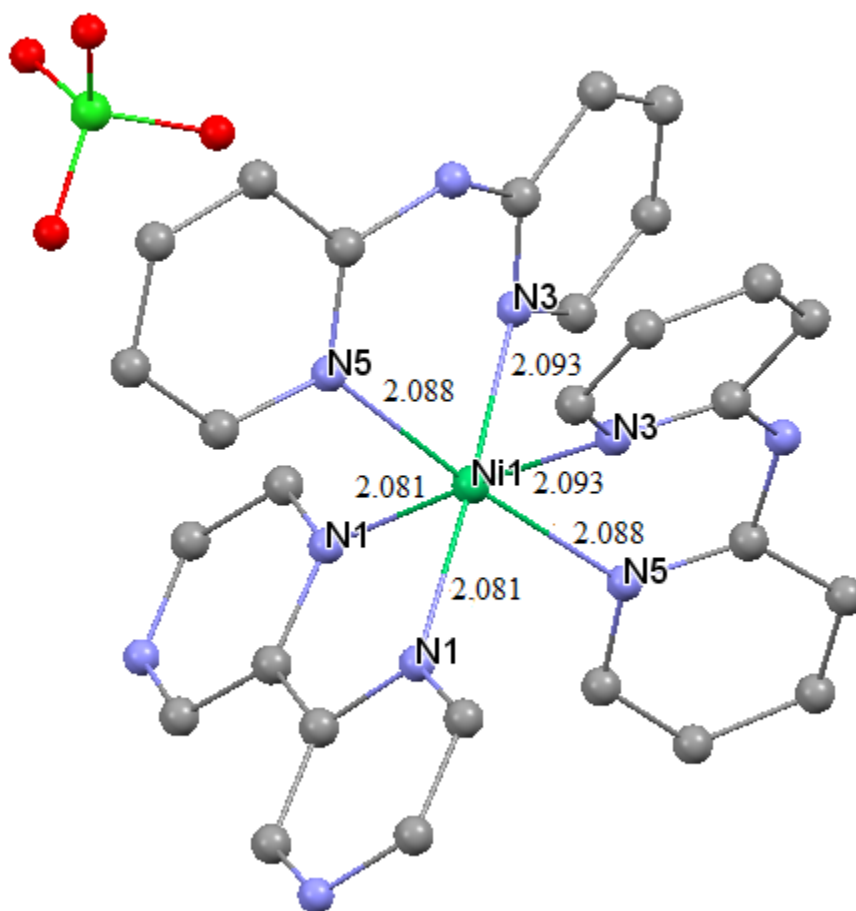


**Figure 3.41** View the distance between Ni metal and nitrogen ligands of  $[\text{Ni}(\text{dipyam})_2(\text{bpz})](\text{ClO}_4)_2$  complex.

The perchlorate anions link the complex cations to form a chain structure through N—H•••O close contacts and C—H•••O hydrogen bonds of 2,2'-dipyridylamine, beside to 2,2'-bipyrazine ligand binds through C—H•••N as what shown in the figure 3.42 and 3.43 below

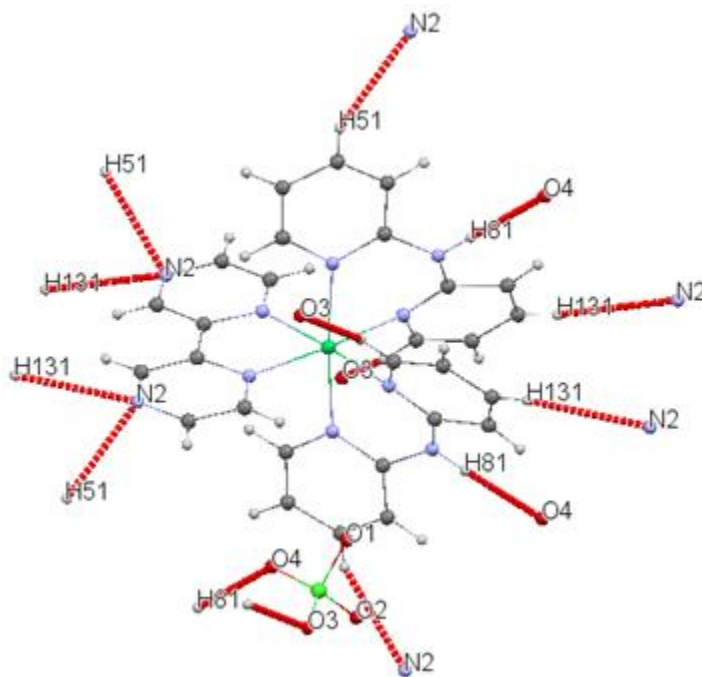


**Figure 3.42** View the inter-interaction H-bonds of the [Ni(dipyam)<sub>2</sub>(bpz)](ClO<sub>4</sub>)<sub>2</sub> complex

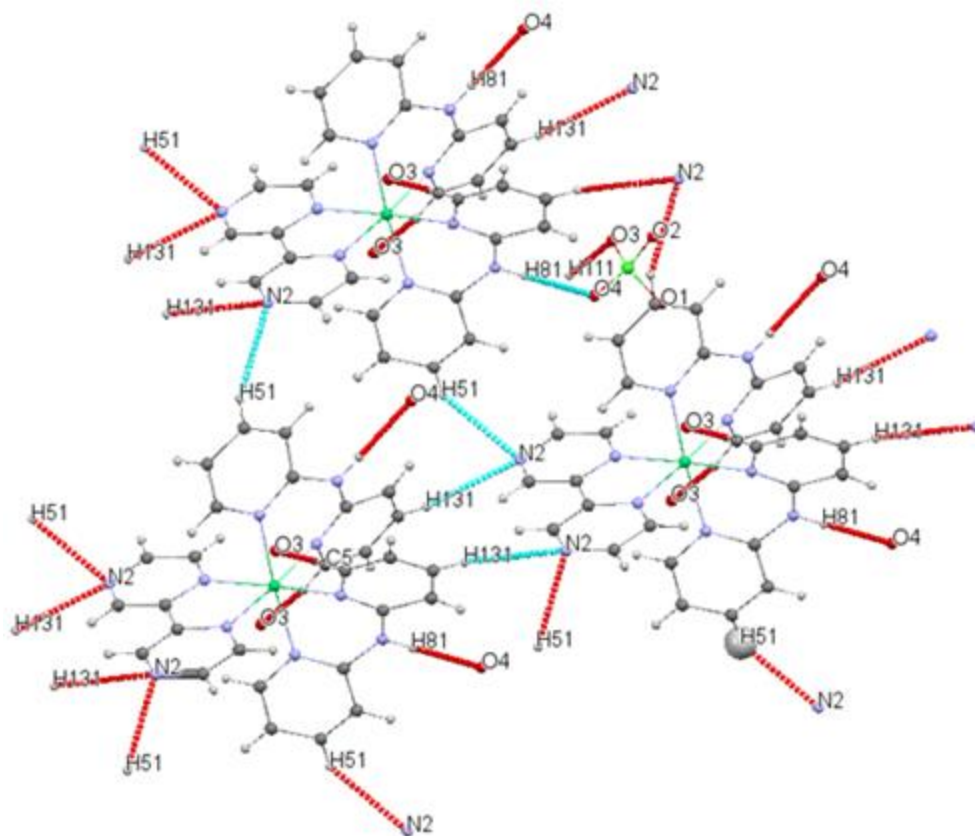


**Figure 3.43** View the crystal packing of  $[\text{Ni}(\text{dipyam})_2(\text{bpz})](\text{ClO}_4)_2$  complex with showing the inter-interaction H-bonds.

The table 3.21 below displays the corresponding D-H,  $\text{H}\cdots\text{A}$  and  $\text{D}\cdots\text{A}$  bond distances and  $\text{D}-\text{H}\cdots\text{A}$  bond angles, where D: donor, A: acceptor.

**Table 3.21** Hydrogen geometry ( $\text{\AA}$ ,  $^\circ$ ) of  $[\text{Ni}(\text{dipyam})_2(\text{bpz})](\text{ClO}_4)_2$  complex

D—H $\cdots$ A	D—H	H $\cdots$ A	D $\cdots$ A	D—H $\cdots$ A
N4—H81 $\cdots$ O4 <sup>ii</sup>	0.88	2.11	2.984 (4)	172
C5—H111 $\cdots$ O3	0.925	2.607	3.372	140.50
C7—H131 $\cdots$ N2	0.926	2.749	3.531	142.74
C12—H51 $\cdots$ N2	0.932	2.633	3.350	134.18

The studies perspective of that O—H $\cdots$ N hydrogen bonds leads to procedure a 1D sheet, the tangled of O—H $\cdots$ N and N—H $\cdots$ O hydrogen bonds create the 2D, while 3D

formed by face to face  $\pi$ - $\pi$  and edge to face C—H $\cdots$  $\pi$  [261] Accordingly, it can be concluded to that perchlorate anion acts as bridge with the cations of the complex; to form two-dimensional sheet as what the figure 3.44 shown. These sheets linked with others via the oxygen atoms of perchlorate with NH and C-H groups of 2,2'-dipyridylamine ligand with distance value 2.984 (4) and 3.372 Å, and via weak interaction between the nitrogen atoms of 2,2'-bipyrazine with C-H groups of 2,2'-dipyridylamine ligand in adjacent structure unit with distance value 3.531 and 3.350 Å. The oxygen atom of perchlorate are linked with C-H(dipyam) in weak interactions in distance 2.607 Å which are in the normal range of the weak interactions. [167b, 242, 261, 280a]

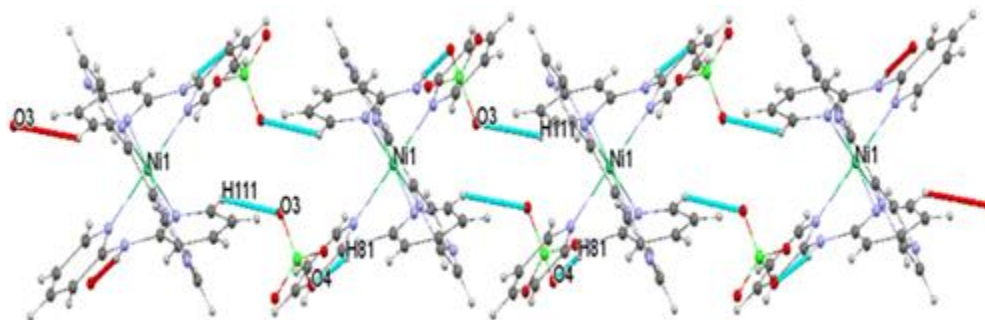


**Figure 3.44** View that perchlorate anion links with the cations of the  $[\text{Ni}(\text{dipyam})_2(\text{bpz})](\text{ClO}_4)_2$  complex; forming two-dimensional sheet.

On one hand, not only the hydrogen bond contributed in construction of the supramolecular in the crystal packing, but also the  $\pi\cdots\pi$  and/or C-H $\cdots\pi$  interactions that established by aromatic rings of pyridyl and pyrazinyl groups from adjacent sheet. [167b, 242, 261, 266] Adjacent Ni chains overlapping with others by  $\pi$ - $\pi$  stacking interactions connecting each 2,2'-bipyrazine and 2,2'-dipyridylamine ligands at 3.722 - 3.839 Å, closest connection, resulting in forming of 3D sheets, as what shown in figure 3.45

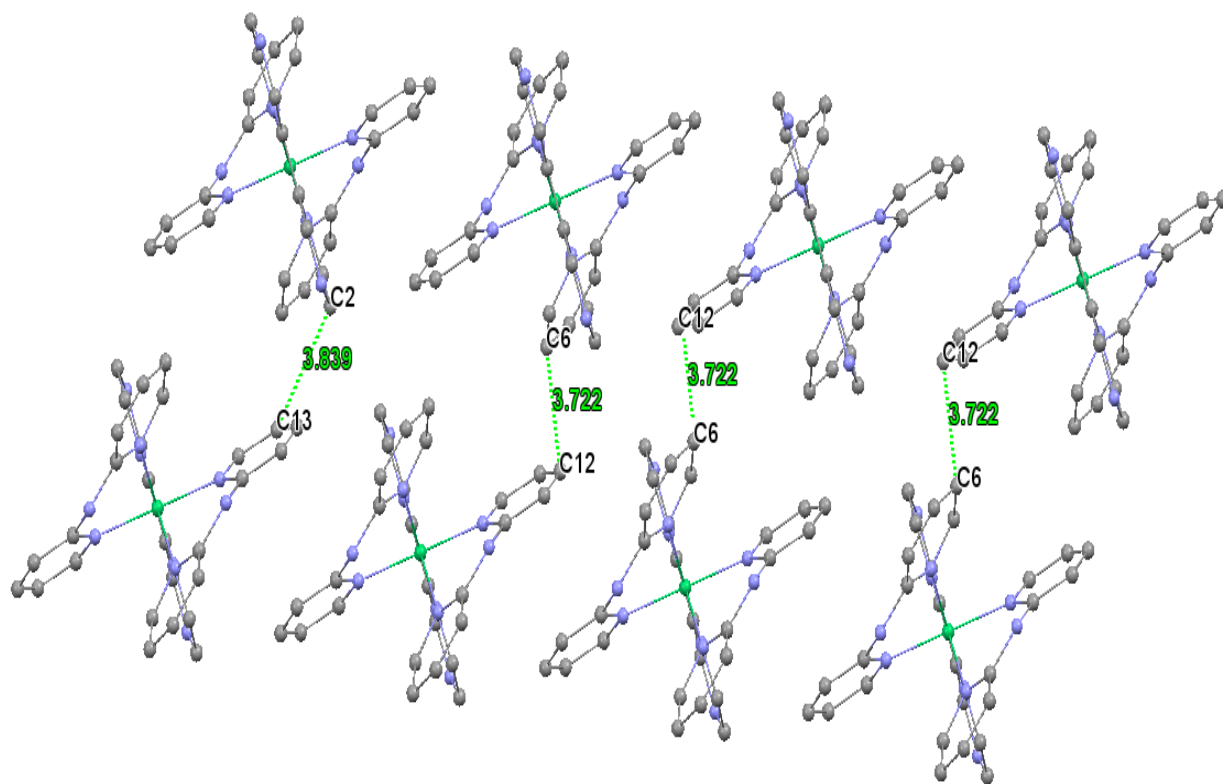


**Figure 3.45** View the distance of  $\pi$ - $\pi$  stacking interactions connecting each 2,2'-bipyridine and 2,2'-dipyridylamine ligands at 3.722 - 3.839 Å

### 3.6 [Cu(amp)<sub>2</sub>(NO<sub>3</sub>)<sub>2</sub>] complex

The complexation of transition metals with 2-(aminomethyl)pyridine ligand (amp) has attention in recent time, as they have good magnetic properties, biological activity, and structural diversity. They can functionalize as chelating or bridging, in organic and inorganic chemistry. Also, they can serve as pro-drugs in medicine filed as anti-tumor, antibacterial and anticancer agents. [185c, 192, 330(a-c)]

By the time, researchers also found that the using different of nitrate forms including NO, NO<sub>2</sub> and NO<sub>3</sub> as ligands in the complexation synthesis either as monodentate or bidentate, has an important impact in the applications of compounds.[331] The following complexes are evidenced examples about what said above. First, [Ni(C<sub>6</sub>H<sub>8</sub>N<sub>2</sub>)<sub>3</sub>]Cl<sub>2</sub>.2(H<sub>2</sub>O) complex, (where C<sub>6</sub>H<sub>8</sub>N<sub>2</sub> = 2-aminomethylpyridine) in which it is a semiconductor and so used in the electronic and optoelectronic applications. [185c, 192, 330(a-c)] Second, [Ni(amp)<sub>2</sub>]<sup>2+</sup> complex (where amp = 2-aminomethylpyridine)

used as building block in the forming of metal ion which is coordinated strongly in the equatorial plane.[332] Third,  $[\text{Ni}(-\text{amp})_2]_3[\text{Fe}(\text{CN})_6]_2 \cdot 6\text{H}_2\text{O}$  complex (where amp= 2-aminomethylpyridine) has a critical role in gaining visions in the studies of magneto structural correlation of the cyano-bridged hetero-polynuclear compounds. [258] Forth,  $[\text{Cu}(\text{NH}_2\text{CH}_2\text{CH}(\text{R})\text{Y})_2(\text{NO}_3)_2]$  complex (Where R= H, Y= $\text{NH}_2$ ) used as viable precursors in the chemical vapor deposition (CVD) and inkjet printing of metallic copper. Current modern copper(II) formate ink contains situ copper(II) formate solutions with co-complexing agents, in which they commonly are amines and their derivatives. [254]

At least,  $[\text{Cu}(\text{bpy})(\text{NO}_3)_2]$  (1) and  $[\text{Cu}(\text{L}2)\text{NO}_3]$  (2) complexes (L=2-tert-butyl-6-(quinoline-2-ylhydrazonomethyl)pheno) have biological activities as they have ability to interact with DNA. The complex (1) used as grove binding agents, and complex (2) behaves as efficient DNA binders. [249, 251] In this work a new complex of copper(II) with 2-(aminomethyl)pyridine ligand (amp) which was successfully synthesized at room temperature and slow evaporation of solvent. Its structure  $[\text{Cu}(\text{amp})_2(\text{NO}_3)_2]$  was confirmed by different technical ways as IR spectroscopy, thermal analysis and X-ray diffraction.

### **3.6.1 Infrared Spectroscopy**

#### **3.6.1.1 2-(aminomethyl)pyridine ligand**

The infrared absorption frequencies obtained for the 2-(aminomethyl)pyridine are listed in (table 3.22), and spectra are given in (fig. 3.46).

**Table 3.22:** Infrared frequencies ( $\text{cm}^{-1}$ ) for the 2-(aminomethyl)pyridine and assignments. [271, 332(a-b)]

<b>Assignment</b>	<b>Frequencies (<math>\text{cm}^{-1}</math>)</b>
$\nu(\text{NH}_2)$	3360 m, 3286m
$\nu(\text{CH})_{\text{alp}}$	3054m, 3008m
$\nu(\text{CH}_2)$	2910m, 2847m,
$\delta(\text{NH}_2)$	1590vs
$\nu(\text{CC})$	1568s
$\delta(\text{CH}_2)$	1474s, 1434vs
t( $\text{NH}_2$ )	1294w
$\nu$ (skeletal)	1149m, 1047m, 994s
Ip bending in py ring	1074sh
t( $\text{CH}_2$ )	881m
r( $\text{CH}_2$ ), w( $\text{NH}_2$ )	752vs
sym str in py ring, wagging in $\text{NH}_2$	627m, 596w

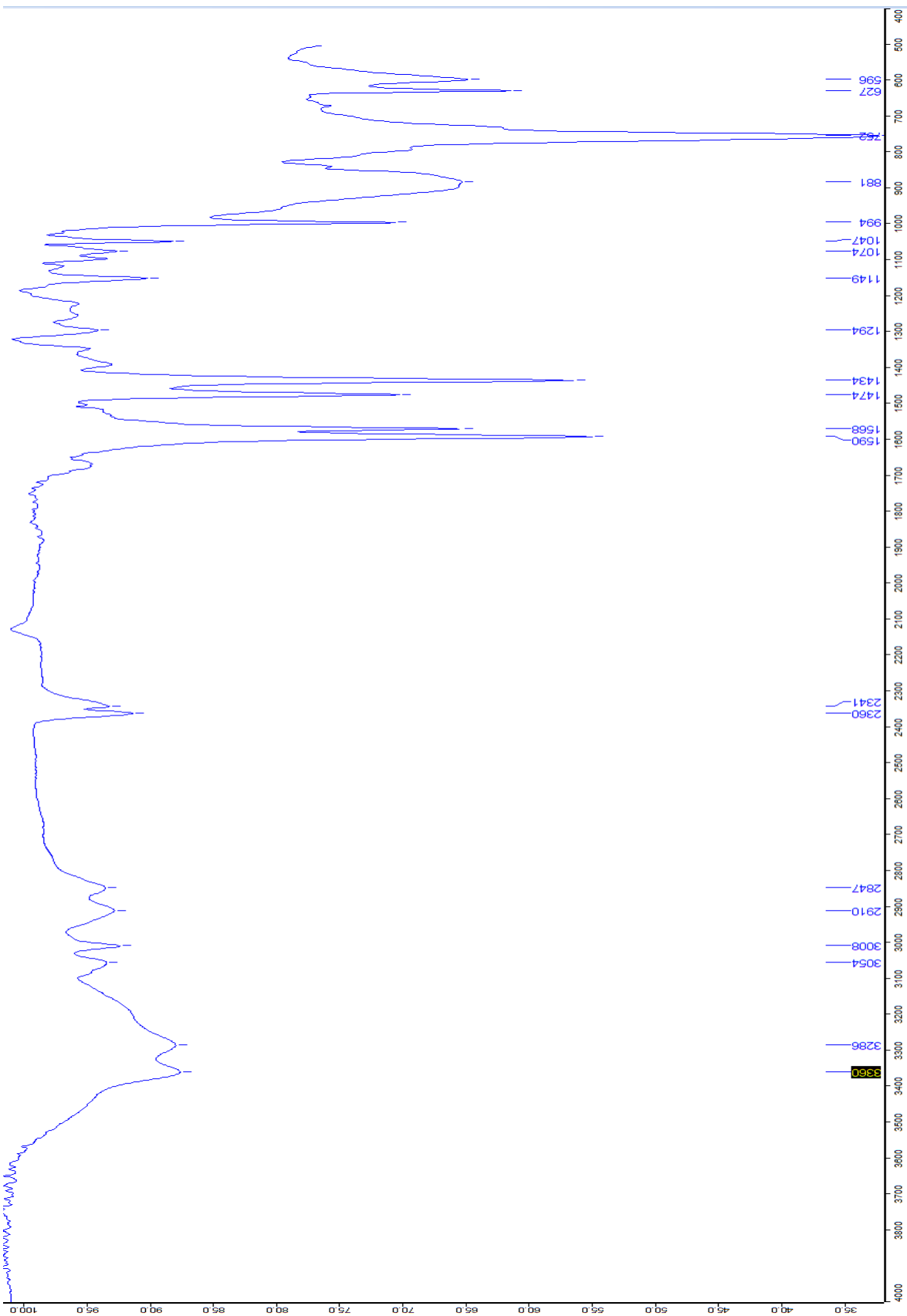


Figure 3.46 FTIR for 2-(aminomethyl)pyridine ligand.

### 3.6.1.2 Infrared spectroscopy for $[Cu(amp)_2(NO_3)_2]$

**Table 3.23:** Comparison Infrared frequencies ( $cm^{-1}$ ) of 2-(aminomethyl)pyridine ligand of  $[Cu(amp)_2(NO_3)_2]$  complex with the 2-(aminomethyl)pyridine ligand.

$[Cu(amp)_2(NO_3)_2]$	Assignment	Frequencies ( $cm^{-1}$ ) for 2-(aminomethyl)pyridine
3293w, 3216w, 3152w	$\nu(NH_2)$	3360 m, 3286m
3042w	$\nu(CH)$	3054m, 3008m
2930vw, 2852vw	$\nu(CH_2)$	2910m, 2847m
1636w	$\nu(C=N)$	1617sh
1591w	$\delta(NH_2), \nu(CC)$	1590vs
1478w, 1464w	$\delta(CH_2)$	1474s, 1434vs
1199m, 1181m	scissoring in pyridine ring	1191w
1147s, 1107s, 1089s and 1018s	$\nu(\text{skeletal})$	1149m, 1047m, 994s
1054s	Ip bending in py ring	1074w
845m, 825s	t( $CH_2$ )	881m
774m	r( $CH_2$ ), w( $NH_2$ )	752vs
621m	sym str in py ring, wagging in $NH_2$	627m, 596w

The IR spectrum of the  $[Cu(amp)_2(NO_3)_2]$  complex was compared with that of the free 2-(aminomethyl)pyridine ligand (fig. 3.47). The assignments of the most characteristic IR bands of 2-(aminomethyl)pyridine ligand are given in the table 3.22 above. The shifting of bands to lower or higher wave number because of the coordinated metal or crystal packing. [280a]

The FTIR spectra of 2-(aminomethyl)pyridine ligand has many characteristic bands which are  $\nu(NH_2)$ ,  $\nu(CH)$ ,  $\nu(CH_2)$ ,  $\nu(C=N)$ ,  $\delta(NH_2)$ ,  $\nu(CC)$ ,  $\delta(CH_2)$ , w( $CH_2$ ), in plane bending of C–H, scissoring in py ring,  $\nu(\text{skeletal})$ , t( $CH_2$ ), r( $CH$ ) in py ring, r( $NH_2$ ). The weak bands and broad absorption bands at 3293 and 3216  $cm^{-1}$  related to  $NH_2$  vibration. The weak absorption at 1591  $cm^{-1}$  for  $\delta(NH_2)$  group at bending out-of-plane. Also, there two medium bands at frequency 1199 and 621  $cm^{-1}$  belongs to scissoring in py ring and rocking vibrations for r( $NH_2$ ), respectively. The weak absorption at 3042  $cm^{-1}$  is for CH of the aromatic pyridine ring. The very weak peaks at 2930 and 2852  $cm^{-1}$  correspond to  $CH_2$  group of aliphatic chain. The weak peak at 1478 and 1464  $cm^{-1}$  are for  $\delta(CH_2)$ , while the w( $CH_2$ ) has strong peak at 1376  $cm^{-1}$ , the strong intensity at 825  $cm^{-1}$  and the medium peak at 845  $cm^{-1}$  are referred to t( $CH_2$ ). The weak peak at 1636  $cm^{-1}$  related to C=N vibration,

and the weak peak at  $1525\text{ cm}^{-1}$  assigned to (CC) vibration. The very strong peak at  $1314\text{ cm}^{-1}$  related to in plane bending of C-H, while the medium peaks at  $1199$  and  $1181\text{ cm}^{-1}$  correspond to scissoring in py ring. The skeletal vibration has strong peaks around  $1147$ ,  $1107$ ,  $1089$ ,  $1054$ ,  $1029$  and  $1018\text{ cm}^{-1}$ . The rocking of C-H in py ring has medium peak at  $774\text{ cm}^{-1}$ . [233, 258, 332(a-b)]

The coordinated nitrate molecule has absorption bands at  $1525\text{w}$ ,  $1376\text{s}$ ,  $1314$  and  $1029\text{ cm}^{-1}$ . These values assured that the monodentate coordination mode of the nitrate group. The spectra of the complex contain these bands, but not appeared in the spectra of free ligand. [244, 250, 331, 333]

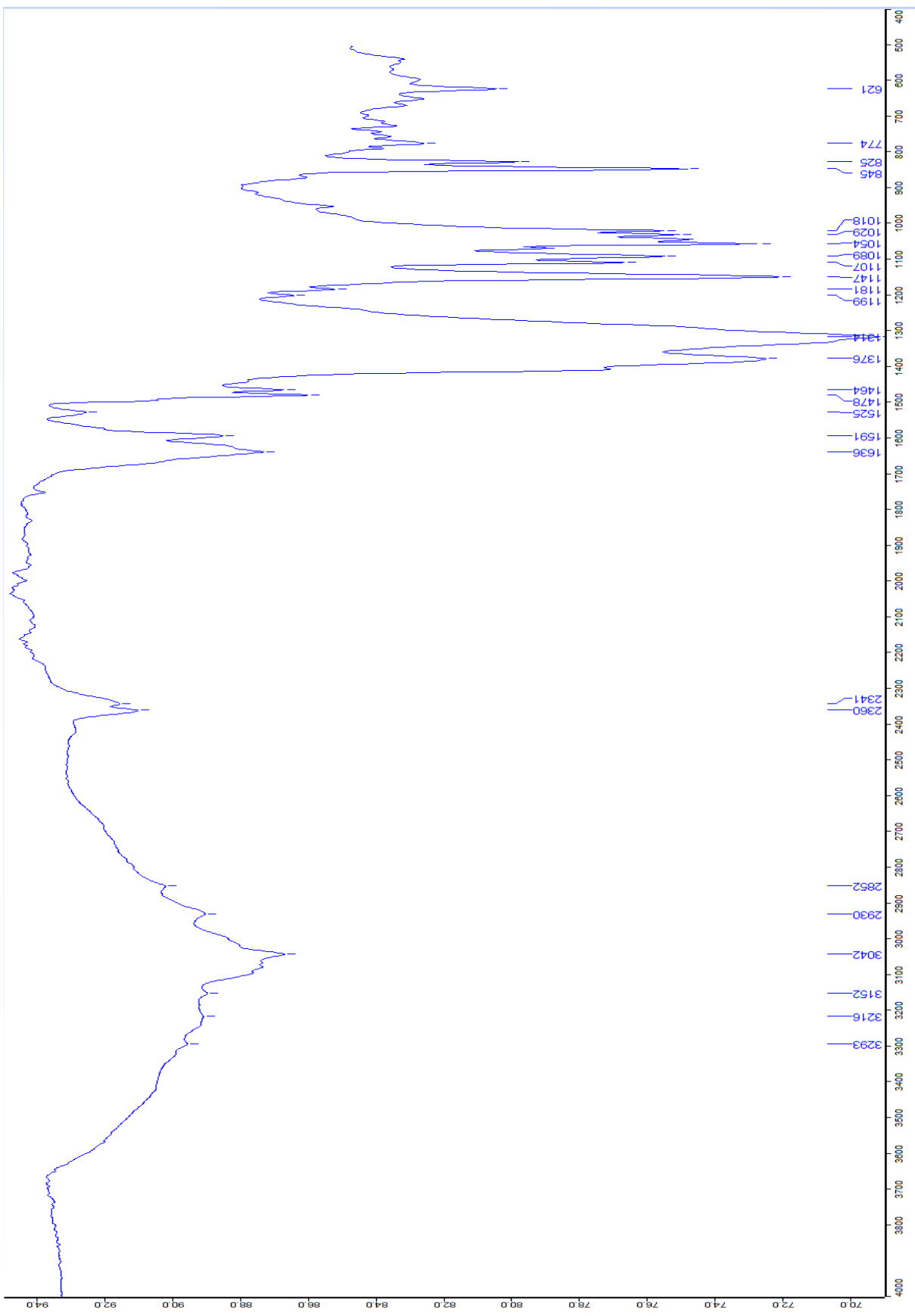
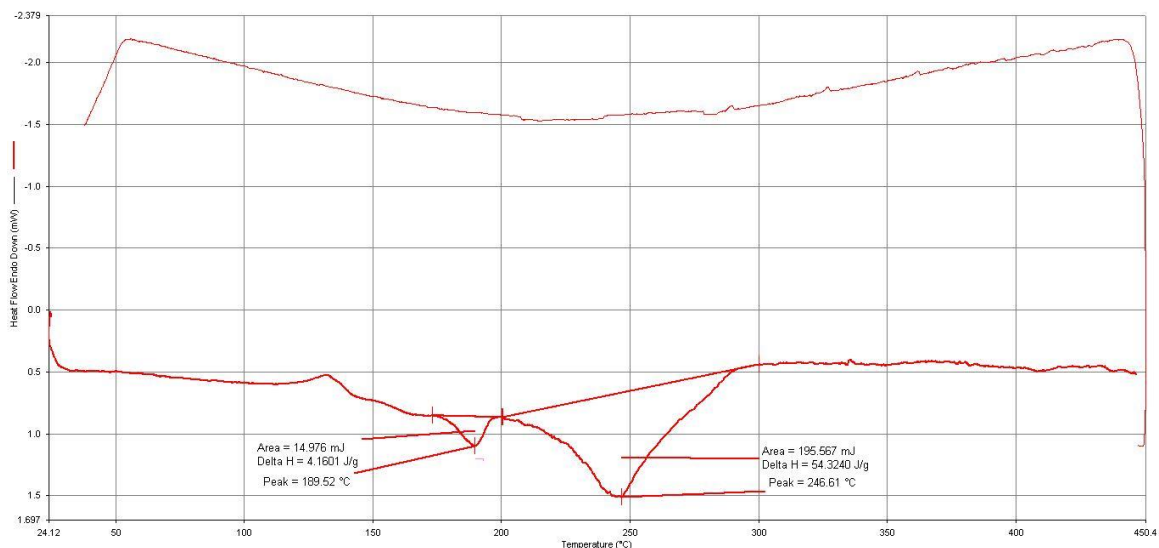


Figure 3.47 The infrared spectra of [Cu(amp)<sub>2</sub>(NO<sub>3</sub>)<sub>2</sub>] complex

### **3.6.2 Thermal analysis**

The Differential Scanning Calorimetry (DSC) thermal analysis for the  $[\text{Cu}(\text{amp})_2(\text{NO}_3)_2]$  complex were performed using Perkin Elmer DSC equipment. Samples about 6 mg of complex with aluminum pans, nitrogen gas flow and a scan rate  $5^\circ\text{C}/\text{min}$  from 25 up to  $350^\circ\text{C}$ , and then the cooling was done in the same range. The DSC curve (fig. 3.48) displayed an endothermic peak associated with enthalpy of  $4.1601 \text{ J/g}$  at  $T_{\text{max}} = 189.52^\circ\text{C}$ , followed by another endothermic peak associated with enthalpy of  $54.3240 \text{ J/g}$  at  $T_{\text{max}} = 246.61^\circ\text{C}$  that expect to melting point process.



**Figure 3.48** Differential Scanning Calorimetry (DSC) of  $[\text{Cu}(\text{amp})_2(\text{NO}_3)_2]$  complex

### **3.6.3 Crystal structure for $[\text{Cu}(\text{amp})_2(\text{NO}_3)_2]$ complex:**

The structure of complex  $[\text{Cu}(\text{amp})_2(\text{NO}_3)_2]$  consists of Cu(II) center, in which it is six coordinated with four nitrogen atoms of 2-(aminomethyl)pyridine ligands, and with two oxygen atoms of the coordinated nitrate molecule, as what shown in the figure 3.49 below

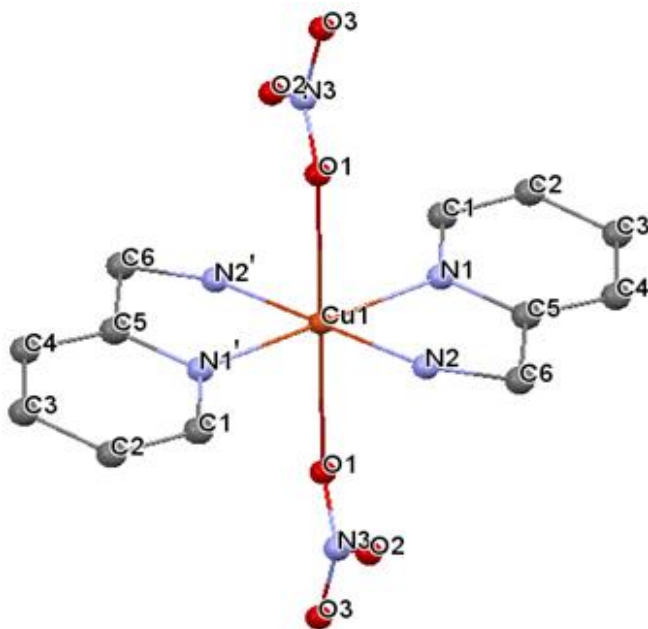


**Figure 3.49** View the structure of  $[\text{Cu}(\text{amp})_2(\text{NO}_3)_2]$  complex, with showing the atomic numbering

There are four half molecules of  $[\text{Cu}(\text{amp})_2(\text{NO}_3)_2]$  complex per unit cell, as what shown in the figure 3.50 below. They are bonded through electrostatic interactions, Van der Waals forces and hydrogen bonds.

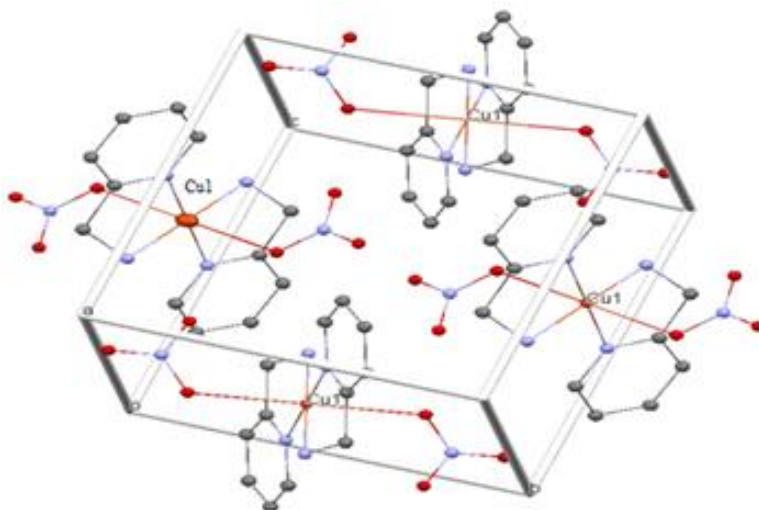


**Figure 3.50** View the structure packing of  $[\text{Cu}(\text{amp})_2(\text{NO}_3)_2]$  complex within unit cell.

The N1, N2, N1' and N2' atoms are surrounded the Cu metal and formed a coplanar. The bond angles within the 'plane' are so significant from each other. That leads to shape a

distorted octahedron with N1-Cu-N2 is  $81.86(6)^\circ$  and N1'-Cu-N2 is  $98.14(7)^\circ$  as what shown in figure 3.51. The angle of other bonds are near to predicted angles of octahedral geometry. [332], and the same as the other coordinated amp ligand, N1'-Cu1-N2 is  $98.14(6)^\circ$  and N1—Cu1—N2 is  $81.86(6)^\circ$

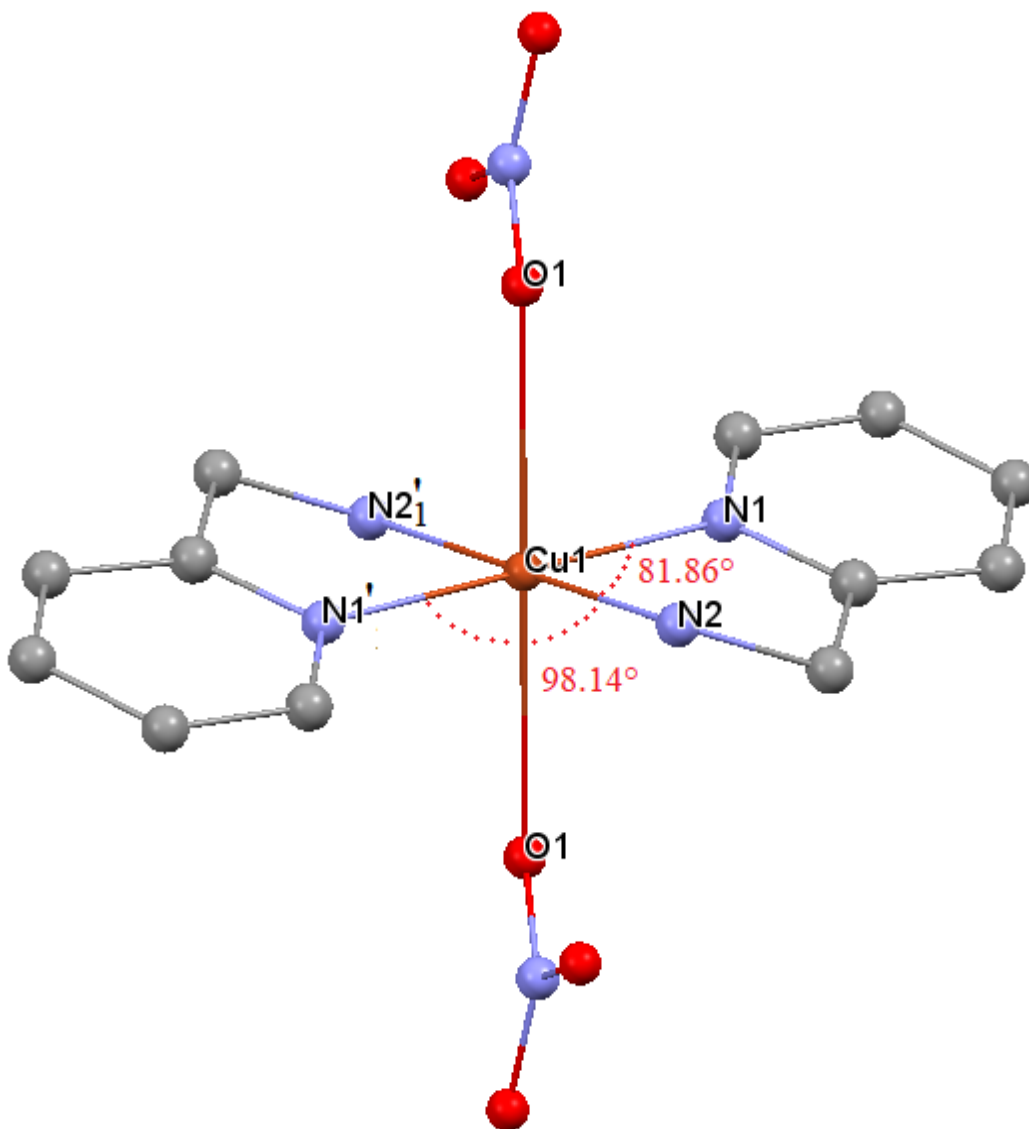


**Figure 3.51** View the angles between N1-Cu-N2 & N1-Cu- N2'of the  $[\text{Cu}(\text{amp})_2(\text{NO}_3)_2]$  complex according to the X-ray complex.

As what mentioned above, the nitrate molecules act as monodentate ligand with a Cu-O<sup>1</sup>,Cu-O<sup>2</sup> distances of  $2.5790 \text{ \AA}$  which is closed to distance between Zn, Ni and oxygen of nitrate (Zn(1)-O(2)) of  $2.051 \text{ \AA}$  [268], ((Ni -O) is  $2.1665 \text{ \AA}$ ) [258] and that ideal for

monodentate nitrate. The bond distances of copper-nitrogens: one of pyridine is 2.022 Å and other of imino is 1.995 Å (fig. 3.52). These values are considered normal according to comparing with  $[\text{Ni}(\text{ampy})_2(\text{NO}_3)_2]$  complex and  $[\text{Zn}(\text{SALAMP})(\text{NO}_3)_2]$  complex, where SALAMP is 2-[[2-(2-pyridinylmethyl)amino]methyl]phenol. [258, 268]

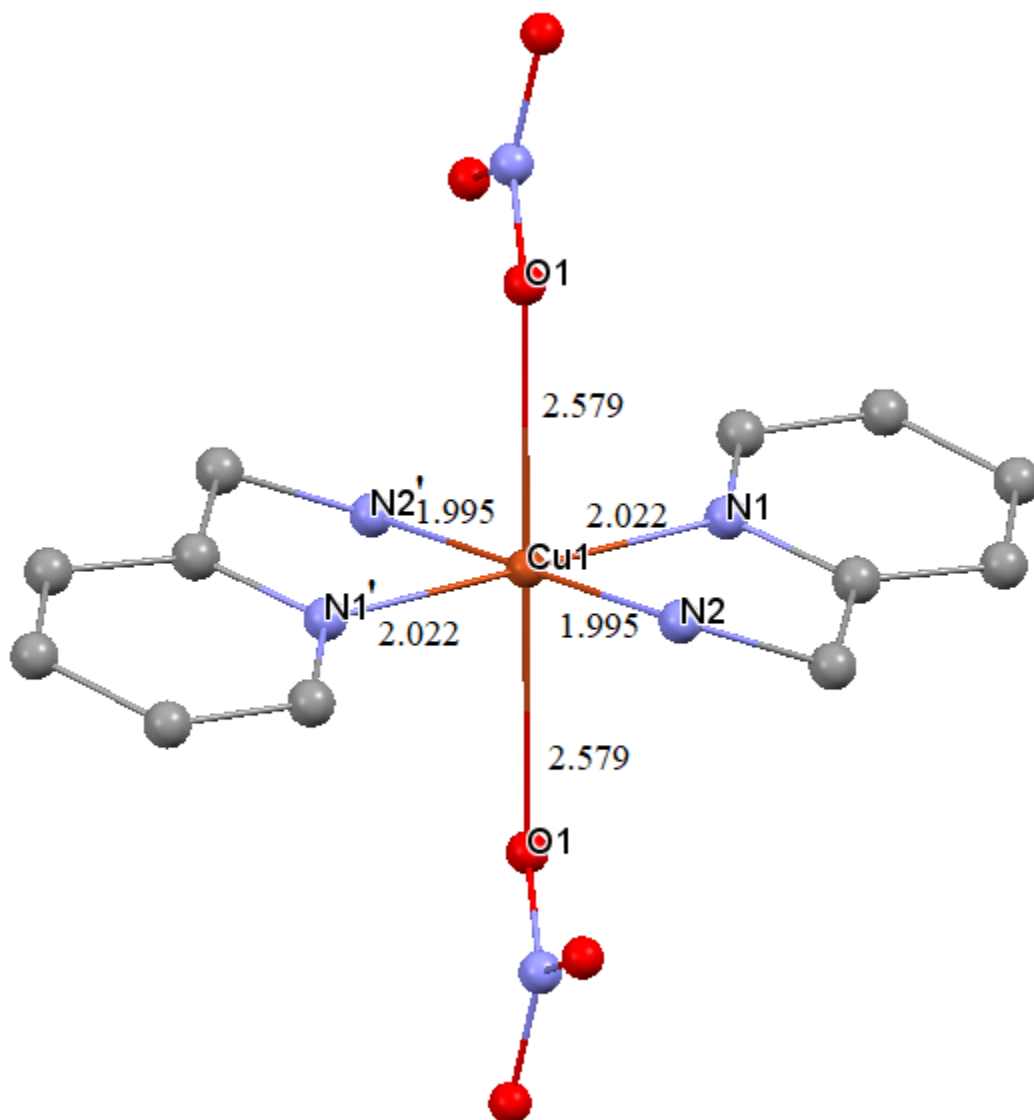


**Figure 3.52** View the distance between the Cu-amp ligand of the  $[\text{Cu}(\text{amp})_2(\text{NO}_3)_2]$  complex according to the X-ray

The crystal structure of  $[\text{Cu}(\text{amp})_2(\text{NO}_3)_2]$  complex exposed that Cu(II) atom has distorted octahedral coordination geometry, because of four chelating ligands bind with Cu(II) metal, including two 2-(aminomethyl)pyridine (amp) located at equatorial plane, while two

coordinated nitrate molecules occupied the axial plane. The geometry is confirmed via value of angles between nitrogen and oxygen atoms that bonded with Cu(II) metal, including N2-Cu-N1 [81.86 (6)], N1-Cu-O1 [90.66 (6)], N2'-Cu-O1'[92.85 (6)], O1-Cu-O1' [179.996], N2-Cu-N2' [179.994], N1-Cu-N1' [179.994]. These values are less deviated from the perfect bond angles of 90° and 180°. The figures below clarify the bond angles (fig. 3.53a and fig. 3.53b) [261, 329] and the table 3.24 shows the angle between atoms.

**Table 3.24:** Bond angle [deg.] of [Cu(amp)<sub>2</sub>(NO<sub>3</sub>)<sub>2</sub>] complex

O1 <sup>i</sup> —Cu1—N1 <sup>i</sup>	90.66 (6)	Cu1—N1—C5	113.52 (13)
O1 <sup>i</sup> —Cu1—N2 <sup>i</sup>	92.85 (7)	C1—N1—C5	118.82 (17)
N1 <sup>i</sup> —Cu1—N2 <sup>i</sup>	81.86 (6)	Cu1—N2—C6	109.63 (12)
O1 <sup>i</sup> —Cu1—N1	89.34 (6)	O1—N3—O2	119.63 (19)
N1 <sup>i</sup> —Cu1—N1	179.994	O1—N3—O3	120.10 (19)
N2 <sup>i</sup> —Cu1—N1	98.14 (7)	O2—N3—O3	120.3 (2)
O1 <sup>i</sup> —Cu1—N2	87.15 (7)	Cu1—O1—N3	123.08 (13)
N1 <sup>i</sup> —Cu1—N2	98.14 (6)	N1—C1—C2	122.0 (2)
N2 <sup>i</sup> —Cu1—N2	179.994	C1—C2—C3	119.0 (2)
N1—Cu1—N2	81.86 (6)	C2—C3—C4	119.1 (2)
O1 <sup>i</sup> —Cu1—O1	179.996	C3—C4—C5	119.4 (2)
N1 <sup>i</sup> —Cu1—O1	89.34 (6)	C4—C5—N1	121.57 (19)
N2 <sup>i</sup> —Cu1—O1	87.15 (6)	C4—C5—C6	122.44 (19)
N1—Cu1—O1	90.66 (6)	N1—C5—C6	116.00 (17)
N2—Cu1—O1	92.85 (6)	C5—C6—N2	110.27 (17)
Cu1—N1—C1	127.64 (14)		

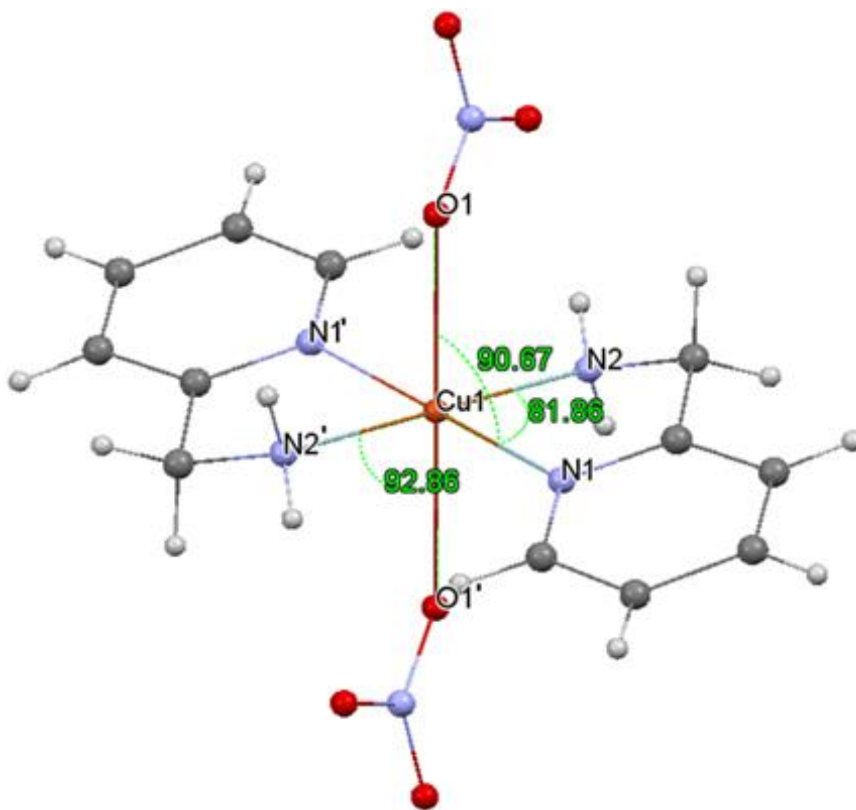


**Figure 3.53a** The angles between N and O atoms of the ligands and Cu metal of  $[\text{Cu}(\text{amp})_2(\text{NO}_3)_2]$  complex according to the X-ray complex.

The distortion geometry of the complex originated from the short bite angle of amp ligands  $[\text{N1}^i\text{—Cu1—N2}^i]$  which is  $81.86(6)^\circ$  (fig. 3.55, table 3.24), slightly less than  $90^\circ$ . [261, 329] The distance between Cu metal and nitrogen atoms range between  $1.955 - 2.022 \text{ \AA}$  (table 3.25, fig. 3.54). The amp ligands via the pyridine end and imino end. The Cu-amp bond distances are very similar to those observed in other amp ligands. [185c, 192, 330(a-c)]

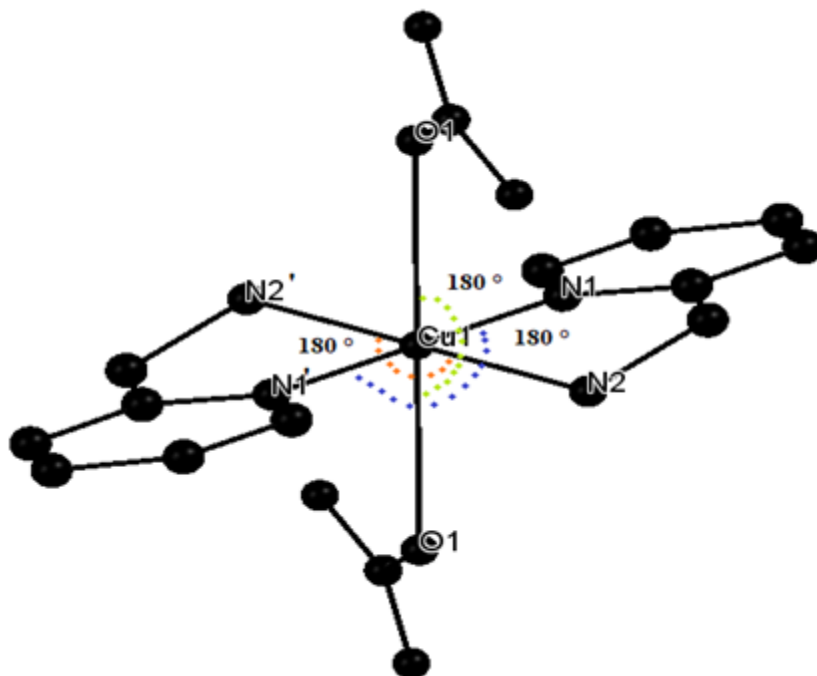


**Figure 3.53b** View the values of angles between nitrogen that bonded with Cu(II) metal of  $[\text{Cu}(\text{amp})_2(\text{NO}_3)_2]$  complex, the color used to distinguish between them.

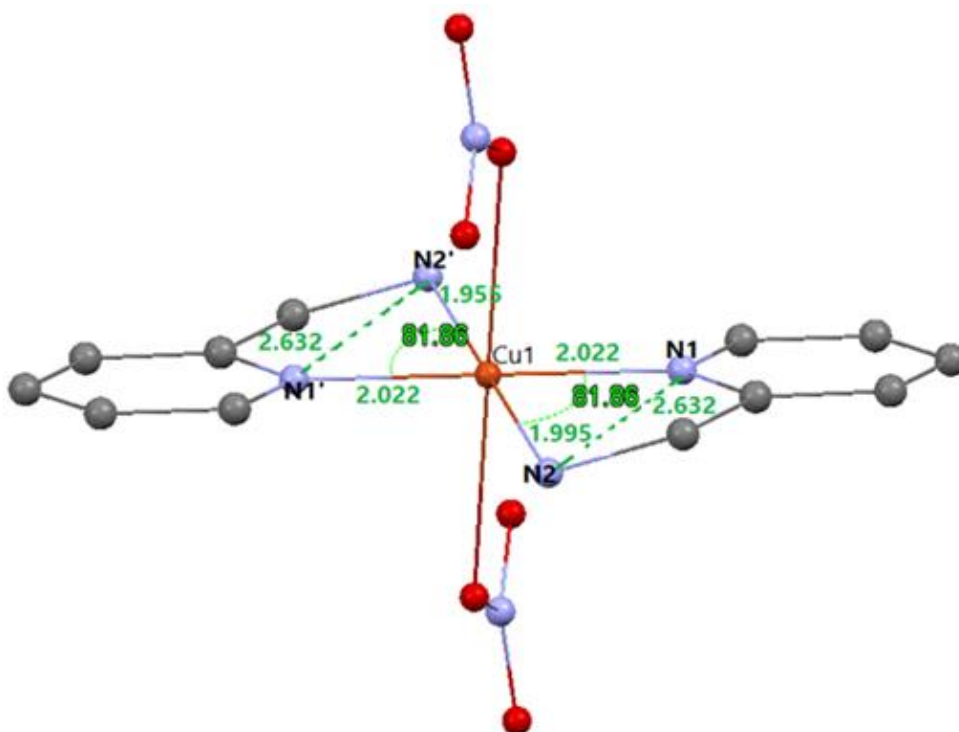


**Figure 3.54** View the bite distance and the bite angles between N atoms of ligands and Cu metal of  $[\text{Cu}(\text{amp})_2(\text{NO}_3)_2]$  complex according to the X-ray complex.

**Table 3.25:** Bond length [Å] of [Cu(amp)<sub>2</sub>(NO<sub>3</sub>)<sub>2</sub>] complex

Atom 1	Atom 2	Length	Atom 1	Atom 2	Length
Cu1	O1 <sup>i</sup>	2.5790 (18)	N3	O1	1.251 (2)
Cu1	N1 <sup>i</sup>	2.0219 (16)	N3	O2	1.243 (2)
Cu1	N2 <sup>i</sup>	1.9951 (16)	N3	O3	1.221 (3)
Cu1	N1	2.0219 (16)	C1	C2	1.379 (3)
Cu1	N2	1.9951 (16)	C2	C3	1.379 (3)
Cu1	O1	2.5790 (18)	C3	C4	1.372 (3)
N1	C1	1.346 (2)	C4	C5	1.387 (3)
N1	C5	1.339 (3)	C5	C6	1.498 (3)
N2	C6	1.473 (3)			

The crystal packing is stabilized by C-H...O and N-H...O hydrogen bonds between the pyridine and amino groups of amp ligand with the oxygen atoms of coordinated nitrate molecule as what shown in figure 3.55 and figure 3.56 below.

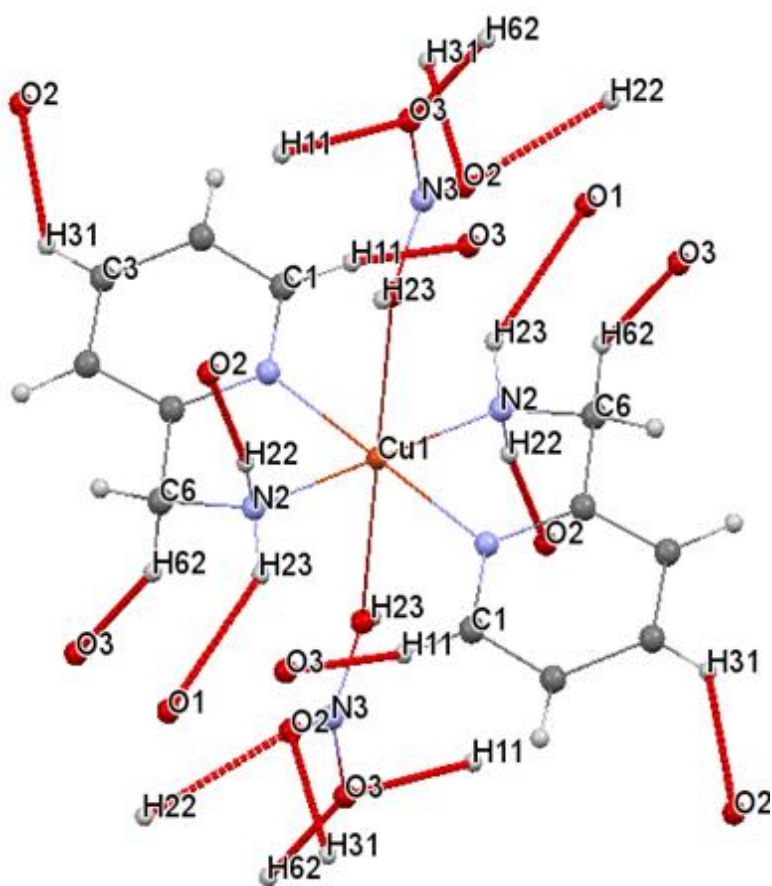


**Figure 3.55** View the inter-interaction H-bonds of the [Cu(amp)<sub>2</sub>(NO<sub>3</sub>)<sub>2</sub>] complex

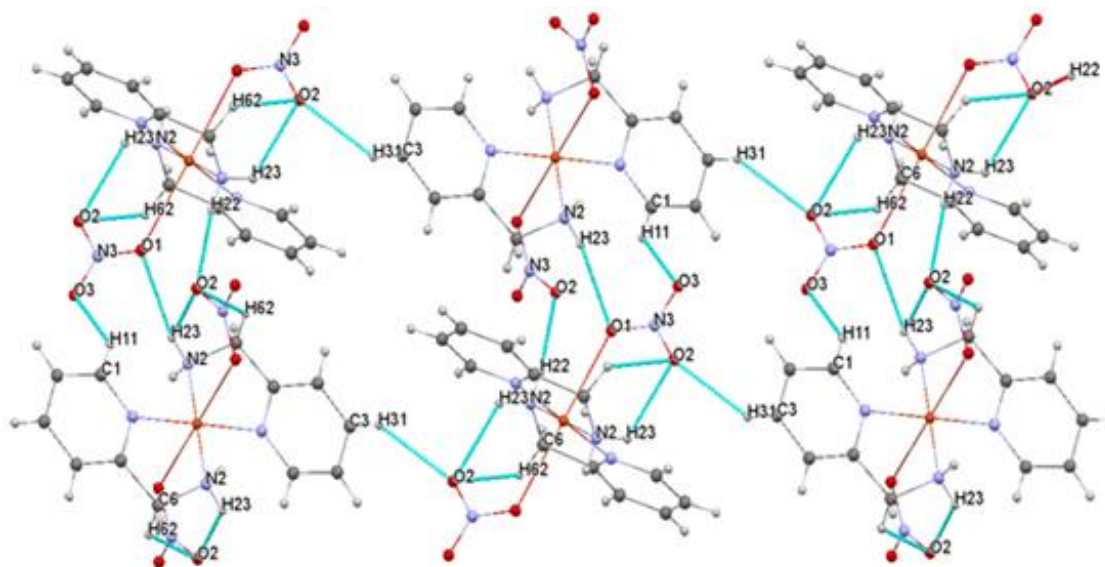


**Figure 3.56** View the crystal packing of  $[\text{Cu}(\text{amp})_2(\text{NO}_3)_2]$  complex with showing the inter-interaction H-bonds.

Hydrogen bonding interactions lead to create a two-dimensional network structure through combination of  $\text{C}-\text{H}\cdots\text{O}$  and  $\text{N}-\text{H}\cdots\text{O}$ , where the  $\text{NH}_2$  group of the amp ligand participate in intermolecular hydrogen bonding with the oxygen atom of nitrate ligand of adjacent chain with distance value 3.044 (3), 3.070 (3) and 2.999 (3) Å (table 3.26), that making one-dimensional chains as shown in fig. 3.57 [233, 261, 318, 326, 329]

The table 3.26 below displays the corresponding D-H,  $\text{H}\cdots\text{A}$  and  $\text{D}\cdots\text{A}$  bond distances and  $\text{D}-\text{H}\cdots\text{A}$  bond angles, where D: donor, A: acceptor.

**Table 3.26:** Hydrogen geometry (Å, °) of  $[\text{Cu}(\text{amp})_2(\text{NO}_3)_2]$  complex

D—H $\cdots$ A	D—H	H $\cdots$ A	D $\cdots$ A	D—H $\cdots$ A
C1—H11 $\cdots$ O3 <sup>ii</sup>	0.94	2.49	3.233 (3)	135
C3—H31 $\cdots$ O2 <sup>iii</sup>	0.93	2.47	3.212 (3)	137
N2—H22 $\cdots$ O2 <sup>iv</sup>	0.88	2.17	3.044 (3)	171
N2—H23 $\cdots$ O1 <sup>v</sup>	0.85	2.37	3.070 (3)	140
N2—H23 $\cdots$ O2	0.85	2.45	2.999 (3)	123

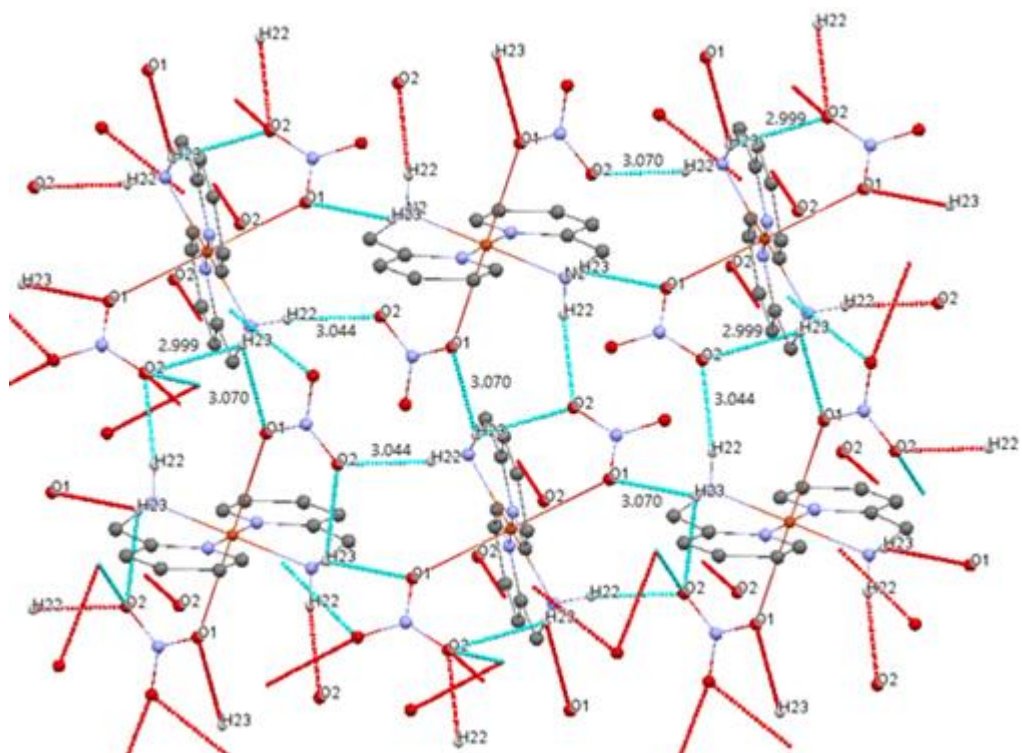


**Figure 3.57** View the distance value of intermolecular hydrogen bonding between  $\text{NH}_2$  group of the amp ligand with the oxygen atom of nitrate ligand of adjacent chain of  $[\text{Cu}(\text{amp})_2(\text{NO}_3)_2]$  complex; forming two-dimensional sheet.

Beside to that, the chains are additionally reinforced by  $\text{C-H}\cdots\text{O}$  interactions by the CH group of the amp ligand with oxygen atom of nitrate ligand of adjacent chain with distance value 3.233 (3) and 3.212 (3) Å as shown in (table 3.26, fig. 3.58) [233, 261, 318, 326, 329].

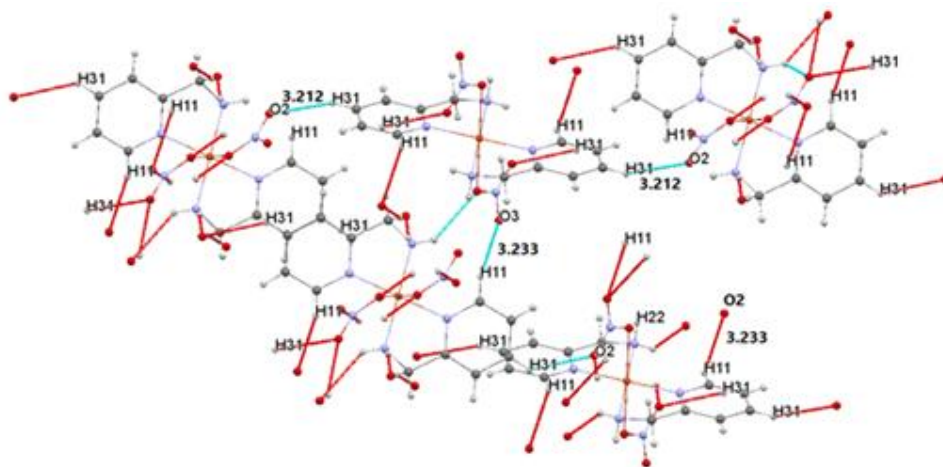


**Figure 3.58** View the distance value of C-H...O interactions by the CH group of the amp ligand with oxygen atom of nitrate ligand of adjacent chain  $[\text{Cu}(\text{amp})_2(\text{NO}_3)_2]$  complex.

The most exciting structural merit is existing the  $\pi$ - $\pi$  stacking interactions, which involving the pyridyl moieties of neighboring mononuclear entities. That results to infinite chains and weak magnetic interactions arised across  $\pi$ -stacking which noticed in several compounds. [258, 261, 329] The  $\pi$ - $\pi$  stacking interactions connecting by two 2-(aminomethyl)pyridine (amp) ligand at 3.375 Å resulting in forming of 3D sheets (fig. 3.59).[185c, 192, 330(a-c)]

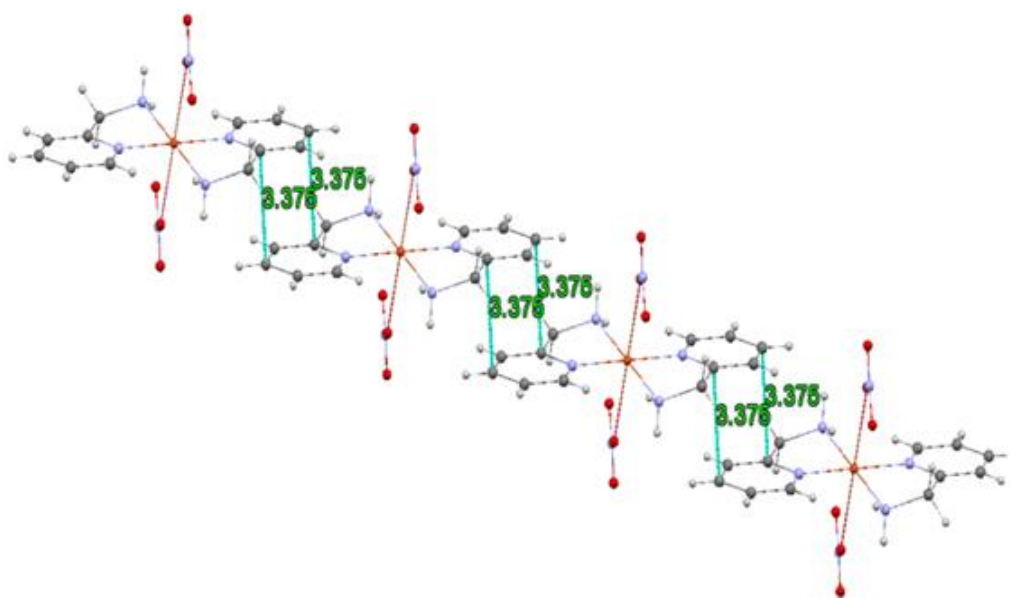


**Figure 3.59** View the distance of  $\pi$ - $\pi$  stacking interactions connecting amp ligand at 3.375 Å in the  $[\text{Cu}(\text{amp})_2(\text{NO}_3)_2]$  complex

## Chapter Four

---

### 4.1 Conclusion:

The work of thesis is conclude to synthesise series of homoleptic and mixed-ligand chelates that contain either copper(II) or nickel(II) metal atom with different ligands as 2,2'-bipyrazine, 2,2'-dipyridylamine, 2-(aminomethyl)pyridine. These compounds are characterized based on several techniques as single crystal X-ray diffraction, FTIR spectroscopy and thermal analysis (DSC), and characterized in detail of ligands by FTIR spectroscopy.

The ligands were used in this work have huge attention in different applications especially biological searches, for example, bonding in DNA, and in architectures studies because of their ability to make many different coordination modes and outer nitrogen atom.

This work has been successfully synthesized and characterized of six coordination compounds, five of them new complexes which are  $[(\text{bpz})\text{Cu}(\text{OH})(\text{ClO}_4)(\text{H}_2\text{O})]_2 \cdot \text{H}_2\text{O}$ ,  $[\text{Cu}(\text{amp})_2(\text{NO}_3)_2]$ ,  $[\text{Cu}(\text{bpz})_3](\text{ClO}_4)_2 \cdot 2\text{CH}_3\text{CN}$ ,  $[\text{Cu}(\text{dipyam})(\text{H}_2\text{O})(\text{pca})]\text{ClO}_4$ ,  $[\text{Ni}(\text{dipyam})_2(\text{bpz})](\text{ClO}_4)_2$  and  $[\text{Cu}(\text{bpz})_2(\text{H}_2\text{O})](\text{NO}_3)_2$  complex, where (bpz = 2,2'-bipyrazine and dipyam = 2,2'-dipyridylamine, amp = 2-(aminomethyl)pyridine, pca = 2-pyrazine carboxylate).

Although, all complexes had synthesized and characterized under normal laboratory conditions, the copper(II) center metal atom of  $[\text{Cu}(\text{dipyam})(\text{H}_2\text{O})(\text{pca})]\text{ClO}_4$  complex binds with new forming ligand which is 2-pyrazinecarboxylate (pca), this ligand was not in the reactant materials but formed during the preparation of complex, in which its supposed molecular formula was  $[\text{Cu}(\text{dipyam})(\text{bpz})](\text{ClO}_4)_2$ . It mean that, the aim was to prepare  $[\text{Cu}(\text{dipyam})(\text{bpz})](\text{ClO}_4)_2$ , but the product was  $[\text{Cu}(\text{dipyam})(\text{H}_2\text{O})(\text{pca})]\text{ClO}_4$  complex.

The forming of new ligand (pca) will encourage scientists to new methodology for C-C / C-N bond cleavage. The proposed forming of this ligand is discussed by hypothesis mechanisms. Suggest mechanism is that the ligand is attached by nucleophile, then the ring of 2,2'-bipyrazine (bpz) ligand is broken and  $\text{CO}_2$  gas is caught from atmosphere. The

crystal structure of  $[\text{Cu}(\text{dipyam})(\text{H}_2\text{O})(\text{pca})]\text{ClO}_4$  complex is a novel copper(II) chelates with a distorted square pyramid geometry. The Cu(II) center is five coordinated by two nitrogen atoms of 2,2'-dipyridylamine, one nitrogen and one oxygen of 2-pyrazinecarboxylate ligand, one oxygen atom of coordinated water. The perchlorate anions link the complex cations to form a chain structure through  $\text{O}-\text{H}\cdots\text{O}$  close contacts and  $\text{C}-\text{H}\cdots\text{O}$  hydrogen bonds.

The second coordination compound is  $[(\text{bpz})\text{Cu}(\text{OH})(\text{ClO}_4)(\text{H}_2\text{O})]_2\cdot\text{H}_2\text{O}$ , in which it was synthesized by Abu sharkh. K in 2017. Nevertheless, the distinguish merit in this work is the preparation of the complex by new methodology. The geometry description of complex is a distorted elongated tetragonal octahedral geometry around each copper ion. Also, the structure composed di- $\mu$ -hydroxo-copper(II) dimer with 2,2'-bipyrazine as outer ligand. The structure of complex formed 2D sheet according to hydrogen bond interactions including water molecules and compound, and so the 3D sheet are formed according to oxygen atom of perchlorate and  $\pi\cdots\pi$  interactions of polypyridyl ligands of other adjacent sheets.

The third coordination compound is  $[\text{Cu}(\text{bpz})_3](\text{ClO}_4)_2\cdot 2\text{CH}_3\text{CN}$ , this is an unexpected complex, because two mixed ligands: 2,2'-bipyrazine and tricyclohexylphosphine( $\text{C}_{18}\text{H}_{33}\text{P}$ ) are used during its preparing. The single crystal X-ray diffraction reveals the tricyclohexylphosphine does not exist in the crystal structure. Its coordination is a distorted octahedral geometry and crystal packing reveals that there are different types of hydrogen bonds are formed between atoms, which are first between hydrogen atoms of acetonitrile and nitrogen atom of bpz ligands. Second is between the hydrogen atoms of bpz ligand and nitrogen atoms of other bpz ligand. Third is between the oxygen atoms of perchlorate molecules and hydrogen atom of bpz ligands. Forth is between hydrogen atom of acetonitrile and oxygen atom of perchlorate. The interaction Van Deer Waal force is noticed between the C-H of bpz with oxygen atom of  $\text{ClO}_4$ . Also, the  $\pi\cdots\pi$  interaction has a role in the parking structure between adjacent sheets.

The forth coordination compound is  $[\text{Cu}(\text{bpz})_2(\text{H}_2\text{O})](\text{NO}_3)_2$ , which its crystal structure is a distorted trigonal bipyramidal geometry. The Cu(II) center is five coordinated with four nitrogen atoms of 2,2'-bipyrazine ligands, and with one oxygen atom of the water molecule. The nitrate anions link the complex cations to form a chain structure through

hydrogen bonds. The adjacent coordination spheres are held together through C–H··O hydrogen bonds formed between the H-atoms on bpz and O-atoms on nitrate anion, the complex cations of [Cu(bpz)<sub>2</sub>(H<sub>2</sub>O)](NO<sub>3</sub>)<sub>2</sub> are stacked in the closest approach between the 2,2'-bipyrazine rings of 4.990 Å, indicating no significant π---π stacking interactions.

The fifth coordination compound is [Cu(amp)<sub>2</sub>(NO<sub>3</sub>)<sub>2</sub>], which its crystal structure is an distorted octahedral coordination geometry. The Cu(II) center atom has six coordinated with four nitrogen atoms of 2-(aminomethyl)pyridine ligands, and with two oxygen atoms of the coordinated nitrate molecule. The crystal packing is stabilized by C–H··O and N–H··O hydrogen bonds between the pyridine and amino groups of amp ligand with the oxygen atoms of coordinated nitrate molecule. Beside to that, the chains are additionally reinforced by C–H---O interactions by the CH group of the amp ligand with oxygen atom of nitrate ligand of adjacent chain. Adjacent Cu chains overlapping with others by π–π stacking interactions connecting by two 2-(aminomethyl)pyridine (amp) ligand.

Finally, the sixth coordination compound is [Ni(dipyam)<sub>2</sub>(bpz)]ClO<sub>4</sub>, nickel complexes have been an attractive area of research because they are considered as a potential alternative to cis-platin. Ni(II) center of complex is a hexacoordinated by two nitrogen atoms of 2,2'-bipyrazine ligand located at equatorial positions, and four nitrogen atoms of 2,2'-dipyridylamine ligands located at equatorial plane and at axial position, the complex has a distorted octahedral geometry. The perchlorate anions link the complex cations by hydrogen bond to form a chain structure through its oxygen with NH and C–H groups of 2,2'-dipyridylamine ligand, beside to nitrogen atoms of 2,2'-bipyrazine with C–H groups of 2,2'-dipyridylamine ligand in adjacent structure unit. Furthermore, aromatic rings of pyridyl and pyrazinyl groups from adjacent sheet are linked through π•••π and/or C–H•••π interactions.

## **4.2 Future work:**

As a continuation of this work, I propose to do further measurements as magnetic susceptibility at different temperature, to examine the applications of [Cu(dipyam)(H<sub>2</sub>O)(pca)]ClO<sub>4</sub> complex, in which 2-pyrazinecarboxylic acid and its metal complexes have efficient role in organic–inorganic hybrid material. Beside to their various applications such as development of selective catalysis, molecular recognition, electro-optic materials, semiconductor materials and magnetic materials. Also, study the applications [Cu(bpz)<sub>3</sub>](ClO<sub>4</sub>)<sub>2</sub>·2CH<sub>3</sub>CN complex, where its structure resembles to [Ni(bpz)<sub>3</sub>](ClO<sub>4</sub>)<sub>2</sub>·H<sub>2</sub>O, that has special interest in research areas, especially in biological studies, where it shows good affinity in interaction with DNA and vital usage in designing of pharmaceutical molecules.

Furthermore, I suggest a new procedure for synthesis of [Cu(dipyam)(H<sub>2</sub>O)(pca)](ClO<sub>4</sub>)<sub>2</sub> complex with 2,2'-bipyrazine ligand, and complex of Cu(II) and Ni(II) with different phosphine ligand and 2,2'-bipyrazine. It may lead to produce new structurally and magnetically properties.

Finally, the six synthesized complexes are good suggestions for using as start material for preparation of supramolecular compounds continues multinuclear, for example, reacting them with Ag(I), Cu(II), and Ni(II) salts.

## Chapter Five

---

### References:

1. Blake, A. J., Champness, N. R., Cooke, P. A., Nicolson, J. E., and Wilson, C. “Multi-Modal Bridging Ligands; Effects of Ligand Functionality, Anion and Crystallisation Solvent in Silver(i) Co-Ordination Polymers<sup>†</sup>.” *Journal of the Chemical Society, Dalton Transactions*, no. 21, 2000, pp. 3811–3819.
2. Navarro, J. A., and Lippert, B. “Simple 1:1 and 1:2 Complexes of Metal Ions with Heterocycles as Building Blocks for Discrete Molecular as Well as Polymeric Assemblies.” *Coordination Chemistry Reviews*, vol. 222, no. 1, 2001, pp. 219–250.
3. Benesperi, I., Singh, R., and Freitag, M. “Copper Coordination Complexes for Energy-Relevant Applications.” *Energies*, vol. 13, no. 9, 2020, pp. 1-19.
4. Conry, R.R. “Copper: Inorganic & Coordination Chemistry.” In Conry R.R. and Karlin K.D. (eds), *Encyclopedia of Inorganic and Bioinorganic Chemistry, first edition*, Waterville, ME, USA: John Wiley & Sons, Ltd, 2011, pp. 1-19.
5. Conway, J. R., Adeleye, A. S., Gardea-Torresdey, J., and Keller, A. A. “Aggregation, Dissolution, and Transformation of Copper Nanoparticles in Natural Waters.” *Environmental Science & Technology*, vol. 49, no. 5, 2015, pp. 2749–2756.
6. Persson, I., Persson, P., Sandström, M., and Ullström, A. S. “Structure of Jahn–Teller Distorted Solvated Copper(II) Ions in Solution, and in Solids with Apparently Regular Octahedral Coordination Geometry.” *Journal of the Chemical Society, Dalton Transactions*, no. 7, 2002, p. 1256- 1265.
7. Li, X., Cheng, D., Lin, J., Li, Z., and Zheng, Y. “Di-, Tetra-, and Hexanuclear Hydroxy-Bridged Copper(II) Cluster Compounds: Syntheses, Structures, and Properties.” *Crystal Growth & Design*, vol. 8, no. 8, 2008, pp. 2853–2861.
8. Tisato, F., Marzano, C., Porchia, M., Pellei, M. and Santini, C. “Copper in Diseases and Treatments, and Copper-Based Anticancer Strategies.” *Medicinal Research Reviews*, vol. 30, no. 4, 2010, pp. 708-749.
9. Gaur, A., Klysubun, W., Nair, N. N., Shrivastava, B. D., Prasad, J., and Srivastava, K. “XAFS Study of Copper(II) Complexes with Square Planar and Square Pyramidal Coordination Geometries.” *Journal of Molecular Structure*, vol. 1118, 2016, pp. 212–218.
10. Klepka, M. T., Drzewiecka, A., Wolska, A., and Ferenc, W. “XAS Studies on Cu(II) Complexes with Derivatives of Phenoxyacetic and Benzoic Acids.” *Chemical Physics Letters*, vol. 553, 2012, pp. 59–63.
11. Sandroni, M., Pellegrin, Y., and Odobel, F. “Heteroleptic Bis-Diimine Copper(I) Complexes for Applications in Solar Energy Conversion.” *Comptes Rendus Chimie*, vol. 19, no. 1-2, 2016, pp. 79–93.
12. De Almeida, K. J. “Optical and Magnetic Properties of Copper(II) Compounds.” *PhD dissertation, Department of Theoretical Chemistry, School of Biotechnology, Royal Institute of Technology, Stockholm*, 2008, pp. 1-53.

13. Belousoff, M. J., Graham, B., Mobaraki, B., Murray, K. S., and Spiccia, L. "Oxalato-Bridged Dinuclear Copper(II) Complexes of *n*-Alkylated Derivatives of 1,4,7-triazacyclononane: Synthesis, X-ray Crystal Structures and Magnetic Properties." *European Journal of Inorganic Chemistry*, vol. 2006, no. 23, 2006, pp. 4872–4878.
14. Huang, X. Y., Deng, F., Yamaji, N., Pinson, S. R., Fujii-Kashino, M., Danku, J., Douglas, A., Guerinot, M.L., Salt, D.E., and Ma, J.F. "A Heavy Metal P-Type ATPase OsHMA4 Prevents Copper Accumulation in Rice Grain." *Nature Communications*, vol. 7, no. 1, 2016, pp. 1-13.
15. Krasnovskaya, O., Naumov, A., Guk, D., Gorelkin, P., Erofeev, A., Beloglazkina, E., and Majouga, A. "Copper Coordination Compounds as Biologically Active Agents." *International Journal of Molecular Sciences*, vol. 21, no. 11, 2020, pp. 1-37.
16. Hussain, A., AlAjmi, M.F., Rehman, M., Amir, S., Husain, F.M., Alsalmeh, A., Siddiqui, M.A., AlKhedhairy, A.A., and Khan, R.A. "Copper(II) Complexes as Potential Anticancer and Nonsteroidal Anti-Inflammatory Agents: In Vitro and in Vivo Studies." *Scientific Reports*, vol. 9, no. 1, 2019, pp. 1-17.
17. Komaei, S.A., Van Albada, G.A., Haasnoot, J.G., Kooijman, H., Spek, A.L., and Reedijk, J. "Synthesis, Spectroscopic, Magnetic Properties and X-Ray Crystal Structure of Di- $\mu$ -Hydroxo-Bis( $\mu$ -Perchlorato-O,*o'*)-Bis-[Bis(2-Amino-4-Methylpyrimidine)Copper(II)]: Bridging Perchlorate Results in Significant Deviation from the Predicted Magnetic Exchange." *Inorganica Chimica Acta*, vol. 286, no. 1, 1999, pp. 24–29.
18. Festa R.A., and Thiele D.J. "Copper: An Essential Metal in Biology." *Current Biology*, vol. 21, no. 21, 2011, pp. R877-R883.
19. Osredkar, J., and N. Sustar. "Copper and Zinc, Biological Role and Significance of Copper/Zinc Imbalance." *J Clin Toxicol*, vol. S3, no. 001, 2011, pp. 1-14.
20. Raman, N., Joseph, J., Sakthivel, A. and Jeyamurugan, R. "Synthesis, Structural Characterization and Antimicrobial Studies of Novel Schiff Base Copper(II) Complexes." *Journal of the Chilean Chemical Society*, vol. 54, no. 4, 2009, pp.354-357.
21. Bartyzel, A. "Synthesis, Thermal Behaviour and Some Properties of Cu<sup>II</sup> Complexes with N,O-Donor Schiff Bases." *Journal of Thermal Analysis and Calorimetry*, vol. 131, no. 2, 2018, pp. 1221-1236.
22. Yruela, I. "Copper in Plants: Acquisition, Transport and Interactions." *Functional Plant Biology*, vol. 36, no. 5, 2009, pp. 409-430.
23. Gao, S., Yan, R., Cao, M., Yang, W., Wang, S. and Chen, F. "Effects of Copper on Growth, Antioxidant Enzymes and Phenylalanine Ammonia-Lyase Activities in *Jatropha Curcas* L. Seedling." *Plant Soil Environment*, vol. 54, no.3, 2008, pp.117-122.
24. Coelho, F.C., Squitti, R., Ventriglia, M., Cerchiaro, G., Daher, J.P., Rocha, J.G., Rongioletti, M.C. and Moonen, A.C. "Agricultural Use of Copper and its Link to Alzheimer's Disease." *Biomolecules*, vol. 10, no. 6, 2020, pp. 1-19.

25. Van Nguyen, D., Nguyen, H.M., Le, N.T., Nguyen, K.H., Nguyen, H.T., Le, H.M., Nguyen, A.T., Dinh, N.T.T., Hoang, S.A. and Van Ha, C. "Copper Nanoparticle Application Enhances Plant Growth and Grain Yield in Maize Under Drought Stress Conditions." *Journal of Plant Growth Regulation*, vol. 41, no. 1, 2022, pp. 364-375.
26. Świdorski, G., Świsłocka, R., Łyszczek, R., Wojtulewski, S., Samsonowicz, M. and Lewandowski, W. "Thermal, Spectroscopic, X-ray and Theoretical Studies of Metal Complexes (Sodium, Manganese, Copper, Nickel, Cobalt and Zinc) with Pyrimidine-5-carboxylic and Pyrimidine-2-carboxylic acids." *Journal of Thermal Analysis and Calorimetry*, vol. 138, no. 4, 2019, pp. 2813-2837.
27. Lee, H., Wu, X. and Sun, L. "Copper-Based Homogeneous and Heterogeneous Catalysts for Electrochemical Water Oxidation." *Nanoscale*, vol. 12, no. 7, 2020, pp. 4187-4218.
28. Colombo, A., Dragonetti, C., Roberto, D. and Fagnani, F. "Copper Complexes as Alternative Redox Mediators in Dye-Sensitized Solar Cells." *Molecules*, vol. 26, no. 1, 2021, pp. 1-20.
29. Zhao, P., Zhai, S., Dong, J., Gao, L., Liu, X., Wang, L., Kong, J. and Li, L. "Synthesis, Structure, DNA Interaction, and SOD Activity of Three Nickel(II) Complexes Containing L-phenylalanine Schiff Base and 1,10-phenanthroline." *Bioinorganic chemistry and applications*, vol. 2018, 2018, pp. 1-16.
30. Shahabadi, N., Kashanian, S., Khosravi, M. and Mahdavi, M. "Multispectroscopic DNA Interaction Studies of a Water-Soluble Nickel(II) Complex Containing Different Dinitrogen Aromatic Ligands." *Transition Metal Chemistry*, vol. 35, no. 6, 2010, pp. 699-705.
31. Haghighi, F.H., Hadadzadeh, H., Darabi, F., Jannesari, Z., Ebrahimi, M., Khayamian, T., Salimi, M. and Rudbari, H.A. "Polypyridyl Ni(II) Complex, [Ni(Tppz)<sub>2</sub>]<sup>2+</sup>: Structure, DNA- and BSA Binding and Molecular Modeling." *Polyhedron*, vol. 65, 2013, pp.16-30.
32. Genchi, G., Carocci, A., Lauria, G., Sinicropi, M.S. and Catalano, A. "Nickel: Human Health and Environmental Toxicology." *International journal of environmental research and public health*, vol. 17, no. 3, 2020, pp. 1-21.
33. Li, Y., Dong, J., Zhao, P., Hu, P., Yang, D., Gao, L. and Li, L. "Synthesis of Amino Acid Schiff Base Nickel(II) Complexes as Potential Anticancer Drugs in Vitro." *Bioinorganic chemistry and applications*, vol. 2020, 2020, pp. 1-15.
34. Jabłońska-Trypuć, A., Wydro, U., Wołejko, E., Świdorski, G. and Lewandowski, W. "Biological Activity of New Cichoric Acid–Metal Complexes in Bacterial Strains, Yeast-Like Fungi, and Human Cell Cultures in Vitro." *Nutrients*, vol. 12, no. 1, 2020, pp. 1-21.
35. Macomber, L., and Hausinger, R.P. "Mechanisms of Nickel Toxicity in Microorganisms." *Metallomics*, vol. 3, no. 11, 2011, pp. 1153-1162.
36. Wang, J., Zhang, L., Jiang, H., Chen, K. and Liu, H. "Application of Nickel(II) Complexes to the Efficient Synthesis of  $\alpha$ - or  $\beta$ -amino Acids." *Chimia International Journal for Chemistry*, vol. 65, no. 12, 2011, pp. 919-924.
37. Kumar, S., and Trivedi, A. V. "A Review on Role of Nickel in the Biological System." *Int. J. Curr. Microbiol. Appl. Sci.*, vol. 5, no. 3, 2016, pp. 719-727.

38. Henrion, M., de P. Cardoso, B., César, V., Chetcuti, M.J. and Ritleng, V. "Nickel(II) Complexes of Highly  $\sigma$ -Donating Cyclic (Alkyl)(Amino)-and Malonate-Carbenes: Syntheses and Catalytic Studies." *Organometallics*, vol. 36, no.6, 2017, pp. 1113-1121.
39. W Wang, Z., Yu, S.L., Wei, Z.B., An, D.L., Li, Y.Y. and Gao, J.X. "Synthesis, Characterization of Novel Nickel(II) Complexes with P<sub>x</sub>N<sub>y</sub>-Type Ligands and Their Application in Reduction of Ketones." *Journal of Organometallic Chemistry*, vol. 898, 2019, pp. 1-6.
40. Klein, A., Kaiser, A., Sarkar, B., Wanner, M. and Fiedler, J. "The Electrochemical Behaviour of Organonickel Complexes: Mono-, Di-and Trivalent Nickel." *European journal of inorganic chemistry*, vol. 2007, no. 7, 2007, pp. 965-976.
41. Feizi, H., Shiri, F., Bagheri, R., Singh, J.P., Chae, K.H., Song, Z. and Najafpour, M.M. "The Application of a Nickel(II) Schiff Base Complex in Water Oxidation: the Importance of Nanosized Materials." *Catalysis Science & Technology*, vol. 8, no. 15, 2018, pp. 3954-396.
42. Anitha, P., Manikandan, R., Vijayan, P., Prakash, G., Viswanathamurthi, P. and Butcher, R.J. "Nickel(II) Complexes Containing ONS Donor Ligands: Synthesis, Characterization, Crystal Structure and Catalytic Application towards CC Cross-Coupling Reactions." *Journal of Chemical Sciences*, vol. 127, no. 4, 2015, pp. 597-608.
43. Das, K.K., Reddy, R.C., Bagoji, I.B., Das, S., Bagali, S., Mullur, L., Khodnapur, J.P. and Biradar, M.S. "Primary Concept of Nickel Toxicity—an Overview." *Journal of basic and clinical physiology and pharmacology*, vol. 30, no. 2, 2018, pp. 141-152.
44. Kumar, A., Balouch, A., Pathan, A.A., Jagirani, M.S., Mahar, A.M., Zubair, M. and Laghari, B. "Remediation of Nickel Ion from Wastewater by Applying Various Techniques: a Review." *Acta Chemica Malaysia*, vol. 3, no.1, 2019, pp. 1-15.
45. Sivaramakrishna, A., Clayton, H.S. and Muralikrishna, U. "Synthesis, Structure, Chemistry, and Applications of Tetravalent Nickel Complexes." *Journal of Coordination Chemistry*, vol. 64, no .8, 2011, pp. 1309-1332.
46. Lisdiana, A., Solihin and Onggo, D. "Potential Application of Lateritic Nickel as Nickel(II)triazole Complexes: Electronic Spectral Studies." *AIP Conference Proceedings*, vol. 2232, no. 1, AIP Publishing LLC, 2020, pp. 1-6.
47. Noël, S., Alamarguy, D., Correia, S. and Laurat, P. "Fretting Behavior of Nickel Coatings for Electrical Contact Applications." *Proc. 57th IEEE Holm Conf. on Electrical Contacts, Minneapolis (USA), Spt., 2011*, 2011, pp. 78-85.
48. Aderonke, A.V., Dede, A.H., Oluwatobi, A.I. and Ezekiel, N.Y.A.N. "Role of Nickel(II) Salicylhydroxamic Acid and its Aniline Adduct as an Antimicrobial Substitute." *Biomedical Journal of Scientific & Technical Research*, vol. 18, no .1, 2019, pp. 13273-13276.
49. Besson, T. and Thiéry, V. "Microwave-Assisted Synthesis of Sulfur and Nitrogen-Containing Heterocycles." In Van der Eycken, E. and Kappe, C.O. (eds), *Microwave-Assisted Synthesis of Heterocycles. Topics in Heterocyclic Chemistry, vol. 1*. Springer, Berlin, Heidelberg, 2006, pp. 59-78.

50. Kalal, P., Gandhi, D., Prajapat P. and Agarwal S. "Biological and Synthetic Studies of Four, Five and Six Membered." *Heterocyclic Letters*, vol. 7, no.2, 2017, pp. 513-540.
51. Hopkinson, M.N., Richter, C., Schedler, M. and Glorius, F. "An Overview of N-Heterocyclic Carbenes." *Nature*, vol. 510, no. 7506, 2014, pp. 485-496.
52. Balaban, A.T., Oniciu, D.C. and Katritzky, A.R. "Aromaticity as a Cornerstone of Heterocyclic Chemistry." *Chemical reviews*, vol. 104, no. 5, 2004, pp. 2777-2812.
53. Majumdar, P., Pati, A., Patra, M., Behera, R.K. and Behera, A.K. "Acid Hydrazides, Potent Reagents for Synthesis of Oxygen-, Nitrogen-, and/or Sulfur-Containing Heterocyclic Rings." *Chemical reviews*, vol. 114, no. 5, 2014, pp. 2942-2977.
54. Kaur, N. "Benign Approaches for the Microwave-Assisted Synthesis of Five-Membered 1,2-N, N-heterocycles." *Journal of Heterocyclic Chemistry*, vol. 52, no. 4, 2015, pp. 953-973.
55. Kaur, N. "Microwave-Assisted Synthesis of Five-Membered O, N-heterocycles." *Synthetic Communications*, vol. 44, no. 24, 2014, pp. 3509-3537.
56. Kaur, N. "Insight into Microwave-Assisted Synthesis of Benzo Derivatives of Five-Membered N, N-heterocycles." *Synthetic Communications*, vol. 45, no. 11, 2015, pp. 1269-1300.
57. Kaur, N. "Synthesis of Fused Five-Membered N, N-heterocycles Using Microwave Irradiation." *Synthetic Communications*, vol. 45, no. 12, 2015, pp. 1379-1410.
58. Kaur, N. "Review of Microwave-Assisted Synthesis of Benzo-Fused Six-Membered N, N-heterocycles." *Synthetic Communications*, vol. 45, no. 3, 2015, pp. 300-330.
59. Kaur, N. "Environmentally Benign Synthesis of Five-Membered 1, 3-N, N-heterocycles by Microwave Irradiation." *Synthetic Communications*, vol. 45, no. 8, 2015, pp. 909-943.
60. Kaur, N. "Synthesis of Five-Membered N, N, N-and N, N, N, N-heterocyclic Compounds: Applications of Microwaves." *Synthetic Communications*, vol. 45, no. 15, 2015, pp. 1711-1742.
61. Kaur, N. and Kishore, D. "Microwave-Assisted Synthesis of Seven-and Higher-Membered N-heterocycles." *Synthetic Communications*, vol. 44, no. 18, 2014, pp. 2577-2614.
62. Kaur, N. "Six-Membered N-heterocycles: Microwave-Assisted Synthesis." *Synthetic Communications*, vol. 45, no. 1, 2015, pp. 1-34.
63. Kaur, N. "Microwave-Assisted Synthesis of Fused Polycyclic Six-Membered N-heterocycles." *Synthetic Communications*, vol. 45, no. 3, 2015, pp. 273-299.
64. Kaur, N. "Advances in Microwave-Assisted Synthesis for Five-Membered N-heterocycle Synthesis." *Synthetic Communications*, vol. 45, no. 4, 2015, pp. 432-457.

65. Kaur, N. "Greener and Expeditious Synthesis of Fused Six-Membered N, N-heterocycles Using Microwave Irradiation." *Synthetic Communications*, vol. 45, no. 13, 2015, pp. 1493-1519.
66. Kaur, N. "Recent Impact of Microwave-Assisted Synthesis on Benzo Derivatives of Five-Membered N-heterocycles." *Synthetic Communications*, vol. 45, no. 5, 2015, pp. 539-568.
67. Kaur, N. "Six-Membered Heterocycles with Three and Four N-heteroatoms: Microwave-Assisted Synthesis." *Synthetic Communications*, vol. 45, no. 2, 2015, pp. 151-172.
68. Kaur, N. "Microwave-Assisted Synthesis: Fused Five-Membered N-heterocycles." *Synthetic Communications*, vol. 45, no. 7, 2015, pp. 789-823.
69. Kaur, N. "Microwave-Assisted Synthesis of Five-Membered S-heterocycles." *Journal of the Iranian Chemical Society*, vol. 11, no. 2, 2014, pp. 523-564.
70. Kaur, N. "Polycyclic Six-Membered N-heterocycles: Microwave-Assisted Synthesis." *Synthetic Communications*, vol. 45, no. 1, 2015, pp. 35-69.
71. Kaur, N. "Application of Microwave Irradiation in the Synthesis of Fused Six-Membered Heterocycles with N-heteroatom." *Synthetic Communications*, vol. 45, no. 2, 2015, pp. 173-201.
72. Kaur, N. "Green Synthesis of Three-to Five-Membered O-heterocycles Using Ionic Liquids." *Synthetic Communications*, vol. 48, no. 13, 2018, pp. 1588-1613.
73. Dabiri, M., Salehi, P. and Baghbanzadeh, M. "Ionic Liquid Promoted Eco-Friendly and Efficient Synthesis of 2,3-dihydroquinazolin-4 (1H)-ones." *Monatshefte für Chemie-Chemical Monthly*, vol. 138, no. 11, 2007, pp. 1191-1194.
74. Kaur, N. "Perspectives of Ionic Liquids Applications for the Synthesis of Five-and Six-Membered O, N-heterocycles." *Synthetic Communications*, vol. 48, no. 5, 2018, pp. 473-495.
75. Frizzo, C.P., Moreira, D.N. and Martins, M.A. "Ionic Liquids: Applications in Heterocyclic Synthesis." In Prof. Alexander Kokorin. (ed), *Ionic Liquids: Applications and Perspectives*, InTechOpen, 2011, pp. 415-438.
76. Kaur, N. "Application of Silver-Promoted Reactions in the Synthesis of Five-Membered O-heterocycles." *Synthetic Communications*, vol. 49, no. 6, 2019, pp. 743-789.
77. Eftekhari-Sis, B., Zirak, M. and Akbari, A. "Arylglyoxals in Synthesis of Heterocyclic Compounds." *Chemical reviews*, vol. 113, no. 5, 2013, pp. 2958-3043.
78. Majumder, A., Gupta, R. and Jain, A. "Microwave-Assisted Synthesis of Nitrogen-Containing Heterocycles." *Green chemistry letters and reviews*, vol. 6, no. 2, 2013, pp. 151-182.
79. Ghaemi, M. and Pordel, M. "Isoxazolo [4, 3-e] Indazole as a new Heterocyclic System: Design, Synthesis, Spectroscopic Characterization, and Antibacterial Activity." *Chemistry of Heterocyclic Compounds*, vol. 52, no. 1, 2016, pp. 52-57.
80. Kaur, N. "Ionic Liquid Assisted Synthesis of Six-Membered Oxygen Heterocycles." *SN Applied Sciences*, vol. 1, no. 8, 2019, pp. 1-20.

81. Heravi, M.M. and Zadsirjan, V. "Prescribed Drugs Containing Nitrogen Heterocycles: an Overview." *RSC Advances*, vol. 10, no. 72, 2020, pp. 44247-44311.
82. Kaur, N. "Metal Catalysts: Applications in Higher-Membered N-heterocycles Synthesis." *Journal of the Iranian Chemical Society*, vol. 12, no. 1, 2015, pp. 9-45.
83. Kaur, N. "Photochemical Reactions as Key Steps in Five-Membered N-heterocycle Synthesis." *Synthetic Communications*, vol. 48, no. 11, 2018, pp. 1259-1284.
84. (a) Martins, M.A., Frizzo, C.P., Moreira, D.N., Zanatta, N. and Bonacorso, H.G. "Ionic Liquids in Heterocyclic Synthesis." *Chemical reviews*, vol. 108, no. 6, 2008, pp. 2015-2050. (b) Omar, A. "Review Article; Anticancer Activities of Some Fused Heterocyclic Moieties Containing Nitrogen and/or Sulfur Heteroatoms." *Al-Azhar Journal of Pharmaceutical Sciences*, vol. 62, no. 2, 2020, pp. 39-54.
85. Kaur, N. *Metal and Nonmetal Assisted Synthesis of Six-Membered Heterocycles*. Netherlands: Elsevier Science, 2020.
86. Compain, P. "Olefin Metathesis of Amine-Containing Systems: Beyond the Current Consensus." *Advanced Synthesis & Catalysis*, vol. 349, no. 11-12, 2007, pp. 1829-1846.
87. Mermer, A., Keles, T. and Sirin, Y. "Recent Studies of Nitrogen Containing Heterocyclic Compounds as Novel Antiviral Agents: A Review." *Bioorganic Chemistry*, vol. 114, 2021, p. 105076.
88. Pearce, S. "The Importance of Heterocyclic Compounds in Anti-Cancer Drug Design." *Drug Discovery World (DDW)*, 2017, pp. 66-70.
89. Kerru, N., Gummidi, L., Maddila, S., Gangu, K.K. and Jonnalagadda, S.B. "A Review on Recent Advances in Nitrogen-Containing Molecules and their Biological Applications." *Molecules*, vol. 25, no. 8, 2020, pp. 1-42.
90. Ju, Y. and Varma, R.S. "Aqueous N-heterocyclization of Primary Amines and Hydrazines with Dihalides: Microwave-Assisted Syntheses of N-azacycloalkanes, Isoindole, Pyrazole, Pyrazolidine, and Phthalazine Derivatives." *The Journal of organic chemistry*, vol. 71, no. 1, 2006, pp. 135-141.
91. Sharma, P.K., Amin, A. and Kumar, M. "A Review: Medicinally Important Nitrogen Sulphur Containing Heterocycles." *The Open Medicinal Chemistry Journal*, vol. 14, no. 1, 2020, pp. 49-64.
92. Bur, S.K. and Padwa, A. "The Pummerer Reaction: Methodology and Strategy for the Synthesis of Heterocyclic Compounds." *Chemical reviews*, vol. 104, no. 5, 2004, pp. 2401-2432.
93. Kaur, N. "Synthesis of Seven and Higher-Membered Heterocycles Using Ruthenium Catalysts." *Synthetic Communications*, vol. 49, no. 5, 2019, pp. 617-661.
94. Kaur, N. "Synthesis of Six-Membered N-heterocycles Using Ruthenium Catalysts." *Catalysis Letters*, vol. 149, no. 6, 2019, pp. 1513-1559.

95. Kaur, N. "Metal Catalysts for the Formation of Six-Membered N-polyheterocycles." *Synthesis and Reactivity in Inorganic, Metal-Organic, and Nano-Metal Chemistry*, vol. 46, no.7, 2016, pp. 983-1020.
96. Kaur, N. "Palladium Catalysts: Synthesis of Five-Membered N-heterocycles fused with Other Heterocycles." *Catalysis Reviews*, vol. 57, no. 1, 2015, pp. 1-78.
97. Polshettiwar, V. and Varma, R.S. "Greener and Expeditious Synthesis of Bioactive Heterocycles Using Microwave Irradiation." *Pure and Applied Chemistry*, vol. 80, no. 4, 2008, pp. 777-790.
98. Kaur, N. "Palladium-Catalyzed Approach to the Synthesis of Five-Membered O-heterocycles." *Inorganic Chemistry Communications*, vol. 49, 2014, pp. 86-119.
99. Katritzky, A. R. "Introduction: heterocycles." *Chem. Rev*, vol. 104, no. 5, 2004, pp. 2125-2126.
100. Kaur, N. "Ruthenium Catalysis in Six-Membered O-heterocycles Synthesis." *Synthetic Communications*, vol. 48, no. 13, 2018, pp. 1551-1587.
101. Kaur, N. "Photochemical Mediated Reactions in Five-membered O-heterocycles Synthesis." *Synthetic Communications*, vol. 48, no. 17, 2018, pp. 2119-2149.
102. Hu, X.Q., Chen, J.R., Wei, Q., Liu, F.L., Deng, Q.H., Beauchemin, A.M. and Xiao, W.J "Photocatalytic Generation of N-Centered Hydrazonyl Radicals: A Strategy for Hydroamination of  $\beta$ ,  $\gamma$  -Unsaturated Hydrazones." *Angewandte Chemie*, vol. 126, no. 45, 2014, pp. 12359-12363.
103. Kaur, N. "Nickel Catalysis: Six Membered Heterocycle Syntheses." *Synthetic Communications*, vol. 49, no. 9, 2019, pp. 1103-1133.
104. Li, X., He, L., Chen, H., Wu, W. and Jiang, H. "Copper-Catalyzed Aerobic C(sp<sup>2</sup>)-H Functionalization for C-N Bond Formation: Synthesis of Pyrazoles and Indazoles." *The Journal of organic chemistry*, vol. 78, no. 8, 2013, pp. 3636-3646.
105. Kumar, R. and Joshi, Y.C. "Mild and Efficient One Pot Synthesis of Imidazolines and Benzimidazoles from Aldehydes." *E-journal of chemistry*, vol. 4, no. 4, 2007, pp. 606-610.
106. Xing, X., Zhu, X., Li, H., Jiang, Y. and Ni, J. "Electrochemical Oxidation of Nitrogen-Heterocyclic Compounds at Boron-Doped Diamond Electrode." *Chemosphere*, vol. 86, no. 4, 2012, pp. 368-375.
107. Ameta, K.L. and Dandia, A. (eds). "An Approach towards Green Switch through Nanocatalysis for the Synthesis of Biodynamic Heterocycles." *Green Chemistry: Synthesis of Bioactive Heterocycles, first edition*, chapter 5, Springer: India, 2014, pp. 1 - 412.
108. Kaur, N. "Microwave-Assisted Synthesis of Five-Membered O-heterocycles." *Synthetic Communications*, vol. 44, no. 24, 2014, pp. 3483-3508.
109. Kaur, N. "Review on the Synthesis of Six-Membered N, N-heterocycles by Microwave Irradiation." *Synthetic Communications*, vol. 45, no. 10, 2015, pp. 1145-1182.

110. Kaur, N. "Applications of Microwaves in the Synthesis of Polycyclic Six-Membered N, N-heterocycles." *Synthetic Communications*, vol. 45, no. 14, 2015, pp. 1599-1631.
111. Kaur, N. "Role of Microwaves in the Synthesis of Fused Five-Membered Heterocycles with Three N-heteroatoms." *Synthetic Communications*, vol. 45, no. 4, 2015, pp. 403-431.
112. Kaur, N. and Kishore, D. "Microwave-Assisted Synthesis of Six-Membered S-heterocycles." *Synthetic Communications*, vol. 44, no. 18, 2014, pp. 2615-2644.
113. Kaur, N. "Microwave-Assisted Synthesis of Seven-Membered S-heterocycles." *Synthetic Communications*, vol. 44, no. 22, 2014, pp. 3201-3228.
114. Kaur, N. and Kishore, D. "Microwave-Assisted Synthesis of Seven-and Higher-Membered O-heterocycles." *Synthetic Communications*, vol. 44, no. 19, 2014, pp. 2739-2755.
115. Kaur, N. and Kishore, D. "Microwave-Assisted Synthesis of Six-Membered O-heterocycles." *Synthetic Communications*, vol. 44, no. 21, 2014, pp. 3047-3081.
116. Kaur, N. "Solid-Phase Synthesis of Sulfur Containing Heterocycles." *Journal of Sulfur Chemistry*, vol. 39, no. 5, 2018, pp. 544-577.
117. Badshah, S.L. and Naeem, A. "Bioactive Thiazine and Benzothiazine Derivatives: Green Synthesis Methods and Their Medicinal Importance." *Molecules*, vol. 21, no. 8, 2016, pp. 1-20.
118. Kaur, N. and Kishore, D. "Nitrogen-Containing Six-Membered Heterocycles: Solid-Phase Synthesis." *Synthetic Communications*, vol. 44, no. 9, 2014, pp. 1173-1211.
119. Kaur, N. and Kishore, D. "Solid-Phase Synthetic Approach toward the Synthesis of Oxygen-Containing Heterocycles." *Synthetic Communications*, vol. 44, no. 8, 2014, pp. 1019-1042.
120. Daştan, A., Kulkarni, A. and Toeroek, B. "Environmentally Benign Synthesis of Heterocyclic Compounds by Combined Microwave-Assisted Heterogeneous Catalytic Approaches." *Green chemistry*, vol. 14, no. 1, 2012, pp. 17-37.
121. Dabholkar, V.V. and Ansari, F.Y. "Novel Pyrimidine Derivatives by Sonication and Traditional Thermal Methods." *Green Chemistry Letters and Reviews*, vol. 3, no. 3, 2010, pp. 245-248.
122. Sperry, J.B. and Wright, D.L. "Furans, Thiophenes and Related Heterocycles in Drug Discovery." *Current Opinion in Drug Discovery and Development*, vol. 8, no. 6, 2005, pp. 723-740.
123. Wang, Y., Zhang, W.X. and Xi, Z. "Carbodiimide-Based Synthesis of N-heterocycles: Moving from Two Classical Reactive Sites to Chemical Bond Breaking/Forming Reaction." *Chemical Society Reviews*, col. 49, no. 16, 2020, pp. 5810-5849.
124. Kaur, N. "Ionic Liquid Assisted Synthesis of S-heterocycles." *Phosphorus, Sulfur, and Silicon and the Related Elements*, vol. 194, no. 3, 2019, pp. 165-185.

125. Thanusu, J., Kanagarajan, V. and Gopalakrishnan, M. "Synthesis, Spectral Analysis, and in Vitro Microbiological Evaluation of Ethyl 7, 9-diaryl-1, 4-diazaspiro [4.5] dec-9-ene-6-carboxylates as a New Class of Antibacterial and Antifungal Agents." *Chemistry of Heterocyclic Compounds*, vol. 47, no. 5, 2011, pp. 575-583.
126. Henary, M., Kananda, C., Rotolo, L., Savino, B., Owens, E.A. and Cravotto, G. "Benefits and Applications of Microwave-Assisted Synthesis of Nitrogen Containing Heterocycles in Medicinal Chemistry." *RSC Advances*, vol. 10, no. 24, 2020, pp. 14170-14197.
127. Souldozi, A. "Efficient One-Pot Three-Component Reaction for the Synthesis of (5-aryl-1, 3, 4-oxadiazol-2-yl)(pyridin-2-yl)methanol Derivatives." *Journal of Chemical Research*, vol. 39, no. 3, 2015, pp. 177-179.
128. Asif, M. "An Overview of Various Heterocyclic Imidazopyridine, Triazolopyridine and Quinoline Derivatives Compounds and their Biological Significances." *Moroccan Journal of Chemistry*, vol. 5, no. 2, 2017, pp. 317-324.
129. Díez-González, S. and Nolan, S.P. "8 Carbene and Transition Metal-Mediated Transformations." *Annual Reports Section "B" (Organic Chemistry)*, vol. 101, 2005, pp. 171-191.
130. Kaur, N. "Palladium-Catalyzed Approach to the Synthesis of S-heterocycles." *Catalysis Reviews*, vol. 57, no. 4, 2015, pp. 478-564.
131. Dabiri, M., Salehi, P., Baghbanzadeh, M. and Bahramnejad, M. "A Facile Procedure for the One-Pot Synthesis of Unsymmetrical 2,5-disubstituted 1, 3, 4-oxadiazoles." *Tetrahedron Letters*, vol. 47, no. 39, 2006, pp. 6983-6986.
132. Koradin, C., Dohle, W., Rodriguez, A.L., Schmid, B. and Knochel, P. "Synthesis of Polyfunctionalindoles and Related Heterocycles Mediated by Cesium and Potassium Bases." *Tetrahedron*, vol. 59, no. 9, 2003, pp. 1571-1587.
133. Nakamura, I. and Yamamoto, Y. "Transition-Metal-catalyzed Reactions in Heterocyclic Synthesis." *Chemical reviews*, vol. 104, no. 5, 2004, pp. 2127-2198.
134. Hosseinzadeh, Z., Ramazani, A. and Razzaghi-Asl, N. "Anti-Cancer Nitrogen-Containing Heterocyclic Compounds." *Current Organic Chemistry*, vol. 22, no. 23, 2018, pp. 2256-2279.
135. Zinn, F.K., Viciu, M.S. and Nolan, S.P. "10 Carbenes: Reactivity and Catalysis." *Annual Reports Section "B" (Organic Chemistry)*, vol. 100, 2004, pp. 231-249.
136. Marion, N., Díez-González, S. and Nolan, S.P. "N-Heterocyclic Carbenes as Organocatalysts." *Angewandte Chemie International Edition*, vol. 46, no. 17, 2007, pp. 2988-3000.
137. Galstyan, A., Shen, W.Z., Freisinger, E., Alkam, H., Hiller, W., Sanz Miguel, P.J., Schürmann, M. and Lippert, B. "Supramolecular Isomerism of 2,2'-Bipyrazine Complexes with cis-(NH<sub>3</sub>)<sub>2</sub>PtII: Ligand Rotational State and Sequential Orientation Determine the 3D Shape of Metallacycles." *Chemistry—A European Journal*, vol. 17, no. 38, 2011, pp. 10771-10780.

138. (a) Kom Reddy, V., Rillema, D.P., Nguyen, H. and Kadel, L. "Synthesis and Characterization of 2-(2-Pyridinyl)pyrazine and 2,2'-Bipyrazine Derivatives." *Journal of Heterocyclic Chemistry*, vol. 56, no. 3, 2019, pp. 972-979. (b) Montgomery, T. D. and Rawal, V. H. "Palladium-Catalyzed Modular Synthesis of Substituted Piperazines and Related Nitrogen Heterocycles." *Org Lett*, vol. 18, no. 4, 2016, pp. 740-743. (c) Dolezal, M. and Zitko, J. "Pyrazine Derivatives: A Patent review (June 2012–present)." *Expert Opin Ther Pat*, vol. 25, no. 1, 2015, pp. 33-47. (d) Schultz, D. M.; Sawicki, J. W. and Yoon, T. P. "An Improved Procedure for the Preparation of Ru(bpz)<sub>3</sub>(PF<sub>6</sub>)<sub>2</sub> via a High-Yielding Synthesis of 2,2'-bipyrazine." *J Org Chem*, vol. 11, no. 1, 2015, pp. 61-65. (e) Lin, S.; Ischay, M. A.; Fry, C. G. and Yoon, T. P. "Radical Cation Diels–Alder Cycloadditions by Visible Light Photocatalysis." *J Am Chem Soc*, vol. 133, no. 48, 2011, pp. 19350-19353. (f) Bouilly, L.; Darabantu, M.; Turck, A. and Plé, N. "Aryl-aryl Bonds Formation in Pyridine and Diazine series. Diazines part 41." *J Heterocyclic Chem*, vol. 42, no. 7, 2005, pp. 1423-1428. (g) Graaf, M.D. and Moeller, K.D. "Photoredox Catalysts: Synthesis of the Bipyrazine Ligand." *The Journal of Organic Chemistry*, vol. 80, no. 3, 2015, pp.2032-2035. (h) Toma, L.M., Eller, C., Rillema, D.P., Ruiz-Pérez, C. and Julve, M. "Synthesis and Crystal Structure of the Low-Spin Iron(II) Complex [Fe(bpz)<sub>3</sub>](ClO<sub>4</sub>)<sub>2</sub>·H<sub>2</sub>O (bpz= 2,2'-bipyrazine)." *Inorganica chimica acta*, vol. 357, no. 9, 2004, pp. 2609-2614. (i) Bronner, C. and Wenger, O. S. "Long-Range Proton-Coupled Electron Transfer in Phenol–Ru(2,2'-bipyrazine)<sub>3</sub><sup>2+</sup> Dyads." *Phys Chem Chem Phys*, vol. 16, no.8, 2014, pp. 3617-3622 (j) Wallace, L. and Rillema, D. P. "Photophysical Properties of Rhenium(I) Tricarbonyl Complexes Containing Alkyl-and Aryl-Substituted Phenanthrolines as Ligands." *Inorg Chem*, vol. 32, no. 18, 1993, pp. 3836-3843.
139. Schnebeck, R.D., Freisinger, E. and Lippert, B. "Molecular Architecture with 2,2'-Bipyrazine and Metal Ions: Infinite Loop and Molecular Square." *European Journal of Inorganic Chemistry*, vol. 2000, no. 6, 2000, pp. 1193-1200.
140. Schnebeck, R.D., Freisinger, E., Glahe, F. and Lippert, B. "Molecular Architecture Based on Metal Triangles Derived from 2,2'-Bipyrazine (Bpz) and EnM<sup>II</sup> (M= Pt, Pd)." *Journal of the American Chemical Society*, vol. 122, no. 7, 2000, pp. 1381-1390.
141. Zangrando, E., Casanova, M. and Alessio, E. "Trinuclearmetallacycles: Metallatriangles and Much More." *Chemical Reviews*, vol. 108, no. 12, 2008, pp. 4979-5013.
142. Kulesza, J., Barros, B.S. and Júnior, S.A. "Organic–Inorganic Hybrid Materials: Metallacalixarenes. Synthesis and Applications." *Coordination Chemistry Reviews*, vol. 257, no. 15-16, 2013, pp. 2192-2212.
143. Yeh, T.T., Wu, J.Y., Wen, Y.S., Liu, Y.H., Twu, J., Tao, Y.T. and Lu, K.L. "Luminescent Silver Metal Chains with Unusual  $\mu$  4-bonded 2,2'-bipyrazine." *Dalton Transactions*, no. 4, 2005, pp. 656-658.
144. Xu, Y., Wu, M., Huang, Y., Yuan, D., Jiang, F. and Hong, M. "Synthesis, X-ray Crystal Structure, and Magnetic Property of a 3-D Self-Assembled

- Supermolecule.” *Journal of Coordination Chemistry*, vol. 62, no. 14, 2009, pp. 2307-2315.
145. (a) Baird, D.M., Yang, F.L., Kavanaugh, D.J., Finness, G. and Dunbar, K.R. “Ligand effects on the  $\delta \rightarrow \delta^*$  Band Energies and Intensities in a Series of Diimine Complexes of Dimolybdenum.” *Polyhedron*, vol. 15, no. 15, 1996, pp. 2597-2606. (b) Ernst, S. and Kaim, W. “Coordination Characteristics of Four Isomeric. Alpha.-Diimine Ligands. pi. Molecular Orbital Perturbation Calculations for the Bidiazines and Their Correlation with the Properties of Group 6 Metal Carbonyl Complexes.” *Journal of the American Chemical Society*, vol. 108, no. 13, 1986, pp.3578-3586.
146. Waldhoer, E., Poppe, J., Kaim, W., Cutin, E.H., Garcia Posse, M.E. and Katz, N.E. “EPR Evidence for Low-Lying MLCT States in–Tetracyanoiron and–Ruthenium Complexes with Strongly. Pi.-Accepting Chelate Ligands. Comparison with Isoelectronic Tetracarbonylmetal Species.” *Inorganic Chemistry*, vol. 34, no. 11, 1995, pp. 3093-3096.
147. Ross, H.B., Boldaji, M., Rillema, D.P., Blanton, C.B. and White, R.P. “Photosubstitution in Tris Chelate Complexes of Ruthenium(II) Containing the Ligands 2,2'-bipyrazine, 2,2'-bipyrimidine, 2,2'-bipyridine, and 4,4'-dimethyl-2,2'-bipyridine: Energy Gap Control.” *Inorganic Chemistry*, vol. 28, no.6, 1989, pp. 1013-1021.
148. Haga, M., Dodsworth, E.S., Eryavec, G., Seymour, P. and Lever, A.B.P. “Luminescence Quenching of the tris(2,2'-bipyrazine) ruthenium(II) Cation and its Monoprotonated Complex.” *Inorganic Chemistry*, vol. 24, no. 12, 1985, pp. 1901-1906.
149. Premkumar, P., PK, K.N., Sathishkumar, M., Ramachandran, K.I. and Gopakumar, D. Quantum. “Mechanical Modeling and Molecular Dynamic Simulation of Ruthenium (Ru) Polypyridyl Complexes to Study Feasibility of Artificial Photosynthesis.” In *2009 International Conference on Advances in Recent Technologies in Communication and Computing*, 2009, pp. 461-464.
150. (a) Kajouj, S., Marcélis, L., Lemaur, V., Beljonne, D. and Moucheron, C. “Photochemistry of Ruthenium(ii) Complexes Based on 1,4,5,8-tetraazaphenanthrene and 2,2'-bipyrazine: A Comprehensive Experimental and Theoretical Study.” *Dalton Transactions*, vol. 46, no. 20, 2017, pp. 6623-6633. (b) Campagna, S., Puntoriero, F., Nastasi, F., Bergamini, G. and Balzani, V. “Photochemistry and Photophysics of Coordination Compounds: Ruthenium.” In Balzani, V. and Campagna, S. (eds), *Photochemistry and Photophysics of Coordination Compounds I*, vol. 280, Springer, Berlin, Heidelberg, 2007, pp. 117-214. (c) Nazeeruddin, M.K., Zakeeruddin, S.M., Lagref, J.J., Liska, P., Comte, P., Barolo, C., Viscardi, G., Schenk, K. and Graetzel, M. “Stepwise Assembly of Amphiphilic Ruthenium Sensitizers and Their Applications in Dye-Sensitized Solar Cell.” *Coord. Chem. Rev.*, vol. 248, no. 13-14, 2004, pp. 1317-1328. (d) Grätzel, M. “Recent Advances in Sensitized Mesoscopic Solar Cells.” *Accounts of chemical research*, vol. 42, no. 11, 2009, pp.1788-1798. (e) Carballo, M.S., Urbani, M., Chandiran, A.K., González-Rodríguez, D., Vázquez, P., Grätzel, M., Nazeeruddin, M.K. and Torres, T. “Branched and Bulky Substituted Ruthenium Sensitizers for Dye-Sensitized Solar Cells.”

- Dalton Trans.*, vol. 43, no. 40, 2014, pp. 15085-15091. (f) Canton, S.E., Zhang, X., Liu, Y., Zhang, J., Papai, M., Corani, A., Smeigh, A.L., Smolentsev, G., Attenkofer, K., Jennings, G. and Kurtz, C.A. "Watching the Dynamics of Electrons and Atoms at Work in Solar Energy Conversion." *Faraday Discussions*, 2015, pp.51-68. (g) Tong, L., Zong, R., Zhou, R., Kaveevivitchai, N., Zhang, G. and Thummel, R.P. "Ruthenium Catalysts for Water Oxidation Involving Tetradentate Polypyridine-type Ligands." *Faraday Discussions*, 2015, pp.87-104. (h) Kowacs, T., Pan, Q., Lang, P., O'Reilly, L., Rau, S., Browne, W.R., Pryce, M.T., Huijser, A. and Vos, J.G. "Supramolecular Bimetallic Assemblies for Photocatalytic Hydrogen Generation from Water." *Faraday discussions*, 2015, pp.143-170. (i) Bonnet, S. and Collin, J.P. "Ruthenium-Based Light-Driven Molecular Machine Prototypes: Synthesis and Properties." *Chemical Society Reviews*, vol. 37, no. 6, 2008, pp.1207-1217. (j) Baranoff, E., Barigelletti, F., Bonnet, S., Collin, J.P., Flamigni, L. and Mobian, P. "JP Sauvage in Structure and Bonding: Photofunctional Transition Metals Complexes." In V. W. W. Yam. (ed), *Photofunctional Transition Metal Complexes*, vol. 123, Springer, Berlin, Heidelberg, 2007, pp. 41-78. (k) Gill, M.R. and Thomas, J.A. "Ruthenium(II) Polypyridyl Complexes and DNA—from Structural Probes to Cellular Imaging and Therapeutics." *Chemical Society Reviews*, vol. 41, no. 8, 2012, pp. 3179-3192. (l) Ghesquiere, J., Le Gac, S., Marcelis, L., Moucheron, C. and Kirsch-De Mesmaeker, A. "What Does the Future Hold for Photo-Oxidizing Ru(II) Complexes with Polyazaaromatic Ligands in Medicinal Chemistry?" *Curr. Top. Med. Chem.*, vol. 12, no. 3, 2012, pp.185–196. (m) Van Rixel, V.H.S., Siewert, B., Hopkins, S.L., Askes, S.H.C., Busemann, A., Siegler, M.A. and Bonnet, S. "Green Light-Induced Apoptosis in Cancer Cells by a Tetrapyrrolyl Ruthenium Prodrug Offering Two Trans Coordination Sites." *Chemical science*, vol. 7, no. 8, 2016, pp.4922-4929. (n) Kirsch-De Mesmaeker, A., Jacquet, L. and Nasielski, J. "Ruthenium(II) Complexes of 1,4,5,8-tetraazaphenanthrene (TAP) and 2,2'-bipyridine (bpy). Ground- and Excited-State Basicities of Ru<sup>2+</sup>(bpy)<sub>n</sub>(TAP)<sub>3-n</sub> (n= 0, 1, 2): Their Luminescence Quenching by Organic Buffers." *Inorganic Chemistry*, vol. 27, no. 24, 1988, pp.4451-4458. (o) Rillema, D.P., Allen, G., Meyer, T.J. and Conrad, D. "Redox Properties of Ruthenium(II) Tris Chelate Complexes Containing the Ligands 2,2'-bipyrazine, 2,2'-bipyridine, and 2,2'-bipyrimidine." *Inorganic chemistry*, vol. 22, no. 11, 1983, pp.1617-1622.
151. Bodar-Houillon, F. and Marsura, A. "Synthesis and Luminescence Properties of a New Tripode Containing 2,2'-bipyrazine Subunits: The tris-[(6-methyl-2,2'-bipyrazine-2-yl) methyl]amine." *Tetrahedron letters*, vol. 36, no. 6, 1995, pp. 865-868.
152. Coe, B.J., Peers, M.K. and Scrutton, N.S. "Syntheses and Electronic and Optical Properties of Complexes of the bis(2,2'-bipyrazyl)ruthenium Unit." *Polyhedron*, vol. 96, 2015, pp.57-65.
153. Toma, H.E "Supramolecular Chemistry and Technology." *Anais da Academia Brasileira de Ciências*, vol. 72, no. 1, 2000, pp. 05-26.
154. (a) Motimani, N. "Synthesis and Characterisation of Small Molecule and Macromolecular Photoredox Catalysts for Radical Thiol-ene Reactions." *MS*

- thesis, Faculty of Science, Department of Chemistry, Open UCT Home, 2021, pp. 1-108. (b) Tyson, E.L., Ament, M.S. and Yoon, T.P. "Transition Metal Photoredox Catalysis of Radical Thiol-ene Reactions." *The Journal of organic chemistry*, vol. 78, no. 5, 2013, pp. 2046-2050.
155. Marcélis, L., Ghesquière, J., Garnir, K., Kirsch-De Mesmaeker, A. and Moucheron, C. "Photo-Oxidizing RuII Complexes and Light: Targeting Biomolecules via Photoadditions." *Coordination Chemistry Reviews*, vol. 256, no. 15-16, 2012, pp. 1569-1582.
156. Bevernaegie, R., Marcélis, L., Laramée-Milette, B., De Winter, J., Robeyns, K., Gerbaux, P., Hanan, G.S. and Elias, B. "Trifluoromethyl-Substituted Iridium(III) Complexes: From Photophysics to Photooxidation of a Biological Target." *Inorganic chemistry*, vol. 57, no. 3, 2018, pp. 1356-1367.
157. Deraedt, Q., Marcélis, L., Loiseau, F. and Elias, B. "Towards Mismatched DNA Photoprobes and Photoreagents: "Elbow-Shaped" Ru(II) Complexes." *Inorganic Chemistry Frontiers*, vol. 4, no. 1, 2017, pp. 91-103.
158. Zhang, Y., Zhou, Q., Zheng, Y., Li, K., Jiang, G., Hou, Y., Zhang, B. and Wang, X. "DNA Photocleavage by Non-Innocent Ligand-Based Ru(II) Complexes." *Inorganic chemistry*, vol. 55, no. 9, 2016, pp. 4296-4300.
159. Wehlin, S.A., Troian-Gautier, L., Li, G. and Meyer, G.J. "Chloride Oxidation by Ruthenium Excited-States in Solution." *Journal of the American Chemical Society*, vol. 139, no. 37, 2017, pp. 12903-12906.
160. Gicquel, E., Paillous, N. and Vicendo, P. "Mechanism of DNA Damage Photosensitized by Trisbipyrazyl Ruthenium Complex. Unusual Role of Cu/Zn Superoxide Dismutase." *Photochemistry and photobiology*, vol. 72, no. 5, 2000, pp. 583-589.
161. Hebbar, N., Fiol-Petit, C., Ramondenc, Y., Plé, G. and Plé, N. "A New Series of Rod-Like Conjugated Molecules with a Pyrazine or a Bipyrazine Core. Synthesis and Light Emitting Properties." *Tetrahedron*, vol. 67, no. 12, 2011, pp. 2287-2298.
162. Mathieu, J., Marsura, A., Bouhmaida, N. and Ghermani, N. "Selective Self-Assembly of a Sequential Bipyridine– Bipyrazine Ligand Strand into a Double-Stranded Cu<sup>I</sup> Helicate." *European Journal of Inorganic Chemistry*, vol. 2002, no. 9, 2002, pp. 2433-2437.
163. Sherman, B.D., Sheridan, M.V., Wee, K.R., Song, N., Dares, C.J., Fang, Z., Tamaki, Y., Nayak, A. and Meyer, T.J. "Analysis of Homogeneous Water Oxidation Catalysis with Collector–Generator Cells." *Inorganic chemistry*, vol. 55, no. 2, 2016, pp. 512-517.
164. Wu, J.Y., Hsu, H.Y., Chan, C.C., Wen, Y.S., Tsai, C. and Lu, K.L. "Formation of Infinite Linear Mercury Metal Chains Assisted by Face-to-Face  $\pi$ - $\pi$  (Aryl–Aryl) Stacking Interactions." *Crystal Growth and Design*, vol. 9, no. 1, 2009, pp. 258-262.
165. Wu, M., Yuan, D., Han, L., Wu, B., Xu, Y. and Hong, M. "Inclusion of Metal Complexes into Cavities of 2D Coordination Networks Built from p-Sulfonatothiocalix [4] arene Tetranuclear Clusters." *ur. J. Inorg. Chem*, vol. 2006, no. 3, 2006, pp. 526–530.

166. Shoukry, A.A. and Al-Ahmary, K.M. "Synthesis, Characterization, Mixed-Ligand Complex Formation Reactions, and Equilibrium Studies of Co(II) with 2,2'-dipyridylamine and Some Selected Biorelevant Ligands." *Monatshefte für Chemie-Chemical Monthly*, vol. 144, no. 8, 2013, pp. 1117-1127.
167. (a) Bose, D., Mostafa, G., Fun, H.K. and Ghosh, B.K. "The Mn(II)-2,2'-dipyridylamine-pseudohalide System: Synthesis, Crystal Structure and Luminescence Behaviour of  $[\text{Mn}(\text{dpa})_2(\text{X})_2]\cdot\text{H}_2\text{O}$  and  $[\text{Mn}(\text{dpa})_2(\text{X})(\text{OH}_2)]\text{ClO}_4$  (dpa= 2,2'-dipyridylamine; X=  $\text{N}_3^-$ ,  $\text{NCO}^-$ )." *Polyhedron*, vol. 24, no. 6, 2005, pp. 747-758. (b) Bose, D., Rahaman, S.H., Mostafa, G., Walsh, R.D.B., Zaworotko, M.J. and Ghosh, B.K. "Synthesis, Structure and Properties of  $[\text{Zn}(\text{dpa})(\text{N}_3)_2]$  and  $[\text{Zn}(\text{dpa})(\text{N}_3)(\text{NO}_3)]_2$  (dpa= 2,2'-dipyridylamine): Composition Tailored Architectures." *Polyhedron*, vol. 23, no. 4, 2004, pp. 545-552.
168. (a) Yurdakul, Ş.E.N.A.Y. and Bilkana, M.T. "Spectroscopic and Structural Properties of 2,2'-dipyridylamine and its Palladium and Platinum Complexes." *Optics and Spectroscopy*, vol. 119, no. 4, 2015, pp. 603-619.  
 168 (b) Antonioli, B., Bray, D.J., Clegg, J.K., Gloe, K., Gloe, K., Kataeva, O., Lindoy, L.F., McMurtrie, J.C., Steel, P.J., Sumbly, C.J. and Wenzel, M. "Silver(I) Complexation of Linked 2,2'-dipyridylamine Derivatives. Synthetic, Solvent Extraction, Membrane Transport and X-ray Structural Studies." *Dalton Transactions*, no. 40, 2006, pp. 4783-4794.
169. Gerber\*, T.I.A., Abrahams, A., Mayer, P. and Hosten, E. "2,2'-dipyridylamine Complexes of Rhenium(V)." *J. Coord. Chem*, vol. 56, no. 16, 2003, pp. 1397-1407.
170. Maddock, L.C., Borilovic, I., McIntyre, J., Kennedy, A.R., Aromí, G. and Hevia, E. "Synthetic, Structural and Magnetic Implications of Introducing 2,2'-dipyridylamide to Sodium-Ferrate Complexes." *Dalton Transactions*, vol. 46, no. 20, 2017, pp. 6683-6691.
171. Lescouëzec, R., Marinescu, G., Muñoz, M.C., Luneau, D., Andruh, M., Lloret, F., Faus, J., Julve, M., Mata, J.A., Llusar, R. and Cano, J. " $[\text{Cr}(\text{dpa})(\text{ox})_2]^-$ : A New Bis-oxalato Building Block for the Design of Heteropolymetallic Systems. Crystal Structures and Magnetic Properties of  $\text{PPh}_4[\text{Cr}(\text{dpa})(\text{ox})_2]$ ,  $\text{AsPh}_4[\text{Cr}(\text{dpa})(\text{ox})_2]$ ,  $\text{Hdpa}[\text{Cr}(\text{dpa})(\text{ox})_2]\cdot 4\text{H}_2\text{O}$ ,  $\text{Rad}[\text{Cr}(\text{dpa})(\text{ox})_2]\cdot\text{H}_2\text{O}$  and  $\text{Sr}[\text{Cr}(\text{dpa})(\text{ox})_2]_2\cdot 8\text{H}_2\text{O}$  (dpa= 2,2'-dipyridylamine)." *New Journal of Chemistry*, vol. 25, no. 10, 2001, pp. 1224-1235.
172. Zhou, C., Wang, Y., Li, D., Zhou, L., Liu, P. and Shi, Q. "Polymers or Supramolecules Generated From a New V-Shaped Bis-monodentate Ligand and the Effect of Steric Hindrance on Coordination Modes of the Ligand." *Eur. J. Inorg. Chem*, vol. 2006, no. 12, 2006, pp. 2437-2446.
173. (a) Neville, S.M., Leita, B.A., Halder, G.J., Kepert, C.J., Moubaraki, B., Létard, J.F. and Murray, K.S. "Understanding the Two-Step Spin-Transition Phenomenon in Iron(II) 1D Chain Materials." *Chemistry—A European Journal*, vol. 14, no. 32, 2008, pp. 10123-10133. (b) Seward, C. and Wang, S. "Starburst Complexes of di-2-pyridylamine Derivatives with a Benzene or 1,3,5-triazine Core." *Comments on Inorganic Chemistry*, vol. 26, no. 1-2, 2005, pp. 103-125. (c) Jia, W.L., Liu, Q.D., Song, D. and Wang, S. "Blue Luminescent

- Organosilicon Compounds Based on 2,2'-Dipyridylaminophenyl and 2,2'-Dipyridylaminobiphenyl." *Organometallics*, vol. 22, no. 2, 2003, pp. 321-327.
- (d) Jia, W.L., Song, D. and Wang, S. "Blue Luminescent Three-Coordinate Organoboron Compounds with a 2,2'-Dipyridylamino Functional Group." *The Journal of organic chemistry*, vol. 68, no. 3, 2003, pp. 701-705
- (e) Ni, J., Wei, K.J., Min, Y., Chen, Y., Zhan, S., Li, D. and Liu, Y. "Copper(i) Coordination Polymers of 2,2'-dipyridylamine Derivatives: Syntheses, Structures, and Luminescence." *Dalton Transactions*, vol. 41, no. 17, 2012, pp. 5280-5293.
- (f) Wang, S. "Luminescence and Electroluminescence of Al(III), B(III), Be(II) and Zn(II) Complexes with Nitrogen Donors." *Coordination Chemistry Reviews*, vol. 215, no. 1, 2001, pp. 79-98
174. Mayer, P., Yumata, N.C., Gerber, T.I. and Abrahams, A.R. "Coordination of the Bidentate Ligands 2,2'-dipyridylamine, 1-phenyl-1,3-butadione and N'-(propan-2-ylidene)benzohydrazide to Rhenium(III)." *South African Journal of Chemistry*, vol. 63, 2010, pp. 180-185.
175. Lee, J.H., Park, H.M., Jang, S.P., Eom, G.H., Bae, J.M., Kim, C., Kim, Y. and Kim, S.J. "Construction of HgII Complexes Containing Chelating 2,2'-dipyridylamine Ligands: Anion Effect, Photoluminescence and Catalytic Activities." *Inorganic Chemistry Communications*, vol. 15, 2012, pp. 212-215.
176. Kang, Y., Seward, C., Song, D. and Wang, S. "Blue Luminescent Rigid Molecular Rods Bearing N-7-Azaindolyl and 2,2'-Dipyridylamino and Their Zn(II) and Ag(I) Complexes." *Inorganic chemistry*, vol. 42, no. 8, 2003, pp. 2789-2797.
- 176(a) Kang, Y. and Wang, S. "Syntheses and Photophysical Properties of Rigid-Rod Conjugated Compounds Based on N-7-azaindole and 2,2'-dipyridylamine." *Tetrahedron letters*, vol. 43, no. 20, 2002, pp. 3711-3713.
177. Wang, S., Bruneau, C., Renaud, J.L., Gaillard, S. and Fischmeister, C. "2,2'-Dipyridylamines: More than Just Sister Members of the Bipyridine Family. Applications and Achievements in Homogeneous Catalysis and Photoluminescent Materials." *Dalton Transactions*, vol. 48, no. 31, 2019, pp. 11599-11622.
178. Chelucci, G. "Metal-Complexes of Optically Active Amino- and Imino-Based Pyridine Ligands in Asymmetric Catalysis." *Coordination Chemistry Reviews*, vol. 257, no. 11-12, 2013, pp. 1887-1932.
179. Chelucci, G., Baldino, S. and Baratta, W. "Ruthenium and Osmium Complexes Containing 2-(aminomethyl)pyridine (Ampy)-Based Ligands in Catalysis." *Coordination Chemistry Reviews*, vol. 300, 2015, pp. 29-85.
180. Shirvan, S.A., Khazali, F., Dezfuli, S.H. and Borsalani, A. "Synthesis, Crystal Structure Analysis and Characterization of Mercury(II) Complex Containing 2-(aminomethyl)pyridine and Bromide." *Journal of the Chilean Chemical Society*, vol. 62, no. 1, 2017, pp. 3350-3353.
181. Sirola, K., Laatikainen, M. and Paatero, E. "Effect of Temperature on Sorption of Metals by Silica-Supported 2-(aminomethyl)pyridine. Part II: Sorption Dynamics." *Reactive and Functional Polymers*, vol. 70, no. 1, 2010, pp. 56-62.

182. Baratta, W., Herdtweck, E., Siega, K., Toniutti, M. and Rigo, P. "2-(Aminomethyl)pyridine– Phosphine Ruthenium(II) Complexes: Novel Highly Active Transfer Hydrogenation Catalysts." *Organometallics*, vol. 24, no.7, 2005, pp. 1660-1669.
183. Zhang, X., Lai, Y., Yi, X., Sun, M., Hu, H. and Liu, S. "Investigation on Enthalpies of Combustion and Heat Capacities for 2-aminomethylpyridine Derivatives." *Journal of Thermal Analysis and Calorimetry*, vol. 133, no. 3, 2018, pp. 1627-1633.
184. Shirvan, S.A., Khazali, F., Dezfuli, S.H. and Borsalani, A. "Distorted Square-Based Pyramidal and Trigonal Bipyramidal Geometries in a Mercury(II) Coordination Compound Containing 2-(aminomethyl)pyridine Ligand." *Molecular Crystals and Liquid Crystals*, vol. 656, no. 1, 2017, pp. 105-112.
185. (a) Shirvan, S.A., Khazali, F., Dezfuli, S.H. and Borsalani, A. "Synthesis, Characterization, and Crystal Structure Determination of Mercury(II) Complex Containing 2-(Aminomethyl)pyridine." *Chiang Mai Journal of Science*, vol. 45, no. 1, 2018, pp. 421-426. (b) Yenikaya, C., Sarı, M., Bülbül, M., Ilkimen, H., Çelik, H. and Büyükgüngör, O. "Synthesis, Characterization and Antiglaucoma Activity of a Novel Proton Transfer Compound and a Mixed-Ligand Zn(II) Complex." *Bioorganic & medicinal chemistry*, vol. 18, no. 2, 2010, pp.930-938. (c) Sunkari, S.S., Kharediya, B., Saha, S., Elrez, B. and Sutter, J.P. "Chain of Dimers to Assembly of Trimers: Temperature and Ligand Influenced Formation of Novel Supramolecular Assemblies of Cu(II) with Isomeric (Aminomethyl)pyridines and Azide." *New Journal of Chemistry*, vol. 38, no. 8, 2014, pp. 3529-3539.
186. Barquín, M., Garmendia, M.J.G., Larrínaga, L., Pinilla, E. and Torres, M.R. "Acetato, Formato and Chloride Copper(II) Complexes with 2-(aminomethyl)pyridine: Synthesis, Crystal Structure, Magnetic Properties and EPR Results." *Inorganica Chimica Acta*, vol. 362, no. 7, 2009, pp. 2334-2340.
187. Sales, J.A., Faria, F.P., Prado, A.G. and Airoidi, C. "Attachment of 2-aminomethylpyridine Molecule onto Grafted Silica Gel Surface and its Ability in Chelating Cations." *Polyhedron*, vol. 23, no. 5, 2004, pp. 719-725.
188. Silva Filho, E.C., Santos Júnior, L.S., Santos, M.R., Fonseca, M.G., Sousa, K.S., Santana, S.A. and Airoidi, C. "Thermochemistry of Interaction between Cellulose Modified with 2-aminomethylpyridine and Divalent Cations." *Journal of thermal analysis and calorimetry*, vol. 114, no. 1, 2013, pp. 423-429.
189. Rau, T., Shoukry, M. and van Eldik, R. "Complex Formation and Ligand Substitution Reactions of (2-picolylamine)palladium(II) with Various Biologically Relevant Ligands. Characterization of (2-picolylamine)(1, 1-cyclobutanedicarboxylato)palladium(II)." *Inorganic chemistry*, vol. 36, no. 7, 1997, pp. 1454-1463.
190. Choi, K.Y., Kim, B.R. and Ko, J. "Synthesis, Properties, and Crystal Structures of Copper(II) di-(2-picolyl)amine Complexes Containing Inorganic Salts." *Journal of Chemical Crystallography*, vol. 37, no. 12, 2007, pp. 847-852.

191. Rakesh, K., Sakar, M. and Do, T.O. "2-(Aminomethyl pyridine)SbI<sub>5</sub>: An Emerging Visible-Light Driven Organic–Inorganic Hybrid Perovskite for Photoelectrochemical and Photocatalytic Applications." *Materials Letters*, vol. 242, 2019, pp. 99-102.
192. Yang, J.P., Hu, H.P., Cheng, Z.Y., Qiu, X.J. and Wang, C.X. "Structural Insights into the Coordination and Selective Extraction of Copper(II) by Tertiary Amine Ligands Derived from 2-aminomethylpyridine." *Polyhedron*, vol. 128, 2017, pp. 76-84.
193. Qiu, X., Hu, H., Yang, J., Wang, C., Cheng, Z. and Ji, G. "Selective Removal of Copper from Simulated Nickel Electrolyte by Polystyrene-Supported 2-aminomethylpyridine Chelating Resin." *Chemical Papers*, vol. 72, no. 8, 2018, pp. 2071-2085.
194. Yu, H., Wei, Z., Hao, Y., Liang, Z., Fu, Z. and Cai, H. "Reversible Solid-State Thermochromism of a 2D Organic–Inorganic Hybrid Perovskite Structure Based on Iodoplumbate and 2-aminomethyl-pyridine." *New Journal of Chemistry*, vol. 41, no. 18, 2017, pp. 9586-9589.
195. Ibrahim, M.M., Ramadan, A.M.M., Mersal, G.A. and El-Shazly, S.A. "Synthesis, Superoxide Dismutase, Nuclease, and Anticancer Activities of Copper(II) Complexes Incorporating bis(2-picoyl)amine with Different Counter Anions." *Journal of Molecular Structure*, vol. 998, no. 1-3, 2011, pp. 1-10.
196. Etaiw, S.E.D.H. and El-bendary, M.M. "Crystal Structure, Characterization and Catalytic Activities of Cu(II) Coordination Complexes with 8-hydroxyquinoline and Pyrazine-2-carboxylic acid." *Applied Organometallic Chemistry*, vol. 32, no. 4, 2018, pp. 1-14.
197. El-Medani, S.M., Ali, O.A., Mohamed, H.A. and Ramadan, R.M. "Spectroscopic, Thermal and X-ray Crystal Structure Studies of Some bis-(pyrazine-2-carboxylato)nickel(II) Complexes." *Journal of Coordination Chemistry*, vol. 58, no. 16, 2005, pp. 1429-1437.
198. Ellsworth, J.M. and Zur Loye, H.C. "Metal and Mixed-Metal Coordination Polymers Synthesized with Pyrazine-2-carboxylate." *Dalton transactions*, no. 43, 2008, pp. 5823-5835.
199. Pally, N.K. "Synthesis and Structures of New Three-Dimensional Copper Metal-Organic Frameworks." *MS & SP, Faculty of science, Department of Chemistry, Western Kentucky University, Kentucky*, 2013, pp. 1 -64.
200. Han, L., Ma, Y.R., Chen, L.C., Huo, S.M., Qiu, T.R., Zeng, R.H., Meng, Q.H. and Luo, Y.F. "Synthesis, Structure and Thermal Behavior of a New Coordination Polymer Based on Mixed Pyrazine-2-carboxylate and Oxalate Ligands." *Journal of Chemical Crystallography*, vol. 4, no. 4, 2011, pp. 596-600.
201. (a) Ciurtin, D.M., Smith, M.D. and zur Loye, H.C. "New One- and Two-Dimensional Cadmium Iodide/pyrazinecarboxylate-based Coordination Polymers." *Polyhedron*, vol. 22, no. 22, 2003, pp. 3043-3049. (b) Liang, Y.C., Hong, M.C., Liu, J.C. and Cao, R. "Hydrothermal Syntheses, Structural Characterizations and Magnetic Properties of Cobalt(II) and Manganese(II) Coordination Polymeric Complexes Containing Pyrazinecarboxylate Ligand."

- Inorganica chimica acta*, vol. 328, no. 1, 2002, pp.152-158. (c). Zheng, L.M., Wang, X. and Jacobson, A.J. “Two-and Three-Dimensional Mixed-Valence Cu(I)–Cu(II) Coordination Polymers: Syntheses and Characterization of  $\alpha$ -,  $\beta$ -[Cu<sub>2</sub>X (C<sub>5</sub>H<sub>3</sub>N<sub>2</sub>O<sub>2</sub>)<sub>2</sub>(H<sub>2</sub>O)](X= Cl, Br).” *Journal of Solid State Chemistry*, vol. 152, no. 1, 2000, pp.174-182. (d) Ciurtin, D.M., Smith, M.D. and zur Loye, H.C. “[Cu (pyrazine-2-carboxylate)<sub>2</sub>]<sub>2</sub>Cd<sub>4</sub>I<sub>8</sub>: Unprecedented 1-D Serpentine Inorganic Chains and Regular 2-D Metal–Organic Square Grids in a 3-D Framework.” *Chemical Communications*, no. 1, 2002, pp.74-75.
202. Leciejewicz, J., Ptasiewicz-Bąk, H., Premkumar, T. and Govindarajan, S. “Crystal Structure of a Lanthanum(III) Complex with Pyrazine-2-carboxylate and Water Ligands.” *Journal of Coordination Chemistry*, vol. 57, no. 2, 2004, pp. 97-103.
203. Yang, Q., Zhao, J.P. and Liu, Z.Y. “Single Crystal to Single Crystal Transition in (10,3)-d Framework with Pyrazine-2-carboxylate Ligand: Synthesis, Structures and Magnetism.” *Journal of Solid State Chemistry*, vol. 196, 2012, pp. 52-57.
204. Gao, S., Zhang, S., Chen, S. and Yang, D. “Low-Temperature Heat Capacity and the Standard Molar Enthalpy of Formation of Compound Chromium(III) tri(pyrazine-2-carboxylate).” *Thermochimica acta*, vol. 543, 2012, pp. 118-124.
205. Tanase, S., van Son, M., van Albada, G.A., de Gelder, R., Bouwman, E. and Reedijk, J. “Self-Assembly of Extended Structures Through Non-Coordination Intermolecular Forces: Synthesis, Crystal Structures, and Properties of Metal Complexes with 5-methyl-2-pyrazinecarboxylate.” *Polyhedron*, vol. 25, no. 15, 2006, pp. 2967-2975.
206. Ding, B., Yang, E.C., Guo, J.H., Zhao, X.J. and Wang, X.G. “A Novel Lead(II) Framework Containing Pb–O–Pb and Pb–Cl–Pb helical chains.” *Inorganic Chemistry Communications*, vol. 11, no. 5, 2008, pp. 509-512.
207. Tanase, S., Gallego, P.M., Bouwman, E., Long, G.J., Rebbouh, L., Grandjean, F., de Gelder, R., Mutikainen, I., Turpeinen, U. and Reedijk, J. “Versatility in the Binding of 2-pyrazinecarboxylate with Iron. Synthesis, Structure and Magnetic Properties of Iron(II) and Iron(III) Complexes.” *Dalton Transactions*, no. 13, 2006, pp. 1675-1684.
208. Govindaswamy, P., Therrien, B., Süß-Fink, G., Štěpnička, P. and Ludvík, J. “Mono and Dinuclear Iridium, Rhodium and Ruthenium Complexes Containing Chelating Carboxylato Pyrazine Ligands: Synthesis, Molecular Structure and Electrochemistry.” *Journal of organometallic chemistry*, vol. 692, no. 8, 2007, pp. 1661-1671.
209. Zheng, B., Liu, G., Gou, L., Wang, D.Y. and Hu, H.M. “A one-Dimensional Coordination Polymer of Copper(II) with 2-pyrazinecarboxylate.” *Acta Crystallographica Section E: Structure Reports Online*, vol. 61, no. 3, 2005, pp. m499-m501.
210. Cuevas, A., Kremer, C., Hummert, M., Schumann, H., Lloret, F., Julve, M. and Faus, J. “Magnetic Properties and Molecular Structures of Binuclear (2-pyrazinecarboxylate)-bridged Complexes Containing Re(IV) and M (II)(M= Co, Ni).” *Dalton Transactions*, no. 3, 2007, pp. 342-350.

211. Huang, D., Zhang, X., Chen, C., Chen, F., Liu, Q., Liao, D., Li, L. and Sun, L. "Synthesis, Structural Characterization and Magnetic Properties of 2-pyrazinecarboxylate manganese Compounds  $[\text{Mn}(\text{pyz})_2(\text{H}_2\text{O})_4]$  and  $[\text{MnCl}(\text{pyz})(\text{H}_2\text{O})]_n$  (pyz= 2-pyrazinecarboxylate)." *Inorganica chimica acta*, vol. 353, 2003, pp. 284-291.
212. Świdorski, G., Lewandowska, H., Świsłocka, R., Wojtulewski, S., Siergiejczyk, L. and Wilczewska, A. "Thermal, Spectroscopic (IR, Raman, NMR) and Theoretical (DFT) Studies of Alkali Metal Complexes with Pyrazinecarboxylate and 2,3-pyrazinedicarboxylate Ligands." *Journal of Thermal Analysis and Calorimetry*, vol. 126, no. 1, 2016, pp. 205-224.
213. Chen, C.L., Goforth, A.M., Smith, M.D., Su, C.Y. and zur Loye, H.C. " $[\text{Co}_2(\text{ppca})_2(\text{H}_2\text{O})(\text{V}_4\text{O}_{12})_{0.5}]$ : A Framework Material Exhibiting Reversible Shrinkage and Expansion through a Single-Crystal-to-Single-Crystal Transformation Involving a Change in the Cobalt Coordination Environment." *Angewandte Chemie*, vol. 117, no. 41, 2005, pp. 6831-6835.
214. (a) Gryca, I., Machura, B., Małeck, J.G., Shul'pina, L.S., Pombeiro, A.J. and Shul'pin, G.B. "New P-tolylimido Rhenium(V) Complexes with Carboxylate-Based Ligands: Synthesis, Structures and Their Catalytic Potential in Oxidations with Peroxides." *Dalton Transactions*, vol. 43, no. 15, 2014, pp. 5759-5776. (b) Kirillov, A.M. and Shul'pin, G.B. "Pyrazinecarboxylic Acid and Analogs: Highly Efficient Co-Catalysts in the Metal-Complex-Catalyzed Oxidation of Organic Compounds." *Coordination Chemistry Reviews*, vol. 257, no. 3-4, pp. 732-754.
215. Zhao, M.G., Shi, J.M., Yu, W.T., Wu, C.J. and Zhang, X. "Synthesis and Crystal Structure of a 3-d Polymeric Cobalt(II) and Sodium Complex with Pyrazine-2-carboxylate as a Bridging Ligand." *J. Coord. Chem*, vol. 56, no. 15, 2003, pp. 1351-1356.
216. Hazra, S. and Karmakar, A. "Synthesis, Molecular and Supramolecular Structure of a New Dinuclear Aluminium(III) Complex Derived from 3-aminopyrazine-2-carboxylic Acid." *Zeitschrift für Kristallographie-Crystalline Materials*, vol. 230, no. 7, 2015, pp. 459-465.
217. Ptasiewicz-Bak, H. and Leciejewicz, J. "The Crystal Structure of Monoaquabis (Trans-5-methylpyrazine-2-carboxylato-N,O)copper(II)trihydrate." *Polish Journal of Chemistry*, vol. 74, no. 6, 2000, pp. 877-884.
218. (a) Adediji, J.F., Olayinka, E.T., Adebayo, M.A. and Babatunde, O. "Antimalarial Mixed Ligand Metal Complexes: Synthesis, Physicochemical and Biological Activities." *International Journal of Physical Sciences*, vol. 4, no. 9, 2009, pp. 529-534. (b) Wankhede, D.S., Mandawat, N.D. and Qureshi, A.H. "Mixed Ligand Complexes Derived from 4-(Benzene Azo)salicylaldehyde and 2-amino-4-nitrophenol Using Transition Metal Ions." *Journal of Current Chemical Pharmaceutical Sciences*, vol. 4, no. 3, 2014, pp. 135-141. (c) Thebo, K.H., Shad, H.A., Raftery, J., Malik, M.A., Mahmud, T. and O'Brien, P. "Synthesis, Characterization and X-ray Diffraction of  $[\text{Cu}(\text{malonate})(\text{phen})_2]_2 \cdot 17\text{H}_2\text{O}$  complex." *Journal of Molecular Structure*, vol. 1001, no. 1-3, 2011, pp. 12-15. (d) Ei-Sherif, A.A. and Jeragh, B.J. "Mixed Ligand Complexes of Cu(II)-2-(2-pyridyl)-benzimidazole and Aliphatic or

- Aromatic Dicarboxylic Acids: Synthesis, Characterization and Biological Activity.” *Spectrochimica Acta Part A: Molecular and Biomolecular Spectroscopy*, vol. 68, no. 3, 2007, pp. 877-882.
219. Al-Hamdani, A.A.S., Al-dulyme, N.K.G., Ahmed, S.D. and Basheer, H.M. “Preparation, Spectroscopic, Bioactive and Theoretical Studies of Mixed Ligand Complexes.” *Al-Nahrain Journal of Science*, vol. 20, no. 3, 2017, pp. 49-59.
220. Alimarin, I.P. and Shlenskaya, V.I. “The Analytical Chemistry of Mixed Ligand Complexes.” *Pure and Applied Chemistry*, vol. 21, no. 4, 1970, pp. 461-478.
221. Mohapatra, R.K., Saikishore, V.P., Azam, M. and Biswal, S.K. “Synthesis and Physicochemical Studies of a Series of Mixed-Ligand Transition Metal Complexes and Their Molecular Docking Investigations against Coronavirus Main Protease.” *Open Chemistry*, vol. 18, no. 1, 2020, pp. 1495-1506.
222. Mrinalini, L. and Singh, A.M. “Mixed Ligand Cobalt(III) Complexes with 1-amidino-o-methylurea and Amino Acids.” *Research Journal of Chemical Sciences*, vol. 2, no. 1, 2012, pp. 45-49.
223. Sanap, S.V. and Patil, R.M. “Synthesis, Characterisation and Biological Activity of Chiral Mixed Ligand Ni(II) Complexes.” *Research Journal of Pharmaceutical Sciences*, vol. 2, no. 1, 2013, pp. 1-10.
224. Patil, S.S., Thakur, G.A. and Patil, V.R. “Synthesis, Spectral and Biological Studies on Some Mixed Ligand Ni(II) Complexes.” *Acta Pol Pharm*, vol. 66, no. 3, 2009, pp. 271-277.
225. Bodkhe, A.S., Patil, S.S. and Shaikh, M.M. “Synthesis, Characterization and Antibacterial Studies on Mixed Ligand Copper Complexes with Polydentate Ligands.” *Acta Poloniae Pharmaceutica*, vol. 69, no. 5, 2012, pp. 871-877.
226. Hemalatha, S., Dharmaraja, J., Shobana, S., Subbaraj, P., Esakkidurai, T. and Raman, N. “Chemical and Pharmacological Aspects of Novel Hetero MLB Complexes Derived from NO<sub>2</sub> Type Schiff Base and N<sub>2</sub> Type 1,10-phenanthroline Ligands.” *Journal of Saudi Chemical Society*, vol. 24, no. 1, 2020, pp. 61-80.
227. Pal, T.K., Alam, M.A., Paul, S. and Sheikh, M.C. “Spectral, Magnetic, Thermal, Antioxidant and Biological Studies on New Mixed Ligand Complexes.” *Journal of King Saud University-Science*, vol. 31, no. 4, 2019, pp. 445-451.
228. Kathiresan, S., Mugesh, S., Annaraj, J. and Murugan, M. “Mixed-Ligand Copper(II) Schiff Base Complexes: the Vital Role of Co-Ligands in DNA/Protein Interactions and Cytotoxicity.” *New Journal of Chemistry*, vol. 41, no. 3, 2017, pp. 1267-1283.
229. Alagesan, M., Bhuvanesh, N.S. and Dharmaraj, N. “Potentially Cytotoxic New Copper(II) Hydrazone Complexes: Synthesis, Crystal Structure and Biological Properties.” *Dalton Transactions*, vol. 42, no. 19, 2013, pp. 7210-7223.
230. Patel, N.H., Parekh, H.M. and Patel, M.N. “Synthesis, Physicochemical Characteristics, and Biocidal Activity of Some Transition Metal Mixed-Ligand Complexes with Bidentate (NO and NN) Schiff Bases.” *Pharmaceutical Chemistry Journal*, vol. 41, no. 2, 2007, pp. 78-81.

- 231.(a) Mihsen, H.H. and Shareef, N.K. "Synthesis, Characterization of Mixed-Ligand Complexes Containing 2,2-Bipyridine and 3-aminopropyltriethoxysilane." *In Journal of Physics: Conference Series*, vol. 1032, no. 1, 2018, PP. 1-18. (b) Chandraleka, S., Ramya, K., Chandramohan, G., Dhanasekaran, D., Priyadharshini, A. and Panneerselvam, A. "Antimicrobial Mechanism of Copper(II) 1,10-phenanthroline and 2,2'-bipyridyl Complex on Bacterial and Fungal Pathogens." *Journal of Saudi Chemical Society*, vol. 18, no. 6, 2014, pp. 953-962.
- 232.El-Sherif, A.A., Shehata, M.R., Shoukry, M.M. and Barakat, M.H. "Thermodynamic Investigation and Mixed Ligand Complex Formation of 1,4-Bis-(3-aminopropyl)-piperazine and Biorelevant Ligands." *Bioinorganic chemistry and applications*, vol. 2012, 2012, pp. 1-10.
- 233.Sakr, S.H., Elshafie, H.S., Camele, I. and Sadeek, S.A. "Synthesis, Spectroscopic, and Biological Studies of Mixed Ligand Complexes of Gemifloxacin and Glycine with Zn(II), Sn(II), and Ce(III)." *Molecules*, vol. 23, no. 5, 2018, pp. 1-17.
- 234.(a) Omar, M.M., Abd El-Halim, H.F. and Khalil, E.A. "Synthesis, Characterization, and Biological and Anticancer Studies of Mixed Ligand Complexes with Schiff Base and 2,2'-bipyridine." *Applied Organometallic Chemistry*, vol. 31, no. 10, 2017, pp. 1-11. (b) Mahmoud, W.H., Mahmoud, N.F., Mohamed, G.G., El-Sonbati, A.Z. and El-Bindary, A.A. "Synthesis, Spectroscopic, Thermogravimetric and Antimicrobial Studies of Mixed Ligands Complexes." *Journal of Molecular Structure*, vol. 1095, 2015, pp. 15-25. (c) Patel, R.N., Singh, N., Shukla, K.K., Chauhan, U.K., Niclos-Gutierrez, J. and Castineiras, A. "Magnetic, Spectroscopic, Structural and Biological Properties of Mixed-Ligand Complexes of Copper(II) with N, N, N', N'', N''-pentamethyldiethylenetriamine and Polypyridine Ligands." *Inorganica Chimica Acta*, vol. 357, no. 9, 2004, pp. 2469-2476.
- 235.Obaid, S.M., Jarad, A.J. and Al-Hamdani, A.A.S. "Synthesis, Characterization and Biological Activity of Mixed Ligand Metal Salts Complexes with Various Ligands." *In Journal of Physics: Conference Series*, vol. 1660, no. 1, 2020, pp. 1-13.
- 236.Salga, M.S. and Sabo, S. "Antimicrobial Activities of Some Mixed Ligands Adducts of Benzoylacetone and Salicylaldehyde." *Bayero Journal of Pure and Applied Sciences*, vol. 11, no. 1, 2018, pp. 174-178.
- 237.Lafferty, J.J. and Case, F.H. "The Preparation and Properties of Certain Pyridylpyrimidines and Biazines as Potential Chelating Agents for Iron(II)." *The Journal of Organic Chemistry*, vol. 32, no. 5, 1967, pp.1591-1596.
- 238.Crutchley, R.J. and Lever, A.B.P. "Comparative Chemistry of Bipyrazyl and Bipyridyl Metal Complexes: Spectroscopy, Electrochemistry and Photoanation." *Inorganic Chemistry*, vol. 21, no. 6, 1982, pp. 2276-2282.
- 239.Dhital, R.N., Kamonsatikul, C., Somsook, E. and Sakurai, H. "Bimetallic Gold-Palladium Alloy Nanoclusters: An Effective Catalyst for Ullmann Coupling of Chloropyridines under Ambient Conditions." *Catalysis Science & Technology*, vol. 3, no. 11, 2013, pp. 3030-3035.

240. Qing, W., Xuwu, Y., Shengli, G. and Qizhen, S. "Preparation and the Standard Enthalpy of Formation of 2-Amino-4, 6-dimethoxypyrimidine and the Related Complexes of Copper." *Chemical Papers-Slovak Academy of Sciences*, vol. 57, no. 2, 2003, pp. 97-101.
241. Carranza, J., Grove, H., Sletten, J., Lloret, F., Julve, M., Kruger, P.E., Eller, C. and Rillema, D.P. "Synthesis, X-ray Crystal Structure and Magnetic Properties of Oxalato-Bridged Copper(ii) Complexes with 2,3-Bis(2-pyridyl) pyrazine, 2,3-Bis(2-pyridyl) quinoxaline and 2,2'-Bipyrazine as Peripheral Ligands." *European Journal of Inorganic Chemistry*, vol. 2004, no. 24, 2004, pp. 4836-4848.
242. Wang, H., Zheng, X.F., Shen, X.Q., Zhang, H.Y., Yang, R., Hou, H.W. and Zhu, Y. "Syntheses, Crystal Structures and Thermal Decomposition Kinetics of Ni(II) and Cu(II) Complexes with dpa and dca: [Ni(dpa)<sub>2</sub>(dca)<sub>2</sub>] and [Cu(dpa)<sub>2</sub>(dca)<sub>2</sub>] (dpa= 2,2'-Dipyridylamine, dca= Sodium Dicyanamide) Ligands." *Synthesis and Reactivity in Inorganic and Metal-Organic Chemistry*, vol.36, no. 8, 2006, pp. 609-616.
243. Subramanian, P.S., Suresh, E. and Casella, L. "Supramolecular Helical Architectures Dictated by Folded and Extended Conformations of the Amino Acid in Ternary CuII/Diamine/Racemic Amino Acid Complexes." *Eur. J. Inorg. Chem*, vol. 2007, no. 12, 2007, pp.1654-1660.
244. Singh, V. P. "Synthesis, electronic and ESR Spectral Studies on Copper(II) Nitrate Complexes with some Acylhydrazines and Hydrazones." *Spectrochimica Acta Part A: Molecular and Biomolecular Spectroscopy*, vol. 71, no. 1, 2008, pp.17-22.
245. Yuste, C., Armentano, D., Marino, N., Cañadillas-Delgado, L., Delgado, F.S., Ruiz-Pérez, C., Rillema, D.P., Lloret, F. and Julve, M. "Synthesis, Crystal Structures and Magnetic Properties of Tricyanomethanide-Containing Copper(II) Complexes." *Dalton Transactions*, no. 12, 2008, pp. 1583-1596.
246. Lazarou, K.N., Psycharis, V., Perlepes, S.P. and Raptopoulou, C.P. "Complexes Derived from the Copper(II) Perchlorate/maleamic Acid/2,2'-bipyridine and Copper(II) Perchlorate/Maleic Acid/2, 2'-bipyridine Reaction Systems: Synthetic, Reactivity, Structural and Spectroscopic Studies." *Polyhedron*, vol. 28, no. 6, 2009, pp. 1085-1096.
247. Agwara, M.O., Ndifon, P.T., Ndosiri, N.B., Paboudam, A.G., Yufanyi, D.M. and Mohamadou, A. "Synthesis, Characterisation and Antimicrobial Activities of Cobalt(ii), Copper(ii) and Zinc(ii) Mixed-Ligand Complexes Containing 1,10-phenanthroline and 2,2'-bipyridine." *Bulletin of the Chemical Society of Ethiopia*, vol. 24, no. 3, 2010, pp. 383-389.
248. Yutkin, M.P., Zavakhina, M.S., Samsonenko, D.G. and Fedin, V.P. "Crystal Structure of Metal-Organic Coordination Polymers [Cu(bpy)<sub>2</sub>(H<sub>2</sub>O)<sub>2</sub>](NO<sub>3</sub>)<sub>2</sub>·4.5 C<sub>2</sub>H<sub>5</sub>OH and [Cu<sub>2</sub>(bpy)(H<sub>2</sub>O)(L-pha)<sub>2</sub>](NO<sub>3</sub>)<sub>2</sub>·H<sub>2</sub>O." *Journal of Structural Chemistry*, vol. 52, no. 2, 2011, pp. 365-370.
249. Draksharapu, A., Boersma, A.J., Leising, M., Meetsma, A., Browne, W.R. and Roelfes, G. "Binding of Copper(ii) Polypyridyl Complexes to DNA and

- Consequences for DNA-Based Asymmetric Catalysis.” *Dalton Transactions*, vol. 44, no.8, 2015, pp. 3647-3655.
250. Kwon, J.H., Park, H.J., Chitrapriya, N., Cho, T.S., Kim, S., Kim, J., Hwang, I.H., Kim, C. and Kim, S.K. “DNA Cleavage Induced by  $[\text{Cu}(\text{L})_x(\text{NO}_3)_2]$  (L= 2,2'-dipyridylamine, 2,2'-bipyridine, Dipicolylamine, x= 1 or 2): Effect of the Ligand Structure.” *Journal of Inorganic Biochemistry*, vol. 131, 2014, pp. 79-86.
251. Brissos, R.F., Torrents, E., Mariana dos Santos Mello, F., Carvalho Pires, W., de Paula Silveira-Lacerda, E., Caballero, A.B., Caubet, A., Massera, C., Roubeau, O., Teat, S.J. and Gamez, P. “Highly Cytotoxic DNA-Interacting Copper(II) Coordination Compounds.” *Metallomics*, vol. 6, no. 10, 2014, pp. 1853-1868.
252. Puchonova, M., Mazur, M. and Valigura, D. “Methyl- and Methoxysalicylatocopper(II) Complexes with 2-aminomethylpyridine.” *Acta Chimica Slovaca*, vol. 7, no. 2, 2014, pp. 94-98.
253. Ibrahim, M.M., Ramadan, A.E.M.M., Shaban, S.Y., Mersal, G.A., El-Shazly, S.A. and Al-Juaid, S. “Syntheses, Characterization and Antioxidant Activity Studies of Mixed-Ligand Copper(II) Complexes of 2,2'-bipyridine and Glycine: The X-ray Crystal Structure of  $[\text{Cu}(\text{BPy})(\text{Gly})]\text{ClO}_4$ .” *Journal of Molecular Structure*, vol. 1134, 2017, pp. 319-329.
254. Knapp, C.E., Metcalf, E.A., Mrig, S., Sanchez-Perez, C., Douglas, S.P., Choquet, P. and Boscher, N.D. “Precursors for Atmospheric Plasma-Enhanced Sintering: Low-Temperature Inkjet Printing of Conductive Copper.” *ChemistryOpen*, vol. 7, no. 11, 2018, pp. 850-857.
255. Mangoli, M., Tabatabaee, M., Jamehbozorgi, S., Ramazani, M. and Kučeráková, M. “Hydrothermal Synthesis of a Dinuclear Copper(II) Complex with 2-aminopyrimidine and Bridging Oxalate Ligands: In Situ Degradation of Tartaric Acid to Oxalate and Thermal Decomposition to CuO Nanoparticles.” *Inorganic and Nano-Metal Chemistry*, vol. 50, no.12, 2020, pp. 1353-1357.
256. Nisbet, M.L., Hiralal, E. and Poepelmeier, K.R. “Crystal Structures of Three Copper(II)-2,2'-bipyridine (bpy) Compounds,  $[\text{Cu}(\text{bpy})_2(\text{H}_2\text{O})][\text{SiF}_6] \cdot 4\text{H}_2\text{O}$ ,  $[\text{Cu}(\text{bpy})_2(\text{TaF}_6)_2]$  and  $[\text{Cu}(\text{bpy})_3][\text{TaF}_6]_2$  and a Related Coordination Polymer,  $[\text{Cu}(\text{bpy})(\text{H}_2\text{O})_2\text{SnF}_6]_n$ .” *Acta Crystallographica Section E: Crystallographic Communications*, vol. 77, no. 2, 2021, pp. 158-164.
257. Gao, S., Fronczek, F.R. and Maverick, A.W. “A Copper Complex of an Unusual Hydroxy-Carboxylate Ligand:  $[\text{Cu}(\text{bpy})(\text{C}_4\text{H}_4\text{O}_6)]$ .” *Acta Crystallographica Section E: Crystallographic Communications*, vol. 77, no. 3, 2021, pp. 282-285.
258. Tanase, S., Ferbinteanu, M., Andruh, M., Mathonière, C., Strenger, I. and Rombaut, G. “Synthesis and Characterization of a New Molecular Magnet,  $[\text{Ni}(\text{ampy})_2]_3[\text{Fe}(\text{CN})_6]_2 \cdot 6\text{H}_2\text{O}$ , and Synthesis, Crystal Structure and Magnetic Properties of its Mononuclear Precursor, Trans- $[\text{Ni}(\text{ampy})_2(\text{NO}_3)_2]$  (ampy= 2-aminomethylpyridine).” *Polyhedron*, vol. 19, no. 16-17, 2000, pp. 1967-1973.

259. Lin, Y.C., Lu, T.H., Liao, F.L. and Chung, C.S. "Crystal Structure of (2,2'-Bipyridine-N, N')(2,2',2''-Triaminotriethylamine-N, N', N'', N''')nickel(II) Diperchlorate." *Analytical sciences*, vol. 19, no. 4, 2003, pp. 641-642.
260. Zhou, Y., Li, X., Xu, Y., Cao, R. and Hong, M. "Tris (2,2'-bipyridine)nickel(II) Diperchlorate." *Acta Crystallographica Section E: Structure Reports Online*, vol. 59, no. 5, 2003, pp. m300-m302.
261. Rahaman, S.H., Bose, D., Chowdhury, H., Mostafa, G., Fun, H.K. and Ghosh, B.K. "Two-dimensional Hydrogen Bonded Sheet Structures in Nickel(II)-and Zinc(II)-2,2'-dipyridylamine-azido Complexes." *Polyhedron*, vol. 24, no. 14, 2005, pp. 1837-1844.
262. Pedireddi, V. R., Manishkumar R. Shimpi, and J. V. Yakhmi. "Room-Temperature Ionic Liquids: For a Difference in the Supramolecular Synthesis." *Macromolecular Symposia*, vol. 241, no. 1, 2006, pp. 83-87.
263. Bruda, S., Turnbull, M.M., Landee, C.P. and Xu, Q. "Synthesis, Structures and Magnetic Properties of 2-aminomethylpyridine-Ni(II) Complexes." *Inorganica chimica acta*, vol. 359, no. 1, 2006, pp. 298-308.
264. Wang, C.J., Ren, P.D., Wu, W.P. and Zhang, Z.B. "(2,2'-Bipyridine)(2-formyl-6-methoxyphenolato)nickel(II) Perchlorate." *Acta Crystallographica Section E: Structure Reports Online*, vol. 65, no. 1, 2009, pp. m11-m11.
265. Zianna, A., Psomas, G., Hatzidimitriou, A. and Lalia-Kantouri, M. "Ni(II) Complexes with 2,2-dipyridylamine and Salicylaldehydes: Synthesis, Crystal Structure and Interaction with Calf-Thymus DNA and Albumins." *Journal of Inorganic Biochemistry*, vol. 163, 2016, pp. 131-142.
266. Carballo, R., Covelo, B. and Gómez-Paz, O. "Solid State Coordination Chemistry and Supramolecular Assemblies of M(II)/Benzilato/2,2'-Dipyridylamine Systems." *Struct Chem Crystallogr Commun*, vol. 3, no. 2:6, 2017, pp. 1-7.
267. Křešáková, L., Miňo, A., Holub, M., Kuchár, J., Werner, A., Tomás, M., Čížmár, E., Falvello, L.R. and Černák, J. "Heteroleptic Complexes of Ni(II) with 2,2'-bipyridine and Benzoato Ligands. Magnetic Properties of [Ni(bpy)(Bz)<sub>2</sub>]." *Inorganica Chimica Acta*, vol. 527, 2021, pp. 1-13.
268. Tandon, S.S., Chander, S. and Thompson, L.K. "Ligating Properties of Tridentate Schiff Base Ligands, 2-[[2-(2-pyridinylmethyl)imino]methyl]phenol (HSALIMP) and 2-[[2-(2-pyridinyl)ethyl]imino]methyl]phenol (HSALIEP) with Zinc(II), Cadmium(II), Nickel(II) and Manganese(III) Ions. X-ray Crystal Structures of the [Zn(SALIEP)(NO<sub>3</sub>)<sub>2</sub>] Dimer, [Mn(SALIEP)<sub>2</sub>](ClO<sub>4</sub>), and [Zn (AMP)<sub>2</sub>(NO<sub>3</sub>)<sub>2</sub>]." *Inorganica Chimica Acta*, vol. 300-302, 2000, pp. 683-692.
269. Sunahara, T., Onaka, S., Ito, M., Imai, H., Inoue, K. and Ozeki, T. "Construction of Nano-Channels Based on Zinc(ii) Pyrazine-2-carboxylate Complexes." *European Journal of Inorganic Chemistry*, vol. 2004, no. 24, 2004, pp. 4882-4890.
270. Kopel, P., Trávníček, Z., Zbořil, R. and Marek, J. "Synthesis, X-ray and Mössbauer Study of Iron(II) Complexes with Trithiocyanuric Acid (ttcH<sub>3</sub>): The X-ray Structures of [Fe(bpy)<sub>3</sub>](ttcH)·2bpy·7H<sub>2</sub>O and

- [Fe(phen)<sub>3</sub>](ttcH<sub>2</sub>)(ClO<sub>4</sub>)·2CH<sub>3</sub>OH·2H<sub>2</sub>O.” *Polyhedron*, vol. 23, no.14, 2004, pp. 2193-2202.
271. Hamamci, S., Yilmaz, V.T. and Harrison, W.T. “[Silver \(I\)-Saccharinato Complexes with 2-\(Aminomethyl\)pyridine and 2-\(2-Aminoethyl\)pyridine Ligands:\[Ag \(sac\)\(ampy\)\] and \[Ag<sub>2</sub>\(sac\)<sub>2</sub>\(μ-aepy\)<sub>2</sub>\]](#).” *Zeitschrift für Naturforschung B*, vol. 60, no. 9, 2005, pp. 978-983.
272. Yao, J.C., Ma, L.F. and Yao, F.J. “Crystal Structure of tris(2,2'-bipyridine)cobalt(II)diperchlorate,[CO(C<sub>10</sub>H<sub>8</sub>N<sub>2</sub>)<sub>3</sub>][ClO<sub>4</sub>]<sub>2</sub>.” *Zeitschrift für Kristallographie-New Crystal Structures*, vol. 220, no. 1-4, 2005, pp. 503-504.
273. Malassa, A., Görls, H., Buchholz, A., Plass, W. and Westerhausen, M. “Pyridylmethylenamines as Ligands in Iron Halide Complexes–Coordination Behaviour Depending on the Halide, the Denticity of the Amino Ligand and the Oxidation State of Iron.” *Zeitschrift für anorganische und allgemeine Chemie*, vol. 632, no. 14, 2006, pp. 2355-2362.
274. Talaei, Z., Morsali, A. and Mahjoub\*, A.R. “New Mixed-Anion Zinc(II) Complexes,[Zn(phen)<sub>2</sub>(CCl<sub>3</sub>COO)(H<sub>2</sub>O)](NO<sub>3</sub>) and [Zn(bpy)<sub>2</sub>(CH<sub>3</sub>COO)](ClO<sub>4</sub>)·H<sub>2</sub>O; Synthesis, Characterization and Crystal Structures.” *Journal of Coordination Chemistry*, vol. 59, no. 6, 2006, pp. 643-650.
275. Shen, W.Z. “Cyclic, Cationic Complexes of Pt" and Pd" with Heterocyclic Ligands, Including Nucleobases: Synthesis, Structure, Host-Guest Chemistry with Anions and Non-Covalent Interactions with DNA.” *PhD dissertation, Faculty of Science, Department of Chemistry, Dortmund University, Germany*, 2007, pp. 1-183.
276. Drew, M.G., Nag, S. and Datta, D. “Acid Dissociation of 2,2'-dipyridylamine in Non-Aqueous Medium when Chelated to Some Ru(II)N<sub>4</sub> Cores.” *Inorganica Chimica Acta*, vol. 361, no. 1, 2008, pp. 417-421.
277. Kpogo, K.K. “Evaluation of Earth-Abundant Monometallic and Bimetallic Complexes for Catalytic Water Splitting.” *PhD dissertation, Faculty of Science, Department of Chemistry, Wayne State University, Michigan*, 2017, pp. 1-190.
278. Priya I, A.S., Adaikalasamy<sup>2\*</sup>, K. J. and Sunaja Devi. K. R. “Redox Reactions of Iron(III)-polypyridyl Complexes with Thiodicarboxylic Acids: A Kinetic study.” *IJARSE*, vol. 6, no. 12, 2017, pp. 1269-1280.
279. Annan, N.A., Butler, I.S., Osman, Y.A., Hussein, M.H., Jean-Claude, B.J., Saad, E.M. and Mostafa, S.I. “Complexes Based N,N-donors (2,2'-bipyridyl & 2-(2-aminophenyl) benzimidazole); Synthesis, Characterization, DNA Interaction and Toxicity Assessment Against *Chlorella Vulgaris* Microchlorophyte; X-ray Crystal Structure of [Zn(bpy)<sub>3</sub>][Cl<sub>2</sub>].” *Inorganica Chimica Acta*, vol. 512, 2020, pp. 1-14.
280. (a) Abusharkh. K. “Synthesis and Characterization of Mono- Dinuclear Coordination Compound of Nickel, Copper with 2,2'-Bipyrazine Ligand and 2,2'Dipyridylamine.” *MS thesis, Faculty of Science, Department of Chemistry, Al-Quds University, Abu Dies*, 2017, pp. 1-114. (b) Van Albada, G.A., Mutikainen, I., Turpeinen, U. and Reedijk, J. “Structure, Spectroscopy and Magnetism of a Strong Ferromagnetically Coupled Dinuclear Hydroxo-

Bridged Cu(II) Compound with 4, 4'-dimethyl-2, 2'-bipyridine as a ligand. The First X-ray Structure of a Dinuclear Cu(II) Compound with Dmbipy." *Inorganica Chimica Acta*, vol. 324, no. 1-2, 2001, pp.273-277. (c) Belousoff, M.J., Duriska, M.B., Graham, B., Batten, S.R., Moubaraki, B., Murray, K.S. and Spiccia, L. "Synthesis, X-Ray Crystal Structures, Magnetism, and Phosphate Ester Cleavage Properties of Copper(II) Complexes of N-substituted Derivatives of 1,4,7-triazacyclononane." *Inorganic chemistry*, vol.45, no 9, 2006, pp.3746-3755. (d) Youngme, S., van Albada, G.A., Kooijman, H., Roubeau, O., Somjitsripunya, W., Spek, A.L., Pakawatchai, C. and Reedijk, J. "A Unique Dinuclear CuII Compound with Two Phase Transitions Clearly Visible from Thermal and Magnetic Behaviour; Synthesis, Magnetism and X-ray Structures at Three Temperatures of Bis(di-2-pyridylamine)bis( $\mu$ -hydroxo)bis( $\mu$ -perchlorato-O,O)dicopper(ii)." *European Journal of Inorganic Chemistry*, vol. 2002, no. 9, 2002, pp.2367-2374. (e) De Munno, G., Julve, M., Lloret, F., Faus, J., Verdaguer, M. and Caneschi, A. "Alternating Ferro-and Antiferromagnetic Interactions in Unusual Copper(II) Chains." *Inorganic Chemistry*, vol. 34, no. 1, 1995, pp.157-165. (f) Zerbi, G. and Sandroni, S. "Fundamental Frequencies and Molecular Configuration of Biphenyl—I. Re-Analysis of its Vibrational Spectrum." *Spectrochimica Acta Part A: Molecular Spectroscopy*, vol. 24, no. 5, 1968, pp.483-510. (g) Majeste, R.J. and Meyers, E.A. "Crystal and Molecular Structure of Bisbipyridyl- $\mu$ -dihydroxo-dicopper(II) Nitrate." *The Journal of Physical Chemistry*, vol. 74, no. 19, 1970, pp.3497-3500. (h) Castro, I., Julve, M., De Munno, G., Bruno, G., Real, J.A., Lloret, F. and Faus, J. "Formation in Solution, Preparation, Crystal Structure and Magnetic Characterization of di- $\mu$ -hydroxo-bis [diaqua(2,2'-bipyrimidine)copper(II)]diperchlorate Dihydrate." *Journal of the Chemical Society, Dalton Transactions*, 1992, no. 10, pp.1739-1744. (i) Zheng, Y.Q. and Lin, J.L. "Crystal Structures of  $[\text{Cu}_2(\text{bpy})_2(\text{H}_2\text{O})(\text{OH})_2(\text{SO}_4)] \cdot 4\text{H}_2\text{O}$  and  $[\text{Cu}(\text{bpy})(\text{H}_2\text{O})_2]\text{SO}_4$  with bpy= 2,2'-Bipyridine." *Zeitschrift für anorganische und allgemeine Chemie*, vol. 629, no. 9, 2003, pp.1622-1626. (j)Strukl, J.S. and Walter, J.L. "Infrared and Raman Spectra of Heterocyclic Compounds—IV: The Infrared Studies and normal vibrations of some 1: 1 Transition Metal Complexes of 2,2'-Bipyridine." *Spectrochimica Acta Part A: Molecular Spectroscopy*, vol. 27, no. 2, 1971, pp.223-238. (k) Youngme, S., Chailuecha, C., Van Albada, G.A., Pakawatchai, C., Chaichit, N. and Reedijk, J. "Synthesis, Crystal Structure, Spectroscopic and Magnetic Properties of Doubly and Triply Bridged Dinuclear Copper(II) Compounds Containing Di-2-pyridylamine as a Ligand." *Inorganica chimica acta*, vol. 357, no. 9, 2000, pp.2532-2542. (l) Steiner, T. "The Hydrogen Bond in the Solid State." *Angewandte Chemie International Edition*, vol. 41, no. 1, 2002, pp.48-76. (m) Ray, N., Tyagi, S. and Hathaway, B. "The Preparation and Properties of  $[\text{Cu}(\text{chelate})\text{X}_2]$  Complexes. Crystal Structure and Electronic Properties of [bis(2-pyridyl)amine]dibromocopper(II)." *Journal of the Chemical Society, Dalton Transactions*, no. 1, 1982, pp.143-146. (n) Rodig, O.R., Brueckner, T., Hurlburt, B.K., Schlatter, R.K., Venable, T.L. and Sinn, E. "Relation between

- Structure and Spectra of Pseudo-Tetrahedral Copper(II) Complexes. Crystal Structure of bis(di-2-pyridylamido)copper(II).” *Journal of the Chemical Society, Dalton Transactions*, no. 1, 1981, pp.196-199. (o) Chernyshev, A.N., Morozov, D., Mutanen, J., Kukushkin, V.Y., Groenhof, G. and Haukka, M. “Weak Intermolecular Interactions Promote Blue Luminescence of Protonated 2,2'-dipyridylamine Salts.” *Journal of Materials Chemistry C*, vol. 2, no. 39, 2014, pp.8285-8294
281. Betteridge, P.W., Carruthers, J.R., Cooper, R.I., Prout, K. and Watkin, D.J. “Crystals Version 12: Software for Guided Crystal Structure Analysis.” *Journal of Applied Crystallography*, vol. 36, no. 6, 2003, p.1487
282. Bruker Analytical X-ray Systems, Inc. “APEX2, Version 2 User Manual, M86-E01078.” Madison, WI, 2006.
283. De Meulenaer, J. & Tompa, H. “The Absorption Correction in Crystal Structure Analysis” *Acta Cryst.* Vol. 19, no. 6, 1965, pp. 1014 -1018
284. Palatinus, L. and Chapuis, G. “Superflip—a Computer Program for the Solution of Crystal Structures by Charge Flipping in Arbitrary Dimensions.” *Journal of Applied Crystallography*, vol. 40, no. 4, 2007, pp.786-790.
285. Prince, E. “*Mathematical techniques in crystallography and materials science.*” Springer Science & Business Media. In: Manor. P. (ed), Springer-Verlag, New York Heidelberg Berlin, 1982, pp. 1–192.
286. Watkin, D.A.V.I.D. “The Control of Difficult Refinements.” *Acta Crystallographica Section A: Foundations of Crystallography*, vol. 50, no. 4, 1994, pp.411-437.
287. Watkin, D.J., Prout, C.K., Carruthers, J.R. and Betteridge, P.W. “Chemical Crystallography Laboratory.” *University of Oxford*. 1993
288. Sujatha, S., Rajendiran, T.M., Kannappan, R., Venkatesan, R. and Rao, P.S. “Exogenous Bridging and Nonbridging in Cu(II) Complexes of Mannich Base Ligands: Synthesis and Physical Properties.” *Journal of Chemical Sciences*, vol. 112, no. 6, 2000, pp.559-572.
289. (a) Gennarini, F., David, R., López, I., Le Mest, Y., Reglier, M., Belle, C., Thibon-Pourret, A., Jamet, H. and Le Poul, N. “Influence of Asymmetry on the Redox Properties of Phenoxo- and Hydroxo-Bridged Dicopper Complexes: Spectroelectrochemical and Theoretical studies.” *Inorganic Chemistry*, vol. 56, no. 14, 2017, pp.7707-7719. (b) Bochot, C., Favre, E., Dubois, C., Baptiste, B., Bubacco, L., Carrupt, P.A., Gellon, G., Hardré, R., Luneau, D., Moreau, Y. and Nurisso, A. “Unsymmetrical Binding Modes of the HOPNO Inhibitor of Tyrosinase: From Model Complexes to the Enzyme.” *Chemistry—A European Journal*, vol. 19, no. 11, 2013, pp.3655-3664.
290. (a) Gaur, A., Shrivastava, B.D., Gaur, D.C., Prasad, J., Srivastava, K., Jha, S.N., Bhattacharyya, D., Poswal, A. and Deb, S.K. “EXAFS Study of Binuclear Hydroxo-Bridged Copper(II) Complexes.” *Journal of Coordination Chemistry*, vol. 64, no. 7, 2011, pp. 1265-1275. (b) Meinders, H.C., Van Bolhuis, F. and Challa, G. “The Role of  $\mu$ -hydroxo-Ligands in the Catalytic Properties of Binuclear Copper—Tertiary Amine Complexes.” *Journal of Molecular Catalysis*, vol. 5, no. 3, 1979, pp. 225-233

- 291.(a) Prescimone, A., Sanchez-Benitez, J., Kamenev, K.K., Moggach, S.A., Warren, J.E., Lennie, A.R., Murrie, M., Parsons, S. and Brechin, E.K. "High Pressure Studies of Hydroxo-Bridged Cu(II) Dimers." *Dalton Transactions*, vol. 39, no. 1, 2010, pp.113-123. (b) Bleaney, B. and Bowers, K.D. "Anomalous Paramagnetism of Copper Acetate." *Proceedings of the Royal Society of London. Series A. Mathematical and Physical Sciences*, vol. 214, no. 1119, 1952, pp.451-465. (c) Crawford, V.H., Richardson, H.W., Wasson, J.R., Hodgson, D.J. and Hatfield, W.E. "Relation between the Singlet-Triplet Splitting and the Copper-Oxygen-Copper Bridge Angle in Hydroxo-Bridged Copper Dimers." *Inorganic Chemistry*, vol. 15, no. 9, 1976, pp.2107-2110. (d) Hatfield, W.E. "Exchange Coupling in Triplet Ground State Dimeric Molecules with Specific Reference to bis( $\mu$ -pyridine N-oxide)bis[bis(nitrato)(pyridine N-oxide)copper(II)] and bis(diethyldithiocarbamate)copper(II)." *Inorganic Chemistry*, vol. 22, no. 5, 1983, pp.833-837. (e) Hay, P.J., Thibeault, J.C. and Hoffmann, R. "Orbital Interactions in Metal Dimer Complexes." *Journal of the American Chemical Society*, vol. 97, no. 17, 1975, pp.4884-4899. (f) Palacio, F. "Magnetic Molecular Materials, First edition." In: Gatteschi, D., Kahn, O. and Miller, J.S. (eds), vol. 198, Kluwer Academic, Springer Dordrecht, Netherlands, 1991, pp.1- 412. (g) Ruiz, E., Alemany, P., Alvarez, S. and Cano, J. "Toward the Prediction of Magnetic Coupling in Molecular Systems: Hydroxo-and Alkoxo-Bridged Cu(II) Binuclear Complexes." *Journal of the American Chemical Society*, vol. 119, no. 6, 1997, pp.1297-1303. (h) Ruiz, E., Alemany, P., Alvarez, S. and Cano, J. "Structural Modeling and Magneto- Structural Correlations for Hydroxo-Bridged Copper(II) Binuclear Complexes." *Inorganic chemistry*, vol. 36, no. 17, 1997, pp.3683-3688. (i) Castell, O., Caballol, R., Garcia, V.M. and Handrick, K. "Ab initio CI Determination of the Exchange Coupling Constant of Doubly-Bridged Nickel(II) Dimers." *Inorganic chemistry*, vol. 35, no. 6, 1996, pp.1609-1615. (j) Willett, R.D., Gatteschi, D. and Kahn, O. (eds), "Magneto-structural correlations in exchange coupled systems." no. CONF-8306300-, D. Reidel Publishing Co., Hingham, MA, 1985, pp. 1-616
- 292.(a) Kara, H., Elerman, Y. and Prout, K. "Antiferromagnetic Coupling In A( $\mu$ -Hydroxo)( $\mu$ -Pyrazolato)Dicopper(II) Complex. Synthesis, Crystal Structure, Magnetic Properties, And Theoretical Studies." *Zeitschrift für Naturforschung B*, vol. 56, no. 8, 2001, pp.719-727. (b) Kahn, Y. and Pei, Y. Joumax. "Inorganic Materials." In: Q. W. Bruce and D. O 'Hare (eds), John Wiley & Sons, Chichester, UK, 1992.
- 293.(a) Youngme, S., van Albada, G.A., Roubeau, O., Pakawatchai, C., Chaichit, N. and Reedijk, J. "Synthesis, Crystal Structures and Magnetism of Planar and Roof-Shaped Hydroxo-Bridged Dinuclear Copper(II) Compounds with di-2-pyridylamine as a Ligand." *Inorganica chimica acta*, vol. 342, 2003, pp.48-58. (b) Castell, O. and Caballol, R. "Ab Initio Configuration Interaction Calculation of the Exchange Coupling Constant in Hydroxo Doubly Bridged Cr(III) Dimers." *Inorganic Chemistry*, vol. 38, no. 4, 1999, pp.668-673. (c) Calzado, C.J., Cabrero, J., Malrieu, J.P. and Caballol, R. "Analysis of the

- Magnetic Coupling in Binuclear Complexes. I. Physics of the Coupling.” *The Journal of chemical physics*, vol. 116, no. 7, 2002, pp.2728-2747. (d) Calzado, C.J., Cabrero, J., Malrieu, J.P. and Caballol, R. “Analysis of the Magnetic Coupling in Binuclear Complexes. II. Derivation of Valence Effective Hamiltonians from ab Initio CI and DFT Calculations.” *The Journal of chemical physics*, vol. 116, no. 10, 2002, pp.3985-4000. (e) Melník, M., Kabešová, M., Koman, M., Macášková, L., Garaj, J., Holloway, C.E. and Valent, A. “Copper(II) Coordination Compounds: Classification and Analysis of Crystallographic and Structural Data III. Dimeric Compounds.” *Journal of coordination chemistry*, vol. 45, no. 1-4, 1998, pp.147-359.
- 294.(a) Chambron, J. –C. and Dietrich-Buchecker, C. O., “Magnetism: a Supramolecular Function.” *Long-Range Magnetic Ordering and Bistability in Molecular Magnetism*, In: Kahn, O. (ed), vol. 484, Springer Science & Business Media, 2013, pp. 530 – 554. (b) Morse, P.M. “The Theory of Electric and Magnetic Susceptibilities. (Oxford University Press, 1932).” In: JH van Vleck, (ed), vol. 76, no. 1971, science, 1932, pp.326-328. (c) Van Ruitenbeek, J.M. and van Leeuwen, D.A. “Size Effects in Orbital Magnetism.” *Modern Physics Letters B*, vol. 7, no. 16, 1993, pp.1053-1069. (d) Dingle, R.B. “Some Magnetic Properties of Metals-IV. Properties of Small Systems of Electrons.” *Proceedings of the Royal Society of London. Series A. Mathematical and Physical Sciences*, vol. 212, no. 1108, 1952, pp.47-65.
- 295.(a) Lebernegg, S. “Magneto-Structural Correlations in Doubly Hydroxo-Bridged Cu(II)-dimers.” *Croatica Chemica Acta*, vol. 84, no. 4, 2011, pp.505-513. (b) Charlot, M.F., Jeannin, S., Jeannin, Y., Kahn, O., Lucrece-Abaul, J. and Martin-Frere, J. “Crystal Structure and Magnetic Properties of Tetrakis (Cyclohexylamine) Di-. Mu.-Hydroxo-dicopper(II)perchlorate. The First Example of a Roof-Shaped Hydroxo-Bridged Copper(II) Dimer.” *Inorganic Chemistry*, vol. 18, no. 6, 1979, pp. 1675-1681. (c) Charlot, M.F., Kahn, O., Jeannin, S. and Jeannin, Y. “Exchange Interaction in Roof-Shaped Hydroxo-Bridged Copper(II) Dimers.” *Inorganic Chemistry*, vol. 19, no. 5, 1980, pp.1410-1411. (d) Ruiz, E. and Alvarez, S. “Theoretical Search for New Ferromagnetically Coupled Transition Metal Complexes.” *Chemical Communications*, no. 24, 1998, pp.2767-2768.
- 296.Yeşilel, O.Z., Darcan, C. and Şahin, E. “The First Hydroxo-Bridged Saccharinate Complexes: Syntheses, Spectral, Thermal, Structural Characterization and Antimicrobial Activities of  $[\text{Cu}(\mu\text{-OH})(\text{sac-N})(\text{deten})]_2 \cdot 2\text{H}_2\text{O}$  and  $[\text{Cu}(\mu\text{-OH})(\text{sac-O})(\text{tmen})]_2$ .” *Polyhedron*, vol. 27, no. 3, 2008, pp.905-913
- 297.Larkin, P. “Introduction: Infrared and Raman Spectroscopy.” In Clark M. A. (ed), *Infrared and Raman spectroscopy: principles and spectral interpretation, second edition*, Elsevier, Stamford, CT, United states, 2017, pp. 1 – 286.
- 298.Mardani, Z., Dorjani, S., Moeini, K., Darroudi, M., Carpenter-Warren, C., MZ Slawin, A. and Woollins, J.D. “A novel Ligand Transfer Reaction: Transferring an N3-Donor Amine Ligand from Ni(II) to Cu(II)—Structural, Spectral, Theoretical, and Docking Studies.” *Journal of Chemical Research*, vol. 43(9-10), 2019, pp.330-339

299. Breternitz, J., Godula-Jopek, A. and Gregory, D.H. "Ni(NH<sub>3</sub>)<sub>2</sub>(NO<sub>3</sub>)<sub>2</sub>—A 3-D Network through Bridging Nitrate Units Isolated from the Thermal Decomposition of Nickel Hexammine Dinitrate." *Inorganics*, vol. 6, no. 2, 2018, p.59
300. Gaye, M., Tamboura, F.B. and Sall, A.S. "Spectroscopic Studies of Some Lanthanide(III) Nitrate Complexes Synthesized from a New Ligand 2,6-bis-(salicylaldehyde hydrazone)-4-chlorophenol." *Bulletin of the Chemical Society of Ethiopia*, vol. 17, no. 1, 2003
301. (a) Kostelidou, A., Perdih, F., Kljun, J., Dimou, F., Kalogiannis, S., Turel, I. and Psomas, G. "Metal(II) Complexes of the Fluoroquinolone Fleroxacin: Synthesis, Characterization and Biological Profile." *Pharmaceutics*, vol. 14, no. 5, 2022, pp. 1 – 24. (b) Hathaway, B.J. Copper. "Transition Metal Groups 7 and 8." In Wilkinson, G. (ed), *Comprehensive Coordination Chemistry*, vol. 5, chapter 53, Pergamon Press: Oxford, UK, 1987, pp. 533–773. (c) Addison, A.W.; Rao, T.N.; Reedijk, J.; van Rijn, J.; Verchoor, G.C. "Synthesis, Structure, and Spectroscopic Properties of Copper(II) Compounds Containing Nitrogen–Sulphur Donor Ligands; the Crystal and Molecular Structure of aqua[1,7-bis(Nmethylbenzimidazol-2-yl)-2,6-dithiaheptane]copper(II) perchlorate." *J. Chem. Soc. Dalton Trans.*, no. 7, 1984, pp. 1349–1356. (d) Psomas, G.; Kessissoglou, D.P. "Quinolones and Non-Steroidal Anti-Inflammatory Drugs Interacting with Copper(II), Nickel(II), Cobalt(II) and Zinc(II): Structural Features, Biological Evaluation and Perspectives." *Dalton Trans.* 2013, no. 42, pp. 6252–6276.
302. Jelley, R.E., Blackman, A.G., Gahan, L.R., Schenk, E.B. and Krenske, E.H. "Five-coordinate Transition Metal Complexes and the Value of  $\tau_5$ : Observations and Caveats." *Dalton Transactions*, vol. 49, no. 42, 2020, pp. 14798-14806.
303. Barszcz, B., Masternak, J., Hodorowicz, M. and Jabłońska-Wawrzycka, A. "Cadmium(II) and Calcium(II) Complexes with N,O-bidentate Ligands Derived from Pyrazinecarboxylic Acid: Thermal Data and Crystal Structure Correlation." *Journal of thermal analysis and calorimetry*, vol. 108, no. 3, 2012, pp.971-978
304. (a) Kong, Y.X., Di, Y.Y., Gao, Z.F. and Dou, J.M. "Low-Temperature Heat Capacities and Standard Molar Enthalpy of Formation of 2-pyrazinecarboxylate Cupric(II) Complex Cu(pyza)<sub>2</sub>(H<sub>2</sub>O)<sub>2</sub>." *Journal of Thermal Analysis and Calorimetry*, vol. 124, no. 1, 2016, pp.437-446. (b) Giraud, S., Obbade, S., Suard, E., Steinfink, H. and Wignacourt, J.P. "Structures and Ionic Conductivities in Two Fluorite Type Families: Pb<sub>5</sub>Bi<sub>17</sub>X<sub>5</sub>O<sub>43</sub> and Pb<sub>5</sub>Bi<sub>18</sub>X<sub>4</sub>O<sub>42</sub> (X= P, V and As)." *Solid state sciences*, vol.5, no. 2, 2003, pp.335-341. (c) Allan, J.R., Paton, A.D., Turvey, K., Bowley, H.J. and Gerrard, D.L. "Spectral, Magnetic and Electrical Studies on Complexes of Some First Row Transition Elements with Pyrazinecarboxylic Acid." *Inorganica chimica acta*, vol. 132, no. 1, 1987, pp.41-47. (d) Chutia, P., Kato, S., Kojima, T. and Satokawa, S. "Synthesis and Characterization of Co(II) and Cu(II) Supported Complexes of 2-pyrazinecarboxylic Acid for Cyclohexene Oxidation." *Polyhedron*, vol. 28, no. 2, 2009, pp.370-380.

305. Afzalian, B., Mague, J.T., Mohamadi, M., Ebrahimipour, S.Y. and Kermani, E.T. "Ni(II), Co(II), and Cu(II) Complexes Incorporating 2-pyrazinecarboxylic Acid: Synthesis, Characterization, Electrochemical Evaluation, and Catalytic Activity for the Synthesis of 2H-indazolo[2, 1-b]phthalazine-triones." *Chinese Journal of Catalysis*, vol. 36, no. 7, 2015, pp.1101-1108
306. Fan, G., Xie, G., Chen, S. and Gao, S. "Water Tape Stabilized in a 3D Porous Copper(I) Supramolecular Network." *Journal of Coordination Chemistry*, vol. 60, no. 10, 2007, pp.1093-1099
307. Świdorski, G., Wojtulewski, S., Kalinowska, M., Świsłocka, R., Wilczewska, A.Z., Pietryczuk, A., Cudowski, A. and Lewandowski, W. "The Influence of Selected Transition Metal Ions on the Structure, Thermal and Microbiological Properties of pyrazine-2-carboxylic Acid." *Polyhedron*, no. 175, 2020, p.114173
308. (a) Chattopadhyay, S., Jana, P., Mitra, A., Sarkar, S.K., Ganguly, T. and Mallick, P.K. "Raman Excitation Profiles and Molecular Structures in the Excited Electronic States of 2,2'-dipyridylamine." *Journal of Raman spectroscopy*, vol. 28, no. 8, 1997, pp.559-565. (b) Rodig, O.D., Bell, C.E., Clark, A.K. and Taber D.F. "Organic Chemistry Laboratory: Standard and Microscale Experiments." *Infrared absorption spectroscopy*, 3rd. Saunders College Publishing, 2000, pp. 90-106
309. Du, M., Bu, X.H., Weng, L.H., Leng, X.B. and Guo, Y.M. "Redetermination of [bis(2-pyridyl)amine-N,N']copper(II)diperchlorate." *Acta Crystallographica Section E: Structure Reports Online*, vol. 57, no. 1, 2001, pp.m25-m27
310. Hsiao, C.J., Lai, S.H., Chen, I.C., Wang, W.Z. and Peng, S.M. "Metal–Metal Bonding and Structures of Metal String Complexes Cr<sub>3</sub>(dpa)<sub>4</sub>Cl<sub>2</sub>, Cr<sub>3</sub>(dpa)<sub>4</sub>(NCS)<sub>2</sub>, and [Cr<sub>3</sub>(dpa)<sub>4</sub>Cl<sub>2</sub>](PF<sub>6</sub>) from IR, Raman, and Surface-Enhanced Raman spectra." *The Journal of Physical Chemistry A*, vol. 112, no. 51, 2008, pp.13528-13534
311. Manna, S.C., Mistri, S. and Jana, A.D. "A Rare Supramolecular Assembly Involving Ion Pairs of Coordination Complexes with a Host–Guest Relationship: Synthesis, Crystal Structure, Photoluminescence and Thermal Study." *CrystEngComm*, vol. 14, no. 21, 2012, pp.7415-7422
312. Zafiu, C., Trettenhahn, G., Pum, D., Sleytr, U.B. and Kautek, W. "Structural Control of Surface Layer Proteins at Electrified Interfaces Investigated by in situ Fourier Transform Infrared Spectroscopy." *Physical Chemistry Chemical Physics*, vol. 13, no. 29, 2011, pp.13232-13237.
313. Smit, E., de Waal, D. and Heyns, A.M. "The Spin-Transition Complexes [Fe(Htrz)<sub>3</sub>](ClO<sub>4</sub>)<sub>2</sub> and [Fe(NH<sub>2</sub>trz)<sub>3</sub>](ClO<sub>4</sub>)<sub>2</sub> I. FT-IR Spectra of a Low Pressure and a Low Temperature Phase Transition." *Materials research bulletin*, vol. 35, no. 10, 2000, pp. 1697-1707.
314. Rosenthal, M.R. "The Myth of the Non-Coordinating Anion." *Journal of Chemical Education*, vol. 50, no. 5, 1973, p.331
315. Taghipour, F. and Mirzaei, M. "A Survey of Interactions in Crystal Structures of Pyrazine-Based Compounds." *Acta Crystallographica Section C: Structural Chemistry*, vol. 75, no. 3, 2019, pp.231-247

316. Sigala, P.A., Ruben, E.A., Liu, C.W., Piccoli, P.M., Hohenstein, E.G., Martínez, T.J., Schultz, A.J. and Herschlag, D. "Determination of Hydrogen Bond Structure in Water Versus Aprotic Environments to Test the Relationship Between Length and Stability." *Journal of the American Chemical Society*, vol. 137, no. 17, 2015, pp.5730-5740
317. Pal, S., Ghosh, R., Sarkar, A., Woollins, J.D. and Ghosh, B.K. "Photoluminous Copper(II)-2,2'-dipyridylamine Coordination Frameworks: Two-Dimensional Superstructures Based on Hydrogen Bonds and  $\pi$ ...  $\pi$ /C-H...  $\pi$  Interaction." *Journal of Molecular Structure*, vol. 878, no. 1-3, 2008, pp.32-39
318. Midollini, S. and Orlandini, A. "Hydrogen Bonding in Triamine Copper(II) P, P'-Diphenylmethylenediphosphinate ( $\text{pcp}^{2-}$ ) Hybrids. Syntheses and Crystal Structures of  $[\text{Cu}(\text{pcp})(2,2'\text{-dipyridylamine})(\text{H}_2\text{O})]\cdot 2\text{H}_2\text{O}$  and  $[\text{Cu}(\text{pcp})(2,2':6',2''\text{-Terpyridine})]\cdot 4\text{H}_2\text{O}$ ." *Journal of Coordination Chemistry*, vol. 59, no. 13, 2006, pp.1433-1442.
319. Kennepohl, D and Last, A. "Amines and Heterocycles." *Organic Chemistry II*, In: Sanders, G. (ed), Chapter 24, Athabasca University Digital Media Technology Unit, 2020, pp. 499 – 999
320. Miller, K.L., Williams, B.N., Benitez, D., Carver, C.T., Ogilby, K.R., Tkatchouk, E., Goddard III, W.A. and Diaconescu, P.L. "Dearomatization Reactions of N-heterocycles Mediated by Group 3 Complexes." *Journal of the American Chemical Society*, vol. 132, no. 1, 2010, pp.342-355.
321. Fombona, S., Espinal-Viguri, M., Huertos, M.A., Díaz, J., López, R., Menéndez, M.I., Pérez, J. and Riera, L. "Activation of Aromatic C-C Bonds of 2,2'-Bipyridine Ligands." *Chemistry—A European Journal*, vol. 22, no. 48, 2016, pp.17160-17164.
322. Gillard, R.D., Knight, D.W. and Williams, P.A. "Equilibria in Complexes of N-heterocyclic Molecules, part XXVI. Reactions of Hydroxide and Water with the tris-(2,2'-bipyrazine)iron(II) and tris-[2,2'-bis-(5,6-dihydro-4-H-1,3-oxazine)]iron(II) Ions." *Transition Metal Chemistry*, vol. 4, no. 6, 1979, pp.375-378.
323. Kirgan, R.A. "Diimine Complexes of Ruthenium(ii), Rhenium(i) and Iron(ii): from Synthesis to DFT Studies." *Doctoral dissertation, Wichita State University*, 2007.
324. Dong, L., Lin, L., Han, X., Si, X., Liu, X., Guo, Y., Lu, F., Rudić, S., Parker, S.F., Yang, S. and Wang, Y. "Breaking the Limit of Lignin Monomer Production Via Cleavage of Interunit Carbon-Carbon Linkages." *Chem*, vol. 5, no. 6, 2019, pp.1521-1536.
325. Yue, S., Wang, P., Hao, X. and Zang, S. "Dual Amino-Functionalized Ionic Liquids as Efficient Catalysts for Carbonate Synthesis from Carbon Dioxide and Epoxide under Solvent and Cocatalyst-Free Conditions." *Journal of CO<sub>2</sub> Utilization*, vol. 21, 2017, pp.238-246.
326. Sasaki, Y., Kato, H. and Kudo, A. " $[\text{Co}(\text{bpy})_3]^{3+/2+}$  and  $[\text{Co}(\text{phen})_3]^{3+/2+}$  Electron Mediators for Overall Water Splitting Under Sunlight Irradiation Using Z-scheme Photocatalyst System." *Journal of the American Chemical Society*, vol. 135, no.14, 2013, pp.5441-5449.

327. Nicewicz, D.A. and MacMillan, D.W. "Merging Photoredox Catalysis with Organocatalysis: the Direct Asymmetric Alkylation of Aldehydes." *Science*, vol. 322, no. 5898, 2008, p.p.77-80.
328. Cotton, F.A., Wilkinson, G., Mutillo, C.A. and Bochmann, M. "Advanced Inorganic Chemistry". *Journal of Chemical Education*, vol. 77, no. 3, 2000, p.311.
329. Rajendiran, V., Murali, M., Suresh, E., Palaniandavar, M., Periasamy, V.S. and Akbarsha, M.A. "Non-Covalent DNA Binding and Cytotoxicity of Certain Mixed-Ligand Ruthenium(II) Complexes of 2,2'-dipyridylamine and Diimines." *Dalton Transactions*, no. 16, 2008, pp.2157-2170
330. (a) Jbali, W., Selmi, W., Jouffret, L., Marzouki, R. and Zid, M.F. "Synthesis, Crystal Structure, Spectroscopic Study and Hirshfeld Surface Analysis of  $[\text{Ni}(\text{C}_6\text{H}_8\text{N}_2)_3]\text{Cl}_2 \cdot 2(\text{H}_2\text{O})(1)$ ." *Journal of Molecular Structure*, vol. 1225, 2021, p.129123. (b) Abbas, B.F., Kamel, B.A. and Khamais, W.M. "Preparation, Diagnosis, Biological Activity, and Theoretical Studies of Some Mixed Drug Complexes." *The Scientific World Journal*, vol. 2019, 2019, pp. 1-7. (c) Dan, W.Y., Di, Y.Y., Liu, Y.J., Kong, Y.X. and Tan, Z.C. "Low-Temperature Heat Capacities and Standard Molar Enthalpy of Formation of Dichlorobis(2-aminopyridine)zinc(II),  $\text{ZnCl}_2(\text{C}_5\text{H}_6\text{N}_2)_{2(s)}$ ." *International Journal of Thermophysics*, vol. 31, no. 11, 2010, pp.2103-2118.
331. Wyllie, G.R., Munro, O.Q., Schulz, C.E. and Scheidt, W.R. "Structural and Physical Characterization of (Nitrate) Iron(III)porphyrinates  $[\text{Fe}(\text{por})(\text{NO}_3)]^-$  Variable Coordination of Nitrate." *Polyhedron*, vol. 26, no. 16, 2007, pp.4664-4672
332. (a) Shukla, M., Srivastava, N., Saha, S., Rao, T.R. and Sunkari, S. "Synthesis, Structure, UV-Vis-IR spectra, Magnetism and Theoretical Studies on CuII [(2-aminomethyl) pyridine](thiocyanate)<sub>2</sub> and Comparisons with an Analogous CuII Complex." *Polyhedron*, vol. 30, no. 5, 2011, pp.754-763. (b) Karaagac, D. "Vibrational Spectroscopic and Thermal Investigations of the Cyano-Bridged Polymeric Complexes with 3-aminomethylpyridine." *Eskişehir Technical University Journal of Science and Technology A-Applied Sciences and Engineering*, vol. 20, no. 3, 2019, pp.216-226.
333. (a) Reddy K, R.K., Suneetha, P., Karigar, C.S., Manjunath, N.H. and Mahendra, K.N. "Cobalt(II), Ni(II), Cu(II), Zn(II), Cd(II), Hg(II), UO<sub>2</sub>(VI) and the (IV) Complexes from Onon Schiff Base Ligand." *Journal of the Chilean Chemical Society*, vol. 53, no. 4, 2008, pp.1653-1657. (b) Sharipova, L. and Mamatova, F. "IR-Spectroscopic Analysis of the Coordination Compounds of Zinc Nitrate with Benzamide and Urea." *Science and Innovation*, vol. 2, no. A2, 2023, pp.66-70.

## تحضير ودراسة بنية مركبات تناسقية مختلطة المتصلات للنحاس (II) و النيكل (II) مع

٢،٢-بيبيريزين و القواعد النيتروجينية ثنائية الترابط

إعداد : أفنان ربحي عبدالله منصور

المشرف : د. حسين علقم

### ملخص:

تكوين المركبات ذات البنية الهيكلية المنتظمة يتم اعتمادا على استخدام العديد من المعادن الانتقالية والتي لديها القدرة على تشكيل أشكال هندسية متنوعة في تصميم المركبات المتصلة (اللواقظ/الربيطات). تمثل المركبات الحلقية غير المتجانسة والمحتوية على ذرة النيتروجين مثالا جيدا على اللواقظ/الربيطات والتي تتفاعل مع المعادن الأيونية، مما يوفر دورًا مهمًا في تحسين المركبات الغير العضوية ومجالات التصنيع.

تم تحضير سلسلة من المركبات الجديدة مكونة من النيكل (II) والنحاس (II) سواء مع لاقظ/ ربيطة أو مع لواقظ/ روبيطات متنوعة مثل 2,2'-bipyrazine، 2,2'-dipyridylamine، 2-(aminomethyl)pyridine. البنية الهيكلية للمركبات التناسقية وهي  $[\text{Cu}(\text{amp})_2(\text{NO}_3)_2]$  و  $[\text{Cu}(\text{bpz})_2(\text{H}_2\text{O})](\text{NO}_3)_2$  و  $[\text{Cu}(\text{amp})_2(\text{NO}_3)_2]$  والتي تم تشخيصها وتحليلها باستخدام طرق مختلفة مثل تحليل حيود الأشعة السينية، تحليل مطياف الأشعة تحت الحمراء (FTIR) و دراسة الخواص الحرارية (DSC)، وتمييز و وصف اللواقظ/الروبيطات بشكل تفصيلي باستخدام تحليل مطياف الأشعة تحت الحمراء.

معدن النحاس (II) في المركب الجديد  $[\text{Cu}(\text{amp})_2(\text{NO}_3)_2]$  يمتلك ارتباط تناسقي سداسي مع أربع ذرات نيتروجين من 2-(aminomethyl)pyridine (amp) ومع ذرتين أكسجين من جزئ النترات المرتبط تناسقيا مع النحاس (II) حيث يتشكل تنسيق هندسي غير منتظم ثماني السطوح حول معدن النحاس (II). البلورة من الترتيب البلوري الأحادي، مع مجموعة الفضاء  $P2_1/c$  وأبعاد وحدة الخلية  $a = 8.6377$  (7)،  $b = 8.9833$  (6)،  $c = 9.9958$  (10) Å<sup>3</sup>  $V = 765.14$  (10) Å<sup>3</sup>،  $\beta = 99.430^\circ$ ،  $Z = 2$ ،  $A^\circ = 8$  (8). استقرار ترتيب البلورات يتم من خلال رابطة  $\text{C-H}\cdots\text{O}$  و  $\text{N-H}\cdots\text{O}$  الهيدروجينية بين مجموعتي البيريدين والأمين لـ amp مع ذرات الأكسجين لجزئ النترات المرتبط تناسقيا. السلاسل أيضا تتقوى بالارتباطات الضعيفة  $\text{C-H}\cdots\text{O}$  بين مجموعة  $\text{CH}$  لـ amp و ذرة الأكسجين لجزئ

النترات من السلسلة المجاورة. تتداخل سلاسل النحاس المجاورة مع سلاسل أخرى من خلال تفاعلات  $\pi - \pi$  المتصلة بواسطة اثنين من 2-(aminomethyl)pyridine

دراسة المركب الجديد  $[\text{Cu}(\text{bpz})_2(\text{H}_2\text{O})](\text{NO}_3)_2$  تمت بواسطة تحليل الأشعة السينية لإيجاد أن معدن النحاس (II) يمتلك ارتباط تنسيقي رباعي مع أربع ذرات نيتروجين لـ 2,2'-bipyrazine، ومع ذرة أكسجين واحدة من جزئ الماء. جزئي النترات عبارة عن أيون معاكسة الشحنة. التنسيق الهندسي حول معدن النحاس (II) هو هرم رباعي القاعدة غير منتظم. البلورة من الترتيب البلوري الأحادي، مع مجموعة الفضاء C2/c وأبعاد وحدة الخلية  $a = 15.886(6)$ ,  $b = 7.208(4)$ ,  $c = 18.016(7)$  Å,  $\beta = 107.07(4)^\circ$ ,  $Z = 4$ ,  $V = 1972.2(17)$  Å<sup>3</sup> استقرار ترتيب البلورات يتم من خلال الرابطة الهيدروجينية المتشكلة بفعل أيونات النترات التي تعمل كجسور للربط مع الأيونات الموجبة للمركب خلال الروابط  $\text{O} - \text{H} \cdots \text{N}$  و  $\text{O} - \text{H} \cdots \text{O}$  و  $\text{C} - \text{H} \cdots \text{O}$  والاتصال القريب.

توصلت دراسة الأشعة السينية للمركب الجديد  $[\text{Cu}(\text{bpz})_3](\text{ClO}_4)_2 \cdot 2\text{CH}_3\text{CN}$  إلى أن مركز معدن النحاس (II) يمتلك ترتيب هندسي ثماني الأوجه غير منتظم، والبلورة أحادية، مع مجموعة الفضاء P2<sub>1</sub>/c وأبعاد وحدة الخلية  $a = 11.2508(6)$ ,  $b = 22.1602(12)$ ,  $c = 13.6980(8)$  Å,  $A = 90^\circ$ ,  $b = 90.302(5)^\circ$ ,  $g = 90^\circ$ ,  $Z = 4$ ,  $V = 3415.1(3)$  Å<sup>3</sup>. كشف ترتيب البلورات أنواع مختلفة من الروابط الهيدروجينية، تشمل بين أسيتونيتريل و ذرات النيتروجين لـ bpz، ذرات النيتروجين لـ bpz و ذرات نيتروجين لـ bpz أخرى، ذرات الأكسجين لجزئيات البيركلورات، وذرة الهيدروجين لـ bpz، وبين ذرة الهيدروجين لأسيتونيتريل و ذرة الأكسجين للبيركلورات. بالإضافة إلى رابطة فان دير فان تتكون بين C-H لـ bpz مع ذرة الأكسجين للبيركلورات. ترتبط الصفائح المجاورة من خلال الروابط الضعيفة  $\pi - \pi$ .

المركب الجديد  $[\text{Cu}(\text{dipyam})(\text{H}_2\text{O})(\text{pca})]\text{ClO}_4$  الذي تكون نتيجة انشطار جزئ ٢،٢-بيبيريزين إلى جزئ pca داخل محلول التفاعل. وتمت دراسته بواسطة الأشعة السينية وأظهرت أن معدن النحاس (II) ترتبط بشكل خماسي من قبل ذرتين نيتروجين من 2,2'-dipyridylamine، ذرة نيتروجين وذرة أكسجين من 2-pyrazinecarboxylate (pca)، ذرة أكسجين واحدة من الماء المرتبط تناسقياً مع النحاس (II). جزئ البيركلورات هو أيون معاكس الشحنة، هذه الذرات تشكل ترتيب هندسي هرم رباعي القاعدة غير منتظم حول أيونات النحاس (II). البلورة أحادية، مع مجموعة الفضاء P-1 وأبعاد وحدة الخلية هي  $a = 7.8943(10)$ ,  $b = 9.9511(14)$ ,  $c = 13.412(2)$  Å,  $A = 90^\circ$ ، أيونات البيركلورات ترتبط مع أيونات المركب المعقد الموجبة لتنتج البنية الهيكلية للسلسلة خلال الاتصال القريب  $\text{O} - \text{H} \cdots \text{O}$  و الرابطة الهيدروجينية  $\text{C} - \text{H} \cdots \text{O}$ . في محلول التفاعل تكون متصل جديد (pca) من المتصل ٢،٢-بيبيريزين وهذا يشجع العلماء على افتراض منهجية جديدة لانقسام الرابطة لـ C-C / C-N.

البنية الهيكلية للمركب ثنائي النواة  $[(\text{bpz})\text{Cu}(\text{OH})(\text{ClO}_4)(\text{H}_2\text{O})]_2 \cdot \text{H}_2\text{O}$  تحتوي على جزئين هيدروكسيد تعمل كجسر تربط أيونين نحاس (II) مع متصلين اثنين من ٢،٢-بيبيريزين على طرفي المركب، بالإضافة إلى جزئين ماء، وجزئين من البيركلورات وجزئ ماء يعمل كمذيب. البلورة ثلاثية، مع مجموعة الفضاء P-1 وأبعاد الخلية الواحدة  $a = 8.0391(10)$ ,  $b = 8.1718(9)$ ,  $c = 10.5662(14)$  Å,  $\alpha = 77.973(5)^\circ$ ,  $\beta = 80.465^\circ$

(II) شكل هندسي ممدود ثماني السطوح رباعي الزوايا غير منتظم، حيث ذرات الأكسجين لجزيئي الماء والبيركلوريت والتي تقع في المحاور الرأسية، بينما ذرتين النيتروجين لـ 2,2'-bipyrazine و ذرتي الأكسجين من مجموعات الهيدروكسو تقع في المحاور الأفقية. الرابطة الهيدروجينية تتشكل تبعاً لنيتروجين الـ pyrazine، الأكسجين من مجموعة البيركلوريت، مجموعات الهيدروكسيد، مجموعة الماء المتسقة وجزئ الماء المتبلور.

مركب النيكل ثنائي التكافؤ الجديد  $[\text{Ni}(\text{dipyam})_2(\text{bpz})](\text{ClO}_4)_2$ ، التحليل الهيكلي للأشعة السينية أظهر أن معدن النيكل (II) عبارة عن سداسي الارتباط التنسيقي من خلال ذرتين نيتروجين لـ 2,2'-bipyrazine، وأربع ذرات نيتروجين من جزيئين من 2,2'-dipyridylamine. جزيئي البيركلورات عبارة عن أيون معاكسة الشحنة. الترتيب الهندسي للمركب عبارة عن شكل ثماني السطوح مشوه؛ بسبب وجود ثلاثة من حلقات مخرية ترتبط مع ذرة النيكل (II)، تتضمن جزيئين اثنين من (dipyam)، جزئ واحد من 2,2'-bipyrazine، كل جزئ من 2,2'-dipyridylamine يقع على المحور الأفقي وعلى المحور الرأسية، و 2,2'-bipyrazine تقع على المحاور الأفقية. البلورة أحادية، مع مجموعة الفضاء C2/c، أبعاد الخلية الواحدة  $a = 16.919 (3)$ ،  $b = 11.2635 (18)$ ،  $c = 17.588 (4) \text{Å}$ ،  $\beta = 113.037 (4)^\circ$ ،  $Z = 4$ ،  $V = 3084.4 (10) \text{Å}^3$ . أيونات البيركلورات ترتبط مع الأيونات الموجبة للمركب وتشكل البنية الهيكلية للسلسلة خلال  $\text{N}-\text{H}\cdots\text{O}$  اتصال قريب والرابطة الهيدروجينية  $\text{C}-\text{H}\cdots\text{O}$ ، جنباً إلى روابط الـ 2,2'-bipyrazine خلال  $\text{C}-\text{H}\cdots\text{N}$ . روابط ضعيفة الـ  $\pi\cdots\pi$  و/أو  $\text{C}-\text{H}\cdots\pi$  التي أنشأتها حلقات مجموعات الـ pyridyl و pyrazinyl من الصفحة المجاورة.

هذه المركبات ممكن أن تلعب دوراً مهماً في مجالات مختلفة بغض النظر كانت بالمجال الكيميائي، البيولوجي أو حتى الإلكتروني؛ تبعاً لأن مركباتها المتصلة (الواقظ/الروبيطات) لديها استخدامات واسعة في تطبيقات مختلفة، مثلاً، استخدامها في تطوير فعالية المحفزات، تحضير مركبات مكثفة (مكونة من أكثر من وحدة بنائية)، تصميم جزيئات دوائية جديدة والمستخدمة في دراسات تصنيع الأدوية، بالإضافة لتوظيفها في المواد الكهروضوئية، شبه الموصلات والمواد المغناطيسية.